

**Comparison of metabolic cages -
analysis of refinement measures on the welfare and
metabolic parameters of laboratory mice**

Laura Wittek

Univ.-Diss.

zur Erlangung des akademischen Grades

"doctor rerum naturalium"

(Dr. rer. nat.)

in der Wissenschaftsdisziplin "Physiologie und Pathophysiologie der Ernährung"

eingereicht an der

Mathematisch-Naturwissenschaftlichen Fakultät

Institut für Ernährungswissenschaft

der Universität Potsdam

Potsdam, 09.10.2023

Unless otherwise indicated, this work is licensed under a Creative Commons License Attribution 4.0 International.

This does not apply to quoted content and works based on other permissions.

To view a copy of this license, visit:

<https://creativecommons.org/licenses/by/4.0>

Hauptbetreuer: apl. Prof. Dr. Jens Raila

Betreuerin: Prof. Dr. Stephanie Krämer

Gutachter: Prof. Dr. Bernhard Hiebl

Mentorin: Dr. Tina Nitezki

Published online on the

Publication Server of the University of Potsdam:

<https://doi.org/10.25932/publishup-61120>

<https://nbn-resolving.org/urn:nbn:de:kobv:517-opus4-611208>

Dedicated to the mice

Contents

Summary	I
Zusammenfassung.....	III
1. Introduction.....	1
1.1 The 3R-Concept and scientific validity of laboratory animal research.....	1
1.2 The metabolic cage	2
1.3 Behavioral phenotyping and animal personality	5
1.3.1 Behavioral response and adaptation to a stressor.....	7
1.3.2 Requirements for a species-appropriate husbandry.....	8
1.4 Relevant physiological systems for stress assessment of mice while in the metabolic cage	10
1.4.1 The hypothalamic-pituitary-adrenocortical axis	10
1.4.1.1 Adrenal glands - Glucocorticoids.....	12
1.4.1.2 Biotransformation of glucocorticoids - focus on corticosterone in urine and fecal samples.....	13
1.4.2 Brown adipose tissue - adaptive thermogenesis.....	15
1.4.2.1 Thermoregulatory thermogenesis	15
1.4.2.2 Acute and chronic exposure to cold environmental conditions - cold-induced thermogenesis	16
1.4.2.3 Sympathetic innervation of the brown adipose tissue and uncoupling protein 1.....	17
1.4.3 Brain - neurotransmitters.....	19
1.4.3.1 The dopaminergic system	19
1.4.3.2 The serotonergic system	23
1.4.4 Liver - glycogen metabolism.....	26
2. Objective.....	28
3. Materials and Methods	29
3.1 Animal experiment.....	29
3.1.1 Ethical statement.....	29
3.1.2 Mouse strain and housing conditions	29
3.1.3 Study design.....	30
3.1.4 Description of the metabolic cages	32
3.1.5 Assessment of animal welfare.....	33
3.1.5.1 Fur Score.....	33
3.1.5.2 Mouse Grimace Scale.....	33
3.1.5.3 Assessment of cold stress by thermal imaging camera	35
3.1.6 Analysis of behavior.....	36
3.1.6.1 Behavioral tests.....	36

3.1.6.1.1	Elevated Plus Maze	36
3.1.6.1.2	Open Field Test	36
3.1.6.2	Video observation	37
3.1.6.2.1	Experimental setup and observational periods	37
3.1.6.2.2	Video analysis on the basis of an exclusive ethogram	38
3.1.7	Assessment of metabolic parameters	39
3.1.7.1	Body weight and body composition.....	39
3.1.7.2	Food and water intake	39
3.1.7.3	Feces and urine collection.....	40
3.2	Laboratory analyses.....	41
3.2.1	Organ preparation	41
3.2.2	Histology - Periodic Acid Schiff/Hematoxylin staining	44
3.2.3	Molecular biological methods	45
3.2.3.1	RNA isolation from brown adipose tissue.....	45
3.2.3.2	Complementary DNA synthesis.....	46
3.2.3.3	Quantitative reverse transcription-polymerase chain reaction.....	46
3.2.4	Biochemical methods	47
3.2.4.1	Determination of total protein by Bradford method.....	47
3.2.4.2	Determination of liver glycogen by UV method	47
3.2.4.3	Enzyme Immunoassay - Fecal corticosterone metabolites.....	48
3.2.5	Liquid chromatography tandem-mass spectrometry.....	48
3.2.5.1	Determination of corticosterone concentrations in urine samples.....	48
3.2.5.2	Determination of serotonin and dopamine concentrations in brain areas	51
3.3	Data analysis and statistics.....	53
4.	Results	54
4.1	Animal welfare	54
4.1.1	Fur Score	54
4.1.2	Mouse Grimace Scale	55
4.1.3	Cold stress.....	58
4.1.3.1	Cage temperature	58
4.1.3.2	Body surface temperature	59
4.1.3.3	Uncoupling protein 1 in brown adipose tissue and brown adipose tissue weight	60
4.2	Behavioral patterns	61
4.2.1	Behavioral tests	61
4.2.1.1	Excretion of fecal boli.....	61
4.2.1.2	Time in zone	63

4.2.1.3	Entries into zone.....	65
4.2.1.4	Total distance traveled.....	67
4.2.1.5	Activity: total time (im)mobile	69
4.2.2	Video observation.....	72
4.2.2.1	Counts of behavioral categories for female mice during first restraint.....	72
4.2.2.2	Counts of behavioral categories for female mice during second restraint.....	74
4.2.2.3	Counts of behavioral categories for male mice during first restraint.....	76
4.2.2.4	Counts of behavioral categories for male mice during second restraint.....	78
4.2.3	Neurotransmitter levels in brain areas.....	80
4.2.3.1	Dopamine and its metabolites 3,4-dihydroxyphenylacetic acid and 3-methoxythyramine	80
4.2.3.2	Serotonin.....	85
4.2.3.3	The dorsal mesostriatal system.....	87
4.3	Metabolic parameters.....	91
4.3.1	Body weight change	91
4.3.2	Body composition	93
4.3.2.1	Lean mass change	93
4.3.2.2	Fat mass change	93
4.3.3	Food intake	94
4.3.4	Water intake.....	95
4.3.5	Defecation	95
4.3.6	Urinary excretion.....	96
4.3.7	Glycogen levels in liver	97
4.3.7.1	Periodic Acid Schiff/Hematoxylin staining	97
4.3.7.2	UV method	98
4.3.7.3	Correlation between glycogen concentration and food intake.....	99
4.3.7.4	Liver weight	99
4.4	Stress indicator corticosterone	100
4.4.1	Corticosterone levels in urine.....	100
4.4.2	Corticosterone levels in feces.....	101
4.4.2.1	Correlation between fecal corticosterone metabolites and cold stress parameters .	102
4.4.2.2	Comparison of fecal corticosterone metabolites with Fur Scores of mice	104
5.	Discussion.....	105
5.1	Stress during restraint in metabolic cages affects mouse welfare and behavior	106
5.1.1	Outward appearance of mice after metabolic cage restraint	106
5.1.2	Behavioral response to metabolic cage restraint and reference to neurotransmitters in sampled brain areas	108

5.1.3 Adrenal secretion of corticosterone is reduced during restraint in the Innovative metabolic cage	115
5.2 Indications of cold stress reduction during restraint in the Innovative metabolic cage.....	119
5.2.1 Room temperature and the resulting cage temperature.....	119
5.2.2 Body surface temperature as a proxy for body core temperature	120
5.2.3 Brown adipose tissue: adaptive non-shivering thermogenesis.....	122
5.3 The Innovative metabolic cage effectively preserves energy resources of mice.....	125
5.3.1 Reduced body weight, lean and fat mass loss due to application of the Innovative metabolic cage	125
5.3.2 Increase in food intake during Innovative metabolic cage restraint.....	126
5.3.3 Glycogen stores in the liver are depleted to a lesser extent during restraint in the Innovative metabolic cage	128
5.4 Further refinement measures for the improvement of metabolic cages	130
6. Conclusion	131
References.....	132
List of Abbreviations.....	140
List of Figures.....	142
List of Tables.....	145
Units	146
Supplemental information	147
S1 Materials.....	147
S1.1 Reagents	147
S1.2 Buffers and solutions	148
S1.3 Kits	148
S1.4 Oligonucleotides	148
S1.5 Standards	149
S1.6 Equipment for animal experiment and laboratory analyses	149
S1.7 Consumable material for animal experiment and laboratory analyses	152
S1.8 Software.....	156
Conferences.....	157
<i>Curriculum vitae</i>	158
Acknowledgements	159
Eidesstaatliche Erklärung	160

Summary

The metabolic cage is a versatile tool widely used for a variety of animal experiments including input and output studies, pharmacokinetic and pharmacodynamic studies, and assessment of kidney and/or intestinal function. The utilization of the metabolic cage offers many advantages such as individualized monitoring of water and food intake as well as individualized collection of urine and feces. Nevertheless, the welfare of mice is severely limited by their single housing within the cage, the absence of enrichment material, and the grid cage floor. The impact of metabolic cage restraint on the murine metabolic phenotype has, as yet, not been sufficiently researched. The aim of this thesis was to investigate (1) whether the general stress level and cold stress of the metabolic cage can be reduced, and (2) if the energy resources of mice can be more effectively preserved during metabolic cage restraint.

This study focused on the comparison of two different metabolic cage types. The construction of an Innovative metabolic cage (IMC) possesses substantial refinement measures and was built in the research workshop at the German Institute of Human Nutrition (DIfE) while the metabolic cage from the Tecniplast GmbH (TMC) is commercially available. The IMC features improvements such as a decreased cage volume, an angled food hopper and water supply, and an inserted resting platform on top of the grid cage floor in order to enhance animal welfare during experimental utilization. 25 female and 25 male 10 week old C57BL/6J mice were single housed for 24 h in either the IMC or the TMC. This housing was then repeated after a 6 d resting period. Mice were individually housed in control cages containing bedding material and standardized enrichment to control for the effect of isolation itself. The enrichment included 1 cotton nestlet, 2 tissues, 1 wooden gnawing bar, and 1 cardboard house. Animal welfare, mouse behavior, and metabolic parameters were assessed in the course of the two week experiment. After termination of each experimental group, mice were euthanized, organs were sampled, and laboratory analyses of extracted tissues as well as urine and fecal samples followed.

Indications of reduced animal welfare following restraint in metabolic cages were noted, including altered fur condition, facial expression, and cold stress of the mice. Fur Scores of female and male mice deteriorated after both restraints in the TMC as well as in the IMC in comparison to controls. The ear position scores of the applied Mouse Grimace Scale were significantly higher for both sexes after the second restraint in the TMC compared to the IMC. During the first restraint of female mice, the cage temperature in the TMC was significantly lower in comparison to the IMC. This was also true for male mice during both restraints.

Two different behavioral tests - the Elevated Plus Maze (EPM) and the Open Field Test (OFT) - were conducted directly after both 24 h single housing periods and videos of mice were recorded during both 24 h restraints. It was indicated that all mice, independent of the tested cage type, were stressed merely by solitary housing conditions and/or the novel environment of the testing arenas. In the EPM, females and males spent most of their testing time in the closed arms of the maze, indicating increased anxiety behavior in the mice. Similarly, the middle zone of the OFT was approached most frequently by both sexes, suggesting that the mice did not show a pronounced willingness to explore the field. Concerning the video analyses, an exclusive ethogram was predefined that included "escape behavior" and "other activities" alongside three additional behavioral categories. Escape behavior included jumping, running, gnawing on bars, scratching, and rearing while other activities implied drinking, feeding, urination, and defecation.

Escape behavior was increased during TMC restraint as compared to IMC restraint for both sexes during the first restraint. This was also true for females during the second restraint. Other activities were in turn significantly higher for mice restrained in the IMC as compared to the TMC. This was concomitantly associated with increased food intake in the IMC relative to the TMC for male mice during the first restraint and for both sexes during the second restraint.

The neurotransmitters serotonin (SRT) and dopamine (DA) and its metabolites 3-methoxythiramine (3-MT) and 3,4-dihydroxyphenylacetic acid (DOPAC) were quantified in five different brain areas. DOPAC in the *caudate putamen* was significantly increased in females after IMC restraint compared to controls. A similar trend was also seen in the *nucleus accumbens*. Concerning male mice, DOPAC concentrations in the *hypothalamus* were significantly elevated after restraint in the IMC compared to TMC restraint and control cage housing.

As a physiological stress marker, the concentration of fecal corticosterone metabolites (FCM) were quantified, as well as urinary glucuronidated corticosterone. FCM concentrations of female and male mice restrained in the TMC were significantly higher during both restraints as compared to mice housed in the control cages. Concerning urinary corticosterone, females excreted significantly higher amounts of corticosterone during both TMC restraints compared to IMC restraint.

The gathered metabolic parameters suggested that the metabolic phenotype of mice was more affected by the TMC than by the IMC. The extent of loss in body weight (BW) and lean mass (LM) of both female and male mice were greater during restraint in the TMC compared to the IMC. Analyses of hepatic tissue samples chiefly revealed higher glycogen levels of mice restrained in the IMC compared with those restrained in the TMC. The higher reduction of energy stores in the TMC is attributable to the increased activity of the mice during TMC restraint, which can be observed, for example, by increased escape behavior.

In conclusion, the results of this thesis indicate the high stress potential for mice induced by metabolic cage restraint and how the IMC can contribute to a quantifiable reduction in discomfort for laboratory mice. Taken together, these data clearly indicate that the IMC has less impact on the metabolic phenotype of mice in direct comparison to the TMC. Introducing the IMC represents a first attempt to target stress reduction in laboratory mice by actively incorporating refinement measures during the use of metabolic cages. The IMC thereby supports animal welfare-friendly data collection when the restraint of laboratory mice in metabolic cages is indispensable in the context of specific scientific questions.

Zusammenfassung

Der Stoffwechselkäfig ist ein vielseitiges Instrument, welches für zahlreiche versuchstierkundliche Fragestellungen eingesetzt werden kann, wie Bilanz-Studien, pharmakokinetische und pharmakodynamische Studien oder Studien zur Beurteilung der Nieren- und Darmfunktion. Die Verwendung des Stoffwechselkäfigs bietet viele Vorteile, dazu gehören die tierindividuelle Überwachung der Wasser- und Futteraufnahme sowie die Sammlung von Urin und Kot. Dennoch ist das Wohlergehen der Mäuse durch die Einzelhaltung, das Fehlen von Material zur Käfiganreicherung (*Enrichment*), den Gitter-Boden des Käfigs und somit die Abwesenheit von Einstreu, stark beeinträchtigt. Die Auswirkungen auf den metabolischen Phänotyp der Maus während der Haltung im Stoffwechselkäfig sind noch nicht ausreichend erforscht. Ziel dieser Arbeit war es zu untersuchen, (1) ob das allgemeine Stressniveau und der Kältestress im Stoffwechselkäfig reduziert werden können und (2) ob die Energieressourcen der Mäuse während der Haltung im Stoffwechselkäfig effektiver geschont werden können.

Diese Studie untersuchte den Vergleich von zwei verschiedenen Stoffwechselkäfigtypen. Die Konstruktion des Innovativen Stoffwechselkäfigs (IMC) weist wesentliche *Refinement*-Maßnahmen auf und wurde in der Forschungswerkstatt am Deutschen Institut für Ernährungsforschung (DIfE) angefertigt, wobei der Stoffwechselkäfig des Herstellers Tecniplast GmbH (TMC) kommerziell erhältlich ist. Die Käfigkonstruktion des IMC weist Verbesserungsansätze auf, wie z.B. ein verringertes Käfigvolumen, eine angeschrägte Futter- und Wasserversorgung sowie eine eingefügte Ruheplattform auf dem Gitterboden des Käfigs, um das Wohlbefinden der Mäuse während des Versuchs zu steigern. 25 weibliche und 25 männliche, 10 Wochen alte C57BL/6J-Mäuse wurden für jeweils 24 h entweder im IMC oder im TMC gehalten. Nach einer sechstägigen Ruhephase wurde diese Aussetzung wiederholt. Um allein die Auswirkungen der Isolationshaltung zu untersuchen, wurden die Mäuse einzeln in Kontrollkäfigen mit Einstreu und standardisiertem *Enrichment* gehalten. Das *Enrichment* Material beinhaltete 1 Baumwoll-*Nestlet*, 2 Papiertücher, 1 Beißholz und 1 Papphäuschen. Das Wohlbefinden, das Verhalten der Mäuse und spezifische Stoffwechselfparameter wurden im Laufe des zweiwöchigen Experiments evaluiert. Nach Abschluss der jeweiligen Versuchsgruppe wurden die Mäuse euthanasiert, die Organe entnommen und die Gewebe- sowie die Urin- und Kotproben im Labor analysiert.

Der Zustand des Fells, der Gesichtsausdruck und der Kältestress deuteten darauf hin, dass das Wohlbefinden der Mäuse durch die Haltung im Stoffwechselkäfig beeinträchtigt war. Eine Verschlechterung des *Fur Scores* war für beide Geschlechter sowohl im TMC als auch im IMC im Vergleich zu den Kontrollen zu verzeichnen. Die *ear position scores* der angewendeten *Mouse Grimace Scale* waren für beide Geschlechter nach der zweiten Aussetzung in den TMC signifikant höher als im IMC. Die Käfigtemperatur im TMC war signifikant niedriger während der ersten Aussetzung der weiblichen Mäuse im Vergleich zum IMC. Dies galt auch für die Männchen während beiden Aussetzungen.

Zwei verschiedene Verhaltenstests - der *Elevated Plus Maze* (EPM) und der *Open Field Test* (OFT) - wurden direkt im Anschluss an die beiden 24-stündigen Isolationshaltungen durchgeführt, während Videos von den Mäusen im Laufe der beiden 24-stündigen Haltungszeiträume aufgezeichnet wurden. Alle Mäuse, unabhängig vom getesteten Käfigtyp, zeigten allein durch die Einzelhaltung und/oder die neuartige Umgebung der Testarenen Stressverhalten. Die Weibchen und Männchen verbrachten die längste Zeit in den geschlossenen Armen des EPM was auf ein erhöhtes Angstverhalten der Mäuse hindeuten kann.

Eine entsprechend gering ausgeprägte Explorationsbereitschaft der Mäuse wurde im OFT suggeriert, wo die mittlere Zone von beiden Geschlechtern am häufigsten aufgesucht wurde. Für die Videoanalysen wurde ein exklusives Ethogramm vordefiniert, das neben drei weiteren Verhaltenskategorien "Fluchtverhalten" und "andere Aktivitäten" inkludierte. Das Fluchtverhalten umfasste springen, rennen, nagen an Gitterstäben, kratzen und aufbäumen, während andere Aktivitäten trinken, fressen, urinieren und Defäkation beinhalteten. Für beide Geschlechter konnte ein signifikant erhöhtes Fluchtverhalten im TMC im Vergleich zum IMC während der ersten Aussetzung und bei den Weibchen auch während der zweiten Aussetzung detektiert werden. Andere Aktivitäten wurden wiederum bei Mäusen, die im IMC gehalten wurden, signifikant häufiger als im TMC beobachtet. Dies ging mit einer erhöhten Futterraufnahme im IMC im Gegensatz zum TMC bei männlichen Mäusen während der ersten und bei beiden Geschlechtern während der zweiten Aussetzung einher.

Die Neurotransmitter Serotonin (SRT) und Dopamin (DA) wurden in fünf verschiedenen Gehirnarealen quantifiziert, wobei die DA-Metabolite 3-Methoxythyramin (3-MT) und 3,4-Dihydroxyphenyl-essigsäure (DOPAC) in den Analysen inbegriffen waren. DOPAC war bei weiblichen Mäusen nach der Aussetzung im IMC im Vergleich zu den Kontrollen im *Caudate putamen* signifikant erhöht und ist tendenziell im *Nucleus accumbens* angestiegen. Bei männlichen Mäusen waren die DOPAC-Konzentrationen im *Hypothalamus* nach der IMC- im Vergleich zur TMC-Haltung und zur Kontrollkäfighaltung signifikant erhöht.

Als physiologischer Stressmarker wurde die Konzentration der fäkalen Corticosteron-Metabolite (FCM) und des glucuronidierten Corticosterons im Urin quantifiziert. Die FCM-Konzentrationen von weiblichen und männlichen Mäusen waren während der beiden Aussetzungen im TMC signifikant höher als bei Mäusen, die im Kontrollkäfig gehalten wurden. Bei Betrachtung der renalen Corticosteronausscheidung wurden signifikant höhere Mengen an Corticosteron von den Weibchen im TMC ausgeschieden als während der IMC-Aussetzung.

Die erhobenen Stoffwechselfparameter zeigen, dass der metabolische Phänotyp der Mäuse durch die Aussetzung in den TMC stärker beeinflusst wird als durch den IMC. Der Verlust an Körpergewicht (BW) und Magermasse (LM) war für weibliche als auch für männliche Mäuse während der Aussetzung in den TMC höher als in den IMC. Analysen von Lebergewebeproben zeigten vor allem höhere Glykogenwerte bei Mäusen, welche im IMC gehalten wurden, im Vergleich zum TMC auf. Die stärkere Reduzierung von Energiespeichern im TMC ist auf eine erhöhte Aktivität der Mäuse während der TMC-Aussetzung zurückzuführen, die sich beispielsweise in einem verstärkten Fluchtverhalten zeigte.

Zusammenfassend zeigen die Ergebnisse dieser Dissertation das hohe Stresspotential für die Mäuse während der Haltung im Stoffwechselkäfig auf und wie der IMC zu einer quantifizierbaren Belastungsreduzierung bei Labormäusen beitragen kann. Insgesamt belegen die erhobenen Daten deutlich, dass der IMC, im direkten Vergleich zum TMC, einen geringeren Einfluss auf den metabolischen Phänotyp der Mäuse hat. Die Einführung des IMC stellt den ersten Versuch dar, eine Stressreduktion bei Labormäusen durch die aktive Implementierung von *Refinement*-Maßnahmen bei der Verwendung von Stoffwechselkäfigen zu erzielen. Der IMC unterstützt somit eine tierschutzgerechte Datenerhebung, wenn auf den Einsatz von Stoffwechselkäfigen im Rahmen bestimmter wissenschaftlicher Fragestellungen nicht verzichtet werden kann.

1. Introduction

1.1 The 3R-Concept and scientific validity of laboratory animal research

In 1959, William Russell and Rex Burch formulated the principles of the 3R, which apply to the use of animals for research purposes such as safety and drug testing, basic research or disease models. The 3R represent an internationally applied ethical framework that should be urgently applied when performing experiments on animals. The first “R” stands for replacement, which describes the consideration of alternative methods instead of conducting an animal study. Alternatives include *in vitro* experiments, human testing, or *in silico* models. The use of a different animal species lower in the phylogenetic scale referred to as “relatives replacement” also provides an option. If it is not possible to answer the scientific question with an alternative to animal experimentation, the second “R” should be implemented, which describes the reduction of animal studies and the number of utilized animals due to precise statistical calculations beforehand or reuse of animals. The following issue is to be included: if too few animals are used, there is a risk that these are reasonlessly applied because ambiguous data are generated. Therefore, the gain in knowledge should be as large as possible with a simultaneous reduction of animal numbers within the feasible range [1–4].

Refinement represents the third “R”, which aims to accomplish the reduction of the severity of procedures to the possible minimum by concurrently enhancing animal welfare to the possible maximum [1,2,4]. This, of course, solely includes indispensable animal testing. From this point of view, the expected gain in knowledge should justify the stress on the animals in the experiment. In addition, the selected animal model as well as applied experimental methods should be adequate for the testing of the scientific question (construct validity) [3]. In animal experimental research, there is a need to ensure the scientific validity of results and, at the same time, responsible use of animals. Importantly, high animal welfare standards are a requirement for high-quality research to ensure data validity as well as reproducibility [4]. The most relevant and decisive goal at the moment is the implementation of refinement in experiments that cannot be replaced by alternative methods at the current state of the art. Accordingly, legal documents in Europe and the U.S. are guided by the 3R-principle, focussing on animal welfare protection and the assertion of research integrity while minimizing distress and pain of the animals [1,4–6]. Aspects that contribute to the protection of animal welfare include preserving a good health status, limiting negative states while promoting positive states and ensuring the freedom to exert species-specific behaviors [1].

Refinement measures can be applied in a number of different areas that range from breeding and animal husbandry to experimental performance as well as euthanasia. Improved anesthesia and analgesia procedures are essential in this regard. Metabolic cage housing for experimental usage is often discussed as an animal welfare relevant burden for laboratory mice. Therefore, the scientific reliability and quality of the data collected during metabolic cage restraint as well as shortly before and after the restraint therein might be affected. The central question to ask is indeed: do we measure the stress, perhaps even the pain, of mice induced by the restraint in metabolic cages or the effect of the experimental treatment? In the context of this thesis, therefore, the refinement of metabolic cages for the application with mice was addressed. Internal validity refers to ensuring a causal relationship between the experimental treatment and the variation in the treatment effect [3,4]. As the stress level of mice is increased during restraint in metabolic cages, and the internal validity of data collected during the experiment may be affected, the potential impact on relevant physiological systems to assess the stress level in mice was investigated [7,8].

Here the focus was on the hypothalamic-pituitary-adrenocortical axis with the excretion of corticosterone into the urine and feces, heat generation *via* uncoupling protein 1 in brown adipose tissue, the dopaminergic and serotonergic system in specific brain areas and the hepatic glycogen metabolism. Animal welfare, behavior, and metabolic parameters of mice were also assessed in the course of the experiment. External validity defines the degree of generalization of experimental results beyond the specific conditions of the current experiment, e.g. to other mouse strains and laboratories with different experimental conditions [3,4]. Taking into account the criteria for external validity, both sexes of C57BL/6J mice were used for the present experiments and experimental periods were divided into several independent replicates. The active application of the 3R-concept in experiments parallels the scientific validity in many ways. In the process of designing experiments conflicts between the implementation of the 3Rs, application as well as refinement of specific procedures such as the metabolic cage restraint, might occur in order to enhance scientific validity. However, the objectives of ensuring the highest possible animal welfare standards should not be lost out of sight, in the interest of animals and science.

1.2 The metabolic cage

The metabolic cage possesses a primarily functional construction for the purpose of urine and feces collection as well as the monitoring of food and water consumption [7–12]. The metabolic cage can be applied in biomedical studies where the course of specific biological parameters in the experimental animal is to be analyzed [7,8]. In detail, pharmacokinetic and pharmacodynamic studies, the study of renal and intestinal function as well as input and output studies are examples for its application field [7,8,10,12]. Within the frame of toxicological pharmacokinetic studies, metabolic cages are applied for the performance of absorption, distribution, metabolism, and excretion studies [10]. Metabolic cages can be utilized for multiple species including rats, mice, cats, dogs, goats, rabbits among others [7–12]. They differ in size and exact construction based on the species restrained therein. Many different manufacturers also construct metabolic cages for the same species that differ from one another.

The induction of stress in mice by the restraint in metabolic cages is often discussed and is to be considered multifactorial, such as social animals like mice are kept isolated. Their natural behavioral repertoire is restricted due to the barren cage environment lacking bedding, nesting, enrichment materials, and conspecifics; the smaller-than-usual living space area; and the metal grid which serves as cage floor [7,11–13]. Grid flooring is necessary for the collection and clean separation of urine and feces, but it is dolorogenic in the paws [7,11,13,14]. As nesting material is absent in metabolic cages to avoid contamination of feces and urine, mice are deprived of thermoregulation in the form of nesting at standard room temperatures (20-22°C) maintained in the animal husbandry [2]. Convective heat loss is facilitated by the grid floor since metal is thermally conductive, but also because the cage floor is open and provides neither nesting nor bedding material [9,13]. The animals are further kept isolated and cannot huddle with conspecifics to stay warm [11]. Sahin *et al.* (2022) [13] even suggested that the metabolic cage is a suitable model for studies of social isolation stress in small rodents rather than for metabolic studies. The novel environment of the metabolic cage after switch from the home cage depicts another stressor [9,12]. Based on the previously outlined stress factors, the metabolic cage environment is expected to have an impact on animal welfare and affects the behavior as well as physiology of the animals restrained therein. The nature or magnitude of this effect emanating from the metabolic cage has not been fully characterized so far.

Stechman *et al.* (2010) [15] intended to establish plasma and urinary reference ranges specifically for metabolic cage restraint in three mouse strains: C3H, BALB/c, and C57BL/6J mice. Female and male mice of each mouse strain were kept in the metabolic cage for 7 d. After 3 to 4 d, stable values for urinary output, body weight, and dietary intake were obtained. Within the frame of another study conducted by Kalliokoski *et al.* (2013) [7], male BALB/c mice were restrained in the metabolic cage for three weeks. Their main research question entailed if male mice were able to habituate to metabolic cage restraint. An elevated activity of the hypothalamic-pituitary-adrenocortical (HPA) axis, increased oxidative stress and overall metabolism resulted from the metabolic cage restraint for three weeks. Hoppe *et al.* (2008) [9] were studying the course of mean arterial pressure and heart rate in female and male C57BL/6J/129sv mice during restraint in the metabolic cage. Mean arterial pressure and heart rate of females and males were significantly increased compared to baseline during the first hours in the metabolic cage, 7 h and 11 h, respectively. Tachycardia was sustained based on 24 h averages of heart rate, which remained elevated during the 48 h restraint in the metabolic cage. It is important to mention that in the study of Hoppe *et al.* (2008) [9] mice were acclimatized to the metabolic cage for 24 h prior to experiment start, which agrees with the study outcome of Kalliokoski *et al.* (2013) [7] that mice do not seem to habituate to metabolic cage restraint, not even after three weeks.

Guidelines for metabolic cage use

The European Directive 2010/63/EU addresses the 3R-concept, which shall be considered in the evaluation of scientific projects [2,5]. Specific guidelines for metabolic cage use are included in the European Directive 2010/63/EU and the expert information of the Swiss Confederation for “the restraint of laboratory animals in metabolic cages and metabolism boxes 2.06”. Both regulations define four severity categories. According to the EU Directive 2010/63/EU the following severity categories are applied: “non-recovery”, “mild”, “moderate”, and “severe”. In article 25 of the Swiss animal testing regulation the severity categories 0, 1, 2, and 3 are specified while 0 defines no burden for the animal and the category for “non-recovery” as in the Directive 2010/63/EU does not exist. The severity categories 1, 2, and 3 can be considered analogous to “mild”, “moderate”, and “severe” [5,16–18].

According to the Directive 2010/63/EU, restraint in metabolic cages is assigned to the respective severity categories based on the period of restraint [5]:

- Mild: short-term (< 24 h) restraint
- Moderate: moderate restriction of movement over a prolonged period (up to 5 d)
- Severe: severe restriction of movement over a prolonged period.

The Swiss Confederation states that the duration of metabolic cage restraint should be kept as short as possible and therefore more frequent, brief restraints are favored. Furthermore, the restraint in metabolic cages should be limited to a maximum of 7 d and appropriate recovery periods must be incorporated into the study design. Minimal recovery periods for an animal experiment with the severity category “mild” (severity category 1) after restraint in metabolic cages are defined as follows [16]:

- Up to 8 h: 16 h
- Over 8 h up to 24 h: 6 d
- Over 24 h up to 4 d: restraint period plus 7 d
- Over 4 d up to 7 d: restraint period plus 14 d.

If the severity category of the animal experiment is higher graded, including the severity categories 2 and 3, the resting period should be prolonged appropriately. The Directive 2010/63/EU (section B: species-specific section) gives details about the adequate space that shall be provided for mice during the study independent of the applied cage type. For mice in stock and during procedures the following information is depicted [5]:

Table 1. Recommendation of minimum enclosure size [cm²], floor area per animal [cm²], and minimum enclosure height [cm] for mice in stock and during procedures depending on body weight [g] [5].

Body weight [g]	Minimum enclosure size [cm ²]	Floor area per animal [cm ²]	Minimum enclosure height [cm]
up to 20	330	60	12
over 20 to 25		70	
over 25 to 30		80	
over 30		100	

The Swiss guideline includes recommendations on minimal floor area and height specifically for the restraint of mice in metabolic cages [16]:

Table 2. Recommendation of minimum floor area [cm/cm²] and height of metabolic cages for restraint of mice [16].

Floor area	Remark	Height
∅ 12 cm	Maximum restraint: 2-3 d. Recommendation: grid all around metabolic cage for climbing opportunity.	Animals cannot jump out of cage, but rearing is possible.
120 cm ²		
310 cm ²		
∅ 20 cm	-	

The Swiss expert information for restraint in metabolic cages goes into more detail than the European Directive 2010/63/EU. First, the definition and the purpose for utilization of metabolic cages is given. Second, it is specified which details should be included in animal test applications, such as the dimension of applied metabolic cages and acclimatization time. Third, the Swiss guideline also goes into detail about climatic conditions during metabolic cage restraint by emphasizing that the restricted mobility and open grid floor can either induce loss of body temperature or accumulation of heat production. Fourth, the time periods for metabolic cage restraint, but also the recovery periods, are more clearly defined. The term “prolonged period” for the “severe” category remains undefined in the Directive 2010/63/EU [5,16,18].

The acoustic, olfactory, and visual contact among conspecifics should be ensured at all times during metabolic cage restraint, because mice and rats are social animals [16,19]. In the case of single housing of a social species, the European Directive of 2010/63/EU emphasizes that this husbandry system should be considered as an exception. Solitary husbandry is only optional, which applies to a certain experimental design, such as metabolic cage restraint, or if the animals are aggressive and/or incompatible with their conspecifics [1,5].

The U.S. Guide for “the Care and Use of Laboratory Animals” delineates that a long-term individual restraint in metabolic cages may elicit chronic distress [6]. The Australian Animal Research Review Panel emphasizes in their “Guidelines for the Housing of Rats in Scientific Institutions” that rats should be acclimatized to metabolic cages prior experimental testing. Metabolic cages should further be enriched with e.g. a nest box and a resting platform consisting of a solid floor [19].

The metabolic cage applied for dogs and non-human primates was recently refined within a cooperation project tackling the single housing issue for toxicological absorption, distribution, metabolism, and excretion studies. Group or paired housing of dogs and non-human primates was realized besides further modifications of the cage construction. The metabolic cages can also be temporarily divided for sampling of individual animals. First observations indicated that animals restrained together in metabolic cages were calmer due to the stress reduction. The absence of animal-specific data generation was not considered a disadvantage because the enhancement of animal welfare during metabolic cage restraint was deemed as priority [10]. Advances in refinement of metabolic cage housing conditions for multiple laboratory species have great potential. There is a high demand for research in this area, because international regulatory guidelines require metabolism and toxicity studies in which animals and often metabolic cages are still used.

1.3 Behavioral phenotyping and animal personality

The study of behavior is crucial, because it connects many disciplines such as ecological and physiological questions, but also for behavioral phenotyping of genetically modified mice or characterization of behavioral comorbidities in disorders [20–22]. Each animal species has a species-specific locomotion, posture and vocal expression, which can be compiled in an ethogram. An ethogram describes a list of species-specific behaviors that detail particular behavioral patterns and their function. Ethograms can be divided into experimental and species ethograms while the experimental ethogram is an extract of all known species-specific behaviors tailored to the research question [23].

Due to their high fecundity and breeding efficiency, omnivorous diet and high mutation rates, mice are considered to be highly-adaptive [24]. Their sense of smell is highly developed and mainly defines their actions, which is termed macrosmatic. The organizational structure of the murine olfactory system is far more complex than scientists anticipated, four anatomically separated olfactory subsystems were found to detect distinct groups of sensory stimuli. The vomeronasal organ represents one of the olfactory subsystems, and importantly, a strict categorization of this olfactory organ as a specialized pheromone detector would be simplistic [25]. Inputs to the vomeronasal system are obtained from the vomeronasal organ in the septal walls of the ventral nasal meatus and this system targets the accessory olfactory bulb [25–27]. The detection of pheromones aids to identify a reproduction partner or to receive information about the hormonal and social status of conspecifics (territorial and aggression behavior) [25]. Wild mice live in family groups or solitarily, the latter mainly applies for males. Concerning their locomotion abilities, mice move quickly in short stages, they are proficient climbers, swimmers, jumpers and also express burrowing behavior [23]. The analysis of the animal’s locomotor activity is often applied as a tool for animal welfare monitoring.

Behavioral analyses are generally applied in order to associate gene-, environmental- or stress-induced changes with the animal's phenotype. Two different approaches for behavioral studies are available. The first represents a battery of numerous behavioral tests, which are arena- or maze-based assays, while the second focuses on home-cage behavior. Importantly, the performance and validity of behavioral tests can be challenging for several reasons. Firstly, laboratory rodents are crepuscular animals, but the testing is often performed in the light period since this time frame represents the working hours of animal care takers and scientific staff. Secondly, the rich behavioral repertoire of the animals cannot be reproduced during behavioral testing and solely indicates a snap shot. Thirdly, the transfer of animals into the new environment of a testing arena as well as the experimenter's influence should not be underestimated. These drawbacks can be avoided by investigating the animals in their home-cage, although other disadvantages might come up. These implicate the position of the camera(s), a limited view into specific cage areas such as the nesting area or the often necessary single housing of animals. Home-cage based behavioral phenotyping can be conducted without experimenter-animal-interactions on a continuous time scale. Home-cage activity and behavior can be analyzed in various ways including a video based and/or infrared based system, radiofrequency identification or a sensor plate system [21,28].

Differences in the plasticity of behavior as well as behavioral differences in relation to environmental influences are existent among animals. The concept of animal personality was therefore established describing consistent individual behavioral differences that vary among conspecifics of the same population, but are stable concerning the respective individual. Of course, behavioral traits are susceptible to change since animals need to adapt to their surrounding environment, which will be discussed in chapter **1.3.1** Behavioral response and adaptation to a stressor. In the context of animal personality, a distinction is made between the behavioral type and behavioral syndromes. The behavioral type entails a characteristic that is time- and context-independent and provides behavioral stability of the individual.

Behavioral syndromes are defined as characteristics of a population that maintain behavioral consistency among individuals belonging to the same population [29]. Animal personality in the narrow sense focuses on five repeatable behavioral domains: general activity, exploration, boldness, aggressiveness, and sociability [20,29]. These behavioral traits are commonly analyzed within the frame of behavioral testing, e.g. home cage (general activity), novel environment (exploration), reaction to a conspecific (sociability), in order to extrapolate the personality of the tested animal. The open field test by way of example was proven to reflect the behavior of analyzed animals in nature, at least to a certain degree. A relationship between personality traits that are fitness-related and the resting metabolic rate was further suggested in a context-dependent manner [20,30]. Animal energetics describe the energy costs of particular biological processes such as physical activity. Energy expenditure is therefore suggested to be higher if animals are e.g. more physically active, have a distinct exploratory drive, and are more aggressive. Importantly, physical activity needs to be accurately analyzed including i.a. duration, frequency, speed or intensity. For male mice it was demonstrated that the time spent moving in the home cage was positively correlated with the basal metabolic rate (BMR) [20,31]. However, a comprehensive mechanistic explanation for individual variation in the BMR was not found as yet [20].

1.3.1 Behavioral response and adaptation to a stressor

Stress can be defined as a state in which homeostasis is threatened. Mechanisms are therefore activated with the aim of restoring homeostasis, which is understood as a stress response. This stress response includes behavioral adaptation such as increased analgesia, enhanced awareness or improved cognition [32,33]. Importantly, stress is not inherently detrimental for an animal, as stress is a part of life, except if the biological cost is becoming too high to cope with the stressor and to also protect the animal from the source of stress. Distress can result from the presence of both pain and stress, which has an effect on biological processes and can consequently compromise experimental results. Therefore, the fundamental question to ask is: At which stage of an experiment is nonthreatening stress becoming distress? It is thus highly relevant to be able to distinguish between stress and distress for the maintenance of animal welfare.

Nevertheless, stressful experimental conditions should be avoided or at least reduced to the possible minimum. To emphasize, distress can also develop in the absence of pain as long as the stress factor is present, termed as “nonpain” distress [33]. After the stressful stimulus is perceived by the animal, a stress response is elicited including one or more of the four major defense systems: behavior, autonomic nervous system, neuroendocrine system or immune system. In case of a short exposure to the stressor, the stress response only requires a small portion of available biological resources and thus, the biological cost has little to no effect on the animal’s welfare and the induction of distress is unlikely. But if the stressor is more intense, persistent, or multiple stressors are combined, resources might need to be obtained from other biological functions. This could result in an impairment of animal welfare and distress induction, because of the increased biological cost for the generation of a stress response. At that point, the normal functioning of biological processes is disrupted, the animal enters a prepathological state and animal welfare is no longer preserved. Many different stresses may challenge biological resources and eventually the development of abnormal behavioral patterns is anticipated [33].

The main aim of each individual pursues the optimal adaptation to environmental conditions in order to reach a high biological fitness. The species-specific behavioral repertoire was therefore selected in a natural environment during evolution, but not in an artificial laboratory. The modification of behavior matching the laboratory environment represents a logical consequence. Konrad Lorenz defines a modification as every permanent change in an organism caused by external influences during the individual’s course of life [34]. If a mouse is now transferred out of its home cage, already representing an innovative environment in the evolutionary sense, into a novel surrounding for a short period of time, prolonged behavioral modifications are even more difficult to assess. A detailed behavioral characterization of short and prolonged experimental procedures is thus essential. In case animals cannot cope with environmental challenges the quality of their life is reduced.

Three classes of problems were defined by Fraser *et al.* (1997) [35], which might occur if the adaptation of an animal does not cover all environmental requirements. This classification can also be applied to mice restrained in the metabolic cage environment. (1) The animal possesses adaptations that have no significant function within the innovative environment. This may result in unpleasant subjective experiences even though it is not necessarily associated with the disturbance of biological functions. An example could be the provision of food *ad libitum* in the laboratory, which definitely satisfies the animal’s nutritional needs, but does not promote foraging behavior.

During animal experiments, food is commonly provided *ad libitum* to mice regardless of the cage type in which they are housed, thus this also includes metabolic cage restraint. (2) The animal does not have an appropriate adaptation to counteract the environmental challenges, which could result in functional problems, but an impact on subjective feelings is not necessarily present. Male mice housed in groups cannot act out their territorial behavior, because of space problems or the absence of enrichment material for drawing of boundaries. Concerning metabolic cages, mice are single housed, enrichment material is absent, and the space available is severely limited. (3) The animal possesses adaptations that are suitable to the kind of environmental challenges, but prove to be inadequate in this particular case. Mice are building nests to stay warm in case room temperatures are below their thermoneutral zone. If nesting material is lacking or not enough material is provided, mice cannot appropriately adapt to their environment. Importantly, nesting material is absent in metabolic cages to prevent the contamination of collected urine and fecal samples. Therefore, if an animal cannot cope with the environmental challenges over a prolonged period of time might result in behavioral adaptations [35].

Individual variation in natural populations concerning stress response mechanisms on a neural and endocrine basis is often addressed, but many questions remain. The physiological state, age, and genetics were suggested as modulators for intra-animal differences in the stress response, which can be controlled for in laboratory animals. The hypothalamic-pituitary-adrenocortical (HPA) axis was suggested as a candidate system among other systems to mediate the interconnection of energy expenditure and personality traits. The HPA response by quantification of glucocorticoids such as corticosterone can be applied as a stress marker. Nonetheless, it was demonstrated that not all stressors elicit a HPA response and that the HPA axis responds to threatening as well as nonthreatening stimuli. The animal's condition is often assessed based on behavioral approaches since it represents the least invasive method for stress monitoring. Reliable behavioral changes should furthermore be correlated with biological changes in order to be able to make a well-founded statement on the stress level of the investigated animals. Behavioral indicators for animal welfare include i.a. grooming, activity, aggression, facial expression or appearance. Physiological parameters, which can be utilized for the assessment of animal welfare, include body temperature, weight loss or blood-cell count while biochemical indicators represent corticosteroids, glucagon or catecholamines [20,33].

1.3.2 Requirements for a species-appropriate husbandry

The laboratory mouse stems from many subspecies of the wild mouse *Mus musculus* [36]. Wild mice are crepuscular, flight animals, and prefer an environment with shielding structures over an exposed, open terrain [37]. This is also reflected in the behavior of the laboratory mouse. Concerning the social behavior of wild and laboratory mice, the territoriality of both sexes is more pronounced in males resulting in a higher intolerance towards one another. A despotic hierarchy is established among males in the laboratory due to the lack of space while females build stable groups within cages [38]. Therefore, group-housing of female mice is encouraged since mice are social animals and the isolation stress is considered to be higher than for males. Single housing of male mice often represents the only reasonable husbandry system, because of their potential for aggression, which can further depend on the mouse strain, age, and previous experience of males [39]. Interestingly, the patterns of behavior observed in the wild *Mus musculus* can be reproduced in the laboratory mouse whereby the induction and frequency of specific behavioral patterns varies among different mouse strains.

The housing conditions of animals can also represent a latent source of stress. Animal housing should be arranged in a way that the performance of the natural behavioral repertoire is to the greatest extent possible. Enrichment of the cage environment with nesting materials and refuges among others is crucial to promote exploratory and active behavior of mice [22,40]. Even though environmental enrichment of cages is considered as beneficial, no consensus on standardized enrichment considering the type and quantity does exist [5,22,41]. To date, it is advised to keep mice in groups, to provide nesting and bedding material, and the addition of a refuge is considered an option. Maintaining the comparability of mouse physiology and experimental data is often discussed in case further enrichment is introduced, but in some cases a variance in results could be favored to enhance the universal validity [38]. In addition, different mouse strains, but also females and males of the same strain, appear to react differently to environmental enrichment and that the type of enrichment could further matter [22]. After all, the enrichment of the cage with nesting material represents an unequivocal improvement of housing conditions since nest-building behavior as well as the choice of the microclimate is enabled [41]. The duration of exposure to the enrichment material is decisive for the stimulation of behavioral effects and was suggested to be optimal in the range of three weeks [40].

Behavioral analyses of mice possessing the same genotype in different laboratories showed decisive differences despite standardization of experimental and environmental conditions. It was inferred that the genetic strain interacts with the laboratory environment and that the influence originating from humans should not be neglected due to idiosyncratic odor cues. In a study conducted by Lewejohann *et al.* (2006) [22], no differences in path length regarding the Open Field Test were detected between female C57BL/6N mice kept in enriched (plastic inset and wooden climbing frame) and standard cages. This was true for the six different experimenters and the two different laboratories. During Elevated Plus Maze Testing for one of the six experimenters it could be observed that mice housed in standard cages were less anxious than mice housed in enriched cages. This was expressed as an increase in the proportion of open arms entered compared with total arm entries. Pooled data of both housing conditions aside from the different experimenters and laboratories, however, did not reveal any significant differences in locomotor (Open Field Test) or anxiety-related (Elevated Plus Maze) behavior.

It is generally accepted that environmental enrichment has the potential to reduce anxiety and depression in laboratory animals. In a study conducted by Leger *et al.* (2015) [40], male Naval Medical Research Institute mice were either housed in enriched cages (comprising objects of different shapes, sizes, colors, textures, materials plus a running wheel) or standard cages (comprising nesting material and a cardboard house). Males housed in enriched cages were less active after one week as opposed to standard conditions. After three weeks, time and entries into open arms of the Elevated Plus Maze were significantly higher for male mice kept in enriched cages. Interestingly, serotonin concentrations of mice kept in enriched cages were concomitantly significantly higher in the frontal cortex after three weeks suggesting a relationship between behavioral and neurobiological effects. The two study results [22,40] emphasize the variety of murine reactions to environmental enrichment, which are clearly context-dependent.

1.4 Relevant physiological systems for stress assessment of mice while in the metabolic cage

The barren environment and mainly functional construction of the metabolic cage poses a high stress potential for mice during the restraint therein. Besides the potentially elicited behavioral responses in mice, physiological correlates of animal welfare are addressed here. The aim is to investigate whether the restraint of mice in metabolic cages has an effect on adrenal gland, brown adipose tissue, brain, and liver physiology and whether the chosen physiological measures coincide with behavioral changes.

1.4.1 The hypothalamic-pituitary-adrenocortical axis

The hypothalamic-pituitary-adrenocortical (HPA) axis is a complex regulatory circuit of the endocrine organs *hypothalamus*, pituitary gland, and adrenal cortex. “The HPA axis plays a vital role in adaptation of the organism to homeostatic challenge” [42]. The maintenance of the activity of this axis is equally important for humans and mice where an increase in HPA axis activity results in an elevated release of glucocorticoids from the adrenal cortex including the hormones cortisol (humans) or corticosterone (mice). Both stressed and unstressed circumstances of life affect HPA axis activity. The unstressed condition refers to the daily rhythm of glucocorticoid secretion, which is highest at the beginning of the waking cycle. As opposed to this, stressful conditions define either a “real” or “predicted” stimulus that has the potential to unbalance the homeostasis. “Real” stressful stimuli include actual threats to homeostasis perceived through e.g. somatic sensory pathways such as pain while “predicted” stressful stimuli describe e.g. innate, species-specific programs such as the recognition of danger related to open spaces.

In the case of metabolic cage restraint, “reactive” responses to a “real” stressor could include somatic pain (grid cage floor), cold (absence of nesting material), and humoral homeostatic signals such as glucose status (reduced food intake). “Anticipatory” responses to “predicted” stressors could comprise restraint stress (metabolic cages possess a smaller cage area than type II cages). To maintain an optimal level of HPA axis responsiveness is crucial since it was suggested that mental illness is associated with either hyper- or hyposecretion of glucocorticoids. Hypersecretion of glucocorticoids accompanies long-term metabolic disease states. It is important to emphasize that the generation of an HPA response is energetically costly [42,43].

The focus is set on corticosteroid secretion induced by a stressful condition. The perception of a stressor by somatic nociceptors, visceral afferents or humoral sensory pathways induces an activation of the *nucleus paraventricularis* (PVN) in the *hypothalamus* (HTM) (see **Figure 1**). The PVN receives input from catecholaminergic as well as non-catecholaminergic neurons originating in the area of the nucleus of the solitary tract among others. The effects of norepinephrine (NE), a catecholaminergic neurotransmitter, are suggested to be mediated by glutamatergic interneurons. Serotonergic systems also affect HPA activity while serotonin (SRT) exerts its effects mainly *via* the PVN 5HT_{2A} receptor. Serotonergic innervation of the PVN originates from the dorsal and median raphe nucleus. Regions in the brain lacking an intact blood-brain barrier, such as the organum vasculosum of the lamina terminalis, also relay information to the PVN about blood-borne signals.

Taken together, the PVN in the HTM is well positioned to receive input from multiple brain areas as well as blood- and cerebrospinal fluid-borne factors for integration of the stress response. This hypothalamic nucleus possesses multiple receptor types including androgen, estrogen, prostaglandin receptors among others and is highly vascularized. Cells within the PVN produce and secrete the corticotropin releasing hormone (CRH), which reaches the anterior lobe of the pituitary gland *via* the infundibulum (pituitary stalk) and stimulates corticotrope cells [42,44].

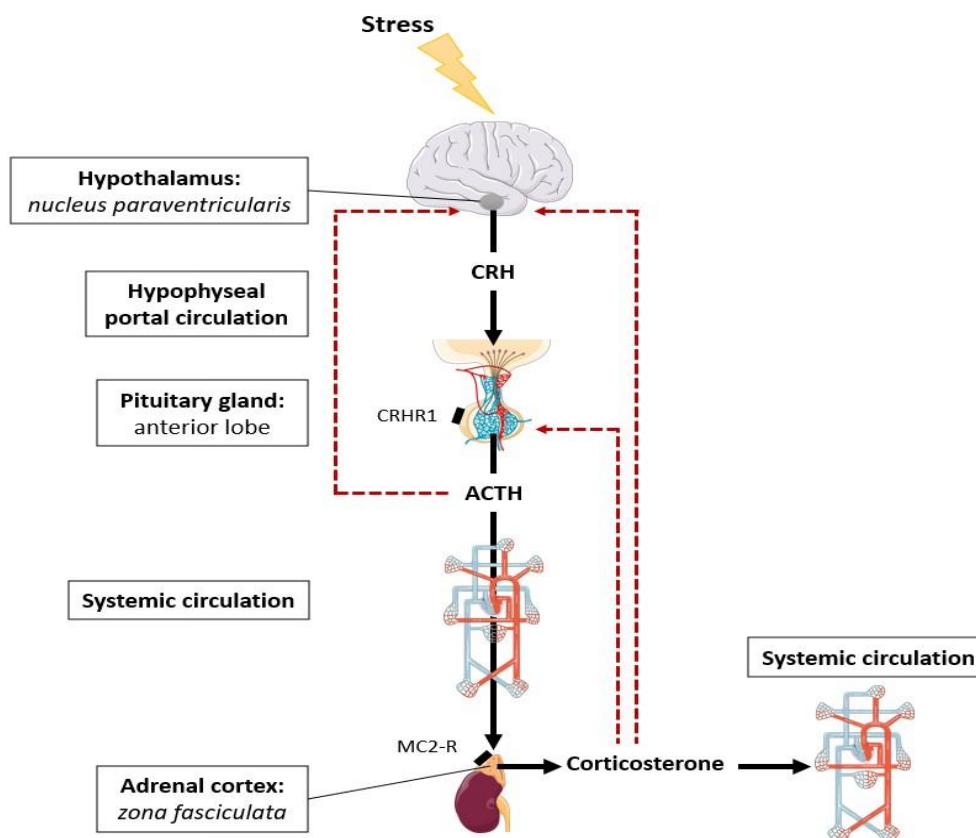


Figure 1. The hypothalamic-pituitary-adrenocortical (HPA) axis schematically displayed. In response to a stressor, the nucleus paraventricularis (PVN) within the hypothalamus (HTM) synthesizes and secretes the corticotropin releasing hormone (CRH). CRH reaches the anterior lobe of the pituitary gland via the hypophyseal portal vessels and binds to the CRH type 1 receptor (CRHR1). In the next step, adrenocorticotropin (ACTH) is released from the anterior pituitary into the systemic circulation. ACTH then binds to the melanocortin type 2 receptor (MC2-R) located on the adrenal cortex. Glucocorticoid synthesis is thereby stimulated, such as corticosterone, the main stress hormone of rodents. Glucocorticoids are synthesized in the adrenal zona fasciculata and secreted into the systemic circulation, where they regulate numerous physiological processes. The red lines indicate the glucocorticoid-dependent inhibition of HPA axis activity by binding to specific receptors located in the brain, but also in peripheral tissues. Modified after [32,42,45,46].

The secretagogue CRH binds to the CRH type 1 receptor on the pituitary gland, stimulates adenylyl cyclase, and the cyclic adenosine monophosphate (cAMP) pathway is subsequently activated. The synthesis and release of adrenocorticotropin (ACTH) into the systemic circulation is thereby induced. The peptide vasopressin, also secreted from the PVN such as CRH, can reinforce the effect of CRH on ACTH synthesis in the anterior lobe of the pituitary gland. ACTH stimulates cells of the *zona fasciculata* located in the adrenal cortex by binding to the melanocortin type 2 receptor. The activation of the melanocortin type 2 receptor stimulates the cAMP pathway resulting in steroidogenesis. ACTH therefore has an immediate effect on the synthesis of glucocorticoids, such as corticosterone, which are released into the systemic circulation.

The synthesis and release of glucocorticoids underlies a glucocorticoid-dependent regulation whereby ACTH release is inhibited due to a negative feedback at the level of the HTM and pituitary. These negative feedback mechanisms can be differentiated into a “fast” and “delayed” feedback. The “fast” feedback is affected by the rate of glucocorticoid secretion while the “delayed” feedback is regulated by circulating glucocorticoid levels. The “delayed” glucocorticoid feedback presumably includes the binding of e.g. corticosterone to specific endogenous receptors located in brain areas decisive for HPA axis activity. Basically two glucocorticoid receptor types within the brain can be distinguished, the mineralocorticoid receptor (MR) and the glucocorticoid receptor (GR). The MR possesses a 5-10 fold higher binding affinity to corticosterone than the GR and is therefore considered to maintain basal HPA axis activity [32,42,43]. Since the GR has a lower binding affinity to corticosterone, higher corticosterone levels after stress exposure induce a negative feedback and thereby inhibit HPA axis activity. The GR is expressed in various brain regions, but mainly in the PVN of the HTM. The GR and MR are both highly expressed in the *hippocampus*. The “fast” feedback is mediated by membrane receptors that structurally differ from the MR and GR [32,42,43].

A glucocorticoid-independent regulation of the HPA axis is also possible since the PVN is innervated by gamma amino butyric acid (GABA) neurons stemming from various brain regions including the HTM, as e.g. the dorsomedial hypothalamic nucleus (cell-type or subregion specific HPA integration). It is not clear to what extent the inhibition of the HPA axis activity by the neurotransmitter GABA in contrast to glucocorticoid concentrations could be decisive. The effects of CRH are additionally regulated by CRH binding proteins located in the pituitary gland as well as in the systemic circulation [32,43].

1.4.1.1 Adrenal glands - Glucocorticoids

The endocrine adrenal glands possess regulatory capacity for a plethora of biological processes including the stress response. The adrenal gland of mammals consists of a cortex and the medulla whereby the cortex is differentiated into the *zona glomerulosa*, *zona fasciculata*, and *zona reticularis*. The *zona reticularis*, the innermost zone of the adrenal cortex, is not existent in mice and rats since the enzyme 17 α -hydroxylase is not expressed leading to absence of androgen synthesis. The innermost zone within the adrenal cortex is the X-zone, which is unique to mice and its functions are still under discussion [47]. Cells of the *zona fasciculata*, the middle zone of the adrenal cortex, secrete glucocorticoids while cells of the *zona glomerulosa*, the outer zone of the adrenal cortex, secrete mineralocorticoids [44].

Glucocorticoids were initially named after their pivotal role in glucose metabolism, hepatic energy mobilization *via* glycogenolysis to be precise. Glucocorticoids exert multiple physiological functions including the fluid and electrolyte balance, the cardiovascular system (vasoconstriction); fat (lipolysis), protein (proteolysis), and muscle metabolism (inhibition of muscle growth) [42,48]. Glucocorticoids therefore support the organism to restore homeostasis after it was disrupted [42]. Furthermore, glucocorticoids take part in the regulation of the duration and magnitude of HPA axis activity [32]. Cortisone, cortisol, and corticosterone are assigned to the glucocorticoids while corticosterone represents the major stress hormone of rodents.

In the first step of the steroid hormone synthesis, cholesterol is hydroxylated to form the prohormone pregnenolone, which is catalyzed by cholesterol-monoxygenase (CYP11A1) (see **Figure 2**). The primary source of cholesterol are plasma lipoproteins. The main representative gestagen progesterone is synthesized from pregnenolone in the next step, which is mediated by 3 β -hydroxysteroid-dehydrogenase. Pregnenolone and progesterone count as central starting compounds for the steroid hormone biosynthesis including mineralocorticoids, glucocorticoids, and sexual hormones. Corticosterone synthesis starts with progesterone, which is converted to the mineralocorticoid deoxy-corticosterone by 21 α -hydroxylase (CYP21A2). The mitochondrial enzyme of the *zona fasciculata*, 11 β -hydroxylase (CYP11B1/2), catalyzes the synthesis of the glucocorticoid corticosterone by hydroxylation of deoxy-corticosterone [44,49].

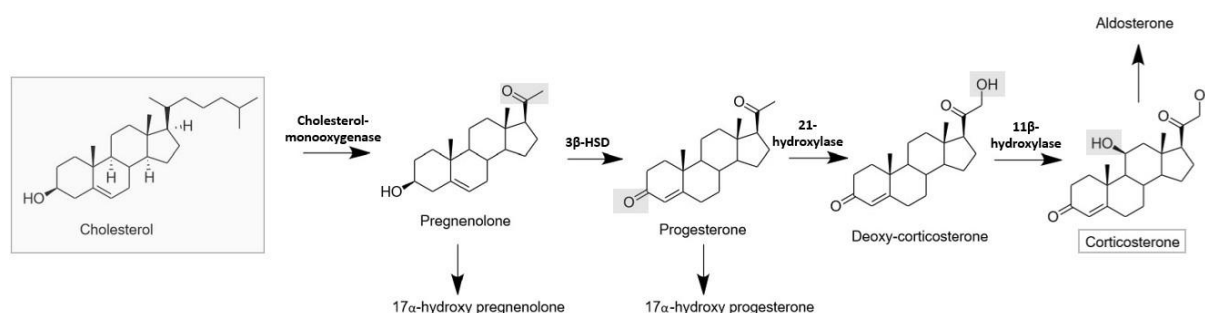


Figure 2. Biosynthesis of corticosterone. Cholesterol is converted to pregnenolone by cholesterol-monoxygenase. In the next step, 3 β -hydroxysteroid-dehydrogenase (3 β -HSD) catalyzes the formation of progesterone. Deoxy-corticosterone is formed by 21-hydroxylase. The key enzyme 11 β -hydroxylase forms corticosterone. Modified after [44,49].

1.4.1.2 Biotransformation of glucocorticoids - focus on corticosterone in urine and fecal samples

The majority of free glucocorticoids are metabolized within the liver contrary to glucocorticoids bound to the carrier protein corticosteroid-binding globulin or to albumin. Since corticosterone is a hydrophobic steroid, conversion into a water-soluble metabolite is required through biotransformation, which can be differentiated into phase I and phase II metabolism. During phase I metabolism, a functional group is added to the molecule or revealed, and its activity is thereby modified. The phase II metabolism entails conjugation reactions resulting in an inactivation of the compound, an increase in water-solubility, and polarity. Phase I and II metabolism reactions do not necessarily have to proceed in sequence, such as corticosteroids can directly undergo 21-sulfation (phase II metabolism). The excretion of metabolized corticosterone is either realized *via* the kidney (urine) or *via* the biliary tract (feces). Metabolized steroids from the biliary tract reach the gastrointestinal tract where they are further modified by bacteria of the microbiome. Metabolites can also be reabsorbed into the intestine and directed into the enterohepatic circulation where they are further metabolized by the liver [44].

Phase I metabolism includes reactions such as A-ring reduction or interconversion of hydroxy- and keto-groups at positions 11, 17, and 20 of the steroid in the context of oxidation and reduction. Cytochrome P450 (CYP) enzymes are also involved in phase I metabolism of steroid hormones, catalyzing hydroxylation, C-C bond cleavages, and further oxidations. Phase II conjugation reactions of steroids mainly proceed through sulfation and glucuronidation where the steroids are converted into a water-soluble form and the concentration as well as excretion in urine is facilitated. Sulfation is mediated by sulfotransferases utilizing 3'-phosphoadenosine-5'-phosphosulfate as cosubstrate while glucuronidation is realized by uridine diphosphate (UDP) glucuronosyltransferase using UDP-glucuronic acid as cosubstrate. It is also possible that steroids undergo methylation or are conjugated with either cysteine or glutathione. Esterification with fatty acids represents another potential phase II metabolization. Steroid conjugates are mainly excreted in the urine and bile [44,45,50–53].

Native, unmetabolized glucocorticoids are practically absent in fecal matter while steroid conjugates make up the main part. Nevertheless, the influence of intestinal bacteria should not be neglected, which possess hydrolase activities that can generate unconjugated steroids [44]. Corticosteroids are taken up into the liver and intestines of mice and rats, are primarily excreted through the gastrointestinal tract while only a small share is excreted *via* urine [54]. Analysis of glucocorticoids such as corticosterone in this matrix offers several advantages including an easy collection and more importantly, this non-invasive sampling procedure is feedback free. Fecal corticosterone metabolites (FCM) are assumed to indicate the integrated average of the previously secreted and circulating corticosterone in the blood.

FCM are therefore less impacted by fluctuations in corticosterone secretion due to the experimental design since capture-induced increases in corticosterone secretion are absent. The daily rhythm of corticosterone secretion needs to be considered and a minimum sampling period for 24 h is advisable. The lag time of FCM excretion is also to be taken into account, because it depends on the gut passage time. Mice possess a gut passage time of approximately 9–10 h. The precise composition of FCM is not completely known and is suggested to vary between sex, species, and even among mouse strains. Of course, FCM levels can be affected by the sample storage time and the environmental conditions during sampling, which is why fecal samples should be frozen as quickly as possible without chemical treatment. The immediate extraction of FCM would be even more suitable [45,50–52,55].

Steroid conjugates from the blood pool are taken up in the kidney cells *via* organic anion symport or exchange. Conjugates reach the lumen of the nephron by carriers using an electrochemical gradient. The excretion of unconjugated steroids in urine is low [44]. Sampling of urine is more challenging than the collection of fecal pellets and cannot be considered as feedback free. As already stated for fecal samples, it is advisable to sample 24 h urine collections due to the diurnal secretion rhythm of glucocorticoids. The lag time for corticosterone secretion in urine amounts to approximately 2 h after intraperitoneal injection of radiolabelled corticosterone [52]. Urine of laboratory mice can be mainly sampled by applying cages possessing a grid floor such as metabolic cages, mice can be placed on clear plastic wrap or hold over a petri dish besides modifications to these methods [14]. Additionally, hydrophobic sand was introduced as an alternative to the metabolic cage restraint for urine collection of laboratory rodents [56]. The two corticosterone metabolites 11 β -hydroxy-3,20-dioxopregn-4-en-21-oic acid (HDOPA) and 11 β ,20 α -dihydroxy-3-oxopregn-4-en-21-oic acid (DHOPA) were identified in the urine of mice after experimental peroxisome proliferator-activated receptor (PPAR α) activation and acetaminophen intoxication.

The oxidized products HDOPA and DHOPA are therefore suggested as urinary biomarkers as part of a stress response by the organism, which includes the stimulation of the adrenal cortex through the HPA axis. Liver tissue was shown to be decisive for the metabolism of corticosterone to 21-carboxylic acids where corticosterone represents the precursor. The metabolite HDOPA is formed after several reaction steps while DHOPA represents the end product. These 21-carboxylic acids are channeled from the liver to the kidney where they accumulate and are subsequently excreted *via* urine [57–59]. DHOPA was also mainly detected in the liver and small intestine of male BALB/cJ mice after intraperitoneal injection of [4-¹⁴C]corticosterone [54].

1.4.2 Brown adipose tissue - adaptive thermogenesis

Adaptive thermogenesis in brown adipose tissue (BAT) can be distinguished between thermoregulatory and metaboloregulatory thermogenesis to serve two different purposes. Thermoregulatory thermogenesis provides heat for the regulation of body temperature while metaboloregulatory thermogenesis serves for additional energy combustion [60,61]. Thermoregulatory thermogenesis is often referred as cold-induced thermogenesis and metaboloregulatory thermogenesis as diet-induced thermogenesis. Within the scope of the present study, heat generation *via* the uncoupling protein 1 (*Ucp1*) in BAT called non-shivering thermogenesis was analyzed by focussing on thermoregulatory thermogenesis.

1.4.2.1 Thermoregulatory thermogenesis

In the case animals are exposed to the cold mechanisms must take effect that can compensate for the heat loss. Therefore, extra heat production is initiated for regulation of the body temperature [60]. The thermoneutral zone defines a temperature range where the basal metabolic rate (BMR) is sufficient to compensate heat losses resulting from the existent temperature gradient between the ambient and the body temperature [62,63]. The thermoneutral zone is demarcated by the lower critical temperature and the upper critical temperature (see **Figure 3**). Mice possess a thermoneutral zone at approximately 30°C [60,62–64]. Cold stress therefore describes temperatures below the thermoneutral zone [65]. Cold stress is also often defined as the acute exposure of animals kept at ~20°C to ~5°C within a specific experimental setup. As a consequence, the animal needs to permanently produce extra heat for the sake of body temperature maintenance [60]. The additional heat demand for body temperature defense is reduced in relative magnitude the larger the animal becomes. This can be explained with an increased BMR in proportion to the body weight (BW) to the power of 0.75, equivalent to 11 ml O₂·min⁻¹·kg^{-0.75}. Animals possessing a higher BW can thus carry more heat insulation [60]. Standardized room temperatures at 20-22°C are maintained in animal houses and it is often addressed how mice are coping with potential cold stress. Interestingly, when comparing the BMR with energy expenditure (EE), mice kept at thermoneutral conditions (30°C) show a 1.6 times higher EE compared to BMR, whereas for mice kept at standard conditions (21°C) the EE/BMR ratio increases to 2.6 and 3.5 for day- and night-time respectively [66].

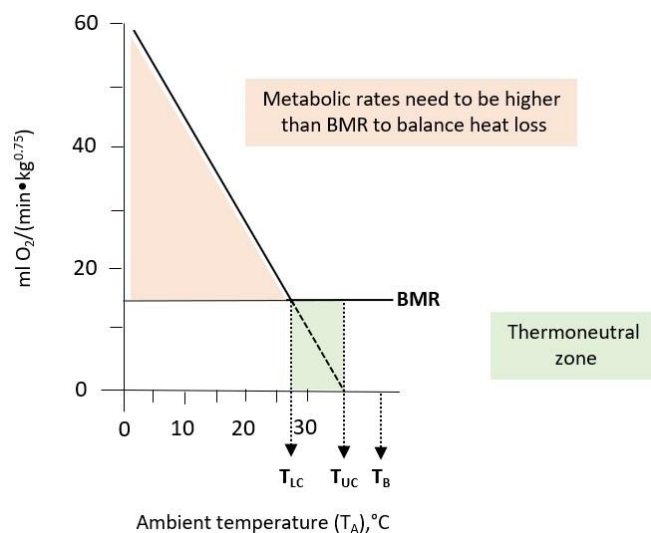


Figure 3. Thermoregulatory response depending on ambient temperature. This scheme is based on data gathered in previous studies [60,63,67]. BMR: basal metabolic rate, T_{LC} : lower critical temperature, T_{UC} : upper critical temperature, T_B : body temperature, T_A : ambient temperature. The slope of the thermoregulatory line in the lower range of the thermoneutral zone depends on the heat insulation. The lower the slope, the higher the insulation. The light pink area indicates the higher metabolic rates needed to balance heat loss. The light green area indicates the thermoneutral zone between the T_{LC} and T_{UC} .

1.4.2.2 Acute and chronic exposure to cold environmental conditions - cold-induced thermogenesis

Shivering, referring to the contraction of skeletal muscles, is the first-line response for heat production in terms of acute cold exposure, while prolonged cold periods enhance capacities for non-shivering thermogenesis in BAT [60,61,68]. Non-shivering thermogenesis is simply defined as replacement of the heat production by shivering. [60]. This type of thermogenesis is considered to be exclusively located in the BAT, which was demonstrated in a study conducted with *Ucp1*-ablated mice. These mice were consistently shivering in comparison with wild type mice after being kept in the cold for several months proving that they were incapable of triggering an alternative source of non-shivering thermogenesis other than *Ucp1* [69].

The thermoregulatory response depends on whether animals are warm- or cold-acclimated. On the one hand, when warm-acclimated rats ($\sim 30^\circ\text{C}$) are exposed to the cold, shivering thermogenesis might enable for sufficient, acute heat production, but not for a longer period of time. They certainly do not have the endurance for maintaining an increased EE, which is essential for survival. On the other hand, in the case of cold-acclimated rats ($\sim 10^\circ\text{C}$), heat production is sufficient *via* non-shivering thermogenesis [68]. That is why the term “adaptive” non-shivering thermogenesis is often utilized reflecting the thermoregulatory adaptation of BAT to the ambient temperature regime.

1.4.2.3 Sympathetic innervation of the brown adipose tissue and uncoupling protein 1

BAT represents a specialized tissue for non-shivering thermogenesis, which responds to cold exposure and changes in diet [61,70]. The BAT consists of numerous mitochondria, plurivacuolar fat cells and a central nucleus. Fatty acids and alternatively glucose represent the main sources for heat production, while *Ucp1*, which is located in the inner mitochondrial membrane of BAT, is the key factor for this process [60,70]. *Ucp1* expression is high in BAT while its expression is low in white adipose tissue (WAT). After browning of WAT, due to i.a. prolonged cold exposure, beige adipose tissue develops and expresses high *Ucp1* levels during cold stimulation [71]. The BAT is highly vascularized to supply the tissue with sufficient oxygen and substrate. The sympathetic nervous system centrally controls BAT activity and therefore densely innervates this tissue [70] (see **Figure 4**, left side).

The ventromedial hypothalamic nucleus receives input of peripheral tissue regarding information on e.g. reduction of body temperature (cold-induced thermogenesis) or food intake conveyed by i.a. the well researched adipokine leptin (diet-induced thermogenesis). In case adjustment of the heat production is required, NE release by sympathetic nerves is triggered [72]. NE reaches the BAT *via* the sympathetic nervous system and mainly binds to β 3-adrenergic receptors. The breakdown of triglycerides, called lipolysis, is induced and free fatty acids in the cytoplasm become available [70–72]. In detail, the adrenergic receptor binds to a G protein (Gs subtype), adenylyl cyclase is activated, and cyclic adenosine monophosphate (cAMP) is formed. cAMP subsequently activates protein kinase A (PKA), which serves as substrate for thermogenesis [70,72]. Nuclear and cytosolic proteins are phosphorylated by PKA including lipases, such as adipose triglyceride lipase and hormone-sensitive lipase, and perilipin. cAMP/PKA signaling also stimulates p38 mitogen-activated protein, which is crucial for gene expression of peroxisome proliferator-activated receptor gamma coactivator 1-alpha (PGC1 α). PGC1 α is widely expressed in BAT and also plays a part in *Ucp1* stimulation. Another triggered signal pathway includes the Janus kinase/signal transducer and activator of transcription pathway. The Peroxisome proliferator-activated receptors (PPARs), including PPAR α and PPAR γ , are also involved in the control of the expression of genes that take part in thermogenesis [70].

Free fatty acids are mainly combusted within the process of the electron transport chain, which occurs in the inner mitochondrial membrane [71,72]. In detail, nicotinamide adenine dinucleotide (NADH), flavin adenine dinucleotide (FADH₂), and acetyl coenzyme A are generated due to β -oxidation of free fatty acids and glucose (see **Figure 4**, right side). Further electron carriers, NADH and FADH₂, are produced by introducing acetyl coenzyme A into the tricarboxylic acid cycle. NADH and FADH₂ provide electrons for the complexes, which are a part of the electron transport chain.

Ubiquinone transfers electrons of complex I and II to complex III and cytochrome c further channels electrons from complex III to complex IV. Molecular oxygen (O_2) represents the terminal electron acceptor and is subsequently reduced to water (H_2O) [71]. Protons are directed out of the mitochondria by passing through the respiratory chain complexes I, III, and IV. An electrochemical potential gradient is thereby build up [71,72]. The energy of the proton gradient is utilized by the adenosine triphosphate (ATP) synthase complex, F_0/F_1 -ATPase, for ATP production [70,71]. *Ucp1* is localized in the mitochondrial membrane like ATPase and as the name already indicates, *Ucp1* uncouples the proton flux utilized by the ATP synthase [70,73]. The *Ucp1* as transmembrane protein translocates protons in the cytoplasm back into the mitochondrial matrix, which results in dissipation of the electrochemical gradient normally utilized for ATP synthesis [71]. In the process, chemical energy in the form of heat is released from the mitochondrial matrix towards the intermembrane space [73]. Especially when small mammals are living in a cold environment, investigating the share of the BAT in total energy metabolism is crucial since the energy is primarily consumed by BAT. The BAT capacity is therefore adapted to the animals' metabolic requirements depending on environmental conditions [72].

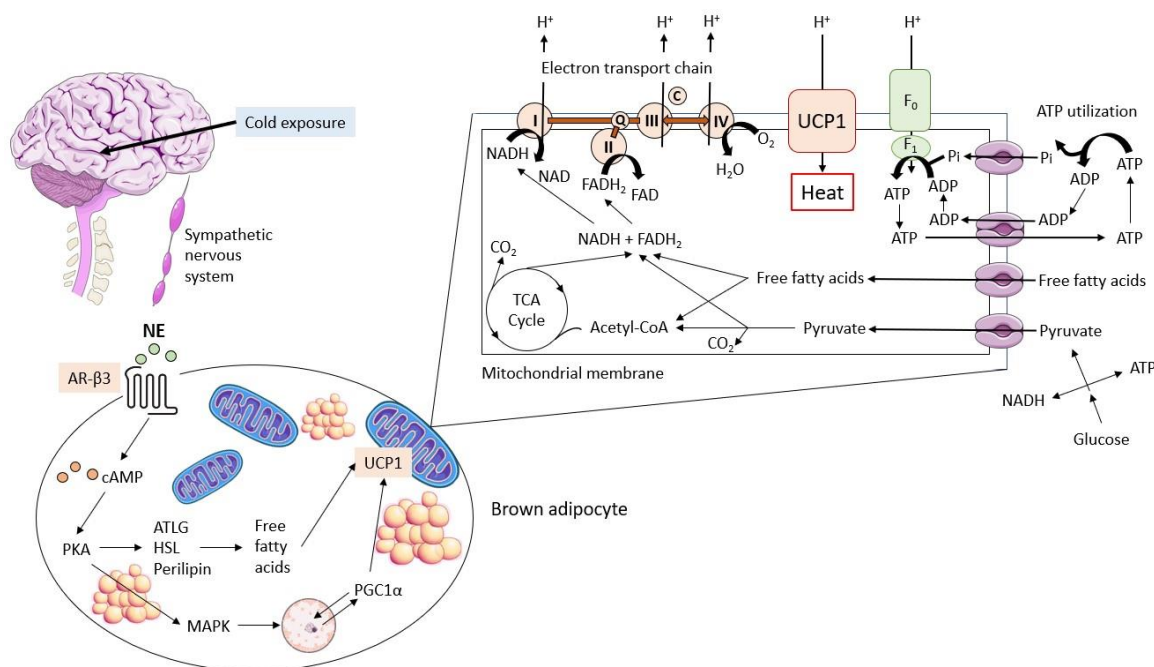


Figure 4. Energy metabolism in mitochondria of the brown adipose tissue (BAT). *Left side - Brain, sympathetic nervous system, BAT:* Cold exposure activates the sympathetic nervous system and induces the release of norepinephrine (NE). NE binds to the β_3 -adrenergic receptor (AR- β_3) located in the BAT membrane and cyclic adenosine monophosphate (cAMP) is formed. Protein kinase A (PKA) is activated by cAMP and phosphorylates proteins such as adipose triglyceride lipase (ATLG), hormone-sensitive lipase (HSL), and perilipin. Free fatty acids are released and are channeled towards mitochondria. PKA can also stimulates p38 mitogen-activated protein kinase (MAPK). MAPK controls the gene expression of peroxisome proliferator-activated receptor gamma coactivator 1-alpha (PGC1 α), which stimulates the uncoupling protein 1 (Ucp1) located in the mitochondrial membrane. *Right side - Mitochondria in BAT:* Nicotinamide adenine dinucleotide (NADH) and flavin adenine dinucleotide (FADH₂) are generated due to β -oxidation of free fatty acids and glucose. The electrons produced during this process are introduced into the electron transport chain. Electrons from complex I and II are transferred to complex III by ubiquinone (Q). Cytochrome c (C) shuttles electrons from complex III to complex IV. Molecular oxygen (O_2) accepts the electrons at the end of the electron transport chain. A proton electrochemical potential gradient is build up while protons (H^+) are pumped out of the mitochondrial membrane by complex I, III, and IV. Protons either re-enter the mitochondrial matrix via the F_0/F_1 -ATPase for the purpose of adenosine triphosphate (ATP) generation or re-enter via Ucp1 by producing heat. Acetyl-CoA: acetyl coenzyme A, TCA: tricarboxylic acid cycle, CO₂: carbon dioxide, ADP: adenosine diphosphate, Pi: phosphate, H₂O: water. Modified after [61,70,71].

1.4.3 Brain - neurotransmitters

1.4.3.1 The dopaminergic system

Dopamine (DA) is assigned to the catecholaminergic and monoamine neurotransmitters, and is highly conserved. Basal ganglia describe interacting forebrain structures located in the basal telencephalon. Basal nuclei include the *caudate putamen* (CPU), the *nucleus accumbens* (NAC), the *globus pallidus*, the ventral pallidum, and the olfactory tubercle. The major nuclei that are associated with the basal nuclei comprise the subthalamic nucleus (STN), the ventral tegmental area (VTA), and the *substantia nigra* (SN) [74]. The following brain areas were analyzed in this study: CPU, NAC, hypothalamus (HTM), VTA, and SN.

The striatum represents the largest part of the basal ganglia and also its primary afferent structure. Dopaminergic neurons project in clearly delineated paths, adding up to four major pathways [75]. Projections to the entire striatum can be classified into the ventral and the dorsal mesostriatal system whereby projections from VTA to NAC are assigned to the ventral and from the *substantia nigra pars compacta* (SNc) to the CPU to the dorsal system (see **Figure 5**, [74,76]). The ventral mesostriatal system mainly controls motivated behavior and exerts cognitive function while the dorsal mesostriatal system primarily controls motor activity [77]. Both systems can be summarized as the mesencephalic DA system besides the diencephalic DA system, which is not focussed here. Besides the two previously described mesostriatal DA systems, the mesolimbocortical DA system involves projections to limbic and cortical areas as well as the amygdala, locus coeruleus (LC) among others [74].

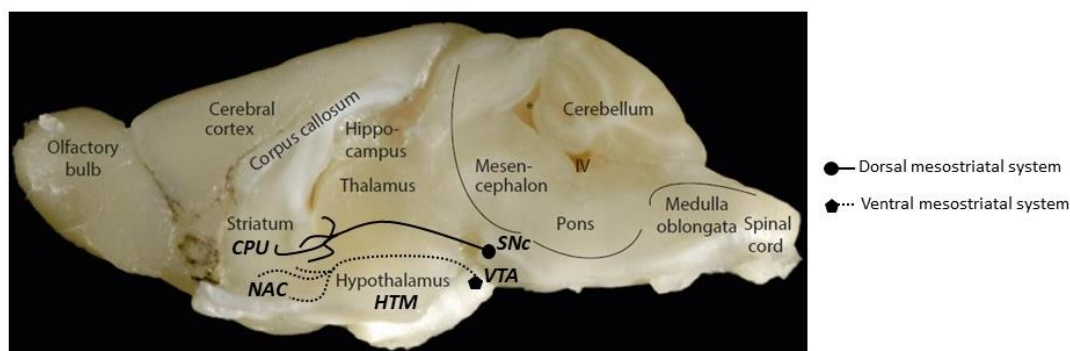


Figure 5. Schematic illustration of the dorsal mesostriatal and the ventral mesostriatal system in the murine brain. Dopaminergic neurons of the dorsal mesostriatal system originate in the *substantia nigra pars compacta* (SNc) and project to the *caudate putamen* (CPU) while dopaminergic neurons of the ventral mesostriatal system emanate from the ventral tegmental area (VTA) and project to the *nucleus accumbens* (NAC). HTM: Hypothalamus. Modified after [27].

The striatum is mainly composed of medium spiny neurons, which can be divided into DA D1 and DA D2 neurons. DA D1-receptor, dynorphin-, substance P expressing striatonigral neurons take part in the direct pathway while DA D2-receptor and enkephalin expressing striatopallidal neurons contribute to the indirect pathway. Medium spiny neurons are densely innervated from dopaminergic neurons originating in the VTA as well as the SNc, and GABA represents their neurotransmitter (see **Figure 6**). Striatal output pathways control movement, but also play a part in behavioral modulation. The direct pathway is suggested to be linked to reward learning (activation of DA D1-receptors) while the indirect pathway is critical for avoidance learning (inactivation of DA D2-receptors). DA exerts different effects depending on the pathway, direct or indirect, in which it acts.

Since the dopaminergic system is well-studied in terms of voluntary movement exertion, the focus is set on the motor loop besides the involvement of DA in four other circuits within the basal ganglia (oculomotor, dorsolateral prefrontal, lateral orbitofrontal, limbic loop). The direct pathway of the motor loop elevates motor tone by disinhibiting thalamic nuclei while the indirect pathway decreases thalamus activity and consequently motor cortex activity [74,76].

In detail, the direct pathway starts with an activating, glutaminergic projection from the cerebral cortex to the striatum. Substance P and GABA are released from the striatum and thereby inhibit the medial globus pallidus (mGP). Thalamic nuclei inhibition is therefore reduced by a decrease in GABA release from the mGP. This results in an increased tone, a glutaminergic projection to the e.g. motor cortex. Concerning the indirect pathway, the striatum is excited by excitatory, glutaminergic projections emanating from the cerebral cortex. Enkephalin and GABA are released and induce the inhibition of the lateral globus pallidus (lGP). Disinhibition of the STN follows, which increasingly stimulates the mGP and *substantia nigra pars reticulata* (SNr) via glutaminergic projections. MGP and SNr then release GABA to the thalamic nuclei and induce a decreased tone in the e.g. motor cortex due to reduced glutamate signalling [74]. An alternatively shorter indirect pathway was suggested by omitting the STN and directly connecting the lGP with the mGP [78]. The hyper indirect pathway was also introduced including cortex projections directly to the STN, which then projects to the mGP [79].

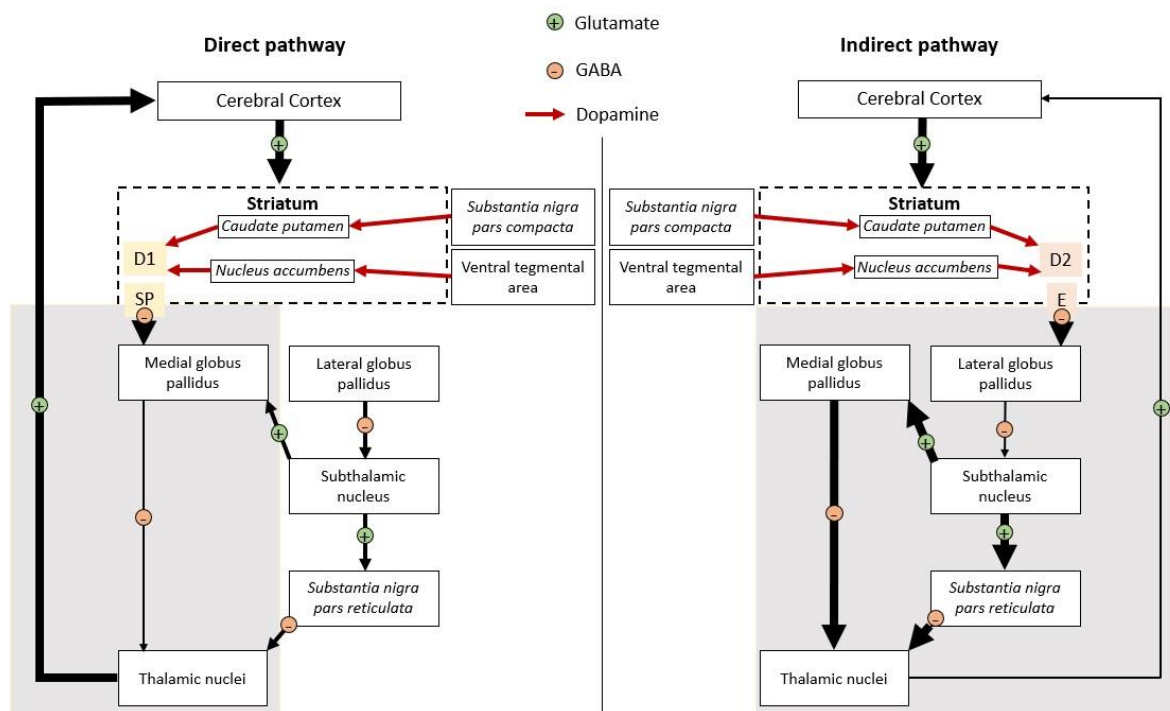


Figure 6. Hypothetical connection between basal nuclei concerning the direct and the indirect pathway proceeding within the dopaminergic system. Left side - direct pathway: The net outcome of the direct pathway entails an increased cerebral cortex activation by reducing the inhibition of the thalamic nuclei. Glutamatergic projections are emitted from the cerebral cortex and stimulate the striatum. The striatum releases gamma amino butyric acid (GABA) and substance P (SP), which inhibit the medial globus pallidus (mgp). Thalamic nuclei inhibition through the mgp is thereby reduced and the activity of the cerebral cortex is enhanced. **Right side - indirect pathway:** The net outcome of the indirect pathway entails a decreased cerebral cortex activation by enhancing the inhibition of the thalamic nuclei. Excitatory, glutamatergic projections from the cerebral cortex are sent to the striatum. The striatum then releases GABA and enkephalin (E) to inhibit the lateral globus pallidus (lgp). The substantia nigra pars reticulata (SNr) and the mgp are stimulated by enhanced glutamatergic projections from the subthalamic nucleus (STN), resulting from a decrease of STN inhibition. Stimulation of the mgp and SNr results in an amplified inhibition of thalamic nuclei activity, which in turn leads to a reduction of cerebral cortex activity. The thickness of the arrows indicate an increase or decrease regarding glutamatergic (green circles with plus sign) and GABAergic (red circles with minus sign) projections within the dopaminergic system. Red arrows indicate dopamine (DA) signalling. D1: DA D1-receptor, dynorphin-, substance P-expressing striatonigral neurons, D2: DA D2-receptor and enkephalin-expressing striatopallidal neurons. Modified after [74,76].

DA synthesis in the brain takes place within the cytosol of catecholaminergic neurons. It starts with the amino acid L-tyrosine, which is hydroxylated by the enzyme tyrosine hydroxylase in ortho position to the existing hydroxy group (see **Figure 7**). This reaction represents the rate-limiting step whereby the cofactor tetrahydrobiopterin needs to be available. L-dihydroxy-phenylalanine is decarboxylated by dopamine decarboxylase and DA is thereby synthesized. A classical and an alternative pathway for DA biosynthesis was suggested, but the alternative pathway only contributes a small share of the total DA biosynthesis. DA is channeled into, concentrated in, and transported within synaptic vesicles, which is mediated by the vesicular monoamine transporter 2 (VMAT2). DA is directly converted into norepinephrine (NE) *via* dopamine β -hydroxylase in noradrenergic and adrenergic neurons within the synaptic vesicles [74,80,81].

In case of an excitation of the dopaminergic neurons, DA stored within the synaptic vessels is released into the synaptic cleft where it interacts with postsynaptic DA receptors or presynaptic DA autoreceptors. DA needs to be eliminated from the synaptic cleft in order to stop the signalling. DA is therefore either taken up by glial cells and subsequently degraded or is taken up by dopaminergic neurons and recycled. Within the glial cells, the two enzymes monoamine oxidase (MAO) and catechol-O-methyltransferase (COMT) are involved in DA degradation. MAO deaminates DA including its metabolites and COMT converts DA and its metabolites into inactive methoxy compounds. 3-Methoxytyramine (3-MT) is synthesized from DA by COMT. MAO catalyzes the conversion of 3-MT into 3-methoxy-4-hydroxyphenylacetaldehyde. The metabolite 3,4-dihydroxyphenylacetic acid (DOPAC) is formed in a two-step process. First, DA is converted to 3,4-dihydroxyphenylacetaldehyde by MAO and then to DOPAC by aldehyde dehydrogenase (AD). Homovanillic acid is formed from both DA metabolites, 3-methoxy-4-hydroxyphenylacetaldehyde and DOPAC, catalyzed by either AD or COMT [74,80,81]. DA, 3-MT, and DOPAC were the neurotransmitters of investigation in the present study, which are highlighted in gray boxes in **Figure 7**.

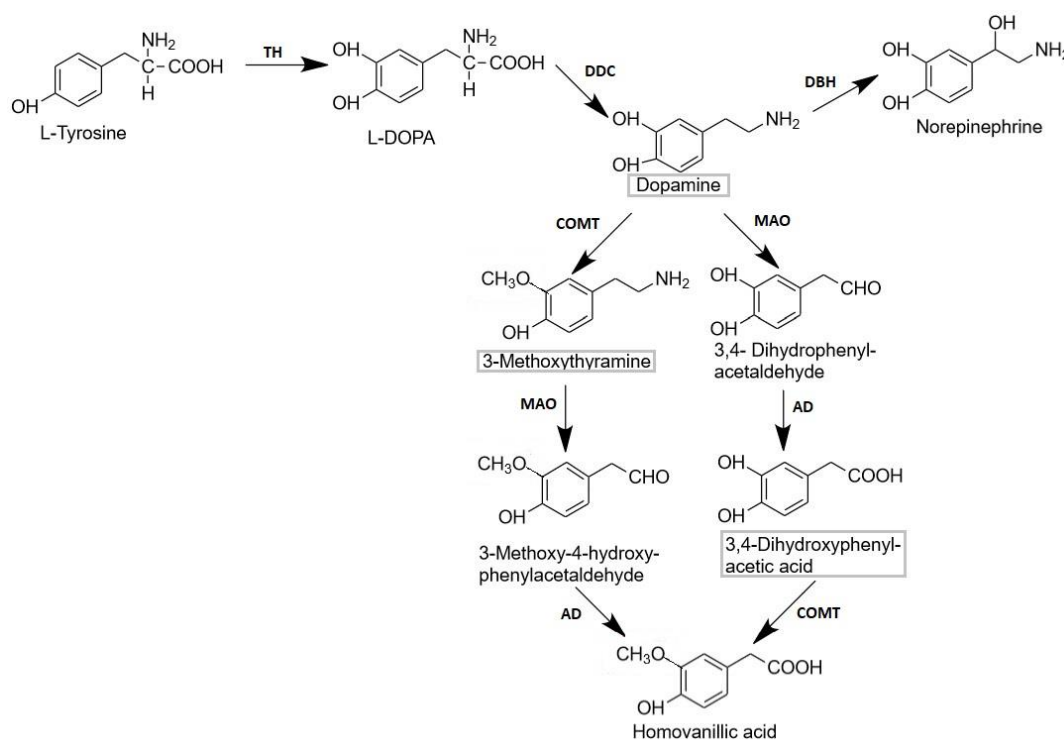


Figure 7. Biosynthesis and degradation of dopamine (DA). **Biosynthesis of DA:** The synthesis of DA starts with the hydroxylation of the amino acid L-tyrosine, which is mediated by the enzyme tyrosine hydroxylase (TH). This is the rate-limiting step of DA synthesis. Dopamine decarboxylase (DDC) then decarboxylates L-dihydroxyphenylalanine (L-DOPA) to form DA. DA is converted into norepinephrine (NE or noradrenaline) by dopamine β -hydroxylase (DBH). **Degradation of DA:** DA degradation mainly involves the enzymes monoamine oxidase (MAO) and catechol-O-methyltransferase (COMT). DA is converted into either 3-methoxytyramine (3-MT) by COMT or into 3,4-dihydroxyphenylacetaldehyde (DHPA) by MAO. 3-methoxy-4-hydroxyphenylacetaldehyde (MHPA) is then formed from 3-MT via the action of MAO. Aldehyde dehydrogenase (AD) converts MHPA into homovanillic acid (HVA). Within the other degradation reaction chain, DHPA is converted into 3,4-dihydroxyphenylacetic acid (DOPAC) by AD and then into HVA by COMT. Investigated compounds in the present study are marked with gray boxes. Modified after [80,81].

1.4.3.2 The serotonergic system

SRT is an indolamine, which is assigned to the monoamine neurotransmitters as DA. SRT is found in many different areas of the brain, takes part in multiple different biological processes within the central nervous system, and is involved in the modulation of various behaviors such as cognitive, motor, and autonomic functions [82]. This monoamine neurotransmitter represents a key neuromodulator, which regulates emotions, sensory processing, and reward among others. Physiological interactions of SRT can convey stress and pain, which act *via* the HPA-axis on the neuronal system [83]. One of SRT's main functions include the reduction of stress and anxiety as well as the mediation of contentment and happiness [82,83]. Disturbances within the serotonergic system, mostly by a reduction in SRT levels in the brain, are connected with a depressive mood, mood fluctuation, and anxiety states. In addition, a SRT transporter deficiency was shown to increase anxiety [84]. During the development of the brain including its neurotransmitter systems, serotonergic neurons evolve from two groups located in the anterior and posterior hindbrain, what is termed the metencephalon. The metencephalon of rodents is divided into seven or eight compartments during embryonic development, which give rise to nine raphe nuclei B1-B9 (see **Figure 8**) [85,86].

Serotonergic neurons are organized in raphe nuclei and can be divided into two raphe-complexes according to their projection areas. The anterior group of raphe nuclei, B9-B5, form the rostral raphe-complex, which projects to the cortical and cerebellar areas. The posterior caudal raphe-complex, B4-B1, solely innervates the medulla. In detail, the rostral raphe-complex primarily innervates the cortex, the striatum, the *hippocampus*, the *thalamus*, the HTM, and the *amygdala*. The serotonergic neurons of the rostral-raphe complex regulate mood; emotional, social, anxiety behavior; thermoregulation among others. The dorsal raphe nucleus (DRN) represents the biggest group of bundled serotonergic neurons referring to B7 of the rostral raphe-complex. Interestingly, more than half of the serotonergic neurons in the murine brain are located in the DRN. The regulation of serotonergic neurons within the DRN is realized by top-down mechanisms, which suggests that serotonergic neurons have an integrating function by processing information from upstream brain areas. Also GABAergic neurones of the DRN take part in the regulation of serotonergic neurones. The DRN receives primarily input from six brain areas - the *lateral habenula*, the prefrontal cortex, the *amygdala*, the preoptic area, the lateral HTM, and the SN. The *lateral habenula* and the prefrontal cortex are involved in emotional regulation while the HTM takes part in feeding behavior and the reward system. As serotonergic neurons of the DRN project to the midbrain SN, it is suggested that the serotonergic input regulates the basal ganglia circuit. It is therefore hypothesized that the DA and the SRT systems interact with each other, but the anatomical basis for this interaction is not fully explored. For example, the DRN connection with the VTA seems to be unidirectional including serotonergic projections of the DRN to the dopaminergic neurons of the VTA for the most part, but not *vice versa* [85–87].

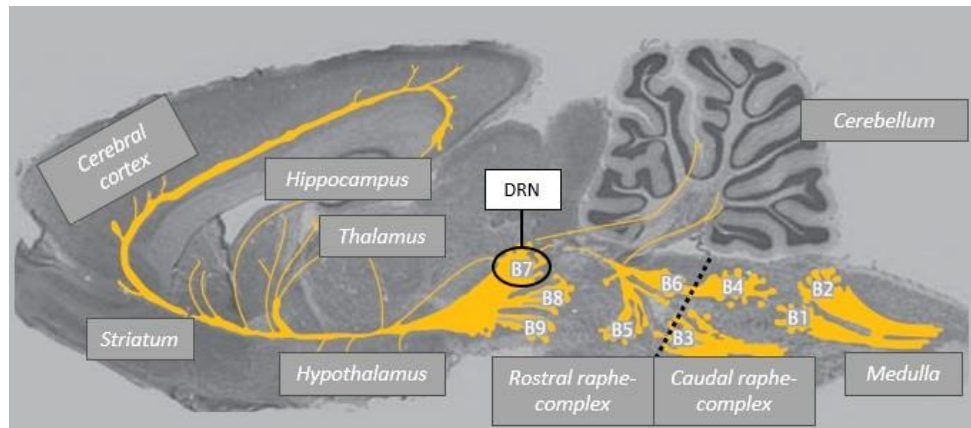


Figure 8. The serotonergic system of the central nervous system. Schematic representation of the rat brain along the sagittal axis with positioning of the raphe nuclei B1-B9. Serotonergic neurons from the rostral raphe-complex, B9-B5, project to the cerebral and cerebellar brain areas. B7 represents the major raphe nucleus, which is the dorsal raphe nucleus (DRN). Serotonergic neurons from the caudal raphe-complex, B4-B1, innervate the medulla. Modified after [85–87].

SRT cannot pass the blood brain barrier and its *de novo* synthesis from the amino acid L-tryptophan is therefore carried out in the brain (see **Figure 9**). Tryptophan hydroxylase (TPH) is the key enzyme for the SRT synthesis, mainly TPH2 in the brain, and is produced within the serotonergic cell bodies of the raphe nuclei [88]. L-Tryptophan is hydroxylated by TPH using molecular oxygen (O_2) to form L-5-hydroxytryptophan (5-HTP). Important co-factors of this reaction step include tetrahydrobiopterin and iron(II) ions, which function as electron donors. The synthesis of 5-HTP is the rate-determining step within the two-step reaction chain. Next, the carboxyl group of 5-HTP is eliminated by L-amino acid decarboxylase and SRT is thereby synthesized. The co-factor pyridoxal phosphate, vitamin B₆, is required for the second reaction step. The synthesis rate of SRT can be affected by the existing concentrations of L-tryptophan, tetrahydrobiopterin, and O_2 . The amino acid precursors L-tryptophan and 5-HTP can pass the blood brain barrier compared to SRT [85].

SRT is stored in intracellular vesicles, such as DA, to ensure a regulated release of SRT. The transport of SRT within these vesicles is realized by VMAT1 and VMAT2, while VMAT2 possesses a two- to three-times higher affinity for monoamine neurotransmitters than VMAT1. Importantly, both transporters show a higher affinity for SRT than for the three catecholamines DA, NE, and epinephrine. VMAT2 is mainly expressed in the central nervous system. SRT is released into the synaptic cleft as a result of an action potential depolarizing the serotonergic neurons, exerts its effect through different postsynaptic SRT receptors, and triggers diverse signal transduction pathways. SRT reuptake is mediated by endocytosis into the presynaptic serotonergic cell bodies and then SRT is either recycled or degraded. SRT degradation depicts a two step process. First, SRT is deaminated by MAO-A or MAO-B, H_2O , O_2 , and FAD^+ functioning as cofactor to form 5-hydroxyindole acetaldehyde, which represents the rate-limiting step. 5-Hydroxyindole acetaldehyde is then oxidized to 5-hydroxyindoleacetic acid (5-HIAA) by AD. 5-HIAA is directed into the blood circulation and is finally excreted *via* the kidneys. MAO-A is mainly located in the periphery and prefers SRT as well as NE as substrate. As opposed to this, MAO-B is primarily found in the central nervous system and presumably has an affinity for DA [85].

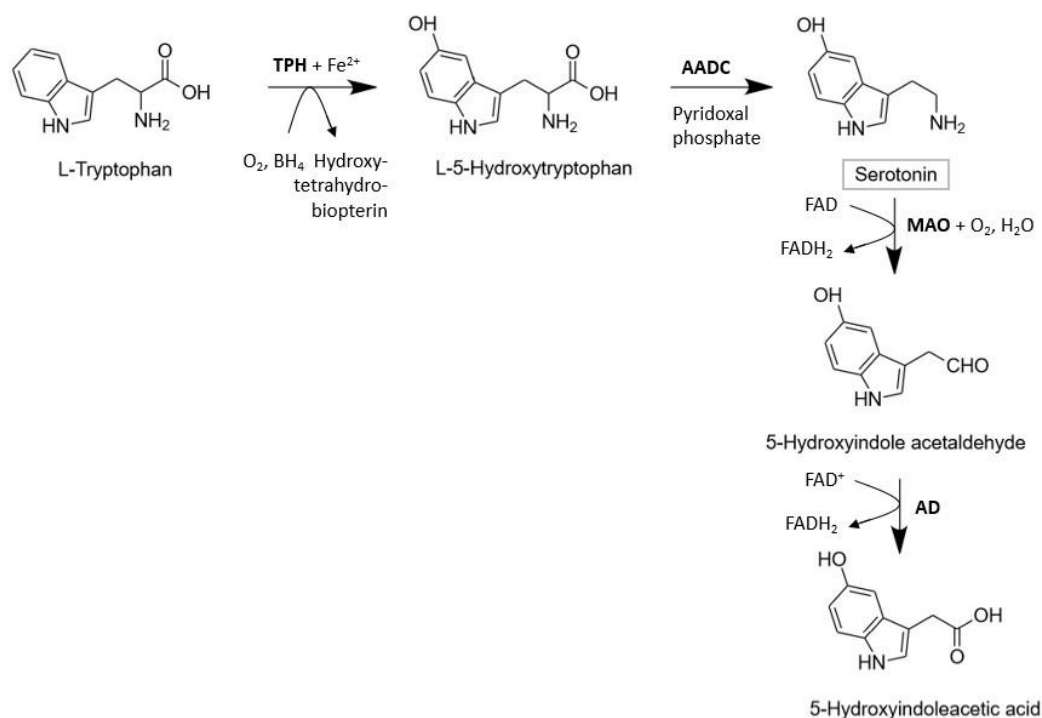


Figure 9. Biosynthesis and degradation of serotonin (SRT). Biosynthesis of SRT: L-Tryptophan is hydroxylated to form L-5-hydroxytryptophan (5-HTP) by tryptophan hydroxylase (TPH). SRT is synthesized in the second reaction step by L-amino acid decarboxylase (AADC), which removes the carboxyl group of 5-HTP. Cofactors required for biosynthesis of SRT: molecular oxygen (O_2), tetrahydrobiopterin (BH_4), iron(II) ions (Fe^{2+}), pyridoxal phosphate. **Degradation of SRT:** Monoamine oxidase (MAO) removes the amino group of SRT and SRT is degraded to 5-hydroxyindole acetaldehyde. 5-hydroxyindoleacetic acid (5-HIAA) is then synthesized through oxidation of 5-hydroxyindole acetaldehyde mediated by aldehyde dehydrogenase (AD). Cofactors required for degradation of SRT: water (H_2O), molecular oxygen (O_2), flavin adenine dinucleotide (FAD^+). SRT is marked with a gray box since this compound was investigated in the present study. Modified after [85].

1.4.4 Liver - glycogen metabolism

The liver represents an important energy storage and is pivotal for maintaining blood glucose since all splanchnic blood runs through the liver prior to entering the systemic circulation. The brain, spinal cord, and erythrocytes are obligatorily dependent on glucose supply during the post resorption phase since fatty acids cannot be utilized as energy source in these tissues. Within the liver, glucose is stored in the form of glycogen and can be released on demand to supply the whole organism with glucose. To ensure that glucose is provided only when needed and not simultaneously with glucose uptake processes, a strict regulation of substrate flows in the hepatocyte is necessary. The liver regulates the glucose metabolism including glycolysis, glycogen synthesis or breakdown (glycogenolysis) as well as gluconeogenesis. Glucose is either synthesized from glycogenolysis or from gluconeogenic precursors (e.g. lactate, alanine, and glycerol) [89]. Gluconeogenesis dominates during prolonged fasting whereas glucose is mainly produced *via* glycogenolysis during short-term fasting periods [90].

The hormones insulin and glucagon act upon the liver, which are in- or decreased relative to the nutritional status of the animal. After the termination of feeding, glucose absorption from ingested food is elevated, which induces higher blood glucose levels. This results in an elevated insulin-glucagon ratio during the postprandial phase. In detail, blood glucose is mainly transported *via* the unlimited and insulin-independent glucose transporter 2 (GLUT2) into the hepatocyte (see **Figure 10**). If sufficient amounts of glucose become available in the liver, insulin induces the glucokinase, which phosphorylates glucose to generate glucose-6-phosphate (G-6-P). Since the intracellular glucose concentration is thereby reduced, more blood glucose is taken up into the liver by GLUT2. G-6-P cannot be transported by GLUT2 and is consequently retained within hepatocytes. In addition, G-6-P is an allosteric inhibitor of glycogen phosphorylase (GPH) and an allosteric activator of glycogen synthase (GS). If there is enough energy obtainable to the organism, glucose-1-phosphate (G-1-P) is formed from G-6-P by phosphoglucomutase. The transfer of glucose to an existing glycogen molecule, representing a branched polymer of glucose, requires a great quantity of energy. G-1-P is therefore not directly converted to glycogen, but G-1-P reacts with uridine triphosphate (UTP) to form uridine diphosphate (UDP) glucose (UDP-G) and pyrophosphate. The generation of UDP-G is catalyzed by UDP-glucose pyrophosphorylase at the expense of the conversion of UTP into UDP. In the last step of glycogen synthesis, UDP-G is hydrolytically cleaved whereby the required energy becomes available to form glycogen. Glycogen formation is catalyzed by GS, which is active in its dephosphorylated form (GS-OH). GS forms α -1,4-glycosidic linkages of glycogen while α -1,6-glycosidic branchpoints are realized by the branching enzyme. In the initial step of glycogen synthesis, the protein glycogenin self-glucosylates in order to form an oligosaccharide primer chain. The process of self-glucosylation starts with the transfer of glucose from UDP-G to a tyrosine residue within glycogenin. Glycogenin then interacts with GS through its C-terminus and α -1,4-glycosidic linkages are formed to reach 10-20 residues [89–92].

A low insulin-glucagon ratio as well as low portal glucose levels occur accordingly during fasting. In this case, blood glucose homeostasis is preserved by the liver regulating glycogenolysis independent of carbohydrate intake. Glycogen is mobilized in the process of glycogenolysis and G-1-P from α -1,4-glycosidic linkages as well as free glucose from α -1,6-glycosidic linkages is available for the organism. GPH in its phosphorylated form (GPH-P) catalyzes the breakdown of glycogen besides the debranching enzyme. G-1-P is converted to G-6-P, G-6-P is transported into the endoplasmic reticulum of hepatocytes where it is dephosphorylated by glucose-6-phosphatase to generate glucose. Glycogen breakdown can also be realized *via* a second pathway including the transfer of glycogen into lysosomes. Glycogen is subsequently hydrolyzed to form glucose, which is catalyzed by the lysosomal α -glucosidase [89–92]. The catecholamines NE and epinephrine, which are synthesized in the adrenal medulla, also exert an effect on glycogen metabolism. They bind to hepatic G-protein coupled beta adrenergic receptors, thereby induce conformational changes in stimulatory protein subunits and subsequently activate the adenylyl cyclase. The adenylyl cyclase increases cAMP levels in the cytosol and cAMP then activates PKA. PKA in the next step can phosphorylate different enzymes, such as GPH and GS, which take part in various metabolic pathways. Within the liver, PKA amplifies glycogen breakdown and gluconeogenesis by activating GPH. Epinephrine stimulates glucagon secretion from pancreatic α -cells while it hinders insulin secretion from pancreatic β -cells and therefore reinforces glycogen breakdown indirectly [90,92].

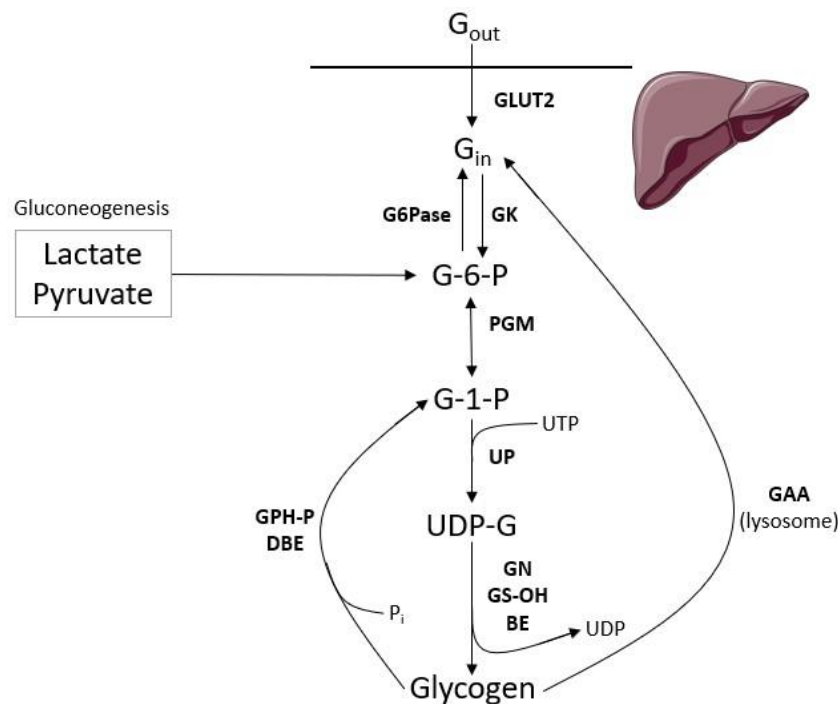


Figure 10. Glycogen metabolism in the liver. Glycogen synthesis: Extracellular glucose (G_{out}) is transported into the liver primarily by the glucose transporter 2 (GLUT2). Glucokinase (GK) converts intracellular glucose (G_{in}) into glucose-6-phosphate (G-6-P). Phosphoglucomutase (PGM) then catalyzes the formation of G-6-P to glucose-1-phosphate (G-1-P). G-1-P and uridine triphosphate (UTP) are converted to uridine diphosphate (UDP) glucose (UDP-G) catalyzed by UDP-glucose phosphorylase (UP). Glycogenin (GN) initiates glycogen synthesis via self-glucosylation by transferring glucose from UDP-G to GN. GN interacts with the dephosphorylated, active glycogen synthase (GS-OH). GS builds α -1,4-glycosidic linkages while the branching enzyme (BE) establishes α -1,6-glycosidic branchpoints within the glycogen molecule. **Glycogenolysis:** Glycogen is converted to G-1-P by glycogen phosphorylase (GPH-P), being active in the phosphorylated state, and by the debranching enzyme (DBE). Glucose can also be directly synthesized from glycogen within lysosomes possessing the lysosomal α -glucosidase (GAA). G6Pase: Glucose-6-phosphatase. Modified after [89,90].

2. Objective

With this thesis, an active contribution to the refinement of metabolic cage restraint for the laboratory mice is to be achieved. The main objective pursues a comprehensive comparison of two different metabolic cage types. The analysis of the extent to which the restraint in metabolic cages affects the metabolic phenotype of mice is based on two separate research foci. The first research focus includes the impact on animal welfare while the second focus comprises effects on metabolic parameters.

Based on these two research foci, the following questions were tested:

- (1) Can the general stress level and the cold stress of mice be alleviated during metabolic cage restraint?
- (2) Can the energy resources of mice restrained in metabolic cages be more effectively preserved?

The two metabolic cages to be compared here include the Innovative metabolic cage (IMC) and the Tecniplast metabolic cage (TMC). The IMC represents a self-built cage construction with integrated refinement measures to improve the housing conditions for mice during restraint therein. The TMC is commercially available and is commonly applied by the scientific community. C57BL/6J mice, exemplary for other mouse strains, were selected for experiments since this inbred mouse strain is most frequently used in biomedical research. Because of the high stress potential emanating from metabolic cages, the restraint was limited to 24 h and was solely repeated once, totalling two restraints.

3. Materials and Methods

3.1 Animal experiment

3.1.1 Ethical statement

The animal experiment was reviewed and approved by the Brandenburg State Authority (Landesamt für Arbeitsschutz, Verbraucherschutz und Gesundheit - LAVG) with the designated animal experiment number: 2347-14-2019. All interventions were performed in compliance with the German Animal Welfare Act. Mice were handled and housed according to recommendations and guidelines of the Federation of European Laboratory Animal Science Associations [93,94] and the Society of Laboratory Animal Science [38].

3.1.2 Mouse strain and housing conditions

Mice (*Mus musculus f. domesticus*) originated from in-house breeding in the central laboratory animal husbandry at the Max Rubner Laboratory (MRL) which is associated with the German Institute of Human Nutrition (DIfE) (Germany). The inbred C57BL/6J strain was used for experiments stemming from the Jackson Laboratory (United States). Female and male mice were utilized for conducting this animal experiment.

Mice were bred and held under specified pathogen free (SPF) conditions. Experiments were also conducted under SPF hygiene standards. Two separate rooms, one for animal husbandry and one for experimental procedures, were used. The SPF-area was surrounded by a barrier. All utilized materials were sprayed with Optisept (2%) during a 30 min sterilization program in the airlock (15 min spray, 15 min ventilate) before entrance into SPF-area. Water, food, and cages with bedding material was autoclaved. Hygiene monitoring of the central animal husbandry of the DIfE is carried out quarterly using litter and contact sentinels according to the recommendations of the Society of Laboratory Animal Science. Young adult sentinels with proven SPF status are transferred into the respective holding rooms for a period of at least three months and are examined by a certified laboratory (GIMmbH, Michendorf, Germany). Blood samples of sentinels are also taken and analyzed by a reference laboratory (Biodoc, Biomedical Diagnostics, Hannover, Germany). Animal care takers and experimenters wore overalls, hairnets, surgical masks, and gloves. Shoes were changed within airlock.

Before the experiment started, mice were housed in groups (n = 5) in open polycarbonate cages of type III. For male mice, single housing in open polycarbonate cages of type II was required after the beginning of experiments due to aggressive behavior against conspecifics. The same type II polycarbonate cage was used for controls. Since open cage systems were used, olfactory as well as visual contact between mice was maintained at all times. Home cages and control cages contained bedding material and standardized enrichment including the following: 1 nestlet, 2 tissues, 1 gnawing bar, and 1 cardboard house. Standard conditions were maintained in the animal husbandry: room temperature 23°C ± 1, relative humidity 50% ± 10, light:dark cycle 12:12 h of artificial light (lights on: 6 am to 6 pm). A commercial pelleted diet was fed to mice (ssniff Spezialdiäten GmbH, Soest, Germany). Acidified water (pH 2.5 - 3) and autoclaved food pellets were provided *ad libitum*. Two animal care takers and two experimenters handled mice during breeding and the experiment in order to minimize stress reactions.

3.1.3 Study design

A sample size calculation was performed in order to define the required animal number for each experimental subgroup. A total of 50 female and male mice aged from 66 d to 73 d were used. Sibling animals were randomly assigned to six study groups: control cage (female: n=5, male: n=5), Tecniplast metabolic cage (TMC; female: n=10, male: n=10), and Innovative metabolic cage (IMC; female: n=10, male: n=10).

The study design is shown in **Figure 11**. On the first day of the experiment baseline values were determined. In order to assess the animal's wellbeing before start of experiments, the Fur Score (FS) was determined and pictures of mice for the Mouse Grimace Scale (MGS) were taken simultaneously in front of white self-built cage borders. Two different behavioral tests, Elevated Plus Maze (EPM) and Open Field Test (OFT), were conducted afterwards. Metabolic parameters were assessed including body weight (BW), body composition (BC) *via* Nuclear Magnetic Resonance (NMR), and feces were collected for Fecal Corticosterone Metabolites (FCM) quantification. Mice were returned to their home cages with familiar group constellations after determination of baseline values.

After a 6 d recovery period, mice were transferred into either control cage, TMC or IMC. Mice were single housed for 24 h and BW as well as BC measurements were conducted before transfer. Pictures of mice within different cage systems were taken with a thermal imaging camera at the beginning and end of the 24 h time period to examine cold stress. To study behavioral patterns during 24 h single housing, videos were recorded at specific time intervals. Shortly before completion of the 24 h period, FS and MGS data were collected. Animals were directly transferred from cages into both behavioral test arenas. After conducting the behavioral tests, BW and BC was measured again. Females were returned to their home cages in groups (n = 5) while males were single housed until the end of the experiments. Metabolic cage data were gathered including total fecal output, urine volume, food and water consumption. Subsequent to first restraint into different cage systems, a 6 d recovery period was repeated following second restraint including the same experimental workflow. Animals were euthanized after deep inhalative isoflurane narcosis by terminal exsanguination.

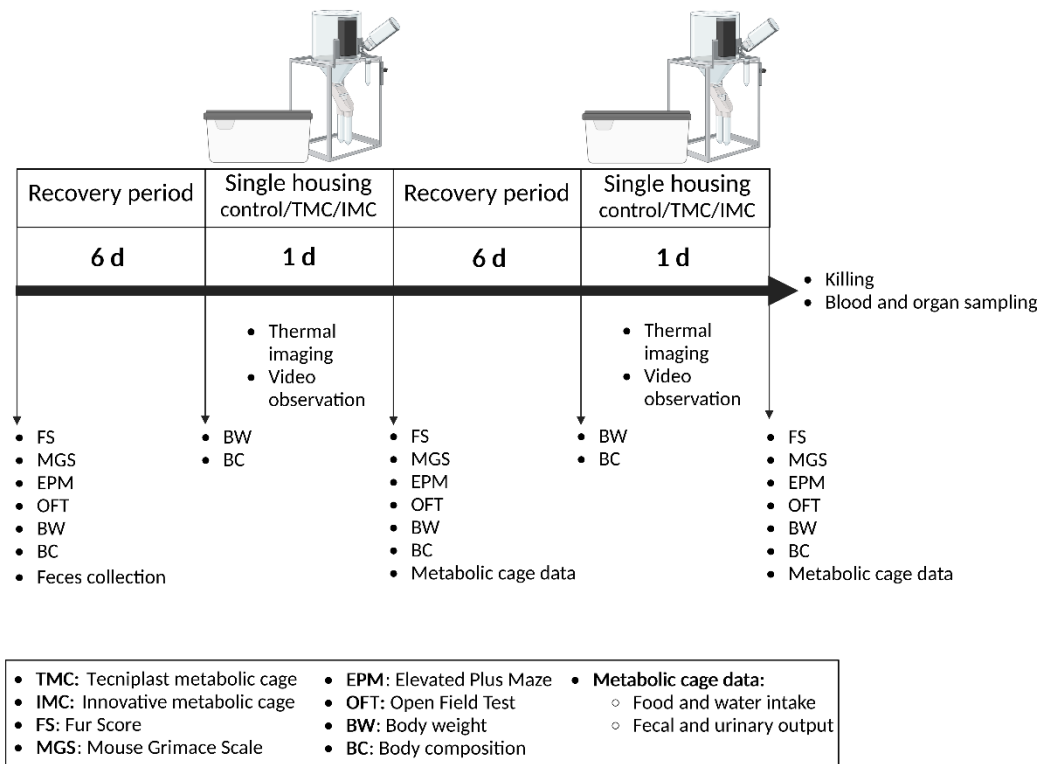


Figure 11. Study design of the conducted animal experiment shown as a time progression. Female and male C57BL/6J mice at the age of 10 weeks were single housed in either control cage (control), Tecniplast metabolic cage (TMC) or Innovative metabolic cage (IMC) for a time period of 1 d. Single housing in the three cage types was repeated once with a 6 d recovery period in between. FS: Fur Score, MGS: Mouse Grimace Scale, EPM: Elevated Plus Maze, OFT: Open Field Test, BW: body weight, BC: body composition.

3.1.4 Description of the metabolic cages

The Innovative metabolic cage (IMC) was constructed in the research workshop of the DfE by modification of a metabolic cage model constructed by Hatteras Instruments, Inc. (model: MMC100, obese design) (see **Figure 12**). We conducted a comparative study by investigating the self-built IMC and the commercially available Tecniplast metabolic cage (TMC, Type 304, Stainless Steel). A design overhaul of the TMC model was performed, which is described in detail in the following.

In general, the metabolic cage is used for continuous collection and clean separation of fecal and urine samples. For this purpose, the cage floor represents a grid of stainless steel with a funnel system underneath guiding samples into collecting vessels. The grid mesh size was reduced from 0.6 x 3.5 cm (TMC) to 0.4 x 0.4 cm (IMC). Front paws of mice show dimensions of 0.3 x 0.5 cm and hind paws of 1.7 x 0.5 cm.

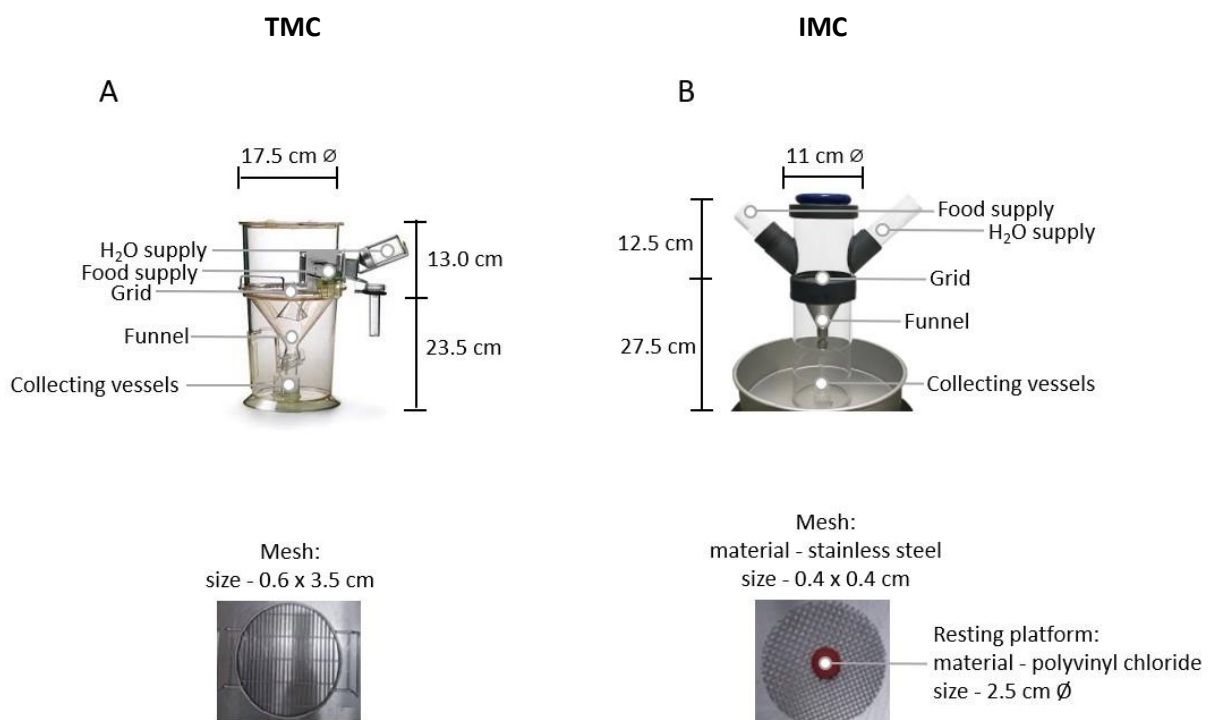


Figure 12. Comparison of applied metabolic cage types in animal experiment. A: Tecniplast metabolic cage (TMC), B: Innovative metabolic cage (IMC). Image source from TMC: www.tecniplast.it; Copyright Tecniplast S.p.A.

In addition to implementation of mesh size reduction, a resting platform ($\varnothing=2.5$ cm) made of plastic material was added centrally on top of the cage grid. Overall cage volume of the IMC was reduced to 1.2 dm³ (used cage space of mice from grid to lid). The metabolic cage construction from Tecniplast GmbH possesses a larger cage volume of 3.1 dm³. Water and food consumption of mice can also be monitored in metabolic cages. An angled food hopper and water supply was mounted on the IMC.

3.1.5 Assessment of animal welfare

3.1.5.1 Fur Score

The Fur Score (FS) represents an objective tool to determine the grooming state of fur in order to draw conclusions on mouse wellbeing and corresponding stress level. Fur quality of mice was assessed between 8 am and 10 am at three points of time: baseline value in front of cage borders, just before expiration of first and second restraint (24 h) in either of three cage systems. Two observers assigned scores at each acquisition date independently and both scores were averaged for each time (mean). The FS comprises a four degree scale and is defined as described in **Table 3** [95]:

Table 3. Fur Score: detailed evaluation scheme (adapted from [95]).

Score	Description		
1	<u>Fur:</u> -well-groomed, smooth, shiny -not tousled, spiky patches	<u>Whiskers:</u> -long -normal	<u>Eye conjunctivae:</u> -clear
2	<u>Fur:</u> -slightly fluffy -some spiky patches	<u>Rest of appearance:</u> -similar to Score 1	
3	<u>Fur:</u> -mostly fluffy -may also have slight staining	<u>Whiskers:</u> -may abnormally trimmed	<u>Eye conjunctivae:</u> -may slightly red
4	<u>Fur:</u> -fluffy, stained, dirty -may have some bald patches/traces/wounds	<u>Eye conjunctivae:</u> -red	

3.1.5.2 Mouse Grimace Scale

The Mouse Grimace Scale (MGS) was originally developed to assess pain in nonhuman animals [96]. This standardized behavioral coding system may also be affected by restraint stress, and thus can be used to determine stress levels of laboratory mice held in metabolic cages. In general, five facial expressions (orbital tightening, nose bulge, cheek bulge, ear position, and whisker change) are scored based on a three-point scale (0: not present, 1: moderate, 2: severe) (see **Figure 13**). Scores were obtained by photographs taken between 8:00 am and 10:00 am in front of inserted cage walls (light grey) during baseline value assessment (see **Figure 13**) or shortly before expiration of 24 h restraint in respective cage systems.

Photos were taken in the setting Shutter Priority (exposure time: 1/1000 s) and without flash adjustment. Three pictures per mouse were selected for scoring afterwards, ideally displaying the front, left, and right side of mouse face. Additionally, pictures were cropped to only show the head of the mouse to negate the influence of body position on scores. Photographs were randomized and rated by three independent scorers. The mean of five facial units was calculated for each scorer separately. Next, the MGS difference score was calculated between MGS scores of baseline values and MGS scores referring to different cage systems after first or second restraint.

Not present: **Moderate:** **Severe:**
0 **1** **2**

Orbital tightening



Nose bulge



Cheek bulge



Ear position



Whisker change



Inserted cage wall

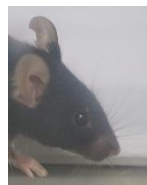


Figure 13. Mouse Grimace Scale (MGS): three-point scale of the five facial units based on sample photos are shown (Image source: [96]).

3.1.5.3 Assessment of cold stress by thermal imaging camera

Thermal images of mice kept in metabolic cages and control cages were taken in order to assess potential cold stress. Pictures taken immediately after transfer of mice into the cages, and shortly before expiration of 24 h restraint, were obtained between 08:00 am and 10:00 am. Cages were removed from shelves and thermal images were taken without cage lids. Cardboard houses were taken out of control cages shortly before thermal imaging. In total, cold stress was assessed for both restraints in respective cage systems. The thermal imaging camera settings were defined as follows: temperature scale 20°C - 38°C, color pallet lava, atmospheric temperature 23°C, object distance 1 m, relative humidity 50%, emittance 0.95, and reflected apparent temperature 20°C. The infrared camera assessed three points within each picture. The middle point (2) was located on the back of each mouse, measuring body surface temperature, and the outer points (1 and 3) assessed cage temperature (see **Figure 14**). Cage temperature of points 1 and 3 was averaged (mean) if the difference between both points was not $> 0.6^{\circ}\text{C}$.

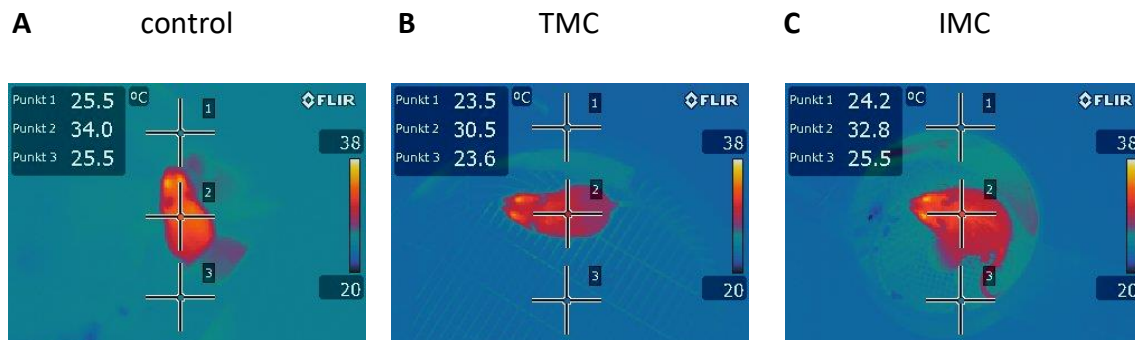


Figure 14. Sample photos of mice taken with the thermal imaging camera during restraint in **A:** control cage, **B:** Tecniplast metabolic cage (TMC), and **C:** Innovative metabolic cage (IMC). Points 1 and 3: cage temperature and point 2: body surface temperature of the mouse.

3.1.6 Analysis of behavior

3.1.6.1 Behavioral tests

Two different behavioral tests, the Elevated Plus Maze (EPM) and Open Field Test (OFT), were conducted between 10:00 am and 12:00 pm directly after 24 h single housing in both metabolic cage types and control cages. Mice were transferred into test arenas, an unknown environment with different smells and lighting conditions [97]. The animal's movements were analyzed by the automated video tracking system ©ANY-maze (version 4.99; Stoelting Europe, Dublin, Ireland). A laptop with tracking software was connected to two identical recording webcams which were placed directly above both arenas, attached to microphone stands. EPM and OFT testing was therefore conducted in parallel. Total runtime of both tests was 5 min, meanwhile mice could freely explore the new environment. Between runs behavioral testing arenas were cleaned with Wofacutan spray, medicinal washing lotion diluted with water. Six parameters collected during behavioral testing were included in analyses: excretion of fecal boli, time in zone [%], entries into zone [%], total distance traveled [m], and activity [%]. Both arenas were produced from light grey plates made out of polyvinyl chloride. This color tone was specifically chosen since mice possessing black fur were used and light grey represents a suitable background for video detection. White sheets, mounted on room-dividers, surrounded test arenas in order to yield comparable visual stimuli. Light sources were installed directly above test arenas to avoid shadowing and to achieve a standardized light intensity of 200 Lux. Behavioral test data were collected during baseline value determination and after first and second restraint in either of three cage types.

3.1.6.1.1 Elevated Plus Maze

The EPM was used to investigate anxiety behavior of laboratory mice [98,99]. During testing, animals are transferred onto an elevated platform and have to make a decision between entering open or closed arms. The cross-shaped EPM was elevated 50 cm above the ground. The EPM apparatus was divided into three zones: open arms (30 cm x 5 cm x 0.3 mm), closed arms (30 cm x 5 cm x 15 cm), and center (5 cm x 5 cm) (see **Figure 15 A**). Open and closed arms were oppositely arranged. Mice were placed in the center, facing a closed arm at the start of each experiment. Anxious mice would stay most of testing phase (total time: 5 min) in closed arms whereas exploratory mice would cross the center region and enter open arms.

3.1.6.1.2 Open Field Test

The OFT is commonly used within the frame of behavioral phenotyping studies [97], in particular to study exploratory drive and motor performance of mice [97–99,99]. In this experiment, a square shape OFT was used. Four wall plates (40 cm x 40 cm) were pinned on a ground plate (50 cm x 50 cm) (see **Figure 15 B**). The OFT arena was divided into center, middle zone, and outer zone. The whole area delimited from walls was covered with a grey-colored matte foil to prevent reflections. At the beginning of testing, mice were placed into the center region. The assumption suggests that less stressed mice actively explore the center region, while stressed mice would walk along the outer zone and stay in corners.

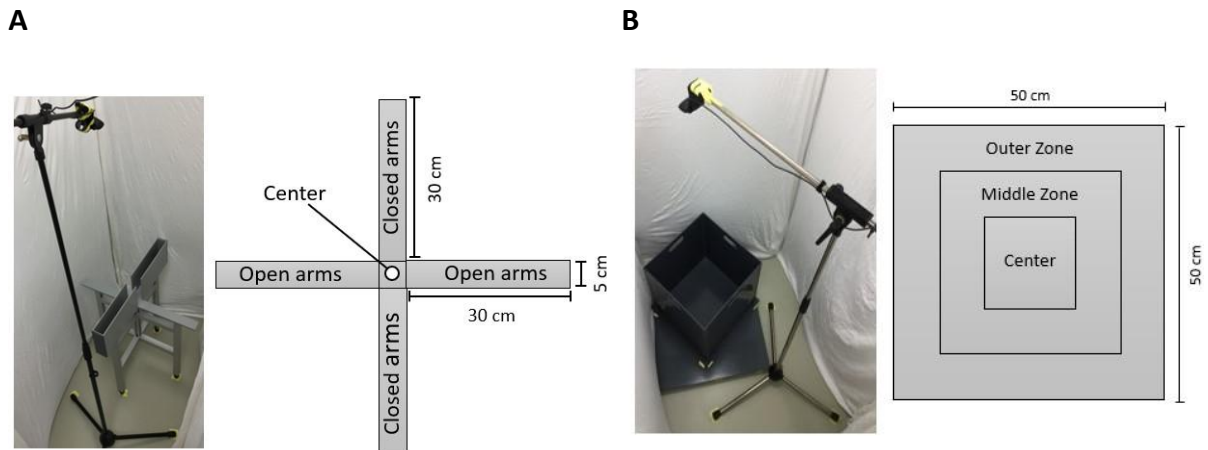


Figure 15. Experimental setup of A: Elevated Plus Maze (EPM) and B: Open Field Test (OFT). *Left: Photograph of apparatus in testing room. Right: Schematic illustration of top view on EPM and OFT with divided zones and dimensions [cm].*

3.1.6.2 Video observation

3.1.6.2.1 Experimental setup and observational periods

In addition to the EPM and OFT behavioral tests, mouse behavior was analyzed on the basis of videos that were recorded during restraint in either IMC, TMC or control cages. Ten control cages were placed in a shelf system comprising four shelves (see **Figure 16 A**). Ten cages of IMC or TMC were placed in an open shelf system, which consisted of three shelves (see **Figure 16 B and C**). A second shelf system including ten infrared cameras was positioned in front of the cage shelf. Each camera focussed on the cage area where the mouse was located and therefore, mice were recorded from the side.

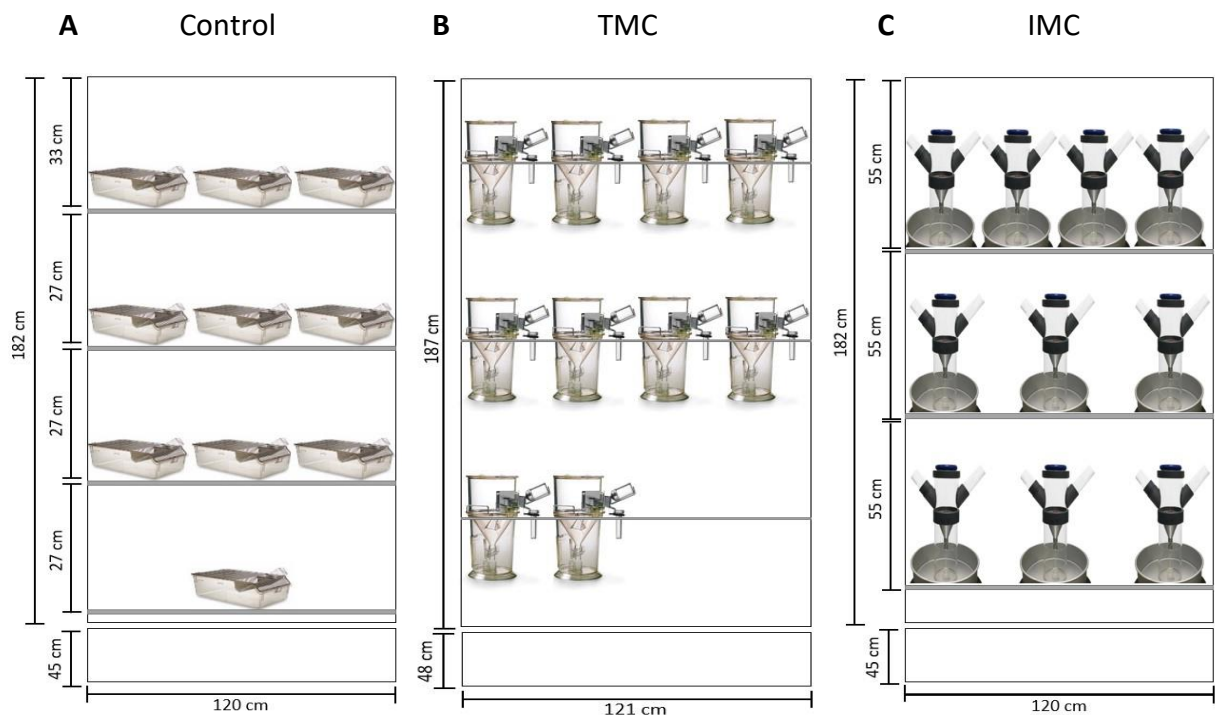


Figure 16. Shelf system and cage position for the video observation of mice during restraint in the control cage and metabolic cages. *A: Control cage, B: Techniplast metabolic cage (TMC), and C: Innovative metabolic cage (IMC).*

Videos of mice during 24 h restraint were recorded with D-ViewCam (D-Link GmbH, Eschborn, Germany) acquisition software. Seven 30 min observational periods were selected while two were in the light phase (12 pm, 3 pm), two in the transition between light and dark phase (6 pm, 6 am), and three in the dark phase (9 pm, 0 am, 3 am; see **Figure 17**). Behavior was scored every 3 min within 30 min time span (0, 3, 6, 9, 12, 15, 18, 21, 24, 27, 30), totalling 11 counts per observation interval. In total, behavior was analyzed 77 times for each mouse per restraint within respective cage system.

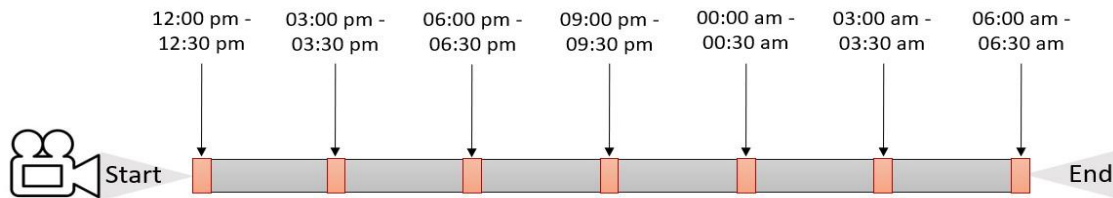


Figure 17. Representation of observation intervals per mouse in the respective cage system.

3.1.6.2.2 Video analysis on the basis of an exclusive ethogram

Recorded videos were analyzed by an independent scorer at the Justus Liebig University Giessen who did not participate in animal experimentation to control for observer bias. An exclusive ethogram was established for behavioral analyses based on suggested behavioral categories by the Stanford University of Medicine [23]. This ethogram type implies that the scorer could assign a behavior exclusively to one behavior category at the selected point in time, which amounted to every 3 min. In order to objectify and simplify assessment of behavioral patterns, behavior was classified into five categories prior to analyses (see **Table 4**). Since mice were single housed within different cage systems, a multitude of behavioral categories were excluded such as group sleeping and allo-grooming. Behavioral patterns of each mouse were altogether captured for 154 times during both 24 h restraints in IMC, TMC or control cage.

Table 4. Exclusive ethogram applied for video analysis of mice during restraint in different cage systems. Adapted from: [23]

Categories	General activity	Escape behavior	Immobility	Grooming	Other activity
Sub-categories	-Walking	-Jumping	-Still and alert	-General: various locations	-Drinking
	-Sniffing	-Running	-Sleeping		-Feeding
	-Coprophagy	-Gnawing on bars	-Resting	-From ears to snout	-Urination
	-Exploratory behavior	-Scratching	-Freezing	-Tail	-Defecation
		-Rearing	-Crouching		

3.1.7 Assessment of metabolic parameters

3.1.7.1 *Body weight and body composition*

BW differences between the start and the end of the 24 h exposure to different cage systems provide an important indicator for assessing animal wellbeing. Mice were transferred to a metal bowl which was positioned on top of a scale and mean value calculation for BW determination of moving mice was selected (F button). In addition to BW, BC of mice was assessed by NMR. This measurement represents a non-invasive technique since mice do not need to undergo anesthesia and are transferred and fixated into a 6 cm \varnothing plexiglass tube. This method is based on dynamic magnetization effects of hydrogen atoms, which are present in the organism in various chemical bonds and are thus excited in the magnetic field. This property is used to distinguish between muscle and fat mass. Mice were placed in the tube directly from the balance after BW measurement. The measuring time is approximately 1.5 min. After BC measurement, the tube containing the mouse was positioned in the home cage in order to release the animal. In total, BW and BC of each mouse was determined five times during the experiment: baseline value, before first restraint, after first restraint, before second restraint and after second restraint.

3.1.7.2 *Food and water intake*

Food and water intake was manually measured over a period of 24 h during restraint in both metabolic cage types. Food and water consumption of mice held in control cages for 24 h was not monitored. Group housed (female) and single housed (male) mice in home cages during the 6 d resting period were also not included in these analyses. Food pellets were filled into the food hoppers of both metabolic cages (see **Figure 18**). Accessibility to food must be ensured, as food pellets could get wedged within food hoppers. For TMC food hoppers, consisting of two pockets, a specific arrangement of food pellets was established. Three pellets were placed in the first front pocket (2 vertically and 1 horizontally on top) and two pieces in the second back pocket (2 vertically). The entire food hopper was weighed before (empty weight) and after filling with food. Food hoppers were hung on the cage apparatus and were additionally fixed with adhesive tape. After exposing mice to 24 h metabolic cage restraint, food hoppers were removed carefully to prevent food pellets from falling through. The food hopper was weighed again to calculate food consumption [g] during 24 h period. The empty weight of each food hopper was included in calculations. Additionally, shredded food from all cage equipment was collected in a weighing dish and its weight was factored in the calculations to avoid overestimation of food consumption.

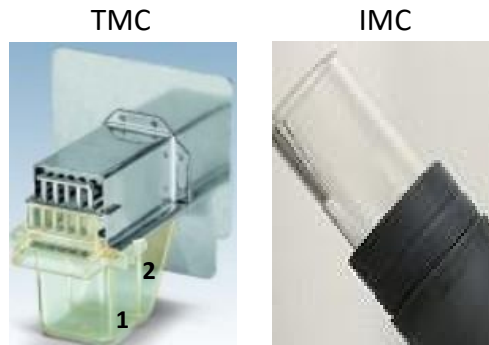


Figure 18. Photographs of food hoppers pertaining to the used metabolic cage types. 1 and 2: pockets of TMC food hopper. TMC: Tecniplast metabolic cage. IMC: Innovative metabolic cage.

Two different water bottle caps were used for metabolic cages, long caps for TMC and short caps for IMC. Autoclaved and acidified water was filled into water bottles up to the mark of 3 oz. (88.7 mL). Prior to this, the empty weight of the water bottle plus cap was determined. In order to acquire water consumption data [g], filled bottles with respective caps were weighted before and after 24 h restraint in metabolic cages. The empty weight of each water bottle plus cap was included in calculations. Water supply was added after the mouse was transferred into the metabolic cage to prevent leakage of the bottle by movement. After termination of the 24 h restraint in metabolic cages, water bottles were removed first.

3.1.7.3 Feces and urine collection

Both metabolic cage types possess separate vessels for collection of excreted urine and feces. Urine was transferred into tubes with a pipette to determine total volume [μL]. Fecal samples were collected with a forceps from collecting vessels, more rarely from the close-meshed IMC grid. Weight of feces [g] was obtained after transfer into tubes from which the empty weight was previously determined. Feces were additionally collected for baseline value determination in life week 10 of mice. Urine and fecal samples were stored at -80°C until analysis.

3.2 Laboratory analyses

3.2.1 Organ preparation

Deep anesthesia was induced by inhalative isoflurane narcosis until the determination of death by reflex check (interdigital reflex, corneal reflex). Exsanguination of euthanized mice *via* puncture of the *Vena cava* followed. Removed organs were either (snap-)frozen in liquid nitrogen and stored at -80°C until analyses or sections were transferred into Histosets and fixed in 4% paraformaldehyde solution for histological analyses.

Brain

Mice were decapitated directly after euthanasia and the mouse head was kept on ice. Ears, fur, and whiskers were removed with scissors. The skull was opened on both sides by cutting from the occipital bone to the frontal bone without incising the brain underneath. The skull cap was lifted with a forceps into the rostral direction. After complete removal of the skull cap, the head was rotated 180 degrees with the cerebral cortex pointing downwards. The brain was lifted out of the skull with forceps starting at the cerebellum. The olfactory bulb and *medulla oblongata* were removed (see **Figure 19**). The extracted brain was placed in a cooled brain block with the ventral region of the brain pointing upwards. Coronal slices representing specific brain areas were prepared.

The bregma (0) was set by identifying the characteristic outer lines of the *hypothalamus* (HTM) and by slicing the brain rostrally located to the HTM. Two spaces (+2 to 0) from the bregma, rostral anterior, defined *caudate putamen* (CPU) as well as *nucleus accumbens* (NAC). HTM was assigned two slices away (0 to -2) from the bregma into caudal posterior direction. Four spaces (-2 to -4) starting from bregma, also into caudal posterior direction, allocated the ventral tegmental area (VTA) and *substantia nigra* (SN) (see **Figure 20**). Brain slices were transferred into cryotubes and fresh weight was determined.

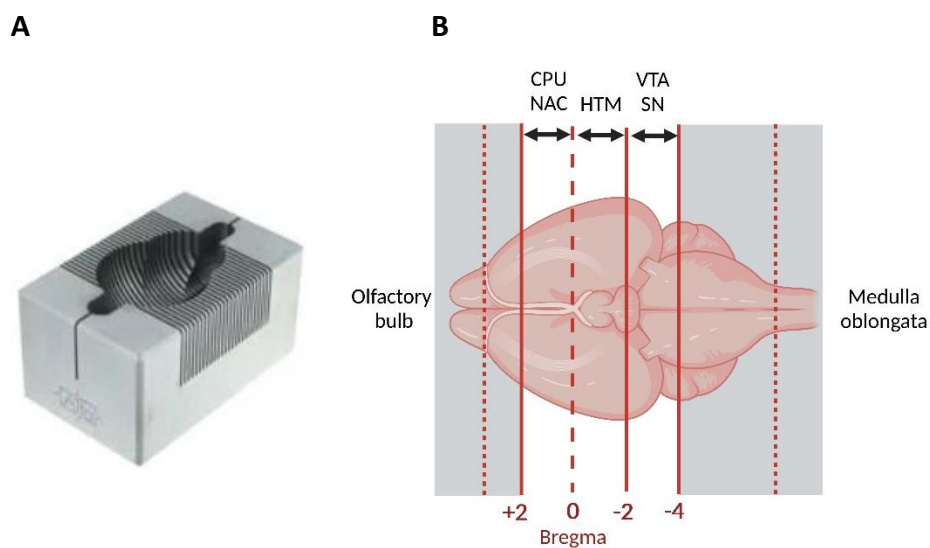


Figure 19. A: Used brain block for the preparation of coronal slices from murine brain. Image source from brain block: www.stoeltingco.com; Copyright Stoelting Co. **B: Dissection of respective brain areas.** CPU: caudate putamen, NAC: nucleus accumbens, HTM: hypothalamus, VTA: ventral tegmental area, SN: substantia nigra.

After decapitation, 70% ethanol was sprayed on fur for disinfection and the abdominal cavity of mice was opened with an incision along the *Linea alba*. Skin and muscles were intersected at once. Organs were removed and fresh weight was determined before division into respective sections depending on subsequent laboratory analyses.

Liver

The liver was fixed with forceps on the ventral side while the portal vein was cut and the tissue was removed without damaging the gallbladder. Connective tissue was detached, and the liver was divided into three sections:

(1) *lobus sinister lateralis hepatis*

(2) *lobus sinister medialis hepatis* and *lobus dexter medialis hepatis*

(3) *lobus dexter lateralis hepatis* and *lobus caudatus hepatis*.

Section 1 was used for histological analyses (Periodic Acid Schiff/Hematoxylin staining) while the other two sections were cryo-preserved in liquid nitrogen. Glycogen concentration was determined in liver Section 2. Section 3 was additionally pulverised under liquid nitrogen.

Brown adipose tissue

Fur of neck region was disinfected with 70% ethanol and incised afterwards. Interscapular brown adipose tissue (BAT) was cut out and excess white adipose tissue was detached. Half of BAT was shock-frozen in liquid nitrogen and served for analyses of *Ucp1* mRNA levels. The other half was utilized for histology.

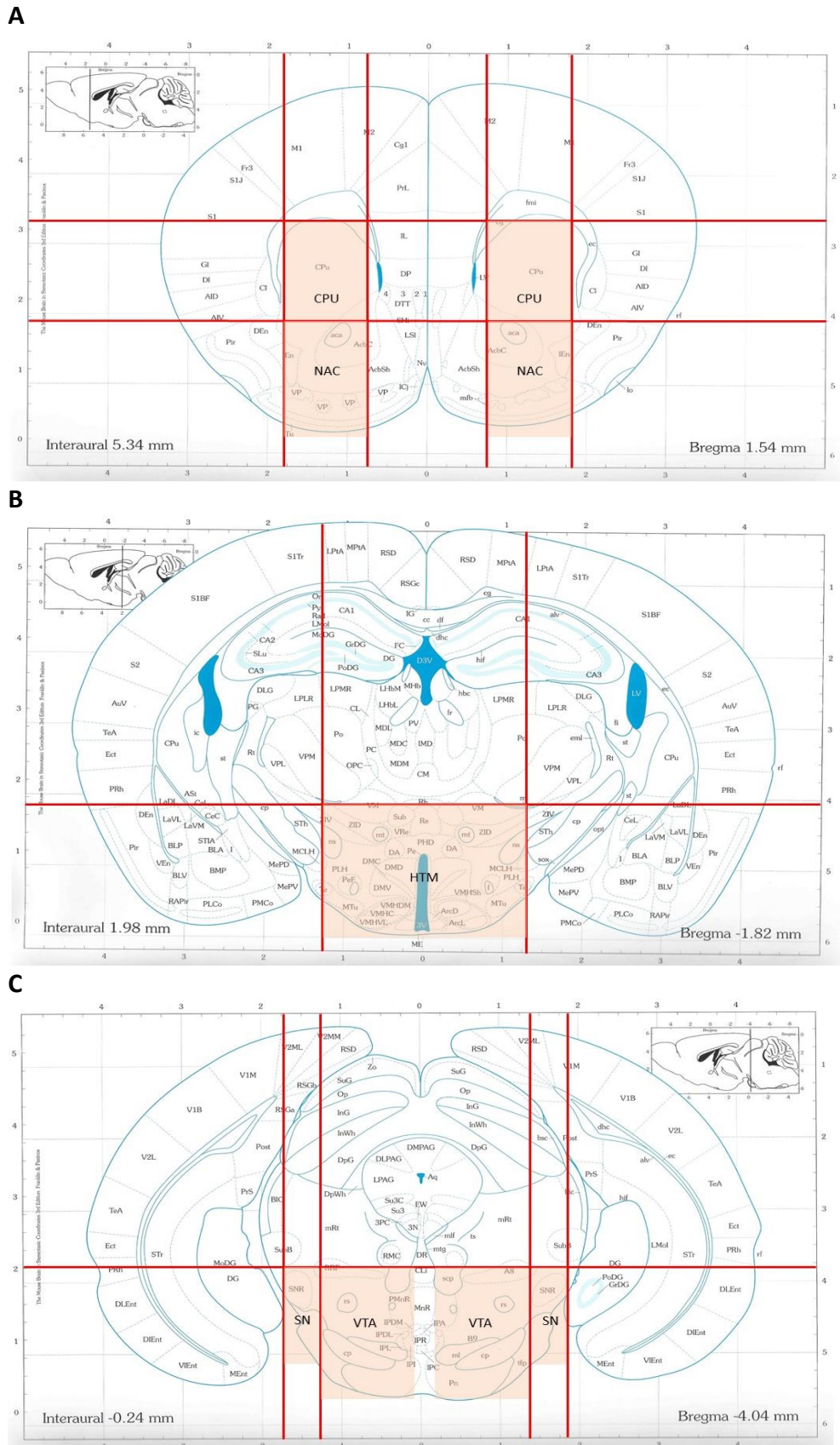


Figure 20. Dissection (red lines) of brain areas (yellow/pink squares) of interest (adapted from [100]). A: caudate putamen (CPU) and nucleus accumbens (NAC); B: hypothalamus (HTM); C: ventral tegmental area (VTA), substantia nigra (SN).

3.2.2 Histology - Periodic Acid Schiff/Hematoxylin staining

The extracted liver was directly transferred into a 4% paraformaldehyde solution for 24 h at room temperature (RT). Fixed tissue was washed with cold tap water for 24 h and was subsequently dehydrated with ethanol solutions in ascending concentrations. Tissue samples were mounted in paraffin, frozen, and sections were cut by using a microtome. Sections (2-4 μm) were transferred onto microscope slides by use of a water bath and were dried thereafter. The sections were deparaffinized:

Toluene	3 min
Toluene	4 min
Ethanol 100%	2 min
Ethanol 100%	3 min
Ethanol 96%	2 min
Ethanol 70%	2 min
ddH ₂ O	2 min

After removing paraffin from slides, staining with Schiff reagent and hematoxylin as counterstaining followed:

1% aq. Periodic Acid Solution	10 min
ddH ₂ O	3 x 2 min
Schiff reagent	15 min
Sulfite H ₂ O (100 mL ddH ₂ O, 6 mL sodium metabisulfite, 5 mL hydrochloric acid)	3 x 2 min
Running tap H ₂ O	15 min
ddH ₂ O	1 min
Hematoxylin	3 min
Running tap H ₂ O	7 min
ddH ₂ O	rinsing

Stained slides were dehydrated starting with 70% ethanol in ascending concentrations (removal of paraffin content in reverse order). Periodic Acid Schiff (PAS) staining is based on a histochemical principle to detect polysaccharides including glycogen. In the first step of the reaction, periodic acid induces oxidation of diols within the polysaccharide structure, resulting in aldehyde formation at the two ends belonging to each broken up monosaccharide ring. Formed aldehydes react with the Schiff reagent, resulting in a purple color formation. Hematoxylin is a base that preferentially colors acidic components of the cell, such as cellular structures (nucleus) containing deoxyribonucleic acid (DNA) and ribonucleic acid (RNA), in a bluish tint. Slides were scanned using a light microscope and pictures were taken with a camera connected to the ocular by applying the imaging software cellSens™ (Evident Europe GmbH, Hamburg, Germany). Stained *versus* unstained pixels, within a predefined range, for either PAS or hematoxylin staining were calculated with ImageJ (NIH) using the Color Deconvolution plugin “Haematoxylin and Periodic Acid of Schiff”.

3.2.3 Molecular biological methods

3.2.3.1 RNA isolation from brown adipose tissue

Total RNA from BAT was isolated by phenol-chloroform extraction with Invitrogen™TRIzol™Reagent (see TRIzol Reagent User Guide: Isolate RNA, Doc. Part No. 15596026.PPS, Pub. No. MAN0001271, Rev. B.0, according to manufacturer's instructions, Thermo Fisher Scientific, Waltham, United States). BAT tissue was pulverised under liquid nitrogen with a mortar. 20 mg of BAT tissue was utilized for RNA isolation. Approximately 10 ceramic beads and 1 mL of TRIzol™Reagent were added to tissue samples. Since TRIzol™Reagent inhibits RNase activity, integrity of RNA was preserved. Tissue samples were homogenized by using a Beadruptor and TRIzol™Reagent thereby disrupts cells and dissolves cell components. Five cycles of homogenization were repeated at the setting *High Speed* for 20 s. Samples were cooled on ice for 1 min between runs. Homogenates were centrifuged for 5 min (12,000 x g; 4°C). The supernatant was transferred to a new tube and incubation for 5 min at RT followed for completing dissociation of the nucleoproteins complex. 0.3 mL of chloroform per 1 mL TRIzol™Reagent was added and thoroughly vortexed. After an incubation for 3 min at RT, samples were centrifuged for 20 min (18,400 x g; 4°C). Thereby, the solution formed three phases: a lower red phenol-chloroform phase, an interphase, and a colorless upper aqueous phase. The upper phase, including RNA, was transferred to a new tube. 0.5 mL of isopropanol was added per 1 mL TRIzol™Reagent. Samples were inverted and incubated at 4°C for 10 min. Another centrifugation step was performed for 45 min (18,400 x g; 4°C). Precipitated RNA formed a white pellet at the bottom of the reaction vessel. Supernatant around the pellet was removed and discarded. The pellet was washed with 1 mL of 75% ethanol per 1 mL of TRIzol™Reagent. After thorough mixing on a vortex mixer, samples were centrifuged for 5 min (7,500 x g; 4°C). The complete supernatant was discarded again. Samples were air-dried for 10 min. The pellet was dissolved in 35 µL of nuclease-free H₂O and subsequently incubated at 58°C for 15 min. Purity and concentration [µg] of isolated RNA was determined with a NanoDrop spectral photometer. Optical density of isolates was measured at 230 nm (absorption of salts), 260 nm (absorption of total nucleic acids), and 280 nm (absorption of proteins). An adequate purity of isolates was defined in the range of 1.8 to 2.0 for ratios of 260 nm to 280 nm. If ratios of 260 nm to 230 nm were falling below 2.0, contamination of salts within the samples could not be excluded. If measured ratios were not within defined range, RNA isolation of pulverised tissue was repeated. For additional purification of RNA isolates, DNase from *E. coli* cells was added to samples in order to digest remaining single- and double-stranded DNA. 8 µg of isolated RNA was subjected to digestion with DNase, 2 µL of DNase (1 u/µL) was added, and the reaction mixture was filled up to 30 µL with reaction buffer (DNase I, RNase-free Kit, Thermofisher Scientific, Waltham, United States). The mixture was incubated for 30 min (600 rpm, 37°C). 1 µL of ethylenediaminetetraacetate (50 mM) was added and incubated for 10 min (600 rpm, 65°C) in order to terminate digestion with DNase. Isolated RNA samples were stored at -80°C.

3.2.3.2 Complementary DNA synthesis

For analysis of gene expression *via* polymerase chain reaction (PCR), reverse transcription of RNA into complementary DNA (cDNA) was conducted with the Revertaid™ First Strand cDNA Synthesis Kit (ThermoFisher Scientific, Waltham, United States). The first cDNA strand was generated from an initial hybrid consisting of isolated messenger RNA (mRNA) and cDNA. mRNA was degraded with RNase resulting in RNA fragments and an intact single-stranded cDNA. RNA fragments were then completed complementary to single-stranded cDNA resulting in a double-stranded cDNA, which could be used for quantitative reverse transcription PCR (qRT-PCR).

2 µg of RNA was subjected to reverse transcription and reaction mixture was filled up to 11 µL with nuclease-free H₂O. 1 µL of oligo (dT)₁₈ primers was added and the mixture was incubated for 5 min (65°C) by using a thermocycler in order to remove secondary RNA structures. Samples were cooled to 4°C. A master mix for each sample was prepared consisting of: 4 µL of 5x reaction buffer, 1 µL nuclease-free H₂O, 2 µL of deoxyribonucleotide triphosphate mix (10 mM) and 1 µL RevertAid M-MuL V Reverse Transcriptase. Samples were returned to the thermocycler and the amplification run was performed:

Reverse Transcription	60 min	45°C
Inactivation of Reverse Transcriptase	5 min	70°C
Stop	∞	4°C

cDNA was stored at -20°C until performance of qRT-PCR. Reaction mixtures without Reverse Transcriptase were applied as controls for validation of absence of DNA in RNA isolates. 1 µL of nuclease-free H₂O was exchanged for 1 µL of Reverse Transcriptase in master mix.

3.2.3.3 Quantitative reverse transcription-polymerase chain reaction

Expression of the target gene uncoupling protein 1 (*mUcp1*) and two reference genes, β-actin (*mβ-actin*) and hypoxanthine-guanine phosphoribosyltransferase 1 (*mHprt1*), were analyzed within BAT tissue. Oligonucleotide primers from Eurofins Genomics (Ebersberg, Germany) were utilized for qRT-PCR (see **Supplemental Table 4**). Specificity of qRT-PCR run was checked on the basis of melting curve analyses and agarose gel electrophoresis was conducted to verify product size of amplicates. 50 ng in 4.5 µL nuclease-free H₂O of respective cDNA sample was subjected to qRT-PCR. 0.25 µL of 10 µM primers, forward and reverse primer separately, and 5 µL of SYBR Green/Fluorescein qPCR Master Mix (Thermo Fisher Scientific, Waltham, United States) were added to each cDNA sample on a 96-well PCR plate. Quantification of each transcript was carried out in duplicate. Every qRT-PCR amplification run consisted of (LightCycler®, Roche Deutschland Holding GmbH, Mannheim, Germany):

Initial denaturation	10 min	95°C	
	15 s	95°C	
Amplification	15 s	58°C (annealing)	42
	15 s	72°C	cycles

Levels of gene expression are proportional to the measured fluorescent signal and were quantified based on the $2^{-\Delta\Delta CT}$ method [101]. For normalization of the respective target gene to reference gene, the mean of both reference genes referring to the same sample was included in calculations [102].

3.2.4 Biochemical methods

3.2.4.1 Determination of total protein by Bradford method

Protein content in liver samples was quantified by using the Bradford method. The chromophore Coomassie Brilliant Blue G-250 interacts with amino groups and aromatic amino acid residues of proteins under acidic conditions. Protein concentrations were calculated based on the calibration curve with bovine serum albumin standard (sequential dilution: 7.8 - 1000 µg/mL). Liver samples were diluted with H₂O suitable for HPLC at the ratio of 1:50. 70 µL of diluted samples and standards were mixed with 630 µL of Coomassie Brilliant Blue solution. 150 µL of the mixture was subjected to microtiter plates in triplicate. Absorption of the blue colored protein-Coomassie-complex is measured at 595 nm and an additional reference filter at 450 nm was applied (Microplate Manager®6, BioRad Laboratories GmbH, Feldkirchen, Germany).

3.2.4.2 Determination of liver glycogen by UV method

Glycogen analyses of liver tissue was conducted with a Starch Kit (R-Biopharm AG, Darmstadt, Germany) [103]. First, tissue extracts were prepared and the weighing as well as homogenization process was performed according to chapter 3.2.3.1 RNA isolation from brown adipose tissue. 750 µL of 0.1 mol/L sodium hydroxide (per precise weight) was added (instead of TRIzol™ Reagent) to 35 mg of liver tissue. Homogenization of liver samples was performed by the Beadruptor for 5 cycles. Due to intense foaming during homogenization, samples were stored on ice for 30 min before centrifugation for 1 min (12,400 x g; 4°C). The supernatant fraction was transferred into new tubes and heated for 45 min (1,000 rpm; 70°C) subsequently. Samples were cooled down on ice for 5 min, thoroughly vortexed, and centrifuged for 45 min. Transfer of the supernatant into a new tube and 30 min of centrifugation followed. Clear supernatant was transferred into a low binding reaction vessel for storage. In case of a turbid supernatant fraction, centrifugation was repeated. Tissue extracts were stored at -20°C until glycogen analyses.

For the calibration curve, glycogen from bovine liver was dissolved in H₂O suitable for HPLC (10 min ultrasonic bath) to yield a concentration of 20 µg/µL (sequential dilution: 0.01 µg/µL - 3 µg/µL). Two controls consisting of glycogen from bovine liver at a concentration of 0.2 µg/µL were included. 1 µL of concentrated acetic acid was added to 50 µL of sample, standard (control/calibration curve) or blank (0.1 N sodium hydroxide). Either 100 µL of solution 1 containing amyloglucosidase (ca. 84 U) (glycogen) or 100 µL of H₂O suitable for HPLC (glucose) was added to each sample. The enzyme amyloglucosidase catalyzes the cleavage of glycogen to form D-glucose. Samples were vortexed and incubated for 15 min (600 rpm, 60°C) resulting in turbid sample mixtures. A centrifugation step for 10 min (21,000 x g; RT) followed. Triplicate testing of 30 µL each of the supernatant fraction per well was performed. 100 µL of H₂O suitable for HPLC and 100 µL of solution 2 was added to each well. Solution 2 contains adenosine triphosphate (ATP, ca. 190 mg) and nicotinamide adenine dinucleotide phosphate (NADP, ca. 75 mg). The microtiter plate was incubated for 3 min at RT. Measurement was performed at 340 nm in a microplate reader in order to determine self-extinction of ATP and NADP (Microplate Manager®6, BioRad Laboratories GmbH, Feldkirchen, Germany).

Thereafter 12 μL of solution 3 was added to each well followed by incubation for 15 min at RT. Measurement of sample extinction at 340 nm was repeated. Solution 3 contains the enzyme hexokinase (ca. 200 U) and glucose-6-phosphate-dehydrogenase (ca. 100 U). Hexokinase phosphorylates D-glucose to form D-glucose-6-phosphate by simultaneous production of adenosine diphosphate. This method is based on the oxidation of D-glucose-6-phosphate in presence of glucose-6-phosphate-dehydrogenase and NADP, forming D-gluconate-6-phosphate and NADPH (reduced form of NADP). Finally, absorbance of NADPH was measured at 340 nm, which is proportional to the amount of glycogen in the processed sample.

3.2.4.3 Enzyme Immunoassay - Fecal corticosterone metabolites

Fecal Corticosterone Metabolites (FCM) were measured in fecal pellets as this sampling technique represents a non-invasive alternative. The applied Enzyme Immunoassay (EIA) detects FCM with a $5\alpha\text{-}3\beta,11\beta\text{-triol}$ structure. Fecal extracts were prepared in our working group and the EIA was performed at the Department of Behavioural Biology at the University of Osnabrück in the laboratory of Prof. Dr. Touma. All of the excreted feces during 24 h single housing were collected in order to assess the acute stress response of mice. Fecal pellets were collected out of bedding and collecting vessels belonging to control cages and TMC or IMC respectively.

Frozen fecal pellets, stored at -80°C , were dried for 2-3 h at 80°C . Dried feces were ground with a mortar and an aliquot of 0.05 g was subjected to extraction. 1 mL of 80% methanol was added to 0.05 g aliquots, thoroughly homogenized and shaken for 30 min (orbital: 60 rpm, 10 s; reciprocal: 90° , 30 s; vibro/pause: 1° , 3 s). Fecal matter was separated from methanol by centrifugation for 10 min ($4,000 \times g$; RT). Supernatant was stored at -20°C and an aliquot of 500 μL supernatant was sent on dry ice to the University of Osnabrück for subsequent $5\text{-}\alpha\text{-pregnane-}3\text{-}\beta,11\text{-}\beta,21\text{-triol-}20\text{-one}$ EIA analysis [52,104].

3.2.5 Liquid chromatography tandem-mass spectrometry

3.2.5.1 Determination of corticosterone concentrations in urine samples

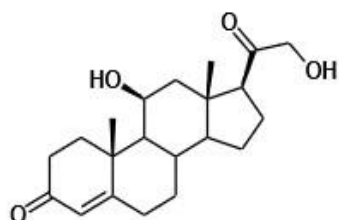
Native and glucuronidated corticosterone (see **Figure 21**) was extracted from mice urine samples collected during 24 h restraint in each metabolic cage type and subsequently quantified *via* liquid chromatography tandem-mass spectrometry (LC-MS/MS; Skyline Targeted Mass Spec Environment, open source). Extraction protocol extended over a period of 2 d and was adapted from Hauser, Deschner, and Boesch (2008) [105].

Extraction of glucuronidated corticosterone

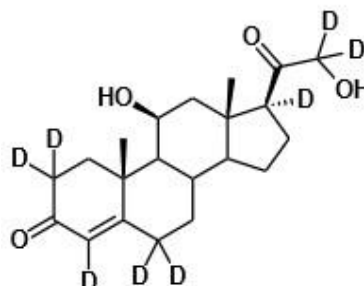
200 μL aliquots of 24 h urine collection were subjected to the extraction. For enzymatic hydrolysis of glucuronidated corticosterone, β -glucuronidase type VII-A from *E. coli* was applied. The lyophilized enzyme was dissolved in 5 mL H_2O suitable for HPLC prior to analyses. 800 μL of 0.25 M sodium phosphate buffer (pH 6.9), 40 μL of β -glucuronidase (200 U), and 10 μL of 1 pmol/ μL internal standard (Corticosterone-d8) were added. After thorough mixing, an incubation of the urine samples for 22 h (220 rpm, 37°C) was carried out.

150 μL of 10% sodium carbonate was added to stop enzymatic reaction (pH 9.6). Liquid-liquid-extraction was conducted in the following step by adding 2 mL of methyl tert-butyl ether and mixing for 10 min under agitation (orbital: 60 rpm, 45 s; reciprocal: 90°, 15 s; vibro/pause: 1°, 3 s). Samples were centrifuged for 10 min (260 x g, RT) and stored at -20°C for at least 30 min to induce a clear phase separation. Ether phase was fully evaporated (no heating, pulse vent: 1) and the residue was resuspended in 500 μL of 80% acetonitrile/0.1% formic acid. Reconstituted samples were transferred into an ultrasonic bath for 5 min, vortexed, and an aliquot of 100 μL was subjected to LC-MS/MS analysis (Mass Hunter, Agilent Technologies Germany GmbH & Co. KG, Waldbronn, Germany).

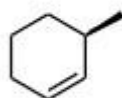
A

Corticosterone: $\text{C}_{21}\text{H}_{30}\text{O}_4$ $[\text{M} + \text{H}]^+ = 347.2$

B

Corticosterone-d8: $\text{C}_{21}\text{H}_{22}\text{D}_8\text{O}_4$ $[\text{M} + \text{H}]^+ = 355.3$

C

Fragment of Corticosterone: C_7H_{12} $[\text{M} + \text{H}]^+ = 97.1$

D

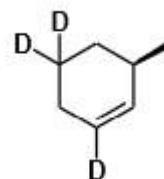
Fragment of Corticosterone-d8: $\text{C}_7\text{H}_9\text{D}_3$ $[\text{M} + \text{H}]^+ = 100.2$

Figure 21. Chemical structures of **A**: Corticosterone, **B**: Corticosterone-d8, **C** and **D**: respective fragments of reactions generating the most abundant product ions used for Multiple Reaction Monitoring (MRM) quantification.

Liquid chromatography tandem-mass spectrometry analysis

The native and glucuronidated corticosterone fractions were quantified by LC-MS/MS analysis directly after extraction (see **Table 5**).

Table 5. LC-ESI-MS/MS parameters for measurement of corticosterone in urine samples.

Column	Kinetex C8 (2.6 μ m, 150 x 4.6 mm)						
Column temperature	40°C						
Flow rate	0.450 mL/min						
Solvents	A	Water + 0.1% formic acid					
	B	Acetonitrile + 0.1% formic acid					
Gradient	1 min	20% B					
	8 - 9 min	100% B					
	9.01 - 12 min	20 % B					
Postrun	4 min	20% B					
Injection volume	5 μ L						
Source parameters	Mode	Positive					
	Capillary	4500 V					
	Drying gas temperature	120°C					
	Drying gas flow (N ₂)	11 L/min					
	Nebulizer	40 psi					
	Nozzle	0 V					
	Sheath gas temperature	400°C					
	Sheath gas flow (N ₂)	12 L/min					
Multiple reaction monitoring	Compound		Retention time [min]	m/z \rightarrow m/z	CE [eV]	Frag [V]	
	Corticosterone	Qualifier	8.50	347.2 \rightarrow 121.1	30	125	
		Quantifier		347.2 \rightarrow 97.1	40	160	
	Corticosterone-d8	Qualifier	8.48	355.3 \rightarrow 125.0	30	125	
		Quantifier		355.3 \rightarrow 100.2	40	160	
	Dwell time	175 ms					
	Cell accelerator voltage	5 V					

3.2.5.2 Determination of serotonin and dopamine concentrations in brain areas

The neurotransmitters dopamine (DA), including its metabolites 3-methoxytyramine (3-MT) and 3,4-dihydroxyphenylacetic acid (DOPAC), and serotonin (SRT) (see **Figure 22**) were quantified in five mouse brain areas (CPU, NAC, HTM, VTA, SN). Brain tissue was rapidly removed and dissected into specific brain areas as indicated in section 3.2.1 Organ preparation. The neurotransmitters were extracted from each brain area and immediately analyzed *via* LC-MS/MS in accordance with Schumacher *et. al.* [82].

Extraction of neurotransmitters

Extraction of neurotransmitter was performed on ice. A multicomponent working standard solution was added to a freshly prepared extraction buffer consisting of 0.002 M sodium thiosulfate in 0.2 M perchloric acid. The multicomponent working standard solution contained 500 nM DOPAC-d5, 50 nM [¹³C¹D⁵]-3-MT, 200 nM SRT-d4 creatinine sulfate complex prepared in ddH₂O and 400 nM DA-d4 hydrochloride prepared in 0.2 M perchloric acid. Approximately 20 ceramic beads and extraction buffer including working standard solution were added to each cryotube. Extraction buffer was added in different volumes depending on the brain area in consideration:

CPU: 1000 μ L; NAC, VTA, SN: 500 μ L; HTM: 300 μ L.

Samples were homogenized by a Beadruptor with the following settings: Speed=3 m/s (low), Time=0.30 s, Cycles=2 (5 s between cycles). The homogenates were centrifuged afterwards for 10 min (21,380 x g, 4°C). A defined volume of supernatant (CPU: 800 μ L; NAC, VTA, SN: 400 μ L; HTM: 200 μ L) was directly transferred onto Spin-X centrifuge tube filters and a centrifugation step for another 10 min followed. Filters were removed after centrifugation and discarded. 50 μ L of extracts were subjected to LC-MS/MS analysis (MassHunter, Agilent Technologies Germany GmbH & Co. KG, Waldbronn, Germany).

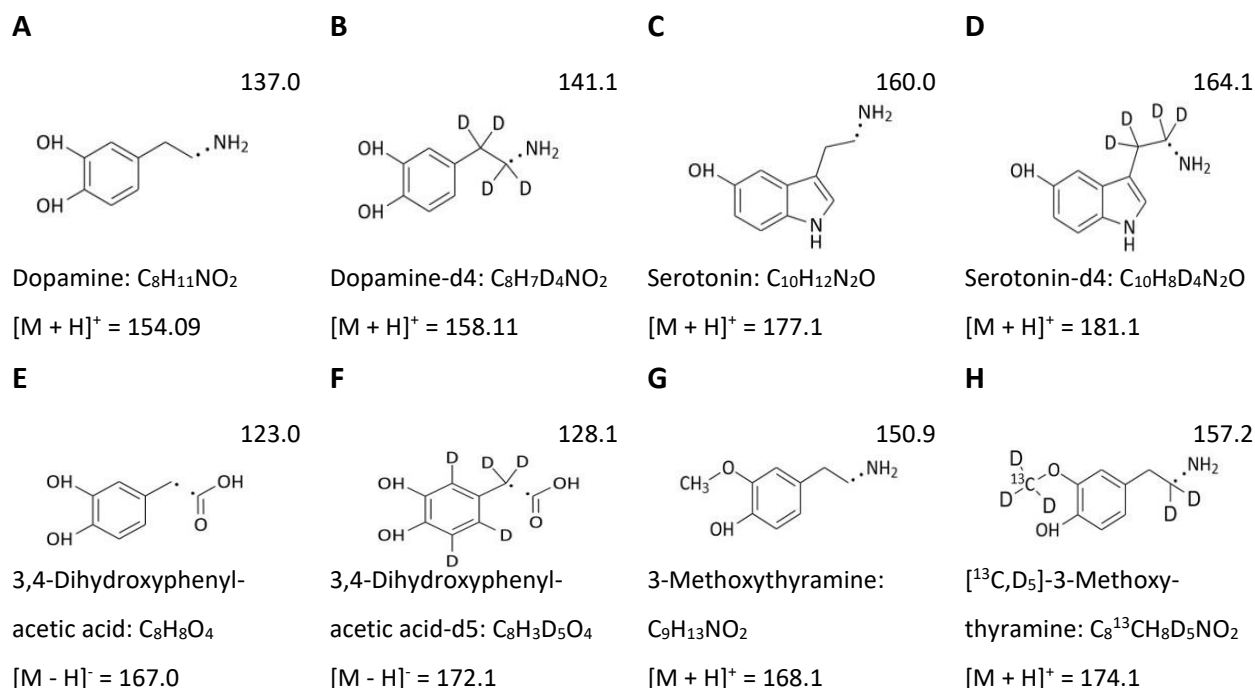


Figure 22. Chemical structures of A: Dopamine, B: Dopamine-d4, C: Serotonin, D: Serotonin-d4, E: 3,4-Dihydroxyphenylacetic acid, F: 3,4-Dihydroxyphenylacetic acid-d5, G: 3-Methoxytyramine, and H: [¹³C, D₅]-3-Methoxytyramine and their fragmentation reactions generating the most abundant product ions used for Multiple Reaction Monitoring (MRM) quantification.

Liquid chromatography tandem-mass spectrometry analysis

The brain extracts were immediately quantified by LC-MS/MS analysis (see **Table 6**).

Table 6. LC-ESI-MS/MS parameters for measurement of neurotransmitters in brain areas.

Column	YMC-Triart PFP (3 μ m, 3 x 150 mm)					
Column temperature	25°C					
Flow rate	0.425 mL/min					
Solvents	A	Water + 10 mM formic acid				
	B	Methanol + 10 mM formic acid				
Gradient	1 - 30 min	0 - 20% B				
	30 - 32 min	20% B				
	32 - 32.01 min	20 - 0 % B				
	32.01 - 36 min	0% B				
Postrun	1 min	0% B				
Injection volume	5 μ L					
Source parameters	Mode	Positive + Negative				
	Capillary	2000 V				
	Drying gas temperature	120°C				
	Drying gas flow (N ₂)	15 L/min				
	Ion funnel RF high	110 V				
	Ion funnel RF low	60 V				
	Nebulizer	40 psi				
	Nozzle	0 V				
	Sheath gas temperature	400°C				
	Sheath gas flow (N ₂)	12 L/min				
Multiple reaction monitoring	Compound		Retention time [min]	m/z \rightarrow m/z	CE [eV]	Polarity
	Dopamine	Quantifier	5.96 \pm 0.27	154.09 \rightarrow 137.0	9	Positive
		Qualifier		154.09 \rightarrow 91.0	25	Positive
	Dopamine-d4	Quantifier	5.94 \pm 0.27	158.11 \rightarrow 141.1	9	Positive
		Qualifier		158.11 \rightarrow 95.0	25	Positive
	Serotonin	Quantifier	16.35 \pm 1.07	177.1 \rightarrow 160.0	4	Positive
		Qualifier		177.1 \rightarrow 115.1	32	Positive
	Serotonin-d4	Quantifier	16.28 \pm 1.06	181.1 \rightarrow 164.1	4	Positive
		Qualifier		181.1 \rightarrow 118.1	32	Positive
	3,4-Dihydroxy-phenylacetic acid	Quantifier	14.46 \pm 1.01	167.0 \rightarrow 123.0	4	Negative
		Qualifier		167.0 \rightarrow 95.0	20	Negative
	3,4-Dihydroxy-phenylacetic acid-d5	Quantifier	14.31 \pm 0.82	172.1 \rightarrow 128.1	4	Negative
		Qualifier		172.1 \rightarrow 100.1	20	Negative
	3-Methoxythyramine	Quantifier	13.35 \pm 0.66	168.1 \rightarrow 150.9	4	Positive
		Qualifier		168.1 \rightarrow 91.0	24	Positive
	[13C1D5]3-Methoxythyramine	Quantifier	13.29 \pm 0.66	174.1 \rightarrow 157.2	4	Positive
Qualifier		174.1 \rightarrow 93.0		24	Positive	

3.3 Data analysis and statistics

Datasets are shown as interleaved scatter (plot individual values) and interleaved symbols (plot summary data) plots depicting means (standard deviation). Scatter plots (no line or error bar) were also used for data presentation. Stacked bars (plot summary data) depict means (standard deviation) or means only while points and connecting line plots solely displayed the means. Plots were generated by GraphPad Prism (version 6; Graphstats Technologies Private Limited, Bangalore, India). Statistical analyses were performed using IBM® SPSS® Statistics (version 20; IBM Deutschland GmbH, Ehningen, Germany).

Differences between two groups were studied by application of an independent-samples t test (normal distribution of data, two-tailed) or Mann-Whitney U test. For statistical analyses of differences between three groups, one-way analysis of variance (ANOVA) was utilized with the following post-hoc tests: Tukey's HSD (normal distribution, equal variances), Bonferroni (no normal distribution, but equal variances), and Dunnett's T3 (no equal variances). The Kruskal Wallis Test was alternatively applied to test for differences between three groups in case data were not normally distributed and to compensate for outliers. For testing of coherence between different data sets, bivariate correlation analyses were conducted by applying either the Pearson (normal distribution of data) or Spearman correlation coefficient. To test for inter-rater-reliability, the Fleiss' and Cohens Kappa (κ) besides intraclass correlation coefficients (ICC, model: two-way mixed, type: absolute agreement) were applied. Statistical significance between tested groups was accepted when * $P \leq 0.05$, ** $P \leq 0.01$, *** $P \leq 0.001$, and **** $P \leq 0.0001$, trends were defined when $0.05 < P < 0.1$.

4. Results

4.1 Animal welfare

4.1.1 Fur Score

Mice were restrained in the Innovative metabolic cage (IMC) or Tecniplast metabolic cage (TMC) or control cage for 24 h. The restraint was repeated once with a 6 d resting period in between what was referred to as first and second restraint. To assess animal welfare, the fur state of mice was rated before (baseline assessment) and after (first and second restraints) single housing in either metabolic cage types, TMC or IMC, or control cages. Whether fur state can be used to assess the distress between metabolic cage types (TMC vs. IMC) or between control cage and metabolic cage types (control vs. TMC, control vs. IMC) was the subject of this investigation. A significant difference in Fur Scores (FS) were observed between control cage and metabolic cage types (control vs. TMC, control vs. IMC, $P \leq 0.001$), but not between the two metabolic cage types (TMC vs. IMC, $P > 0.05$) except for males after 1. restraint ($P \leq 0.001$, see **Table 7**).

The black fur color and generally smooth fur state of the C57BL/6J mice often resulted in equal FS from both independent scorers (i.e. the standard deviation often amounted to 0.00). An ANOVA could therefore not be conducted to investigate differences in FS between the tested cage types. The independent-samples t test or Mann-Whitney U test were applied instead. A clear sex difference concerning the basal grooming state of fur was not apparent.

Table 7. Fur Scores of C57BL/6J mice at baseline, after first, and second restraints in control and metabolic cages.

Cage type	No. of restraint	Mean Fur Score (standard deviation)		Statistics		
Control	baseline	1.00 (0.00)		Control vs. TMC	P = 1.000	
TMC				Control vs. IMC		
IMC				TMC vs. IMC		
Cage type	No. of restraint	Female n=25	Male n=25		Female n=25	Male n=25
Control	first	1.00 (0.00)	1.00 (0.00)	Control vs. TMC	***	***
TMC		2.00 (0.00)	2.75 (0.26)	Control vs. IMC	***	***
IMC			2.00 (0.00)	TMC vs. IMC	P = 1.000	***
Cage type	No. of restraint	Female n=25	Male n=25		Female n=25	Male n=25
Control	second	1.00 (0.00)	1.00 (0.00)	Control vs. TMC	***	***
TMC		2.00 (0.00)	2.50 (0.53)	Control vs. IMC	***	***
IMC			2.00 (0.00)	TMC vs. IMC	P = 1.000	P = 0.063

Fur Score data are depicted as mean (standard deviation) referring to three different cage types. Differences between cage types were calculated by independent-samples t-test or Mann-Whitney U test. Fur Score data were analyzed separately for baseline values, as well as first and second restraints (TMC: Tecniplast metabolic cage, IMC: Innovative metabolic cage; *** $P \leq 0.001$).

4.1.2 Mouse Grimace Scale

Three independent scorers rated pictures of mouse faces referring to the coding system of the Mouse Grimace Scale (MGS) [96]. Fleiss' kappa (κ) statistics and intraclass correlation coefficients (ICC) were used in order to test for inter-rater reliability between the three scorers. Since the single facial action units were scored on a three-point scale (0, 1, 2), resulting in ordinal data, these data were analyzed *via* κ statistics. In order to have a direct comparison, scores for single facial action units were additionally analyzed based on the ICC (model: two-way mixed, type: absolute agreement). Analysis of mean MGS Scores (mean of five facial action units) and overall MGS Scores (sum of five facial action units, max 10) were conducted using ICC, as these measures can be considered as continuous data [106].

Inter-rater reliability with all datasets could not be confirmed among the three scorers (ICC < 0.50, κ < 0.21). The scores of one scorer were excluded from further analyses since pictures of mice were taken by this same person, which may have resulted in bias. Inter-rater reliability analyses were repeated for two scorers by applying the Cohens κ . Mean MGS Scores and overall MGS Scores were not comparable between both scorers, because ICC values were lower than 0.50 for all tested points in time including baseline, and first and second restraints. Subdividing MGS Scores into single facial action units showed sufficient inter-rater reliability for separate facial action units (see **Table 8**).

According to Koo and Li [107], ICC values were defined as follows:

- < 0.50 poor inter-rater reliability
- 0.50 - 0.75 moderate inter-rater reliability
- 0.75 - 0.90 good inter-rater reliability
- > 0.90 excellent inter-rater reliability

According to Landis and Koch [108], Fleiss' κ and Cohens κ were defined as follows:

- < 0 poor inter-rater reliability
- 0.00 - 0.20 slight inter-rater reliability
- 0.21 - 0.40 fair inter-rater reliability
- 0.41 - 0.60 moderate inter-rater reliability
- 0.61 - 0.80 substantial inter-rater reliability
- 0.81 - 1.00 almost perfect inter-rater reliability

Ear Position

Ear position represented the most reliable facial action unit with moderate inter-rater reliability between both scorers at all time points within, the baseline assessment, and after the first restraint, in all three different cage systems (see **Table 8**). Ear position scores were significantly higher after TMC restraint compared to IMC restraint after second restraint for females ($P \leq 0.001$) and males ($P \leq 0.05$, see **Figure 23 A-B**). When combining scores of ear position for both sexes, significantly higher ear position scores after TMC as opposed to IMC restraint were demonstrated after the first ($P \leq 0.01$) and second restraint ($P \leq 0.001$, see **Figure 23 C**).

Since baseline values ($\kappa = 0.410$) and scores after the first ($\kappa = 0.519$) and second restraint ($\kappa = 0.167$, almost fair inter-rater reliability) were comparable among the two scorers, the Difference Score was calculated for both restraints (see **Table 8**). Inter-rater reliability of the Ear Position Difference Score was fair for the first restraint ($\kappa = 0.335$) and approximately fair ($\kappa = 0.199$) for the second. No cage-dependent effect was detected for Difference Scores of ear position after first and second restraint, considering female and male mice separately and together (see **Figure 23 D-F**). Means of Difference Scores of ear position were in the negative range for both investigated time points and sexes. This indicates that the ear position scores did not deteriorate significantly over the course of the experiment compared to baseline.

Orbital Tightening

Orbital tightening indicated fair inter-rater reliability after the first restraint ($\kappa = 0.302$, see **Table 8**). Approximately fair inter-rater reliability was obtained for all time points ($\kappa = 0.191$) and at baseline ($\kappa = 0.188$). For females and males after the first restraint, no significant differences between the three tested cage types were detected (see **Figure 23 G**).

Nose Bulge, Cheek Bulge, Whisker Position

Scores of Nose Bulge indicated fair inter-rater reliability concerning all time points ($\kappa = 0.387$), but not for the three tested time points separately. Cheek bulge ($\kappa = 0.000$) and whisker position ($\kappa = 0.035 - 0.086$) alone showed slight inter-rater reliability.

Table 8. Inter-rater reliability of each facial action unit of the applied Mouse Grimace Scale.

Inter-rater Reliability between 2 Scorers	Ear Position	Orbital Tightening	Nose Bulge	Cheek Bulge	Whisker Position
over all time points n=447	0.517 <i>moderate</i>	0.191	0.387 <i>fair</i>	0.000	0.086
Baseline n=147	0.410 <i>moderate</i>	0.188	0.133	0.000	0.038
1. restraint n=150	0.519 <i>moderate</i>	0.302 <i>fair</i>	0.094	0.000	0.035
2. restraint n=150	0.167	0.016	0.101	0.000	0.044
Difference Score 1. restraint n=147	0.335 <i>fair</i>				
Difference Score 2. restraint n=147	0.199				

Three pictures per mouse were scored (control: 3 x n = 5, Tecniplast metabolic cage and Innovative metabolic cage: 3 x n = 9/10; both sexes: x 2). Results of Cohens kappa (κ) statistics are shown.

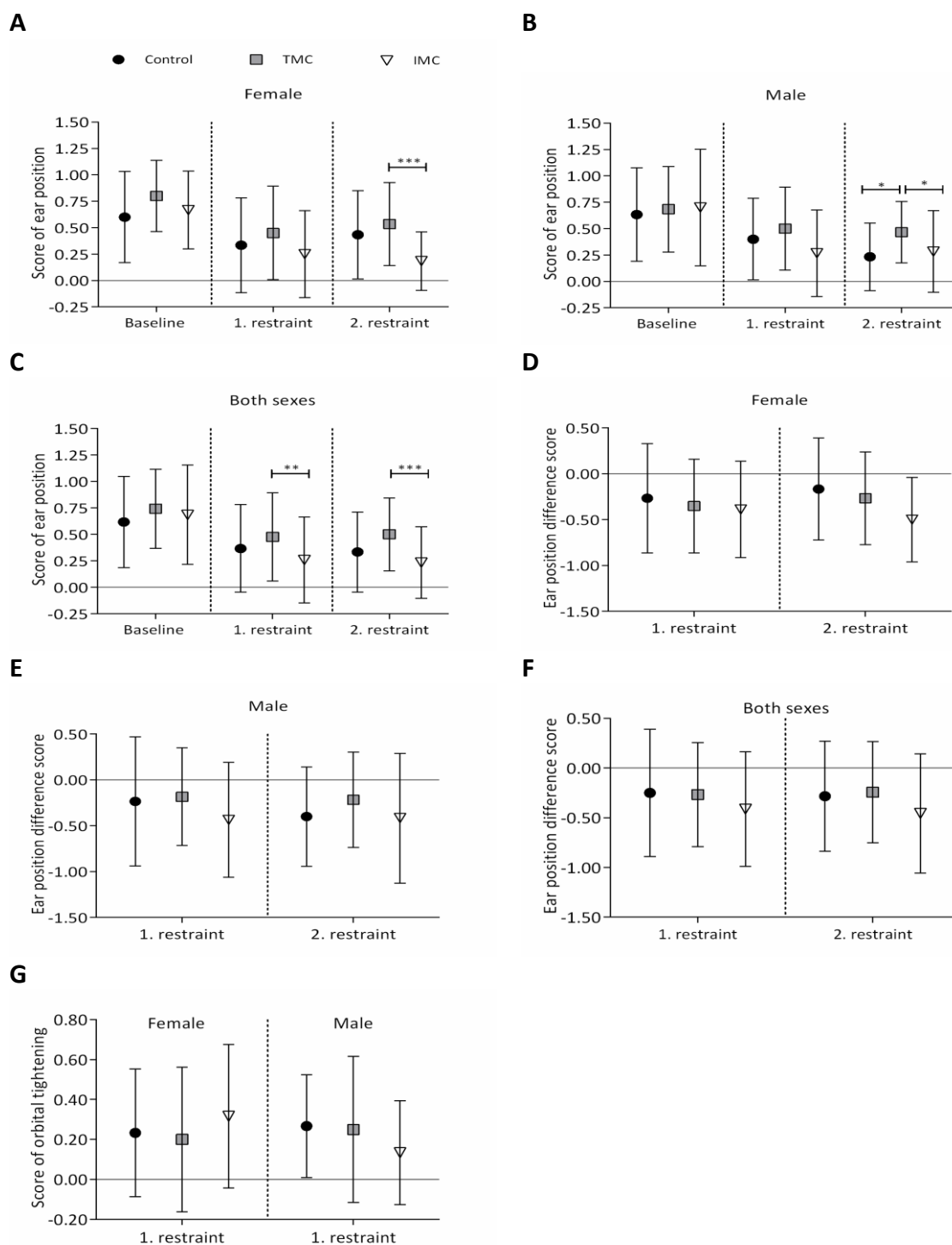


Figure 23. Scores of respective facial action units of the applied Mouse Grimace Scale (MGS) are shown. **A:** Scores of ear position from female mice at baseline, and after first and second restraint (control, $n = 15$; TMC and IMC, $n = 30$). **B:** Scores of ear position from male mice at baseline, and after first and second restraint (control, $n = 15$; TMC and IMC, $n = 30$). **C:** Scores of ear position from both sexes at baseline, and after first and second restraint (control, $n = 30$; TMC and IMC, $n = 60$). **D:** Ear position difference score from female mice after first and second restraint (control, $n = 15$; TMC and IMC, $n = 30$). **E:** Ear position difference score from male mice after first and second restraint (control, $n = 15$; TMC and IMC, $n = 30$). **F:** Ear position difference score from both sexes after first and second restraint (control, $n = 30$; TMC, $n = 60$; IMC, $n = 57$). **G:** Scores of orbital tightening from female and male mice after first restraint (control, $n = 15$; TMC and IMC, $n = 30$). Statistically significant differences between control vs. TMC, control vs. IMC, and TMC vs. IMC were calculated by the Kruskal Wallis Test. Ear position and orbital tightening from baseline, and first and second restraints were analyzed separately (* $P \leq 0.05$, ** $P \leq 0.01$, *** $P \leq 0.001$). Data are presented as mean (standard deviation). Control: control cage, TMC: Tecniplast metabolic cage, IMC: Innovative metabolic cage.

4.1.3 Cold stress

4.1.3.1 Cage temperature

The standard room temperature within animal houses is maintained at $20^{\circ}\text{C} \pm 2$. Mice approximate to their thermoneutral zone of 30°C by means of nest-building and group housing with conspecifics. However, extra energy for heat production must still be spent, resulting in an increased basal metabolic rate [66]. Cold stress, to which mice are generally exposed at mean standard room temperature, is further increased during metabolic cage restraint where mice are single housed in an environment absent of bedding and nesting materials. We therefore investigated the ability of mice to heat up the three tested cage systems in order to draw conclusions on the extent of cage-dependent cold stress. Cage temperatures were assessed with a thermal imaging camera at the beginning and the end of the 24 h test period. Cage temperatures at the end of each restraint are shown in **Figure 24**.

The positive effect of the IMC on the reduction of cold stress was clearly seen for both sexes, where the increase in cage temperature after both restraints was significantly higher compared to the TMC (females - 1. and 2. restraint: $P \leq 0.001$; males - 1. restraint: $P \leq 0.01$, 2. restraint: $P \leq 0.001$; see **Figure 24** A-B). Concerning female mice after both restraints and male mice after second restraint, cage temperatures in IMC were significantly higher compared to controls (females - 1. and 2. restraint: $P \leq 0.001$; males - 2. restraint: $P \leq 0.05$; see **Figure 24** A-B). For male mice after 1. restraint, cage temperature in TMC was significantly lower than in control cages ($P \leq 0.05$, see **Figure 24** B).

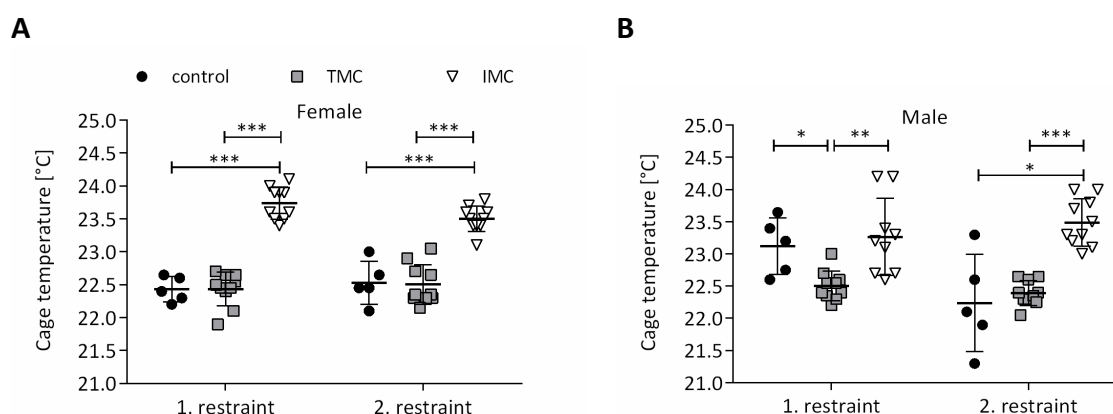


Figure 24. Cage temperature [°C] after 24 h single housing in the three different cage types. A: Female mice (control, $n = 5$; TMC and IMC, $n = 10$). **B:** Male mice (control, $n = 5$; TMC, $n = 10$; IMC, $n = 9$). Differences between control vs. TMC, control vs. IMC, and TMC vs. IMC were calculated by one-way ANOVA. Cage temperature after first and second restraint was analyzed separately (* $P \leq 0.05$, ** $P \leq 0.01$, *** $P \leq 0.001$). Data are presented as mean (standard deviation). Control: control cage, TMC: Tecniplast metabolic cage, IMC: Innovative metabolic cage.

4.1.3.2 Body surface temperature

To gain further insight into cold stress experienced by mice during metabolic cage restraint, we additionally assessed body surface temperature. Measurement of body surface temperature was chosen over e.g. rectal temperature since it represents a non-invasive method that can be realized by use of a thermal imaging camera. As for cage temperature, the body surface temperature at the end of 24 h single housing is shown in **Figure 25**.

After the second restraint, both sexes possessed a significantly higher body surface temperature in the IMC compared to the TMC (females: $P \leq 0.001$, males: $P \leq 0.01$, see **Figure 25 A-B**). Also after the second restraint, female's body surface temperature in the IMC was significantly higher in contrast to the control cage ($P \leq 0.05$, see **Figure 25 A**). Concerning male mice after the second restraint, males possessed a significantly higher body surface temperature in the control cage compared to the TMC ($P \leq 0.05$, see **Figure 25 B**).

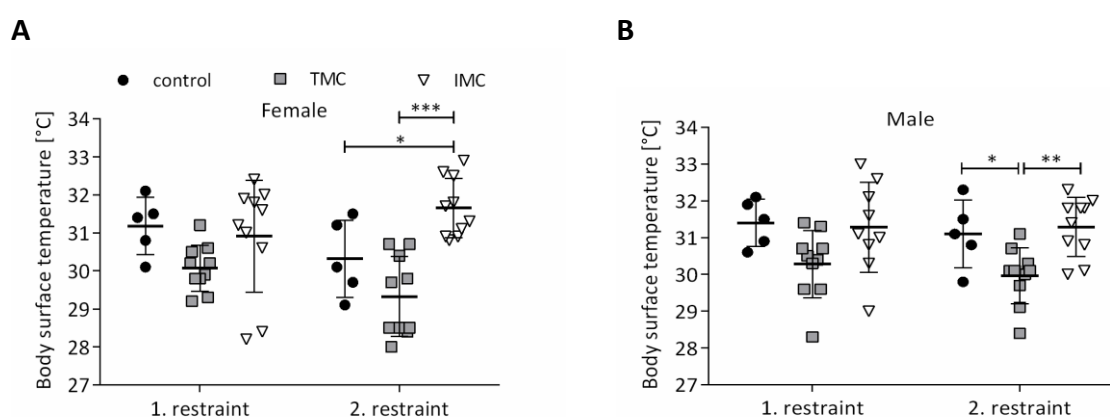


Figure 25. Body surface temperature [°C] after 24 h single housing in the three different cage types. A: Female mice (control, $n = 5$; TMC and IMC, $n = 10$). B: Male mice (control, $n = 5$; TMC, $n = 10$; IMC, $n = 9$). Differences between control vs. TMC, control vs. IMC, and TMC vs. IMC were calculated by one-way ANOVA. Body surface temperature after first and second restraints were analyzed separately ($* P \leq 0.05$, $ P \leq 0.01$, $*** P \leq 0.001$). Data are presented as mean (standard deviation). Control: control cage, TMC: Tecniplast metabolic cage, IMC: Innovative metabolic cage.**

As for the cage temperature, an increase in body surface temperature was assessed at the end of the second restraint in the IMC compared to the TMC. This can be attributed to the improvement of the IMC construction actively supporting the mice in thermoregulation when they are unable to build a nest in the metabolic cage or huddle together with conspecifics. Next, we investigated Uncoupling protein 1 (*Ucp1*) expression in brown adipose tissue (BAT), because we aimed to investigate whether *Ucp1* mRNA is upregulated in the context of cold-induced non-shivering thermogenesis, i.e. metabolic cage restraint.

4.1.3.3 Uncoupling protein 1 in brown adipose tissue and brown adipose tissue weight

After the second 24 h restraint of C57BL/6J mice in one of the three tested cages, mice were euthanized, and the interscapular BAT was extracted. Prior to mRNA expression analyses, RNA extraction and cDNA synthesis preceded. *Ucp1* mRNA expression of mice restrained in either the TMC or IMC was referenced to control mice, which were housed in type II polycarbonate cages containing standardized enrichment. The expression of *Ucp1* in BAT relative to the control group was comparable among all three tested cage types for both sexes (Figure 26).

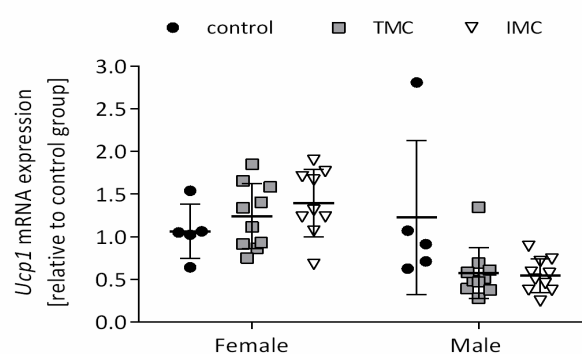


Figure 26. Relative mRNA expression of Uncoupling protein 1 (*Ucp1*) in brown adipose tissue (BAT) of mice after second restraint in the three different cage types. mRNA levels of *Ucp1* in the Tecniplast metabolic cage (TMC, $n = 10$) and in the Innovative metabolic cage (IMC, $n = 10$) were referenced to control mice (control, $n = 5$). Differences between control vs. TMC, control vs. IMC, and TMC vs. IMC were calculated by the Kruskal Wallis Test. Data are presented as mean (standard deviation).

The weight of interscapular BAT was determined after second restraint of mice for each cage type. BAT weight was significantly increased for females restrained in TMC compared to controls ($P \leq 0.05$, see Figure 27). Concerning males, the weight of BAT was comparable among cage types.

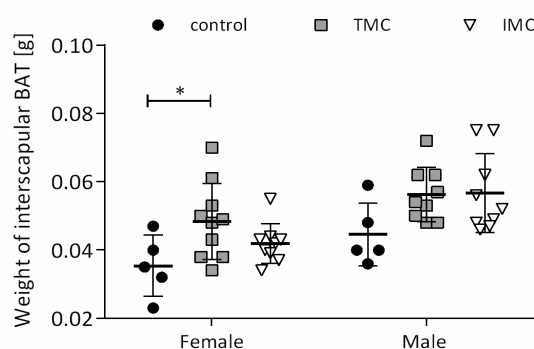


Figure 27. Weight of interscapular brown adipose tissue (BAT) [g] of mice after second restraint in the three different cage types. Differences between TMC vs. IMC, TMC vs. control, IMC vs. control were calculated by one-way ANOVA ($* P \leq 0.05$). Data are presented as mean (standard deviation). Control: control cage, TMC: Tecniplast metabolic cage, IMC: Innovative metabolic cage.

In terms of a multifactorial approach for severity assessment of metabolic cage restraint, the physiological parameter FS and behavioral parameter MGS were applied besides the quantitative parameters cage and body surface temperature together with mRNA expression of *Ucp1* in BAT [109]. The FS is an effective tool to objectively assess the status of animal welfare while a significant increase in FS was detected for female and male mice after metabolic cage restraint compared to controls. Concerning the MGS of both sexes after the second restraint, a significantly elevated ear position score was assessed in the TMC in contrast to the IMC. Cage and body surface temperatures in IMC of both sexes after the second restraint were significantly higher compared to TMC while *Ucp1* mRNA expression in BAT was comparable among cage types. Thus, the parameters collected indicate an improvement in the welfare of the mice during restraint in the IMC compared to the TMC. In the next step, the behavioral patterns of the mice during and after restraint in the three tested cage types were investigated by performing behavioral tests and video analyses as well as quantifying neurotransmitters in brain areas.

4.2 Behavioral patterns

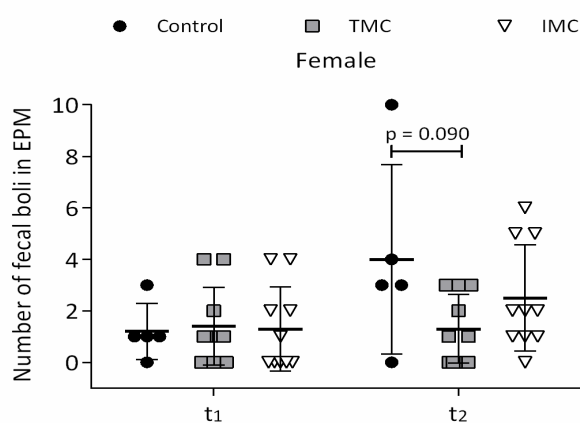
4.2.1 Behavioral tests

Mice were exposed to the new environment of the Elevated Plus Maze (EPM) and Open Field Test (OFT) for five min after first (t_1) and second restraints (t_2) in either control cage, TMC or IMC. Importantly, in order to assess the stress and anxiety level after the 24 h restraint, mice were directly transferred from the three cages into the behavioral test arenas at t_1 and t_2 .

4.2.1.1 Excretion of fecal boli

As the number of excreted fecal boli can serve as an indicator for the stress level, we counted the number of fecal pellets excreted by mice during the 5 min testing phase. At t_1 , the number of female fecal boli was comparable among cage types in the EPM (see **Figure 28 A**). At t_2 , females tended to defecate more after restraint in control cages compared with the TMC ($P = 0.090$). At t_1 and t_2 , male mice excreted significantly more fecal boli after restraint in the IMC in comparison with the TMC ($P \leq 0.01$, see **Figure 28 B**). At t_2 , the number of excreted fecal boli was significantly increased after restraint in control cages compared with TMC restraint ($P \leq 0.001$). Also at t_2 , male mice tended to defecate more after control cage housing in contrast with IMC restraint ($P = 0.094$). This significant increase in fecal boli excretion within the EPM after restraint in the IMC compared with the TMC can be explained by the higher food intake of males during IMC restraint (see chapter **4.3.3 Food intake**, 1st restraint: $P = 0.086$, 2nd restraint: $P \leq 0.001$). Data on food intake during restraint in control cages were not collected.

A



B

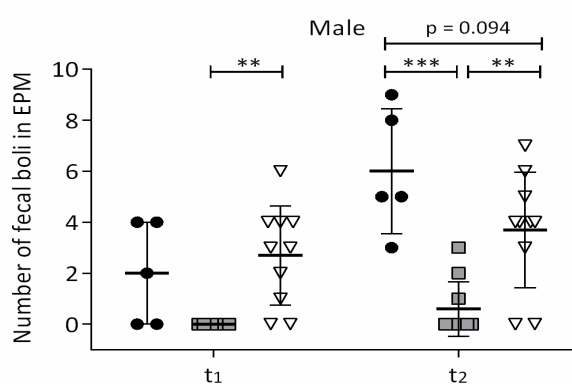
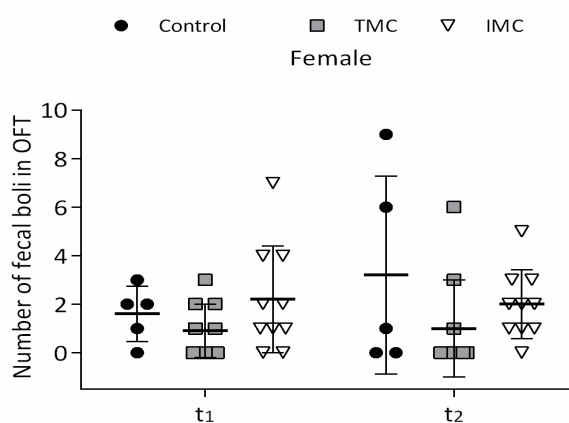


Figure 28. Number of excreted fecal boli within the Elevated Plus Maze (EPM) Arena after first (t_1) and second restraints (t_2) in the three different cage types. **A:** Female mice (control, $n = 5$; TMC and IMC, $n = 10$). **B:** Male mice (control, $n = 5$; TMC and IMC, $n = 10$). Differences among cage types were calculated by the Kruskal Wallis Test or one-way ANOVA and were analyzed separately for each point in time (** $P \leq 0.01$, *** $P \leq 0.001$). Data are presented as mean (standard deviation). Control: control cage, TMC: Tecniplast metabolic cage, IMC: Innovative metabolic cage.

As for female mice in the EPM, at t_1 females in the OFT excreted comparable numbers of fecal boli among tested cages (see **Figure 29 A**). At t_2 , the number of excreted fecal pellets was also comparable between the three cage types. At t_1 , the number of fecal boli concerning male mice was also similar among cage types while at t_2 , males excreted significantly more fecal pellets after housing in control cages compared to restraint in the TMC ($P \leq 0.05$, see **Figure 29 B**).

A



B

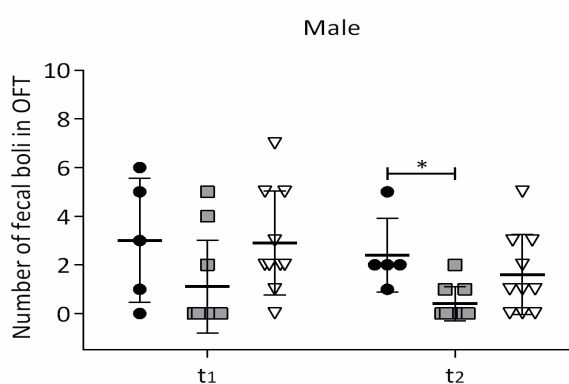
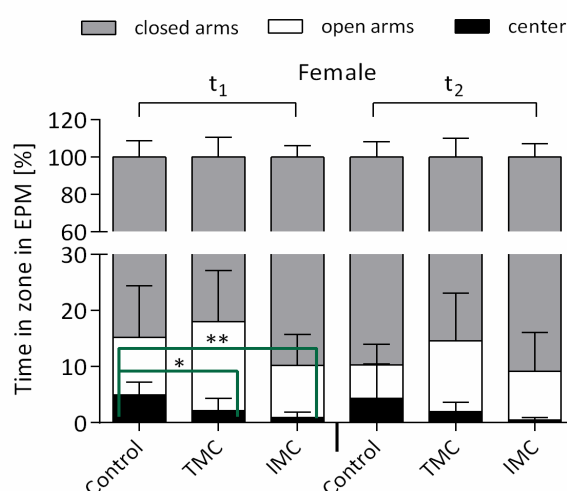


Figure 29. Number of excreted fecal boli within the Open Field Test (OFT) after first (t_1) and second restraints (t_2) in the three different cage types. **A:** Female mice (control, $n = 5$; TMC and IMC, $n = 10$). **B:** Male mice (control, $n = 5$; TMC and IMC, $n = 10$). Differences among cage types were calculated by the Kruskal Wallis Test or one-way ANOVA and were analyzed separately for each point in time ($* P \leq 0.05$). Data are presented as mean (standard deviation). Control: control cage, TMC: Tecniplast metabolic cage, IMC: Innovative metabolic cage.

4.2.1.2 Time in zone

To get an overview of the stress level of mice at t_1 and t_2 , times spent in each predefined zone of the EPM and OFT were analyzed. At t_1 , female mice of the control group explored the center of the EPM significantly longer compared to the TMC ($P \leq 0.05$) and to the IMC ($P \leq 0.01$, see **Figure 30 A**). This observation suggests that controls were less stressed at t_1 in comparison with metabolic cage restraint. After the second restraint, t_2 , spent times in zones within the EPM were similar among tested cage types. Regarding male mice at t_1 and t_2 , the time periods in each zone of the EPM were comparable (see **Figure 30 B**).

A



B

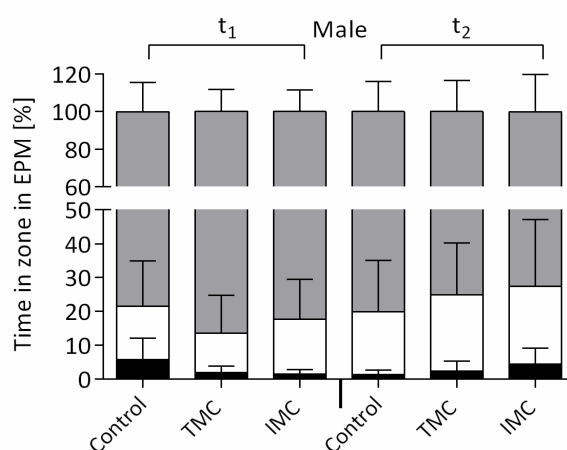
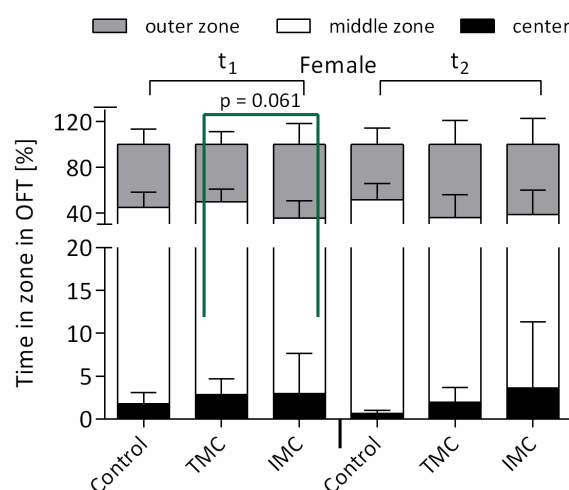


Figure 30. Spent time [%] in either center, open arms or closed arms of the Elevated Plus Maze (EPM) Arena after first (t_1) and second restraints (t_2) in the three different cage types. A: Female mice (control, $n = 5$; TMC and IMC, $n = 10$). B: Male mice (control, $n = 5$; TMC and IMC, $n = 10$). Differences among cage types were calculated by the Kruskal Wallis Test or one-way ANOVA and were analyzed separately for each point in time ($* P \leq 0.05$, $ P \leq 0.01$). Data are presented as mean (standard deviation). Control: control cage, TMC: Tecniplast metabolic cage, IMC: Innovative metabolic cage.**

Both sexes explored the middle zone of the OFT most frequently during the 5 min testing phase (see **Figure 31**). For females at t_1 and t_2 , no significant differences among cage types concerning time spent in either center, middle or outer zone of the OFT, could be detected (see **Figure 31 A**). At t_1 , females tended to spend more time in the middle zone after TMC compared to IMC restraint ($P = 0.061$). This could be explained by an increase in the females' exploratory drive after termination of the TMC restraint. At t_1 , male mice spent significantly more time in the outer zone of the OFT after IMC restraint in comparison with controls ($P \leq 0.05$, see **Figure 31 B**). Also at t_1 , males tended to spend more time in the middle zone of the OFT after control cage housing as opposed to the IMC restraint ($P = 0.063$). This suggests that males were less stressed after first restraint, t_1 , in control cages compared with the IMC due to the longer exploration of the middle zone. At t_2 , males spent comparable periods in each zone of the OFT after restraint in different cage types.

A



B

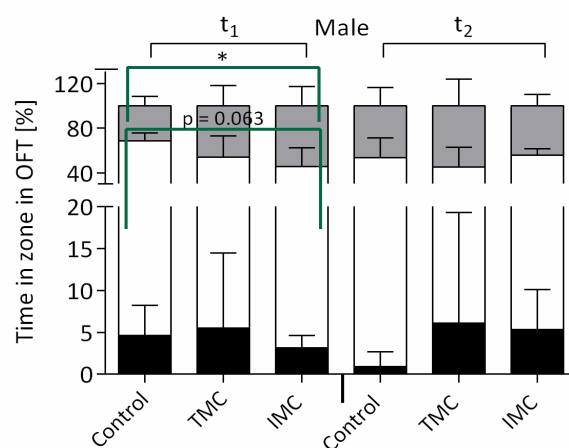
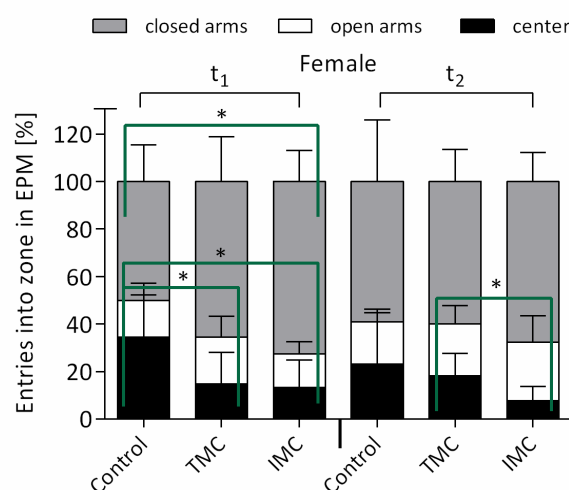


Figure 31. Spent time [%] in either center, middle zone or outer zone of the Open Field Test (OFT) Arena after first (t₁) and second restraints (t₂) in the three different cage types. A: Female mice (control, n = 5; TMC and IMC, n = 10). B: Male mice (control, n = 5; TMC and IMC, n = 10). Differences among cage types were calculated by the Kruskal Wallis Test or one-way ANOVA and were analyzed separately for each point in time (* P ≤ 0.05). Data are presented as mean (standard deviation). Control: control cage, TMC: Tecniplast metabolic cage, IMC: Innovative metabolic cage.

4.2.1.3 Entries into zone

As for spent time in closed arms of the EPM (see **Figure 30**), entries into closed arms was highest for both sexes at t₁ and t₂ (see **Figure 32**). For female mice, entries into particular zones partly coincided with the previously shown results concerning time spent in zones. At t₁, females entered the center significantly more often after housing in control cages as compared with TMC and IMC restraint (P ≤ 0.05, see **Figure 32 A**). In addition to time spent in zone at t₁, females entered the closed arms significantly more often after restraint in IMC than in control cages (P ≤ 0.05). At t₂, entrance into the center was significantly more often observed after TMC than IMC restraint (P ≤ 0.05). Concerning male mice, at t₁ and t₂, entries into respective zones in the EPM were comparable among cage types (see **Figure 32 B**).

A



B

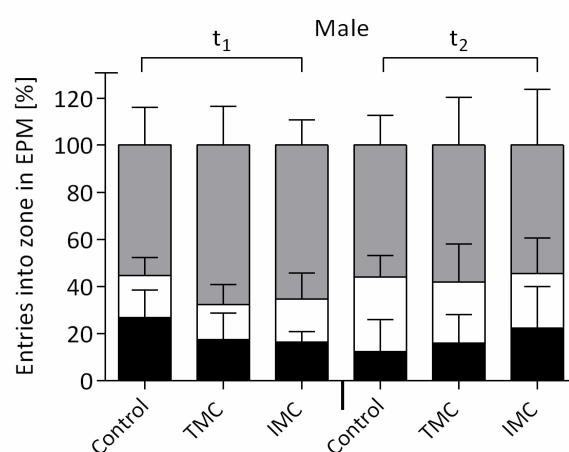
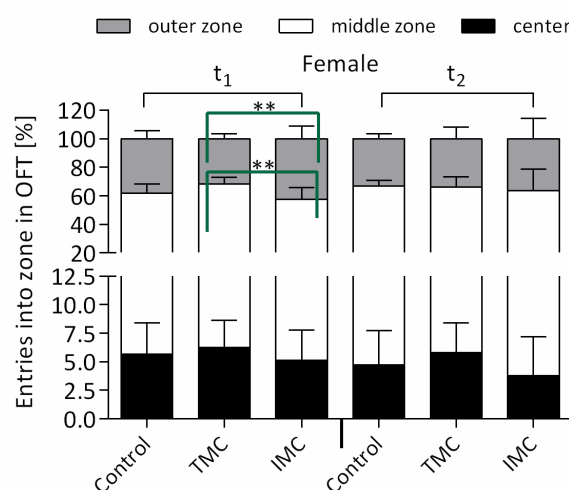


Figure 32. Entries [%] into either center, open arms or closed arms of the Elevated Plus Maze (EPM) Arena after first (t₁) and second restraints (t₂) in the three different cage types. A: Female mice (control, n = 5; TMC and IMC, n = 10). B: Male mice (control, n = 5; TMC and IMC, n = 10). Differences among cage types were calculated by one-way ANOVA and were analyzed separately for each point in time (* P ≤ 0.05). Data are presented as mean (standard deviation). Control: control cage, TMC: Tecniplast metabolic cage, IMC: Innovative metabolic cage.

Percentages of entries into zones of the OFT were more conclusive for females than time spent in the respective zones of the OFT. At t₁, entries into the middle zone after TMC restraint were significantly elevated in comparison with IMC restraint (P ≤ 0.01, see **Figure 33 A**). Conversely, females entered the outer zone significantly more often after IMC than after TMC restraint (P ≤ 0.01). These data from the females regarding entries into respective zones of the EPM and OFT, challenge the hypothesis entailing the anticipated stress reduction during IMC restraint compared with the TMC. Nevertheless, an increase of exploratory drive due to relief after TMC restraint termination can be used as an explanation. At t₁ and t₂, no significant differences among cage types concerning entries into either center, middle or outer zone of the OFT were seen for males (see **Figure 33 B**).

A



B

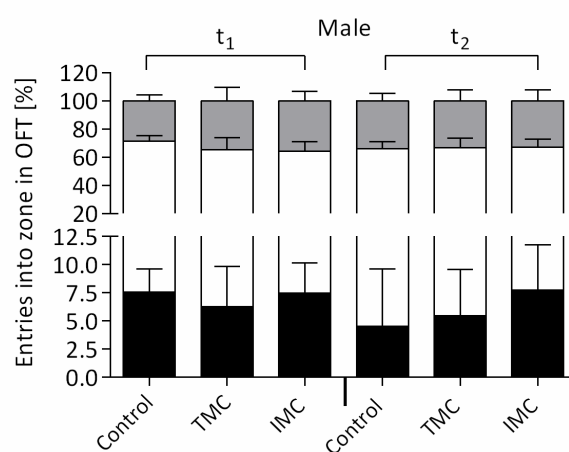
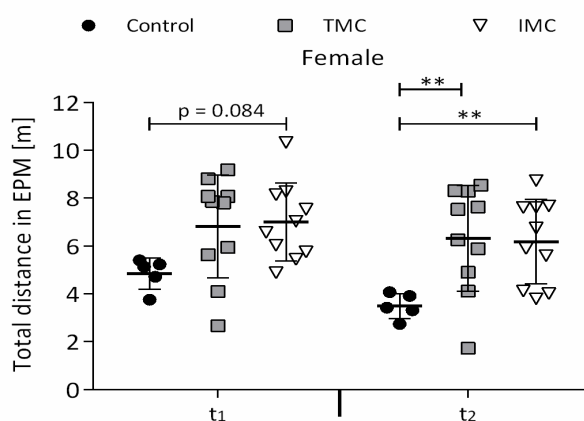


Figure 33. Entries [%] into either center, middle zone or outer zone of the Open Field Test (OFT) Arena after first (t_1) and second restraints (t_2) in the three different cage types. A: Female mice (control, $n = 5$; TMC and IMC, $n = 10$). B: Male mice (control, $n = 5$; TMC and IMC, $n = 10$). Differences among cage types were calculated by one-way ANOVA and were analyzed separately for each point in time ($P \leq 0.01$). Data are presented as mean (standard deviation). Control: control cage, TMC: Tecniplast metabolic cage, IMC: Innovative metabolic cage.**

4.2.1.4 Total distance traveled

Distances traveled in each zone of the EPM and OFT were summed in order to calculate the total distance traveled. At t_1 , females in the EPM tended to cover a longer distance after IMC restraint compared with controls ($P = 0.084$, see **Figure 34 A**). After second restraint (t_2) in both metabolic cages, TMC and IMC, female mice covered a significantly longer distance compared to the control ($P \leq 0.01$). This observed increase in total distance at t_2 after restraint in metabolic cages compared to control cages could be interpreted as an indicator for escape behavior (see chapter **4.2.2** Video observation). Additionally, this observation could indicate relief at the termination of the 24 h restraint in metabolic cages resulting in a higher total distance traveled in the EPM. No significant differences among tested cage types were detected at t_1 and t_2 for total distances covered by males in the EPM (see **Figure 34 B**).

A



B

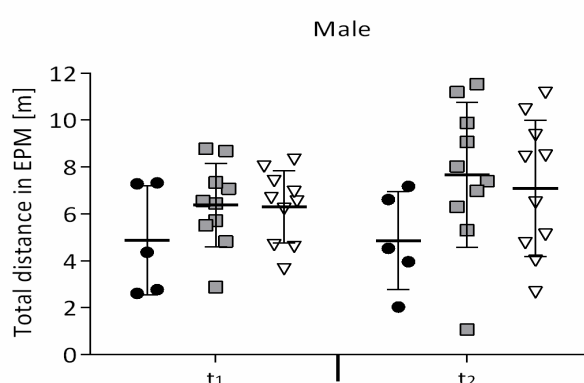
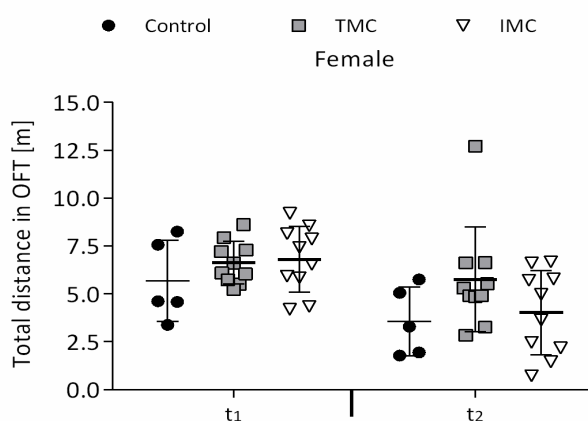


Figure 34. Total distance in the Elevated Plus Maze (EPM) [m] after first (t_1) and second restraints (t_2) in the three different cage types. A: Female mice (control, $n = 5$; TMC and IMC, $n = 10$). B: Male mice (control, $n = 5$; TMC and IMC, $n = 10$). Differences among cage types were calculated by one-way ANOVA and were analyzed separately for each point in time ($P \leq 0.01$). Data are presented as mean (standard deviation). Control: control cage, TMC: Tecniplast metabolic cage, IMC: Innovative metabolic cage.**

At t_1 and t_2 in the OFT, female mice traveled similar distances after restraint in different cage systems (see **Figure 35 A**). Total distances in the OFT at t_1 were comparable among cage types for male mice (see **Figure 35 B**). At t_2 , males traveled a significantly longer distance in the OFT after restraint in the IMC than in the control cage ($P \leq 0.05$). Females and males covered a longer distance in the OFT arena at baseline (t_0) compared to t_1 and t_2 independent of the cage type (data not shown). This can be interpreted as signs of exhaustion due to potential emotional stress during single housing in all three tested cage types. Another point of discussion includes the induced pain in the paws of mice by the grid construction of metabolic cages.

A



B

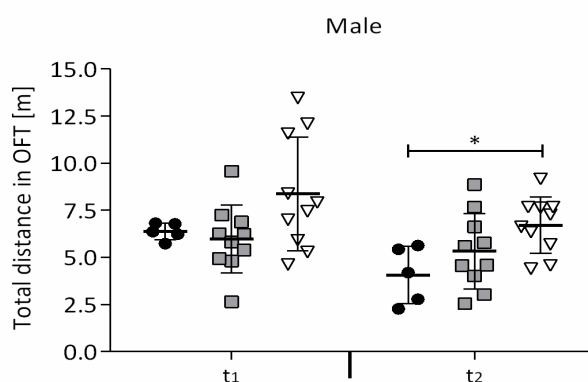
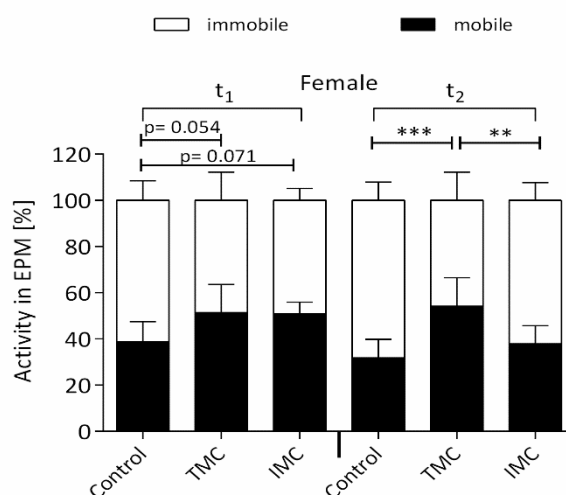


Figure 35. Total distance in the Open Field Test (OFT) [m] after first (t_1) and second restraints (t_2) in the three different cage types. A: Female mice (control, $n = 5$; TMC and IMC, $n = 10$). **B:** Male mice (control, $n = 5$; TMC and IMC, $n = 10$). Differences among cage types were calculated by one-way ANOVA and were analyzed separately for each point in time (* $P \leq 0.05$). Data are presented as mean (standard deviation). Control: control cage, TMC: Tecniplast metabolic cage, IMC: Innovative metabolic cage.

4.2.1.5 Activity: total time (im)mobile

In addition to total distance traveled, activity of mice within the EPM and OFT was further analyzed by subdividing total test time into immobile and mobile phases. At t_1 , female mice tended to be more immobile after control cage housing compared with restraint in the TMC ($P = 0.054$) and in the IMC ($P = 0.071$, see **Figure 36 A**). At t_2 , activity of females was significantly higher after restraint in the TMC as opposed to the control cage ($P \leq 0.001$) and IMC ($P \leq 0.01$). Concerning male mice at t_1 , times mobile and immobile in the EPM were comparable among cage types (see **Figure 36 B**). At t_2 , a significant increase in activity after restraint in both metabolic cage types compared to the control cage was seen ($P \leq 0.05$).

A



B

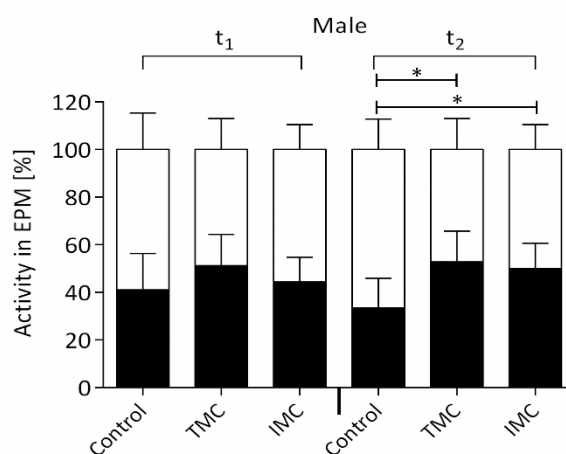
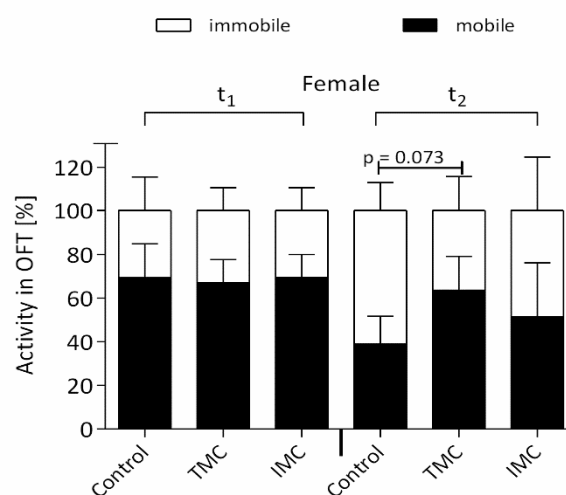


Figure 36. Activity in the Elevated Plus Maze (EPM) Arena [%] subdivided into total time (im)mobile after first (t₁) and second restraints (t₂) in the three different cage types. A: Female mice (control, n = 5; TMC and IMC, n = 10). B: Male mice (control, n = 5; TMC and IMC, n = 10). Differences among cage types were calculated by one-way ANOVA and were analyzed separately for each point in time (* P ≤ 0.05, ** P ≤ 0.01, * P ≤ 0.001). Data are presented as mean (standard deviation). Control: control cage, TMC: Tecniplast metabolic cage, IMC: Innovative metabolic cage.**

At t₁, no significant differences between times (im)mobile in the OFT were observed for female mice among tested cage types (see **Figure 37 A**). At t₂, activity of females tended to increase after restraint in the TMC compared with controls (P = 0.073). No significant differences in activity phases of males in the OFT among cages were seen at t₁ and t₂, but trends were observed (see **Figure 37 B**). At t₁, male mice tended to be more frequently mobile after restraint in the IMC in comparison with control mice (P = 0.062) and TMC restraint (P = 0.062). At t₂, males also tended to be more active after restraint in the IMC as opposed to controls (P = 0.082). In summary, a higher activity of female and male mice was observed after restraint in metabolic cages compared with control cages. The activity data including mobile and immobile timespans confirm the data for total distances traveled while the control mice were the least active and covered the least distances.

A



B

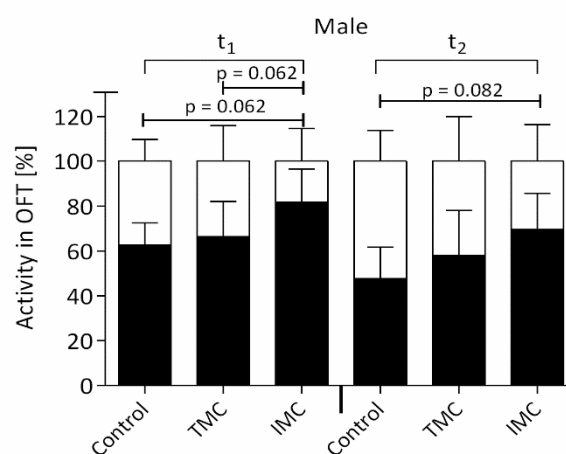


Figure 37. Activity in the Open Field Test (OFT) [%] subdivided into total time (im)mobile after first (t_1) and second restraints (t_2) in the three different cage types. A: Female mice (control, $n = 5$; TMC and IMC, $n = 10$). B: Male mice (control, $n = 5$; TMC and IMC, $n = 10$). Differences among cage types were calculated by one-way ANOVA and were analyzed separately for each point in time. Data are presented as mean (standard deviation). Control: control cage, TMC: Tecniplast metabolic cage, IMC: Innovative metabolic cage.

Summarizing the results from the behavioral tests, it can be concluded that the EPM represents a more challenging test arena for the mice after metabolic cage restraint and that different behaviors may thus be more effectively reflected. Concerning times in zones and entries into zones, trends and tendencies were more frequently observed for females. Closed arms of the EPM as well as the middle zone of the OFT were entered most of the test time. Firstly, results indicate that controls were less stressed compared to mice restrained in metabolic cages. Secondly, after restraint in the TMC, mice showed a higher exploratory drive by visiting the middle zone of the OFT more often compared to the IMC. Interestingly, an increase in distance traveled and time spent mobile after metabolic cage restraint in contrast to the control cage could also be detected. The behavioral test results therefore reflect an end of the stressful metabolic cage restraint that was pronounced as a relief, i.e. increase in activity and exploratory behavior.

4.2.2 Video observation

Recorded videos of mice during two separate 24 h restraints in three different cage types (control, TMC, and IMC) were analyzed based on a predefined ethogram (see chapter 3.1.6.2.2 Video analysis on the basis of an exclusive ethogram). Behavior in the respective cage was assigned to one of the five categories: 1) general activity, 2) escape behavior, 3) immobility, 4) grooming, and 5) other activity. First, scores of behavioral categories were summed over the entire period and averaged (mean) for the respective experimental group (see **Figure 38 A**, **Figure 39 A**, **Figure 40 A**, **Figure 41 A**). In the next step, counts of each behavioral category were summed and averaged (mean) for the respective point in time (see **Figure 38 B-F**, **Figure 39 B-F**, **Figure 40 B-F**, **Figure 41 B-F**). Results were analyzed separately for restraint and sex.

4.2.2.1 Counts of behavioral categories for female mice during first restraint

Concerning females during first restraint, no differences in general activity (walking, sniffing, coprophagy, exploratory behavior) were detected among tested cages when the entire restraint period was considered (see **Figure 38 A**). Analysis of specific time points revealed a significant increase in general activity at 06:00 pm (- 06:30 pm) in the TMC compared to the IMC ($P \leq 0.05$) and controls ($P \leq 0.01$) (see **Figure 38 B**).

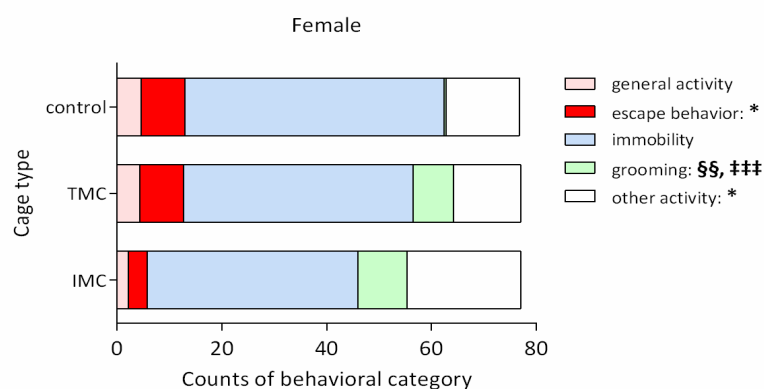
For females in the TMC, a significant increase in escape behavior frequency was seen compared with the IMC ($P \leq 0.05$, see **Figure 38 A**), but this could not be verified for separate points in time (see **Figure 38 C**). At 12:00 pm (- 12:30 pm), frequency of escape behavior of females housed in control cages was significantly increased relative to females in the TMC ($P \leq 0.01$) or IMC ($P \leq 0.001$, see **Figure 38 C**). At 06:00 pm (- 06:30 pm), however, females in the TMC exerted escape behavior significantly more frequently than in control cages ($P \leq 0.05$).

Even if no significant differences in immobility were detected for the whole observational period (see **Figure 38 A**), at 12:00 pm (- 12:30 pm) females in the TMC ($P \leq 0.01$) and in the IMC ($P \leq 0.001$) were significantly more frequently immobile than in control cages (see **Figure 38 D**). At 06:00 pm (- 06:30 pm), female mice in control cages were significantly more immobile than female mice in the TMC ($P \leq 0.001$) and in the IMC ($P \leq 0.001$, see **Figure 38 D**).

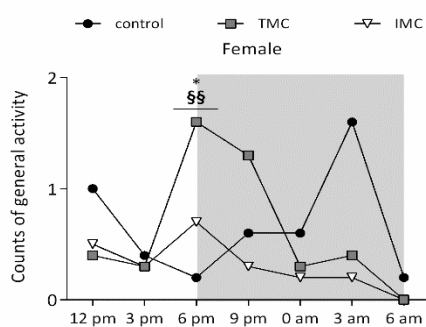
Female mice in the IMC ($P \leq 0.001$) and TMC ($P \leq 0.01$) groomed their fur significantly more often than females in control cages (see **Figure 38 A**). The significant increase in frequency of grooming behavior of females in the TMC and in the IMC compared to controls could be verified at 06:00 pm (- 06:30 pm; $P \leq 0.01$, $P \leq 0.001$) and 03:00 am (- 03:30 am; $P \leq 0.05$, $P \leq 0.01$; see **Figure 38 E**). At 06:00 am (- 06:30 am), a significant increase in grooming behavior was detected for females in the IMC compared to controls ($P \leq 0.05$, see **Figure 38 E**).

Concerning the behavioral category other activity (drinking, feeding, urination, defecation), this behavior was significantly more often assigned to females in the IMC than in the TMC ($P \leq 0.05$, see **Figure 38 A**). Significant differences between both metabolic cage types concerning the category other activity were solely observed when all points in time were considered. At 12:00 pm (- 12:30 pm), controls exerted other activities significantly more often than females in metabolic cages ($P \leq 0.05$) while at 06:00 pm (- 06:30 pm), females in the TMC ($P \leq 0.05$) and IMC ($P \leq 0.001$) showed other activities significantly more frequently than controls (see **Figure 38 F**).

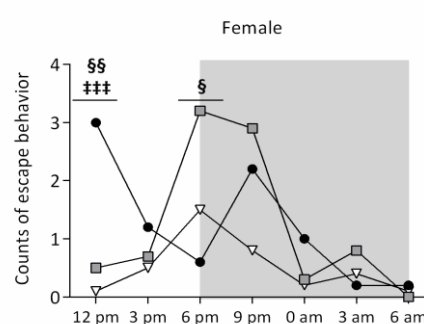
A



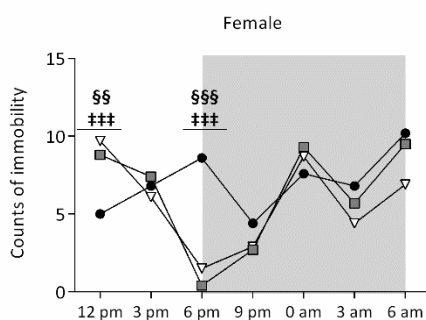
B



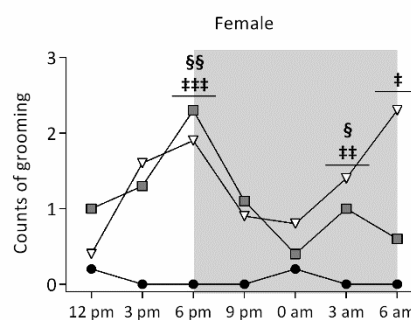
C



D



E



F

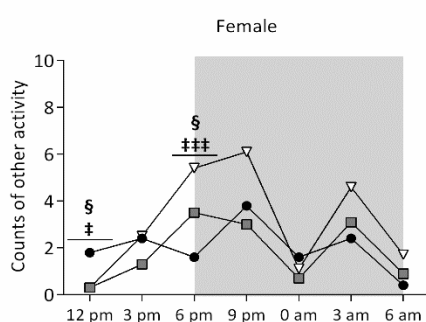


Figure 38. Counts of behavioral categories (general activity, escape behavior, immobility, grooming, other activity) during first restraint of females in the three different cage types. A: All points in time summed. B-F: Seven points in time displayed separately (12:00 pm - 12:30 pm, 03:00 pm - 03:30 pm, 06:00 pm - 06:30 pm, 09:00 pm - 09:30 pm, 00:00 am - 00:30 am, 03:00 am - 03:30 am, 06:00 am - 06:30 am). Grey background indicates the dark phase in the animal house (06:00 pm - 06:00 am). Differences among cage types were calculated by the Kruskal Wallis Test or one-way ANOVA. * $P \leq 0.05$, TMC vs. IMC; § $P \leq 0.05$, §§ $P \leq 0.01$, §§§ $P \leq 0.001$, TMC vs. control; † $P \leq 0.05$, †† $P \leq 0.01$, ††† $P \leq 0.001$, IMC vs. control. Data are presented as mean. Control: control cage ($n = 5$), TMC: Tecniplast metabolic cage ($n = 10$), IMC: Innovative metabolic cage ($n = 10$).

4.2.2.2 Counts of behavioral categories for female mice during second restraint

During the second 24 h single housing period of females, general activity was significantly elevated in control cages compared to the IMC ($P \leq 0.05$) when all investigated points in time were summed (see **Figure 39 A**). This significant difference was confirmed at 00:00 am (- 00:30 am, $P \leq 0.01$; see **Figure 39 B**). General activity for females in the TMC was counted significantly more frequent than in the IMC ($P \leq 0.01$) over the entire period (see **Figure 39 A**), however, this trend could not be confirmed for the single time frames (see **Figure 39 B**).

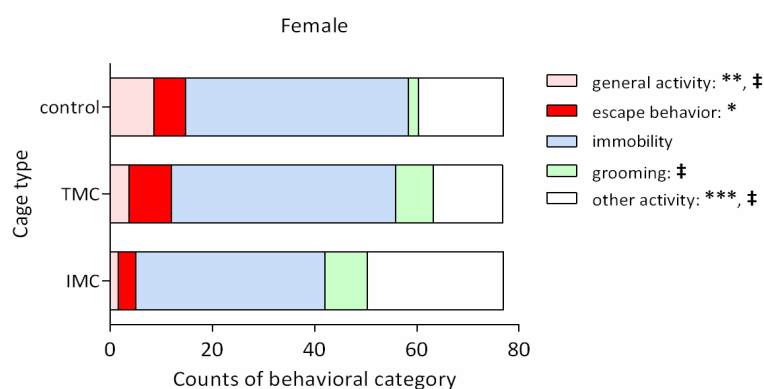
While female escape behavior was significantly higher during restraint in the TMC compared to the IMC over the entire period ($P \leq 0.05$, see **Figure 39 A**), no significant differences in escape behavior were detected when considering separate time periods (see **Figure 39 C**).

Significant differences among cage types concerning total immobility were not detected (see **Figure 39 A**). At 06:00 pm (- 06:30 pm), 09:00 pm (- 09:00 pm), and 06:00 am (- 06:30 am), females in control cages were significantly more frequently immobile than in the IMC ($P \leq 0.01$, $P \leq 0.05$, $P \leq 0.001$; see **Figure 39 D**), which could be explained by the limited view into the nesting area of control cages. Furthermore, immobility was significantly increased for female mice in the TMC compared to the IMC at 09:00 pm (- 09:30 pm) and 06:00 am (- 06:30 am; $P \leq 0.01$, $P \leq 0.05$; see **Figure 39 D**).

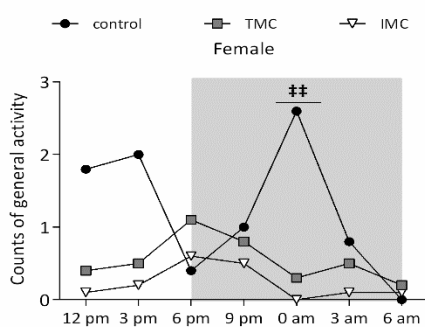
Females in the IMC groomed more often than controls ($P \leq 0.05$) over the entire period (see **Figure 39 A**) and at 06:00 am (- 06:30 am, $P \leq 0.01$; see **Figure 39 E**). Also at 06:00 am (- 06:30 am), females in the IMC groomed significantly more frequently than females in the TMC ($P \leq 0.01$, see **Figure 39 E**).

Other activities were significantly more often scored in the IMC compared with the TMC ($P \leq 0.001$) for all seven points in time (see **Figure 39 A**). At 06:00 pm (- 06:30 pm, $P \leq 0.05$), 09:00 pm (- 09:30 pm, $P \leq 0.001$), and 06:00 am (- 06:30 am, $P \leq 0.01$), this observation was confirmed (see **Figure 39 F**). In total, female mice in the IMC exhibited significantly greater frequencies of behavior that could be assigned to the category other activity compared to controls ($P \leq 0.05$, see **Figure 39 A**). At 06:00 pm (- 06:30 pm, $P \leq 0.05$), 09:00 pm (- 09:30 pm, $P \leq 0.001$), and 06:00 am (- 06:30 am, $P \leq 0.001$), females in the IMC showed other activities significantly more often than females in control cages (see **Figure 39 F**). At 06:00 am (- 06:30 am), females in the TMC exerted other activities significantly more often than controls ($P \leq 0.05$, see **Figure 39 F**).

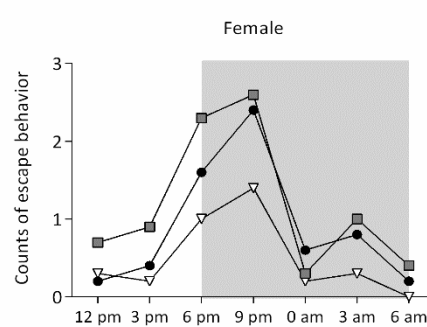
A



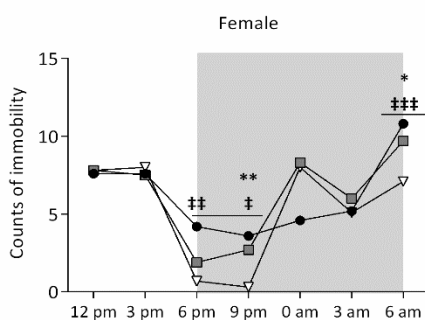
B



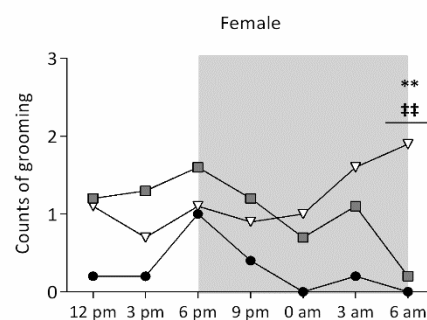
C



D



E



F

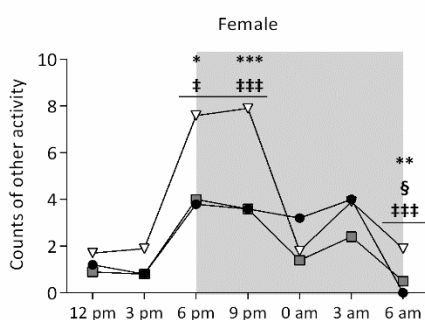


Figure 39. Counts of behavioral categories (general activity, escape behavior, immobility, grooming, other activity) during second restraint of females in the three different cage types. A: All points in time summed. B-F: Seven points in time displayed separately (12:00 pm - 12:30 pm, 03:00 pm - 03:30 pm, 06:00 pm - 06:30 pm, 09:00 pm - 09:30 pm, 00:00 am - 00:30 am, 03:00 am - 03:30 am, 06:00 am - 06:30 am). Grey background indicates the dark phase in the animal house (06:00 pm - 06:00 am). Differences among cage types were calculated by the Kruskal Wallis Test or one-way ANOVA. * $P \leq 0.05$, ** $P \leq 0.01$, * $P \leq 0.001$, TMC vs. IMC; ‡ $P \leq 0.05$, ‡‡ $P \leq 0.01$, ‡‡‡ $P \leq 0.001$, IMC vs. control. Data are presented as mean. Control: control cage ($n = 5$), TMC: Tecniplast metabolic cage ($n = 10$), IMC: Innovative metabolic cage ($n = 10$).**

4.2.2.3 Counts of behavioral categories for male mice during first restraint

During the first 24 h restraint of males, general activity was significantly elevated for male mice in the TMC compared to the IMC ($P \leq 0.01$), but this observation was not confirmed for separate points in time (see **Figure 40 A-B**). At 06:00 pm (- 06:30 pm), general activity of males was significantly more often scored in the TMC and in the IMC compared with controls ($P \leq 0.05$, see **Figure 40 B**).

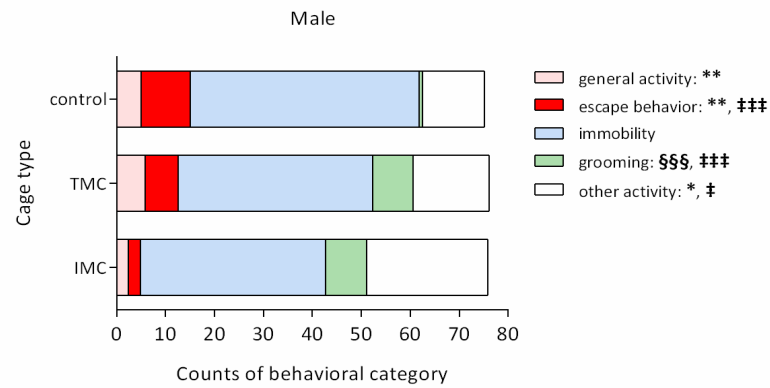
Total escape behavior was significantly increased for males in the TMC relative to those in the IMC ($P \leq 0.01$) and total escape behavior was significantly elevated for controls relative to IMC restraint ($P \leq 0.001$, see **Figure 40 A**). At 12:00 pm (- 12:30 pm, $P \leq 0.001$) and 09:00 pm (- 09:30 pm, $P \leq 0.01$), a significant increase in escape behavior for controls in comparison with the IMC was scored (see **Figure 40 C**). Additionally, at 12:00 pm (- 12:30 pm), a significant elevation of escape behavior for controls compared to TMC restraint was seen ($P \leq 0.01$, see **Figure 40 C**).

No significant differences in counts of immobility were detected for the sum of all seven points in time (see **Figure 40 A**), but were individually seen at 12:00 pm (- 12:30 pm), 06:00 pm (- 06:30 pm), and 03:00 am (- 03:30 am) between both metabolic cage types and controls (see **Figure 40 D**). At 12:00 pm (- 12:30 pm), males in the TMC and in the IMC were significantly more immobile than controls ($P \leq 0.01$, see **Figure 40 D**). At 06:00 pm (- 06:30 pm; $P \leq 0.001$) and 03:00 am (- 03:30 am; $P \leq 0.05$, $P \leq 0.001$) this observation was however reversed with controls being significantly more frequently immobile than males in the TMC and in the IMC (see **Figure 40 D**).

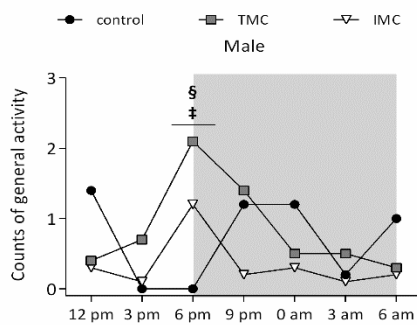
As for females during first restraint, grooming was in total significantly more present in metabolic cages relative to controls ($P \leq 0.001$, see **Figure 40 A**). This observation can be explained by the limited view of the scorer into the nest of control cages, and is why it cannot be excluded that control males also frequently groomed their fur. The significantly increased grooming during restraint in the TMC compared to controls was confirmed at 06:00 pm (- 06:30 pm, $P \leq 0.01$) and 03:00 am (- 03:30 am; $P \leq 0.05$; see **Figure 40 E**). At 03:00 am (- 03:30 am), males in the IMC groomed significantly more frequently than controls ($P \leq 0.001$, see **Figure 40 E**).

For males in the IMC, the behavioral category other activity was significantly more often scored than for the TMC ($P \leq 0.05$) throughout the entire experiment (see **Figure 40 A**) and at 06:00 pm (- 06:30 pm; $P \leq 0.01$; see **Figure 40 F**). The total of other activities was significantly increased in the IMC in comparison to controls ($P \leq 0.05$, see **Figure 40 A**). This observation was confirmed at 06:00 pm (- 06:30 pm, $P \leq 0.001$) and at 03:00 am (- 03:30 am, $P \leq 0.01$), while at 12:00 pm (- 12:30 pm), other activities were significantly elevated for controls compared with IMC restraint ($P \leq 0.05$, see **Figure 40 F**). Additionally, at 12:00 pm (- 12:30 pm) the behavioral category other activity was significantly more often scored for controls than for the TMC ($P \leq 0.05$, see **Figure 40 F**). At 03:00 am (- 03:30 am), however, other activities were significantly elevated for males in the TMC compared with controls ($P \leq 0.05$, see **Figure 40 F**).

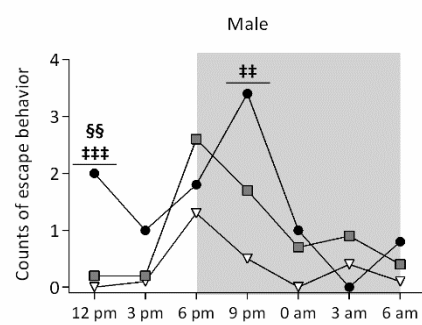
A



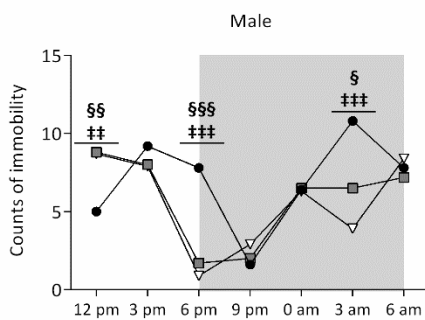
B



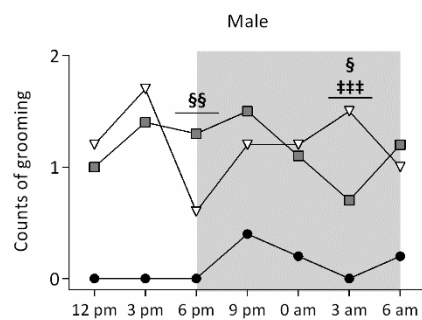
C



D



E



F

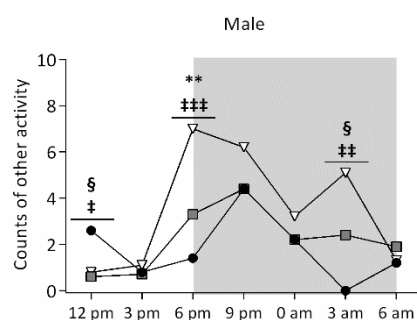


Figure 40. Counts of behavioral categories (general activity, escape behavior, immobility, grooming, other activity) during first restraint of males in the three different cage types. A: All points in time summed. **B-F:** Seven points in time displayed separately (12:00 pm - 12:30 pm, 03:00 pm - 03:30 pm, 06:00 pm - 06:30 pm, 09:00 pm - 09:30 pm, 00:00 am - 00:30 am, 03:00 am - 03:30 am, 06:00 am - 06:30 am). Grey background indicates the dark phase in the animal house (06:00 pm - 06:00 am). Differences among cage types were calculated by the Kruskal Wallis Test or one-way ANOVA. * $P \leq 0.05$, ** $P \leq 0.01$, TMC vs. IMC; § $P \leq 0.05$, §§ $P \leq 0.01$, §§§ $P \leq 0.001$, TMC vs. control; ‡ $P \leq 0.05$, †† $P \leq 0.01$, ††† $P \leq 0.001$, IMC vs. control. Data are presented as mean. Control: control cage ($n = 5$), TMC: Tecniplast metabolic cage ($n = 10$), IMC: Innovative metabolic cage ($n = 10$).

4.2.2.4 Counts of behavioral categories for male mice during second restraint

Concerning the second 24 h restraint of males, total general activity was comparable among tested cage types (see **Figure 41 A**). At 12:00 pm (- 12:30 pm), a significant increase in general activity for controls compared with IMC restraint was counted ($P \leq 0.05$, see **Figure 41 B**).

No statistically significant differences in summed escape behavior was detected between cages (see **Figure 41 A**). At 09:00 pm (- 09:30 pm), male mice in control cages exerted escape behavior significantly more frequently than during restraint in the IMC ($P \leq 0.05$, see **Figure 41 C**).

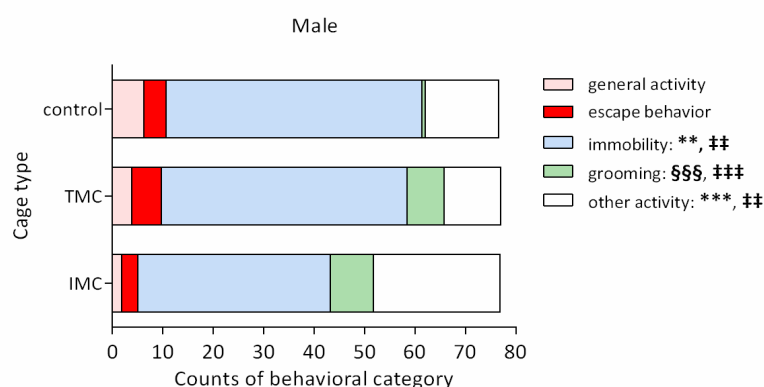
Total immobility was significantly higher during TMC restraint than during restraint in the IMC ($P \leq 0.01$, see **Figure 41 A**). This significant difference was verified at 03:00 am (- 03:30 am; $P \leq 0.001$; see **Figure 41 D**). Overall immobility of controls was significantly more frequently observed compared with the IMC ($P \leq 0.01$, see **Figure 41 A**), which could be confirmed at 03:00 pm (- 03:30 pm, $P \leq 0.05$), 06:00 pm (- 06:30 pm, $P \leq 0.001$), and 03:00 am (- 03:30 am; $P \leq 0.01$; see **Figure 41 D**). In addition, at 03:00 pm (- 03:30 pm, $P \leq 0.001$) and 06:00 pm (- 06:30 pm, $P \leq 0.01$), counts of immobility were significantly elevated for controls compared to restraint in the TMC (see **Figure 41 D**).

As already stated, grooming was significantly more often observed in metabolic cages than for controls ($P \leq 0.001$, see **Figure 41 A**). At 03:00 pm (- 03:30 pm) and at 09:00 pm (- 09:30 pm), males in the TMC ($P \leq 0.001$, $P \leq 0.01$) and in the IMC ($P \leq 0.05$, $P \leq 0.01$) groomed more frequently compared to controls (see **Figure 41 E**). In contrast, at 03:00 am (- 03:30 am) and 06:00 am (- 06:30 am), grooming was only significantly elevated for male mice in the IMC in comparison with the control ($P \leq 0.05$, see **Figure 41 E**).

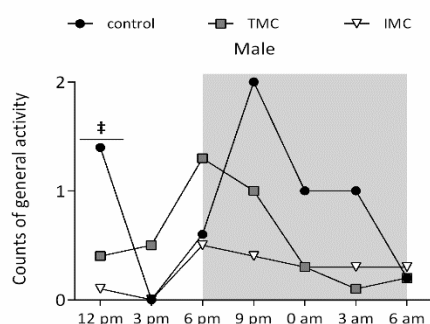
The significant increase in other activities during IMC restraint compared to TMC restraint was more pronounced during the second restraint ($P \leq 0.001$, see **Figure 41 A**) versus the first restraint ($P \leq 0.05$, see **Figure 40 A**). At three points in time - 06:00 pm (- 06:30 pm, $P \leq 0.001$), 09:00 pm (- 09:30 pm, $P \leq 0.01$) and 03:00 am (- 03:30 am, $P \leq 0.05$) - this significant difference was confirmed (see **Figure 41 F**). Total counts of other activity were significantly more frequently present during IMC restraint than for controls ($P \leq 0.001$, see **Figure 41 A**), which was also observed at 06:00 pm (- 06:30 pm; $P \leq 0.001$; see **Figure 41 F**).

The preliminary classification into the respective behavioral categories objectified the behavioral analyses and was also more targeted. Escape behavior was significantly increased for both sexes during both TMC restraints compared with IMC restraint, except for males during second restraint. A significantly elevated grooming behavior was observed during restraint in both metabolic cage types compared with controls, females during second restraint are excluded. Females and males exerted other activities (drinking, feeding, urination, defecation) significantly more often during IMC restraint compared to TMC restraint. To also investigate the effect of metabolic cage restraint on the behavioral response of mice at the molecular level, selected neurotransmitters were subsequently quantified in specific brain areas.

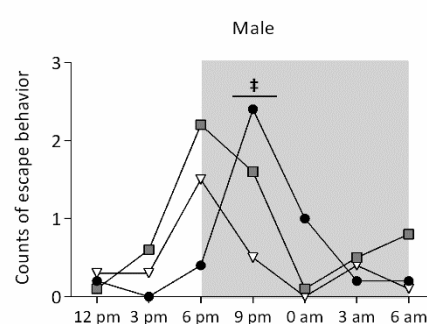
A



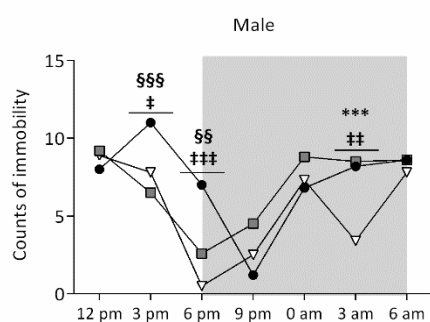
B



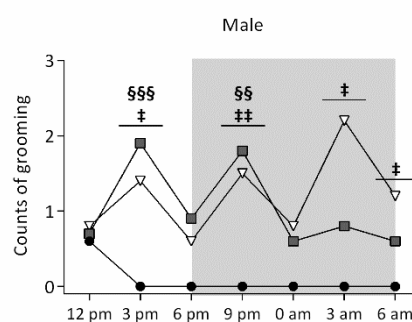
C



D



E



F

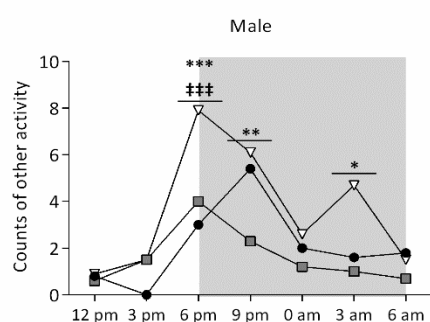


Figure 41. Counts of behavioral categories (general activity, escape behavior, immobility, grooming, other activity) during second restraint of males in the three different cage types. A: All points in time summed. B-F: Seven points in time displayed separately (12:00 pm - 12:30 pm, 03:00 pm - 03:30 pm, 06:00 pm - 06:30 pm, 09:00 pm - 09:30 pm, 00:00 am - 00:30 am, 03:00 am - 03:30 am, 06:00 am - 06:30 am). Grey background indicates the dark phase in the animal house (06:00 am - 06:00 pm). Differences among cage types were calculated by the Kruskal Wallis Test or one-way ANOVA. * $P \leq 0.05$, ** $P \leq 0.01$, * $P \leq 0.001$, TMC vs. IMC; §§ $P \leq 0.01$, §§§ $P \leq 0.001$, TMC vs. control; † $P \leq 0.05$, †† $P \leq 0.01$, ††† $P \leq 0.001$, IMC vs. control. Data are presented as mean. Control: control cage ($n = 5$), TMC: Tecniplast metabolic cage ($n = 10$), IMC: Innovative metabolic cage ($n = 10$).**

4.2.3 Neurotransmitter levels in brain areas

4.2.3.1 Dopamine and its metabolites 3,4-dihydroxyphenylacetic acid and 3-methoxytyramine

Dopamine (DA) concentrations were quantified *via* LC-MS/MS in five specific brain areas of mice after second restraint in either control cage, TMC or IMC (see **Figure 42** A-E). DA concentrations in specific brain areas were comparable and no significant cage-dependent effect was detected:

- *Caudate putamen* (CPU, see **Figure 42 A**)
 - Female: control \bar{x} = 4.52 ng/mg, TMC \bar{x} = 5.02 ng/mg, IMC \bar{x} = 4.24 ng/mg
 - Male: control \bar{x} = 5.03 ng/mg, TMC \bar{x} = 4.75 ng/mg, IMC \bar{x} = 4.52 ng/mg

- *Nucleus accumbens* (NAC, see **Figure 42 B**)
 - Female: control \bar{x} = 2.85 ng/mg, TMC \bar{x} = 2.35 ng/mg, IMC \bar{x} = 3.69 ng/mg
 - Male: control \bar{x} = 2.95 ng/mg, TMC \bar{x} = 2.50 ng/mg, IMC \bar{x} = 3.39 ng/mg

- *Hypothalamus* (HTM, see **Figure 42 C**)
 - Female: control \bar{x} = 0.08 ng/mg, TMC \bar{x} = 0.10 ng/mg, IMC \bar{x} = 0.08 ng/mg
 - Male: control \bar{x} = 0.11 ng/mg, TMC \bar{x} = 0.10 ng/mg, IMC \bar{x} = 0.16 ng/mg

- Ventral tegmental area (VTA, see **Figure 42 D**)
 - Female: control \bar{x} = 0.14 ng/mg, TMC \bar{x} = 0.11 ng/mg, IMC \bar{x} = 0.16 ng/mg
 - Male: control \bar{x} = 0.11 ng/mg, TMC \bar{x} = 0.17 ng/mg, IMC \bar{x} = 0.12 ng/mg

- *Substantia nigra* (SN, see **Figure 42 E**)
 - Female: control \bar{x} = 0.03 ng/mg, TMC \bar{x} = 0.01 ng/mg, IMC \bar{x} = 0.01 ng/mg
 - Male: control \bar{x} = 0.03 ng/mg, TMC \bar{x} = 0.02 ng/mg, IMC \bar{x} = 0.01 ng/mg.

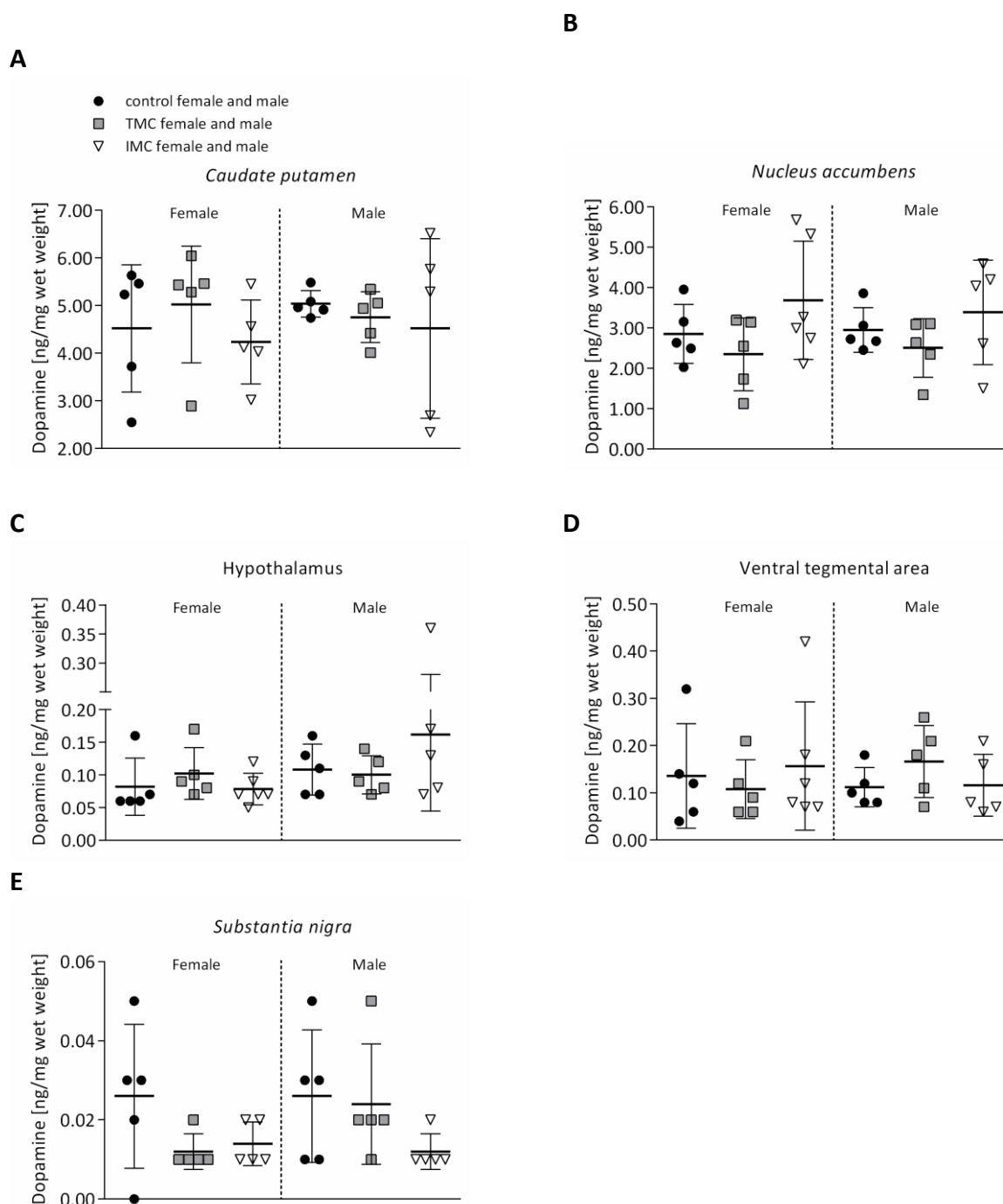


Figure 42. Dopamine concentrations [ng/mg wet weight] in five different brain areas. A-E: Subdivision into extracted brain areas. Differences between control vs. TMC, control vs. IMC, and TMC vs. IMC were calculated by Kruskal-Wallis H Test. Data are presented as mean (standard deviation). Control: control cage (females and males: $n = 5$), TMC: Tecniplast metabolic cage (females and males: $n = 5$), IMC: Innovative metabolic cage (females: $n = 5$ (Caudate putamen, Substantia nigra), $n = 6$ (Nucleus accumbens, Hypothalamus, Ventral tegmental area); males: $n = 5$).

Concentrations of the DA metabolite 3,4-dihydroxyphenylacetic acid (DOPAC) were significantly elevated in female CPU after restraint in the IMC ($\bar{x} = 1.72$ ng/mg) compared to the control cage ($\bar{x} = 0.97$ ng/mg) ($P \leq 0.05$) (see **Figure 43 A**). Concerning males, no significant differences in DOPAC concentrations were detected among tested cage types within the CPU (control $\bar{x} = 1.59$ ng/mg, TMC $\bar{x} = 1.24$ ng/mg, IMC $\bar{x} = 1.31$ ng/mg; see **Figure 43 A**).

Within the NAC, female mice possessed higher DOPAC concentrations in IMC ($\bar{x} = 2.98$ ng/mg) in comparison to controls ($\bar{x} = 2.08$ ng/mg) ($P = 0.059$, see **Figure 43 B**). No differences were observed for males (control $\bar{x} = 2.08$ ng/mg, TMC $\bar{x} = 2.18$ ng/mg, IMC $\bar{x} = 2.59$ ng/mg; see **Figure 43 B**). When taking both sexes into account, the same trend as for females was observed including higher DOPAC concentrations after restraint in IMC compared to the control ($P = 0.055$, data not shown).

Males showed significantly elevated DOPAC concentrations in the HTM following restraint in IMC ($\bar{x} = 0.34$ ng/mg) as compared to controls ($\bar{x} = 0.20$ ng/mg) and TMC ($\bar{x} = 0.19$ ng/mg) ($P \leq 0.05$; see **Figure 43 C**). This observation could not be confirmed for female mice (control $\bar{x} = 0.22$ ng/mg, TMC $\bar{x} = 0.24$ ng/mg, IMC $\bar{x} = 0.37$ ng/mg; see **Figure 43 C**). When including both sexes in the analyses, the same trends as for males were shown with significantly increased DOPAC concentrations after restraint in the IMC compared to the TMC ($P \leq 0.05$) and controls ($P \leq 0.05$, data not shown).

No differences in DOPAC concentrations among cage types were found in the VTA (see **Figure 43 D**). This was true for both sexes (Female: control $\bar{x} = 0.37$ ng/mg, TMC $\bar{x} = 0.33$ ng/mg, IMC $\bar{x} = 0.38$ ng/mg; Male: control $\bar{x} = 0.37$ ng/mg, TMC $\bar{x} = 0.28$ ng/mg, IMC $\bar{x} = 0.34$ ng/mg). DOPAC concentrations were below the detection limit concerning the SN.

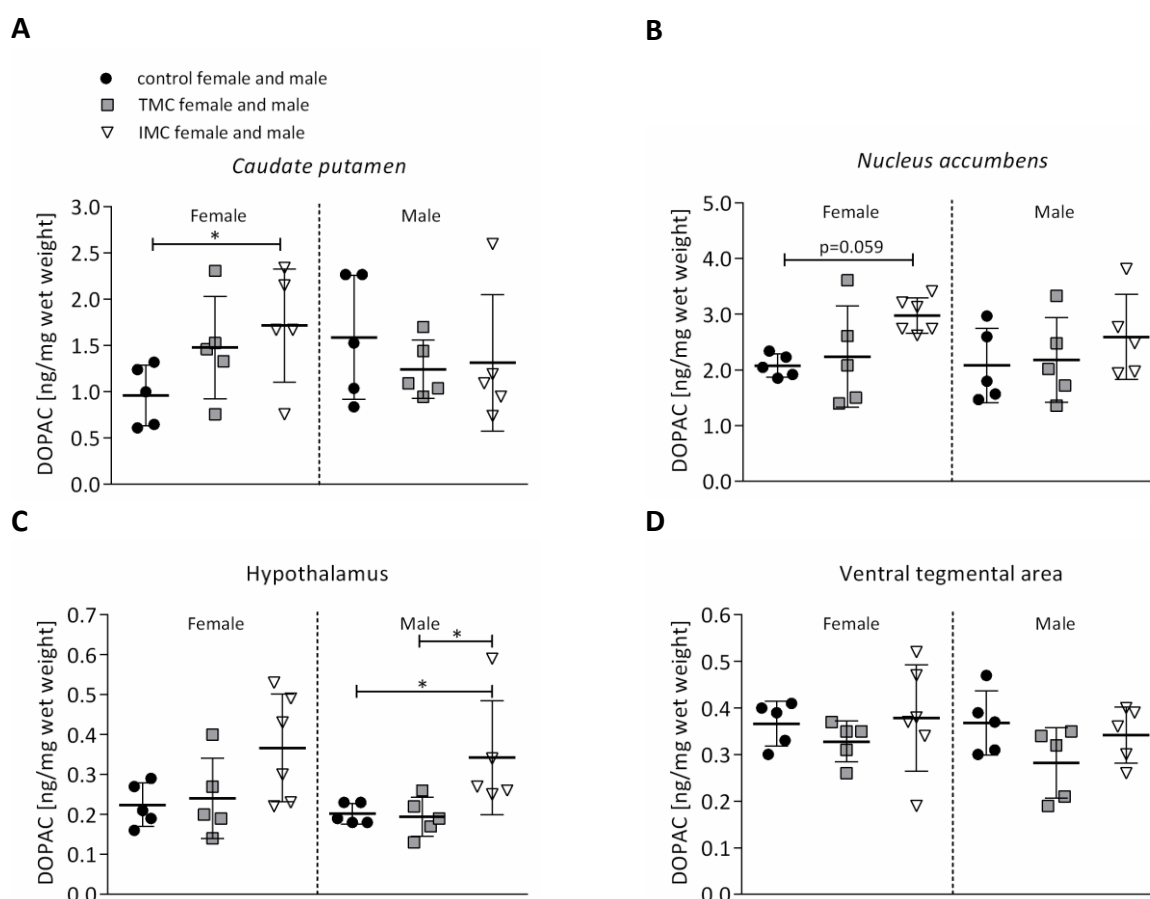


Figure 43. 3,4-Dihydroxyphenylacetic acid (DOPAC) concentrations [ng/mg wet weight] in four different brain areas. A-D: Subdivision into extracted brain areas. Differences between control vs. TMC, control vs. IMC, and TMC vs. IMC were calculated by Kruskal-Wallis H Test. * $P \leq 0.05$. Data are presented as mean (standard deviation). Control: control cage (females and males: $n = 5$), TMC: Tecniplast metabolic cage (females and males: $n = 5$), IMC: Innovative metabolic cage (females: $n = 5$ (Caudate putamen), $n = 6$ (Nucleus accumbens, Hypothalamus, Ventral tegmental area); males: $n = 5$).

Another metabolite of DA, 3-methoxytyramine (3-MT), was quantified in the five different brain areas. 3-MT concentrations were significantly higher in male CPU after housing in control cages (\bar{x} = 1.07 ng/mg) compared to the TMC (\bar{x} = 0.85 ng/mg) ($P \leq 0.05$) (see **Figure 44 A**). This could not be confirmed for female mice (control \bar{x} = 0.81 ng/mg, TMC \bar{x} = 0.98 ng/mg, IMC \bar{x} = 0.78 ng/mg; see **Figure 44 A**).

No significant differences in 3-MT concentrations within the NAC were detected with the focus on cage type (Female: control \bar{x} = 0.65 ng/mg, TMC \bar{x} = 0.60 ng/mg, IMC \bar{x} = 0.83 ng/mg; Male: control \bar{x} = 0.71 ng/mg, TMC \bar{x} = 0.56 ng/mg, IMC \bar{x} = 0.91 ng/mg; see **Figure 44 B**), but if both sexes were taken into account, 3-MT concentrations were elevated in the IMC compared to the TMC ($P = 0.056$, data not shown).

No significant differences in 3-MT concentrations among tested cage types were determined within the HTM, VTA, and SN (see **Figure 44 C-E**):

- HTM (see **Figure 44 C**)
 - Female: control \bar{x} = 0.02 ng/mg, TMC \bar{x} = 0.04 ng/mg, IMC \bar{x} = 0.03 ng/mg
 - Male: control \bar{x} = 0.03 ng/mg, TMC \bar{x} = 0.03 ng/mg, IMC \bar{x} = 0.05 ng/mg

- VTA (see **Figure 44 D**)
 - Female: control \bar{x} = 0.04 ng/mg, TMC \bar{x} = 0.03 ng/mg, IMC \bar{x} = 0.05 ng/mg
 - Male: control \bar{x} = 0.03 ng/mg, TMC \bar{x} = 0.05 ng/mg, IMC \bar{x} = 0.04 ng/mg

- SN (see **Figure 44 E**)
 - Female: control \bar{x} = 0.008 ng/mg, TMC \bar{x} = 0.006 ng/mg, IMC \bar{x} = 0.007 ng/mg
 - Male: control \bar{x} = 0.010 ng/mg, TMC \bar{x} = 0.012 ng/mg, IMC \bar{x} = 0.002 ng/mg.

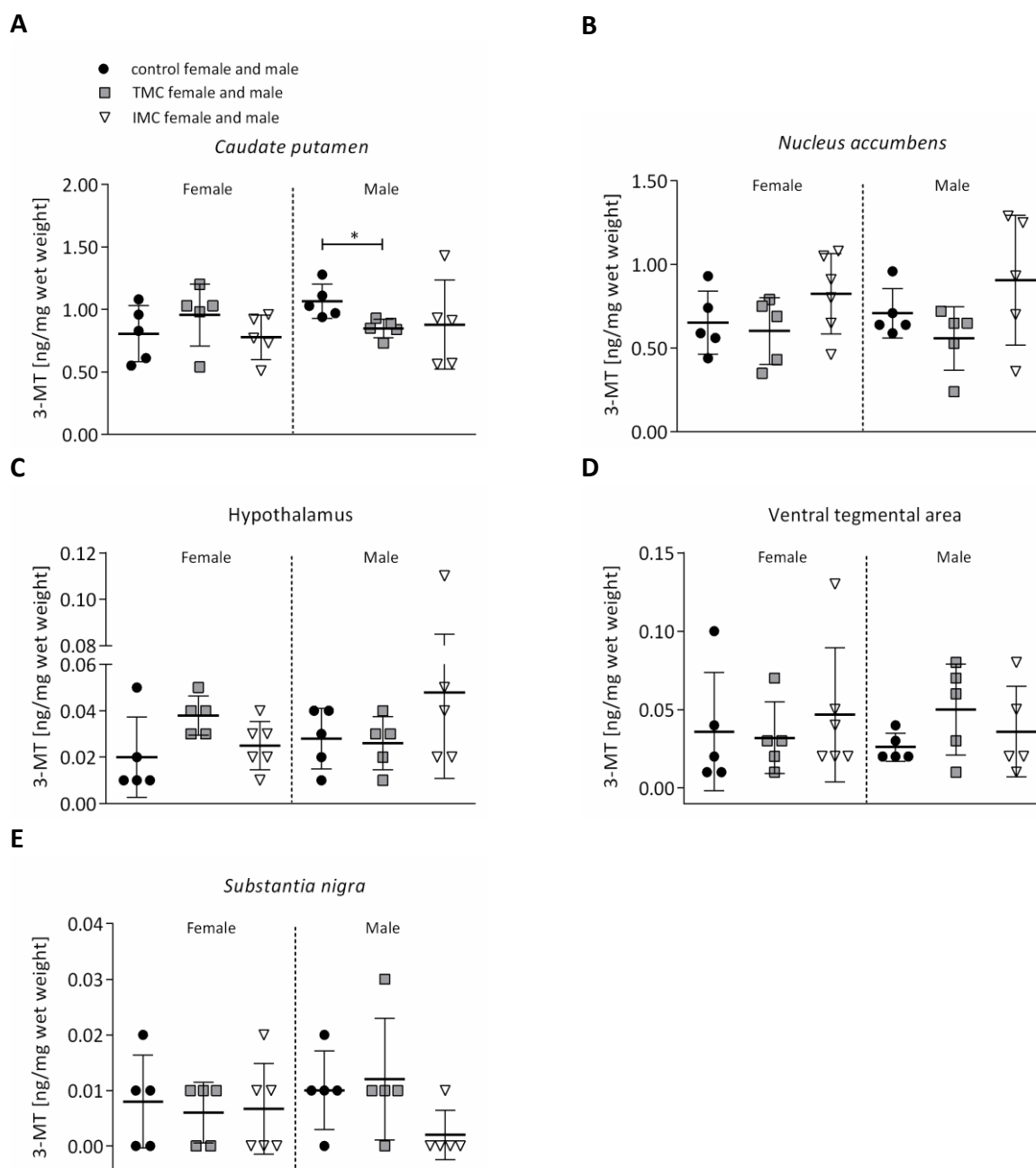


Figure 44. 3-Methoxythyramine (3-MT) concentrations [ng/mg wet weight] in five different brain areas. A-E: Subdivision into extracted brain areas. Differences between control vs. TMC, control vs. IMC, and TMC vs. IMC were calculated by Kruskal-Wallis H Test (* $P \leq 0.05$). Data are presented as mean (standard deviation). Control: control cage (females and males: $n = 5$), TMC: Tecniplast metabolic cage (females and males: $n = 5$), IMC: Innovative metabolic cage (females: $n = 5$ (Caudate putamen), $n = 6$ (Nucleus accumbens, Hypothalamus, Ventral tegmental area, Substantia nigra); males: $n = 5$).

4.2.3.2 Serotonin

No significant effects in serotonin concentrations were detected within specific brain areas between tested cage types (see **Figure 45 A-E**):

- CPU (see **Figure 45 A**)
 - Female: control \bar{x} = 0.46 ng/mg, TMC \bar{x} = 0.37 ng/mg, IMC \bar{x} = 0.33 ng/mg
 - Male: control \bar{x} = 0.36 ng/mg, TMC \bar{x} = 0.42 ng/mg, IMC \bar{x} = 0.40 ng/mg

- NAC (see **Figure 45 B**)
 - Female: control \bar{x} = 0.47 ng/mg, TMC \bar{x} = 0.40 ng/mg, IMC \bar{x} = 0.55 ng/mg
 - Male: control \bar{x} = 0.52 ng/mg, TMC \bar{x} = 0.37 ng/mg, IMC \bar{x} = 0.52 ng/mg

- HTM (see **Figure 45 C**)
 - Female: control \bar{x} = 0.26 ng/mg, TMC \bar{x} = 0.36 ng/mg, IMC \bar{x} = 0.23 ng/mg
 - Male: control \bar{x} = 0.37 ng/mg, TMC \bar{x} = 0.27 ng/mg, IMC \bar{x} = 0.32 ng/mg

- VTA (see **Figure 45 D**)
 - Female: control \bar{x} = 0.23 ng/mg, TMC \bar{x} = 0.25 ng/mg, IMC \bar{x} = 0.34 ng/mg
 - Male: control \bar{x} = 0.18 ng/mg, TMC \bar{x} = 0.31 ng/mg, IMC \bar{x} = 0.23 ng/mg

- SN (see **Figure 45 E**)
 - Female: control \bar{x} = 0.09 ng/mg, TMC \bar{x} = 0.06 ng/mg, IMC \bar{x} = 0.10 ng/mg
 - Male: control \bar{x} = 0.10 ng/mg, TMC \bar{x} = 0.11 ng/mg, IMC \bar{x} = 0.06 ng/mg.

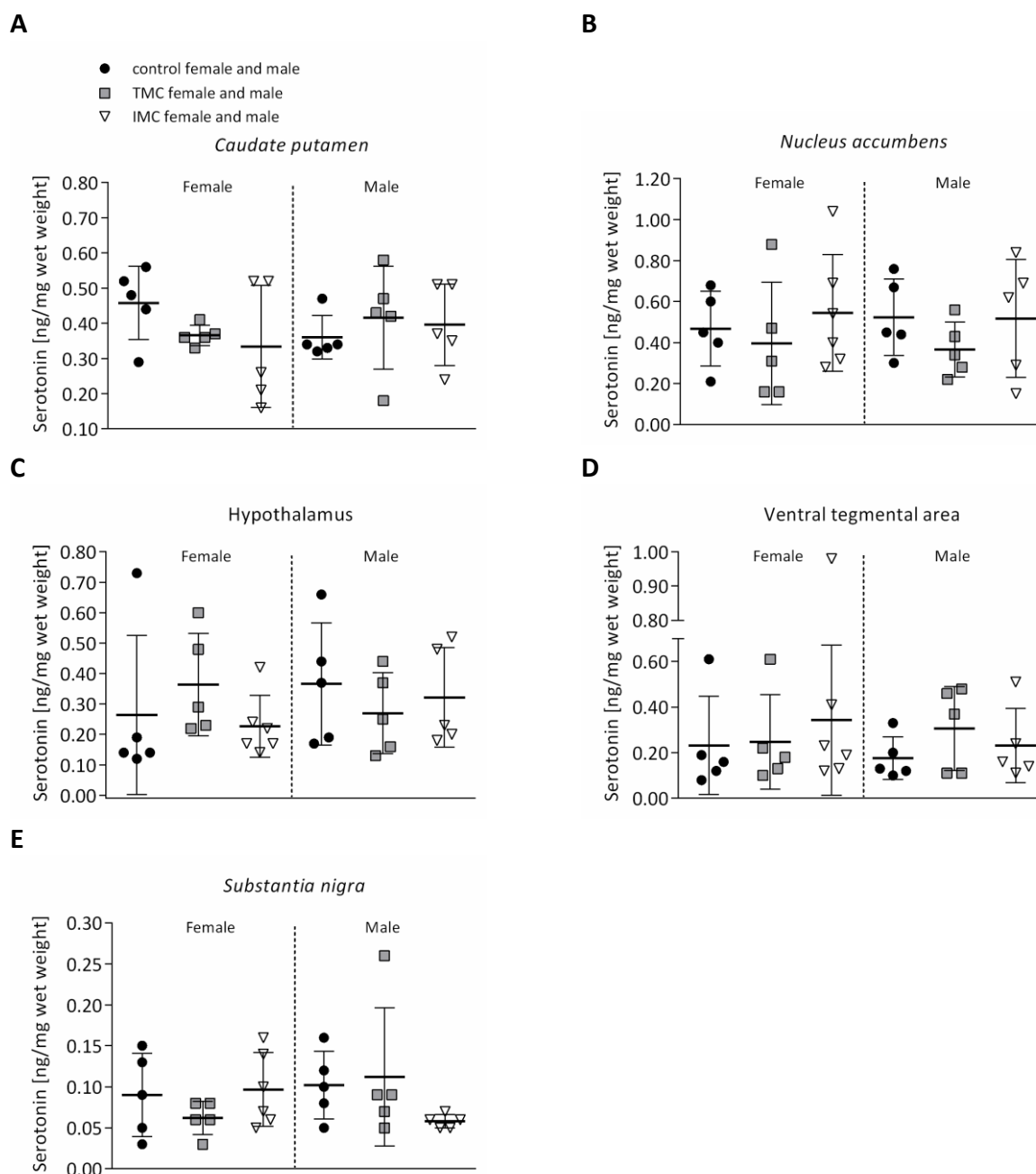


Figure 45. Serotonin concentrations [ng/mg wet weight] in five different brain areas. A-E: Subdivision into extracted brain areas. Differences between control vs. TMC, control vs. IMC, and TMC vs. IMC were calculated by Kruskal-Wallis H Test. Data are presented as mean (standard deviation). Control: control cage (females and males: $n = 5$), TMC: Tecniplast metabolic cage (females and males: $n = 5$), IMC: Innovative metabolic cage (females: $n = 5$ (Caudate putamen), $n = 6$ (Nucleus accumbens, Hypothalamus, Ventral tegmental area, Substantia nigra); males: $n = 5$).

Neurotransmitter analyses of respective brain areas revealed that especially one metabolite of DA, DOPAC, is increased after IMC restraint compared to controls in the CPU and NAC of females as well as in the HTM of males. For males, DOPAC levels in HTM were additionally significantly increased after IMC restraint in contrast to the TMC. There were no significant differences in DA and SRT levels among cage types in different brain areas of both sexes.

4.2.3.3 The dorsal mesostriatal system

The dorsal mesostriatal system originates in the *Substantia nigra pars compacta* (SNc) and projects to the CPU. Since this pathway is involved in motor control and the execution of voluntary movements, collected locomotion parameters during behavioral testing were correlated with DA levels in both brain areas. Data after the second restraint in different cages only were included in the analyses, because the time span between brain extraction and behavioral testing was otherwise too long. 3-MT as a metabolite of DA was included in the analyses, because its concentrations were above detection limit in both brain areas of interest as compared with the other measured metabolite DOPAC.

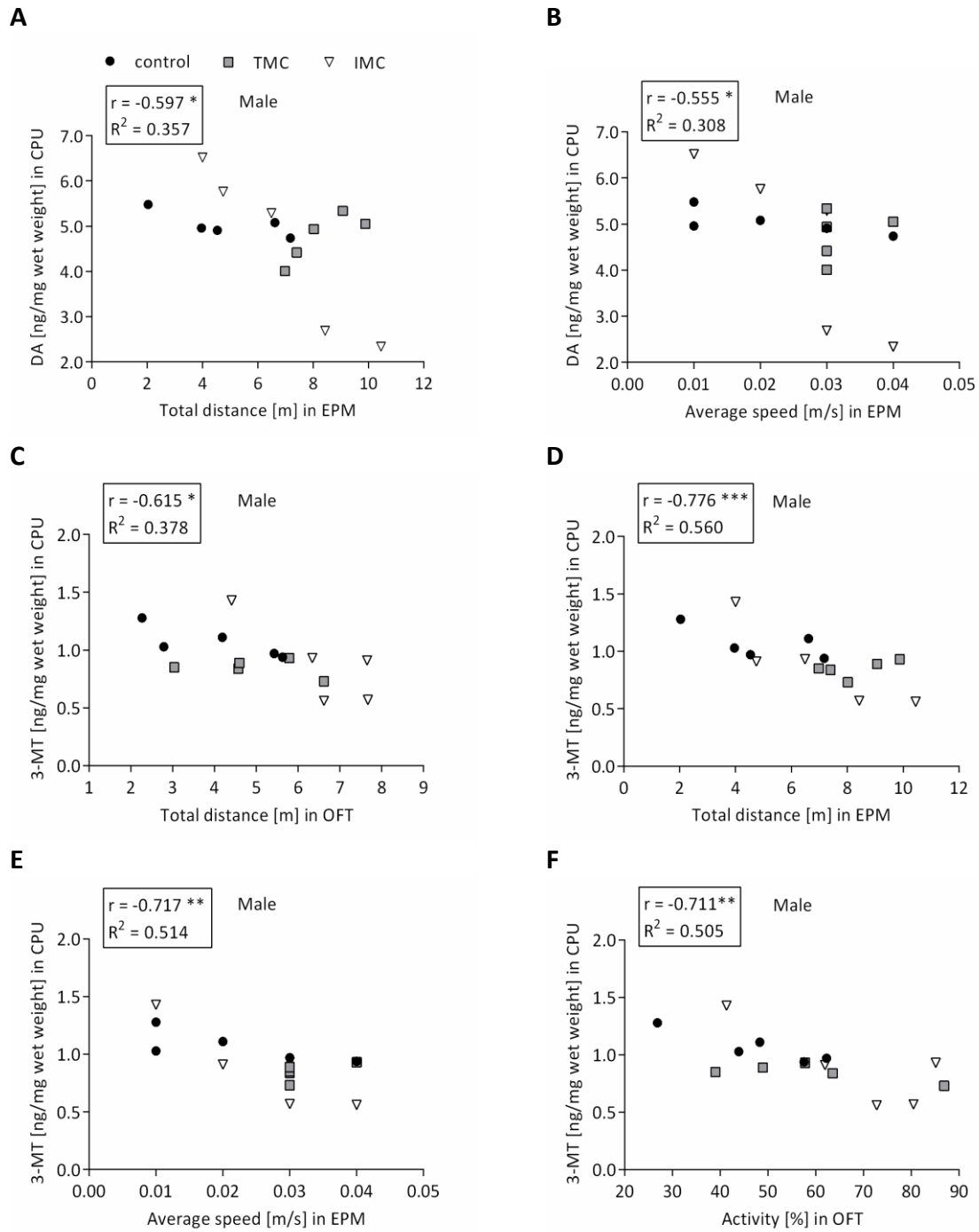
Concerning male mice, total distance in EPM showed significant correlations with DA ($P \leq 0.05$, $r = -0.597$, see **Table 9** and **Figure 46 A**) and 3-MT in the CPU ($P \leq 0.001$, $r = -0.776$, see **Figure 46 D**). The total distance traveled during OFT was also significantly correlated with 3-MT in CPU as well as SN (CPU: $P \leq 0.05$, $r = -0.615$, see **Figure 46 C**; SN: $P \leq 0.05$, $r = -0.596$, see **Figure 46 J**) and DA in the SN ($P \leq 0.001$, $r = -0.745$, see **Figure 46 H**). These results suggest a decrease of DA and 3-MT in the CPU and SN of males that travelled a longer distance.

Average speed alone showed significant correlations for male mice in the EPM concerning levels of DA ($P \leq 0.05$, $r = -0.555$, see **Figure 46 B**) and 3-MT in the CPU ($P \leq 0.01$, $r = -0.717$, see **Figure 46 E**). The faster males explored the EPM arena, the higher the reduction in DA and 3-MT in the CPU.

Activity during OFT was negatively correlated with DA (all mice: $P \leq 0.01$, $r = -0.496$; male: $P \leq 0.05$, $r = -0.639$, see **Figure 46 I**) and 3-MT (all mice: $P \leq 0.05$, $r = -0.366$; male: $P \leq 0.05$, $r = -0.535$, see **Figure 46 K**) in the SN. In addition, activity in the OFT ($P \leq 0.01$, $r = -0.711$, see **Figure 46 F**) and EPM ($P \leq 0.05$, $r = -0.531$, see **Figure 46 G**) was negatively correlated for males concerning 3-MT in the CPU. This indicates that DA and 3-MT concentrations decreased in respective brain areas with increasing activity during 5 min behavioral testing.

Table 9. Correlation between the concentration of the neurotransmitters dopamine (DA) and 3-methoxytyramine (3-MT) [ng/mg wet weight] in the caudate putamen (CPU) or substantia nigra (SN) and the total distance [m], average speed [m/s], and activity [%] in either the Elevated Plus Maze (EPM) or the Open Field Test (OFT) after second restraint. Pearson or Spearman correlation analyses were conducted. Data are expressed as correlation coefficients (* $P \leq 0.05$, ** $P \leq 0.01$, *** $P \leq 0.001$).

Neurotransmitter concentration [ng/mg wet weight]	Parameters for locomotion	All mice n=30	Female n=15	Male n=15
DA in CPU	Total distance [m] in OFT	-0.182	-0.144	-0.309
	Total distance [m] in EPM	-0.104	0.353	-0.597 *
	Average speed [m/s] in OFT	-0.090	0.012	-0.179
	Average speed [m/s] in EPM	-0.206	0.071	-0.555 *
	Activity [%] in OFT	-0.222	-0.102	-0.408
	Activity [%] in EPM	-0.215	-0.105	-0.372
3-MT in CPU	Total distance [m] in OFT	-0.073	0.206	-0.615 *
	Total distance [m] in EPM	-0.172	0.363	-0.776 ***
	Average speed [m/s] in OFT	0.043	0.197	-0.043
	Average speed [m/s] in EPM	-0.286	0.098	-0.717 **
	Activity [%] in OFT	-0.240	0.098	-0.711 **
	Activity [%] in EPM	-0.295	-0.136	-0.531 *
DA in SN	Total distance [m] in OFT	-0.163	-0.033	-0.745 ***
	Total distance [m] in EPM	-0.248	-0.315	-0.372
	Average speed [m/s] in OFT	-0.026	-0.004	0.232
	Average speed [m/s] in EPM	-0.164	-0.067	-0.359
	Activity [%] in OFT	-0.496 **	-0.350	-0.639 *
	Activity [%] in EPM	-0.228	-0.287	-0.418
3-MT in SN	Total distance [m] in OFT	-0.249	0.021	-0.596 *
	Total distance [m] in EPM	-0.147	-0.145	-0.180
	Average speed [m/s] in OFT	0.165	-0.090	0.422
	Average speed [m/s] in EPM	-0.060	0.007	-0.133
	Activity [%] in OFT	-0.366 *	-0.212	-0.535 *
	Activity [%] in EPM	-0.163	-0.023	-0.312



The figure legend is displayed on the following page.

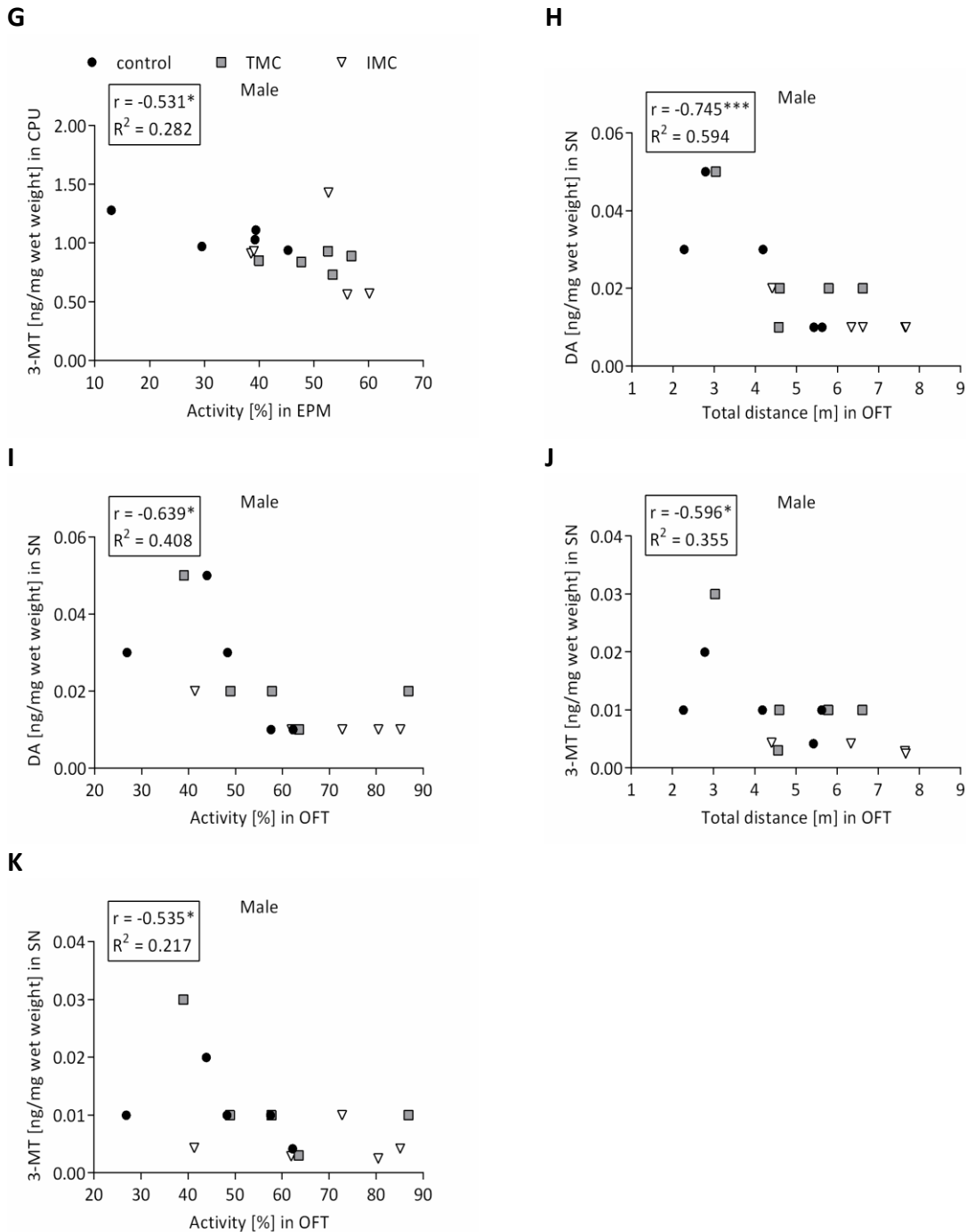


Figure 46. Correlation between the concentration of neurotransmitters dopamine (DA) and 3-methoxytyramine (3-MT) [ng/mg wet weight] in caudate putamen (CPU) or substantia nigra (SN) of male mice and the total distance [m], average speed [m/s], and activity [%] in either the Elevated Plus Maze (EPM) or the Open Field Test (OFT) after second restraint. Pearson or Spearman correlation analyses were conducted. Data are expressed as correlation coefficients, significance level (* $P \leq 0.05$, ** $P \leq 0.01$, *** $P \leq 0.001$), and coefficient of determination (R^2).

4.3 Metabolic parameters

4.3.1 Body weight change

Mice had access to the same pelleted chow *ad libitum* in each of the three tested cage types. Body weight (BW) development was assessed at five points in time during the two week test schedule. All BW data collected were referenced to the baseline measurement (see **Figure 47 A+C**). BW change was additionally calculated, where the percentage weight change was calculated based on BW measured shortly before and shortly after the 24 h restraint (see **Figure 47 B+D**).

Significant reductions in BW were detected after 24 h single housing, especially in the TMC. Female mice lost significantly more BW in TMC compared to controls after the first ($P \leq 0.01$) and second restraints ($P \leq 0.001$, see **Figure 47 A**). Only after the first restraint, BW in IMC was significantly reduced compared to controls ($P \leq 0.01$). Concerning the second 24 h restraint, females lost significantly more BW in the TMC compared to the IMC ($P \leq 0.01$). Male mice lost significantly more BW in the TMC compared to the IMC (1st restraint: $P \leq 0.05$, 2nd restraint: $P \leq 0.01$) and controls (1st restraint: $P \leq 0.01$, 2nd restraint: $P \leq 0.001$; see **Figure 47 C**). In addition, reduction in BW was significantly different between the IMC and controls after the second restraint ($P \leq 0.05$).

When focussing on BW change during either 24 h restraint, the significantly highest BW change was detected for females in TMC (1st restraint: $\bar{x} = -13.2\%$, 2nd restraint: $\bar{x} = -15.0\%$) in contrast to controls (1st restraint: $P \leq 0.01$, $\bar{x} = -3.78\%$; 2nd restraint: $P \leq 0.001$, $\bar{x} = -4.78\%$; see **Figure 47 B**). Female mice lost significantly more BW in the IMC (1st restraint: $P \leq 0.05$, $\bar{x} = -6.94\%$; 2nd restraint: $P \leq 0.01$, $\bar{x} = -6.89\%$) compared to controls. BW change in TMC was significantly higher during both restraints compared to the IMC (1st restraint: $P \leq 0.05$, 2nd restraint: $P \leq 0.01$). Concerning males, BW change was significantly higher in the TMC (1st restraint: $\bar{x} = -13.1\%$, 2nd restraint: $\bar{x} = -14.9\%$) compared to controls (1st restraint: $P \leq 0.01$, $\bar{x} = -6.34\%$; 2nd restraint: $P \leq 0.001$, $\bar{x} = -3.36\%$) and the IMC (1st restraint: $P \leq 0.05$, $\bar{x} = -8.08\%$; 2nd restraint: $P \leq 0.001$, $\bar{x} = -5.82\%$) after both restraints (see **Figure 47 D**). Additionally, female mice were more sensitive to the IMC than male mice since BW change in the IMC was significantly higher compared to controls. In contrast, BW change of males during restraint in the IMC was equivalent to controls. In summary, it can be stated that BW change was tremendous during 24 h single housing in the TMC. After 6 d of resting, the mice gained weight that was comparable to the initial weight.

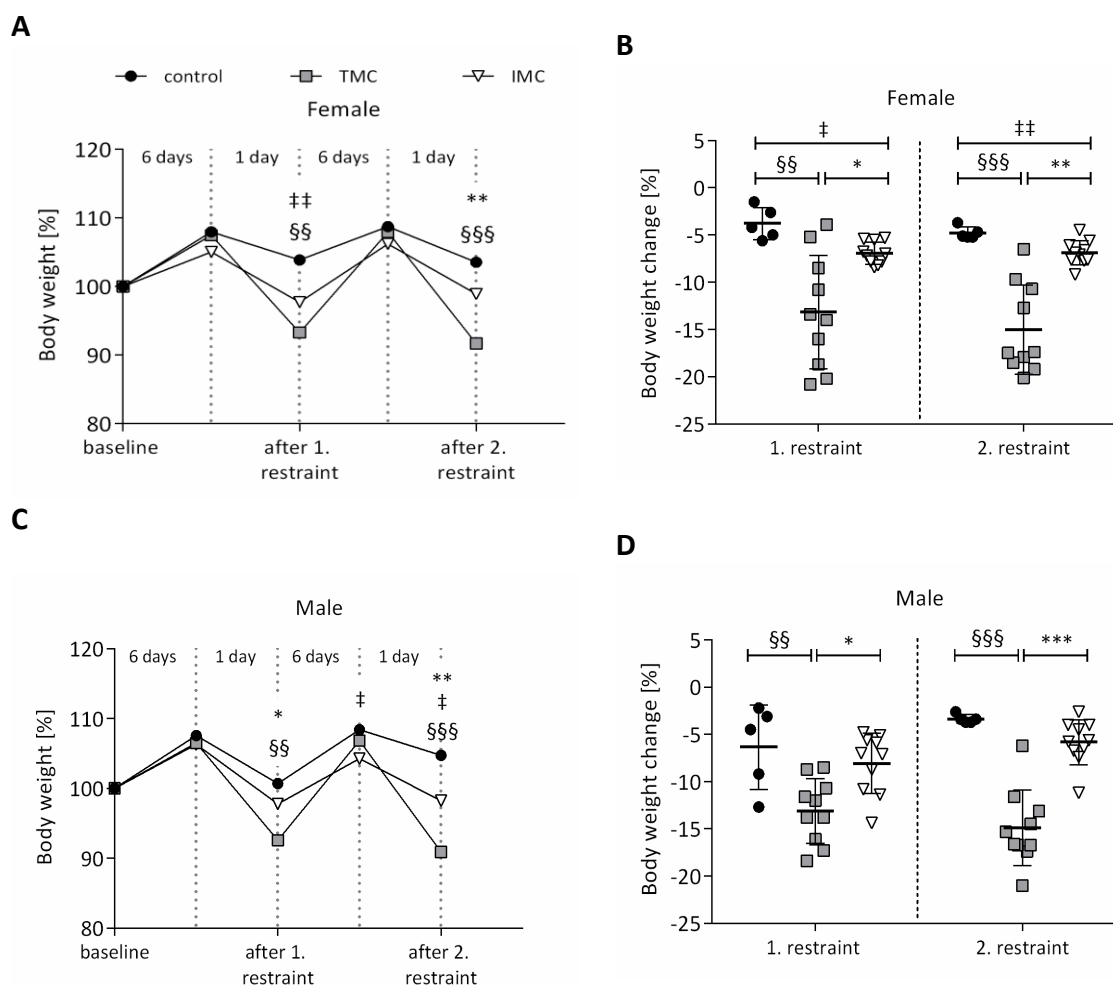


Figure 47. Body weight [%] referenced to baseline measurement and body weight change [%] during restraint in the three tested cage types. A+C: Development of body weight [%] regarding female and male mice in the three different cage types compared to baseline assessment (100%). **B+D:** Body weight change [%] of female and male mice during first and second restraints in the three different cage types. Differences among cage types were calculated by one-way ANOVA. Differences in body weight were analyzed separately for each point in time. * $P \leq 0.05$, ** $P \leq 0.01$, *** $P \leq 0.001$, TMC vs. IMC; §§ $P \leq 0.01$, §§§ $P \leq 0.001$, TMC vs. control; † $P \leq 0.05$, †† $P \leq 0.01$, IMC vs. control. Data are presented as mean (A + C) and mean (standard deviation, B + D). Control: control cage ($n = 5$), TMC: Tecniplast metabolic cage ($n = 10$), IMC: Innovative metabolic cage ($n = 10$).

4.3.2 Body composition

4.3.2.1 Lean mass change

Lean mass (LM) as well as fat mass (FM) of mice were assessed shortly after determination of BW. Change of LM and FM were calculated for each 24 h restraint in the same way as BW change (see **Figure 48**, see **Figure 49**).

After both 24 h restraints of female and male mice, LM loss in the TMC (Females-1st restraint: \bar{x} = -13.0%, 2nd restraint: \bar{x} = -14.5%; Males-1st restraint: \bar{x} = -12.3%, 2nd restraint: \bar{x} = -12.9%) was significantly higher compared to controls (Females-1st restraint: $P \leq 0.01$, \bar{x} = -5.32%, 2nd restraint: $P \leq 0.001$, \bar{x} = -5.91%; Males-1st restraint: $P \leq 0.01$, \bar{x} = -6.04%, 2nd restraint: $P \leq 0.001$, \bar{x} = -4.43%) and IMC restraint (Females-1st restraint: $P \leq 0.01$, \bar{x} = -7.46%, 2nd restraint: $P \leq 0.001$, \bar{x} = -7.92%; Males-1st restraint: $P \leq 0.05$, \bar{x} = -7.59%, 2nd restraint: $P \leq 0.001$, \bar{x} = -5.37%; see **Figure 48 A-B**).

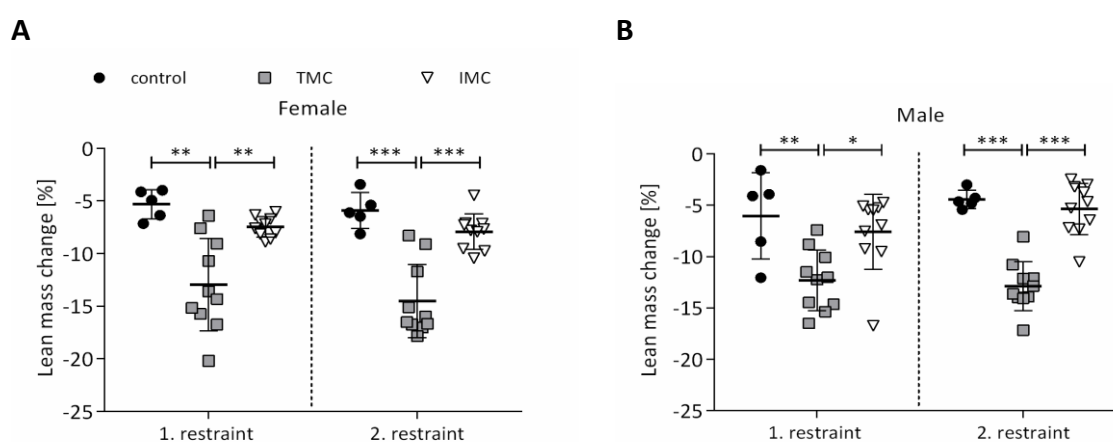


Figure 48. Lean mass change [%] after first and second restraints in the three tested cage types. A: Female mice. B: Male mice. Differences between TMC vs. IMC, TMC vs. control, IMC vs. control were calculated by one-way ANOVA. Differences in lean mass were analyzed separately for each point in time. * $P \leq 0.05$, ** $P \leq 0.01$, *** $P \leq 0.001$. Data are presented as mean (standard deviation). Control: control cage ($n = 5$), TMC: Tecniplast metabolic cage ($n = 10$), IMC: Innovative metabolic cage ($n = 10$).

4.3.2.2 Fat mass change

No effect of the cage type on FM loss was detected for female mice after the first restraint (see **Figure 49 A**). After the second restraint, females lost significantly more FM in the TMC (\bar{x} = -44.8%) compared to the IMC ($P \leq 0.01$, \bar{x} = -20.6%). Concerning male mice, FM loss was significantly higher in the TMC (1st restraint: \bar{x} = -45.4%, 2nd restraint: \bar{x} = -58.3%) in contrast to the IMC (1st restraint: $P \leq 0.01$, \bar{x} = -18.8%; 2nd restraint: $P \leq 0.001$, \bar{x} = -23.9%) and controls (1st restraint: $P \leq 0.05$, \bar{x} = -23.8%; 2nd restraint: $P \leq 0.001$, \bar{x} = -21.1%; see **Figure 49 B**). In summary, it can be stated that body weight as well as body composition change was more pronounced after 24 h single housing in TMC compared to controls and IMC.

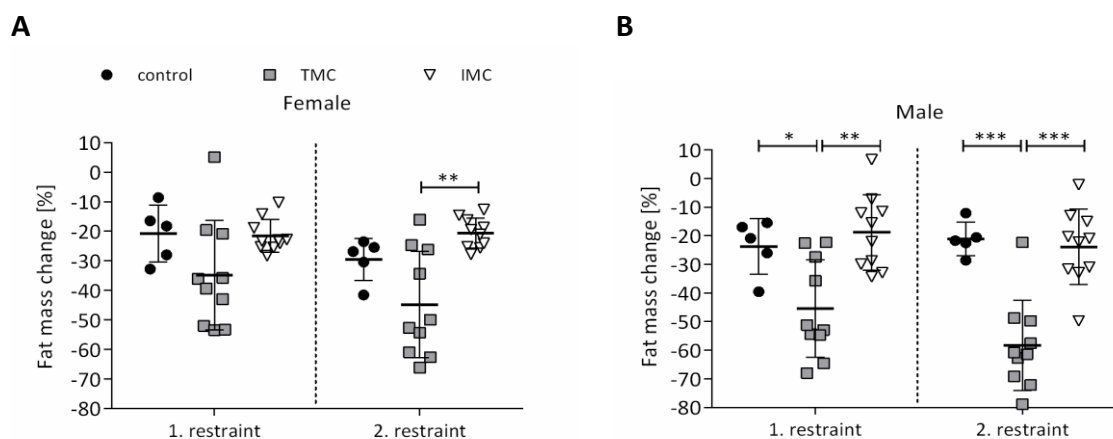


Figure 49. Fat mass change [%] after first and second restraints in the three tested cage types. A: Female mice. B: Male mice. Differences between TMC vs. IMC, TMC vs. control, IMC vs. control were calculated by one-way ANOVA. Differences in fat mass were analyzed separately for each point in time. * $P \leq 0.05$, ** $P \leq 0.01$, *** $P \leq 0.001$. Data are presented as mean (standard deviation). Control: control cage ($n = 5$), TMC: Tecniplast metabolic cage ($n = 10$), IMC: Innovative metabolic cage ($n = 10$).

4.3.3 Food intake

Food intake is expressed per BW to account for the significant variation in BW during metabolic cage restraint (see **Figure 50**). Females tended to consume more food during the second IMC restraint than in the TMC ($P = 0.056$, see **Figure 50 A**). During first restraint, male mice tended to ingest more food during IMC restraint than in the TMC ($P = 0.086$, see **Figure 50 B**). Food intake for male mice was significantly increased in the IMC compared to the TMC after the second restraint ($P \leq 0.001$).

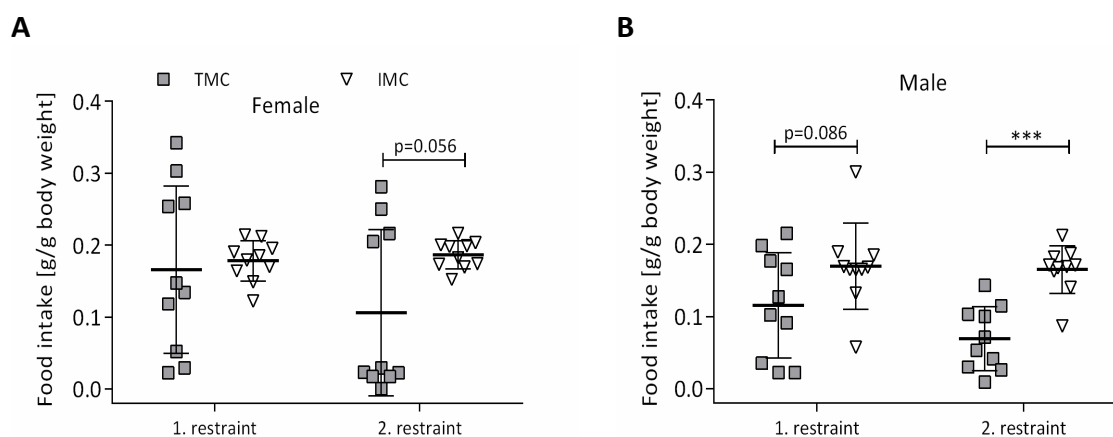


Figure 50. Food intake [g/g body weight] during first and second restraints in the metabolic cage types. A: Female mice. B: Male mice. Food intake during control cage housing was not assessed. The difference between TMC vs. IMC was calculated by independent-samples t-test and analyzed separately for each point in time. *** $P \leq 0.001$. Data are presented as mean (standard deviation). TMC: Tecniplast metabolic cage ($n = 10$), IMC: Innovative metabolic cage ($n = 10$).

4.3.4 Water intake

Water intake was significantly higher for male mice during first restraint in the IMC compared with the TMC ($P \leq 0.01$, see **Figure 51 B**). A statistically significant increase in water intake during IMC restraint relative to TMC restraint was observed after the second restraint for both sexes ($P \leq 0.001$, see **Figure 51 A-B**).

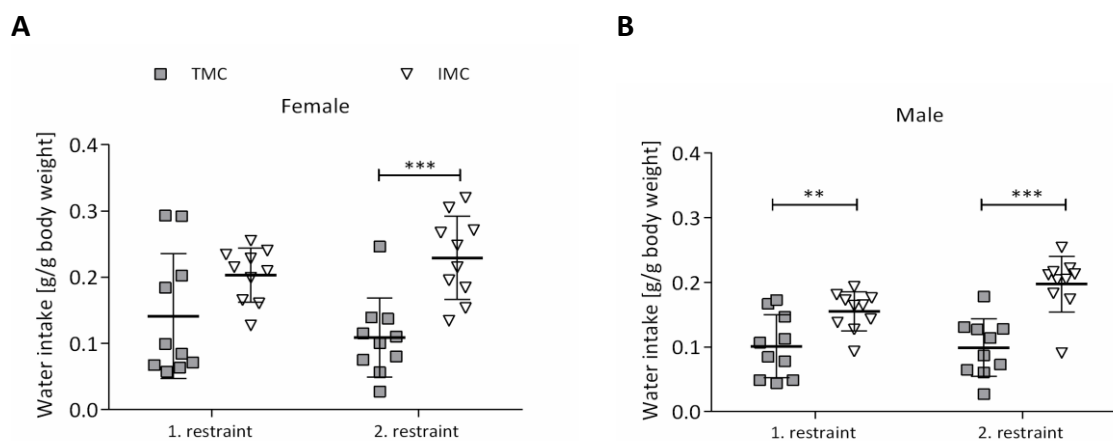


Figure 51. Water intake [g/g body weight] during first and second restraints in the metabolic cage types. A: Female mice. B: Male mice. Water intake during control cage housing was not assessed. The difference between TMC vs. IMC was calculated by independent-samples t-test and analyzed separately for each point in time. ** $P \leq 0.01$, *** $P \leq 0.001$. Data are presented as mean (standard deviation). TMC: Tecniplast metabolic cage ($n = 10$), IMC: Innovative metabolic cage ($n = 10$).

4.3.5 Defecation

The trend already indicated for food intake was even more pronounced for fecal output with a significant increase in defecation during IMC restraint compared to TMC restraint (see **Figure 50 A-B**, **Figure 52 A-B**). This was true for both sexes during both restraints (1st restraint: females - $P \leq 0.01$, males - $P \leq 0.001$; 2nd restraint: females and males - $P \leq 0.001$).

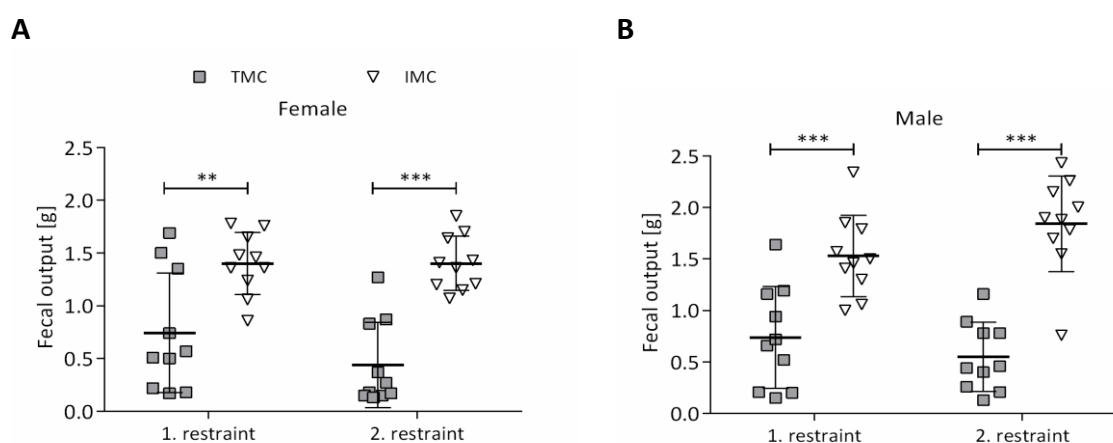


Figure 52. Fecal output [g] during first and second restraints in the metabolic cage types. A: Female mice. B: Male mice. Fecal output during control cage housing was not assessed. The difference between TMC vs. IMC was calculated by independent-samples t-test and analyzed separately for each point in time. ** $P \leq 0.01$, *** $P \leq 0.001$. Data are presented as mean (standard deviation). TMC: Tecniplast metabolic cage ($n = 10$), IMC: Innovative metabolic cage ($n = 10$).

4.3.6 Urinary excretion

The significant increase in water intake during the first (only for males) and second restraints in the IMC (both sexes) in comparison with the TMC was verified by a significantly higher excreted urine volume during first (both sexes) and second restraint (only for females) in the IMC compared to the TMC (see **Figure 51**, **Figure 53**). Females excreted significantly more urine in the IMC at both investigated points in time compared to restraint in the TMC (1st restraint: $P \leq 0.01$, 2nd restraint: $P \leq 0.001$; see **Figure 53 A**). This was also true for males during the first restraint ($P \leq 0.01$, see **Figure 53 B**). To summarize the data gathered during metabolic cage restraint, a tendency or trend for an increased food as well as water intake in the IMC compared to the TMC was detected. This was confirmed by the higher excretion of feces and urine during IMC restraint relative to the TMC. The decreased BW, LM, and FM loss in IMC compared to TMC could be attributed to the increased food intake in IMC.

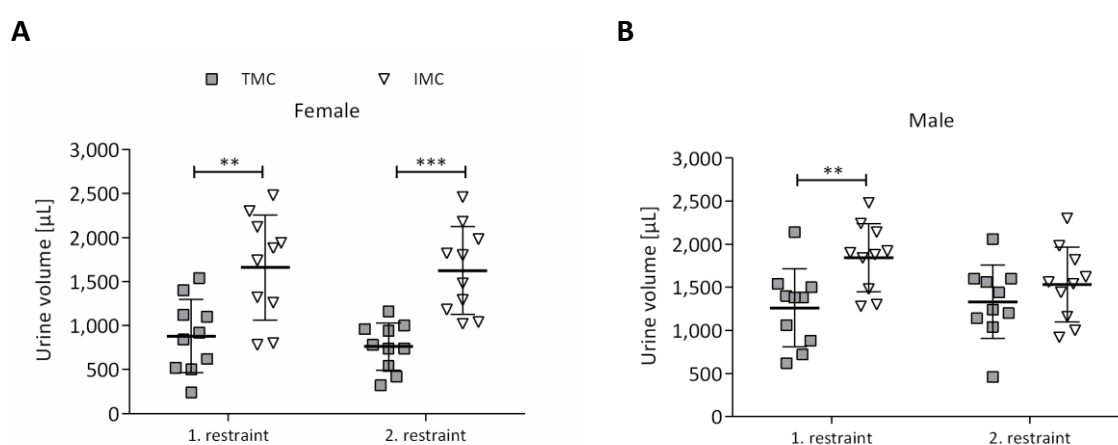


Figure 53. Excreted urine volume [μL] during first and second restraints in the metabolic cage types. A: Female mice. B: Male mice. Excreted urine volume during control cage housing was not assessed. The difference between TMC vs. IMC was calculated by independent-samples t-test and analyzed separately for each point in time. ** $P \leq 0.01$, * $P \leq 0.001$. Data are presented as mean (standard deviation). TMC: Tecniplast metabolic cage ($n = 10$), IMC: Innovative metabolic cage ($n = 10$).**

4.3.7 Glycogen levels in liver

4.3.7.1 Periodic Acid Schiff/Hematoxylin staining

To investigate the glycogen stores of mice after two housing sessions in different cage types, liver slices were stained with Periodic Acid Schiff (PAS) and Hematoxylin was utilized as counterstaining. The reduced glycogen content in liver slices of female and male mice after restraint in the TMC (see **Figure 54** C-D) as opposed to the IMC (see **Figure 54** E-F) was indicated by the reduction in the color intensity of PAS.

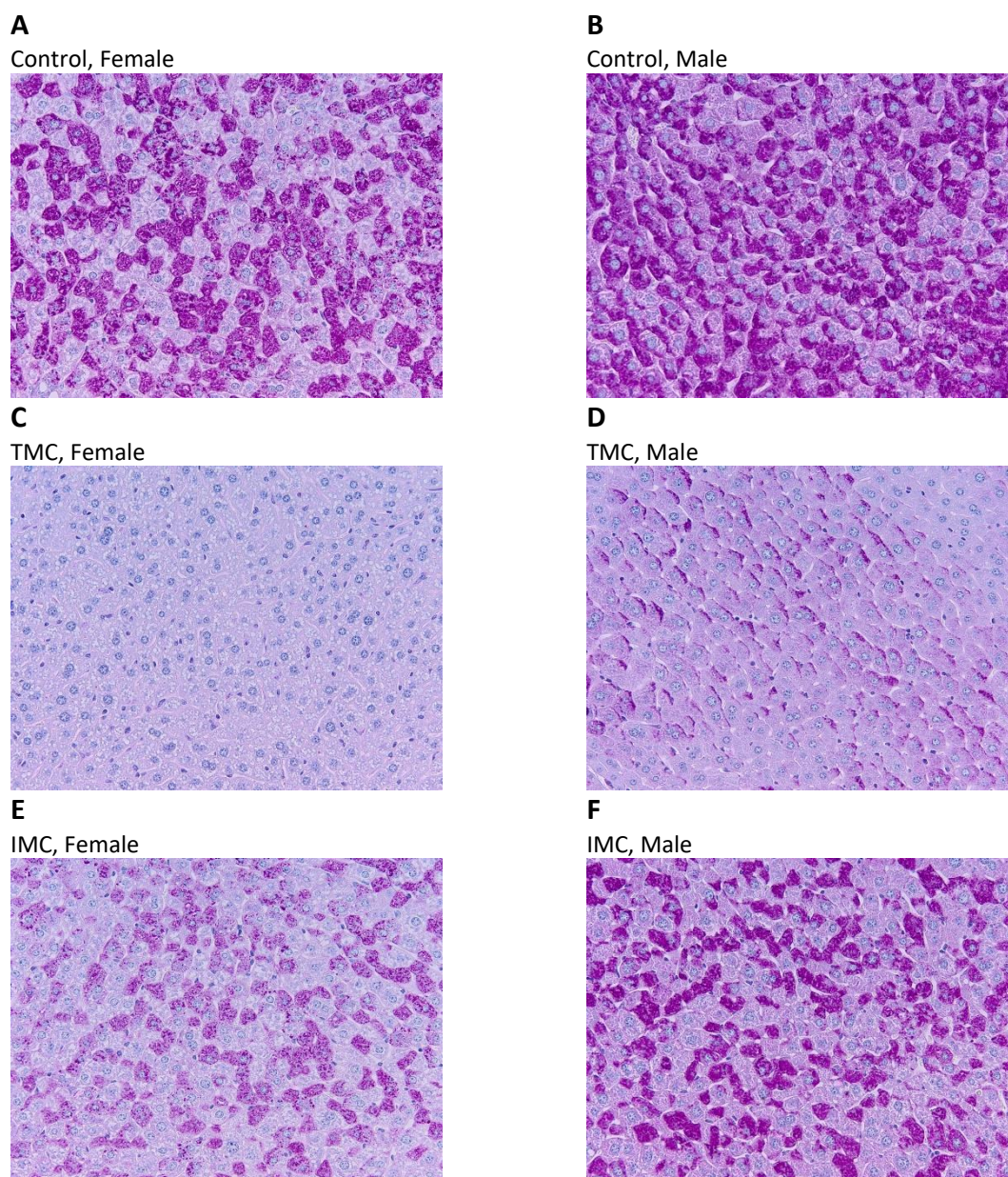


Figure 54. Sample photos of liver slices stained with Periodic acid Schiff (PAS)/Hematoxylin. A: Control, female. **B:** Control, male. **C:** TMC, female. **D:** TMC, male. **E:** IMC, female. **F:** IMC, male. Liver tissue was extracted from female and male mice after second restraint in the control cage (Control), Tecniplast metabolic cage (TMC), and the Innovative metabolic cage (IMC).

In the next step, ratios of PAS to Hematoxylin were calculated based on displayed pixels of the Color Deconvolution plugin “Haematoxylin and Periodic Acid of Schiff” of ImageJ (NIH) (see chapter 3.2.2 Histology - Periodic Acid Schiff/Hematoxylin staining). The calculated ratios for female and male mice in the TMC and IMC were then referenced to controls of each sex (see Figure 55). The percentage area stained positive with PAS relative to controls were significantly lower for female and male mice in the TMC compared to the IMC ($P \leq 0.001$). These results obtained by a histological approach support the results acquired by the applied UV method for glycogen quantification of which the results are shown in the further course of the thesis (see chapter 4.3.7.2 UV method).

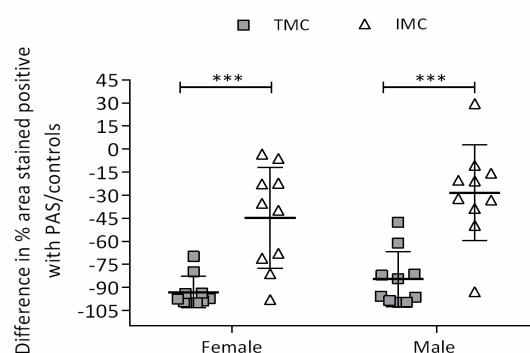


Figure 55. Differences in percentage [%] areas stained positive with Periodic Acid Schiff (PAS) relative to controls ($n = 5$) are depicted for liver slices of female and male mice after second restraint in either Tecniplast metabolic cage (TMC, $n = 10$) or Innovative metabolic cage (IMC, $n = 10$). The difference between TMC vs. IMC was calculated by independent-samples t-test. *** $P \leq 0.001$. Data are presented as mean (standard deviation).

4.3.7.2 UV method

In addition to histological analyses of glycogen content in liver slices by PAS-staining, glycogen in liver tissue was determined by an UV method, following liver lysis and extraction with sodium hydroxide (see chapter 3.2.4.2 Determination of liver glycogen by UV method). Restraint in the TMC induced a significant reduction in liver glycogen concentrations compared to the IMC (female: $P \leq 0.05$, male: $P \leq 0.001$; see Figure 56 A-B). For males, glycogen concentration was also significantly reduced after second restraint in the TMC in comparison with controls ($P \leq 0.001$).

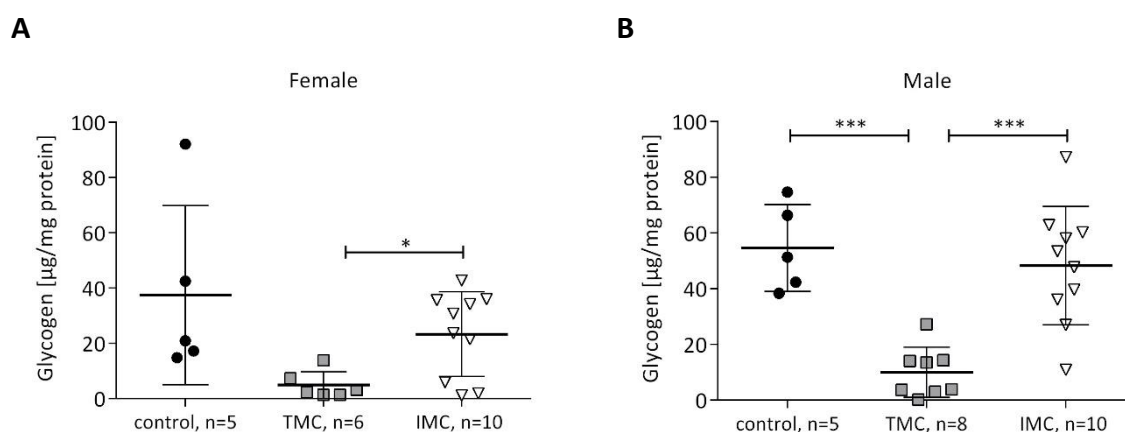


Figure 56. Glycogen concentration [$\mu\text{g}/\text{mg}$ protein] in liver after second restraint in the three different cage types. **A:** Female mice. **B:** Male mice. Differences between TMC vs. IMC, TMC vs. control, IMC vs. control were calculated by one-way ANOVA. * $P \leq 0.05$, *** $P \leq 0.001$. Data are presented as mean (standard deviation). Control: control cage, TMC: Tecniplast metabolic cage, IMC: Innovative metabolic cage.

4.3.7.3 Correlation between glycogen concentration and food intake

In the next step, glycogen concentrations obtained by the UV method were correlated with food intake during the second 24 h restraint in the TMC or IMC. A significant correlation between glycogen concentration in liver and food intake during metabolic cage restraint was determined for both sexes (see **Figure 57** A-B). The correlation between both parameters was more pronounced for males ($P \leq 0.0001$) than for females ($P \leq 0.05$). Glycogen concentrations and food intake in the higher range refer to the IMC, which are depicted as white triangle symbols.

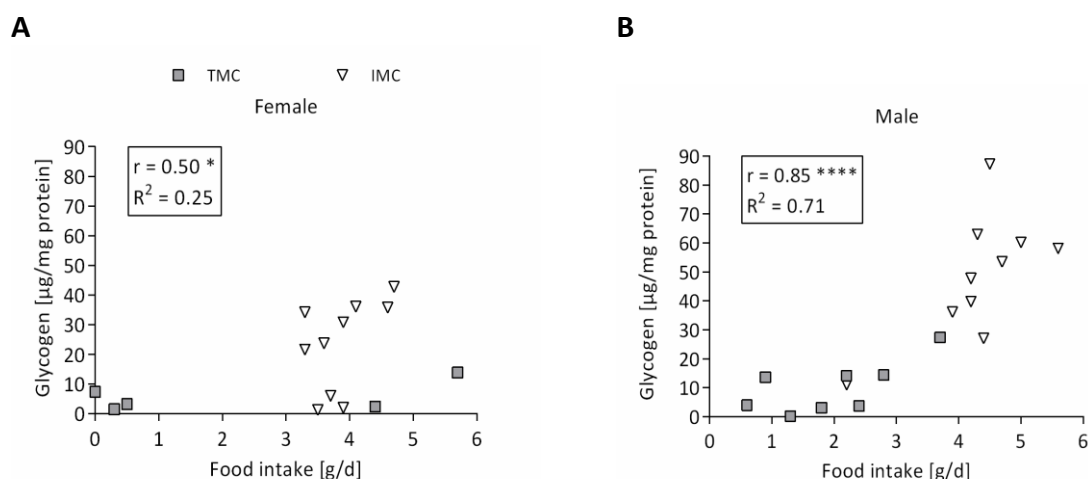


Figure 57. Correlation of glycogen concentration in liver [$\mu\text{g}/\text{mg}$ protein] with food intake [g/d] during metabolic cage restraint. A: Female mice. B: Male mice. Grey squares: Tecniplast metabolic cage (TMC). White triangles: Innovative metabolic cage (IMC). Pearson or Spearman correlation analyses were conducted. Data are expressed as correlation coefficients, significance level ($* P \leq 0.05$, $** P \leq 0.0001$), and coefficient of determination (R^2).**

4.3.7.4 Liver weight

Liver weight of mice was significantly lower after the second restraint in the TMC compared to the IMC for both sexes (female: $P \leq 0.05$, male: $P \leq 0.001$; see **Figure 58**). Liver weight of males housed in the TMC was also significantly lower compared to controls ($P \leq 0.01$). Liver weight is consistent with gathered glycogen data based on histological and biochemical approaches, where the lowest glycogen content as well as organ weight was found in the livers of mice restrained in the TMC.

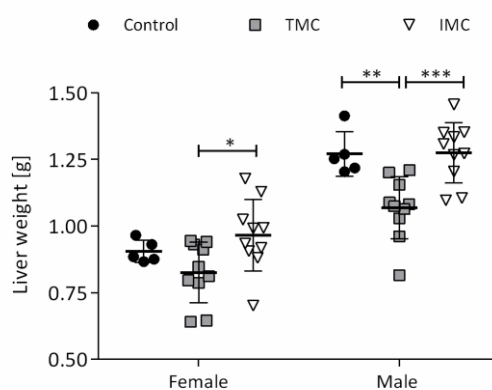


Figure 58. Liver weight [g] of female and male mice after the second restraint in the three different cage types. Differences between TMC vs. IMC, TMC vs. control, IMC vs. control were calculated by one-way ANOVA. $* P \leq 0.05$, $ P \leq 0.01$, $*** P \leq 0.001$. Data are presented as mean (standard deviation). Control: control cage ($n = 5$), TMC: Tecniplast metabolic cage ($n = 10$), IMC: Innovative metabolic cage ($n = 10$).**

4.4 Stress indicator corticosterone

4.4.1 Corticosterone levels in urine

The LC-MS/MS method from Hauser, Deschner, and Boesch (2008) [105] was originally established for quantification of steroids in primate urine. We adapted their LC-MS/MS method for quantification of corticosterone levels in urine of laboratory mice. As described in chapter 3.2.5.1 Determination of corticosterone concentrations in urine samples, we extracted the glucuronidated fraction of corticosterone metabolites besides native corticosterone. For female mice, significantly higher corticosterone concentrations in urine after TMC relative to IMC restraint were detected after both restraints ($P \leq 0.01$, see **Figure 59 A**). No effects of the tested cage types on the corticosterone secretion of male mice in urine could be detected (see **Figure 59 B**).

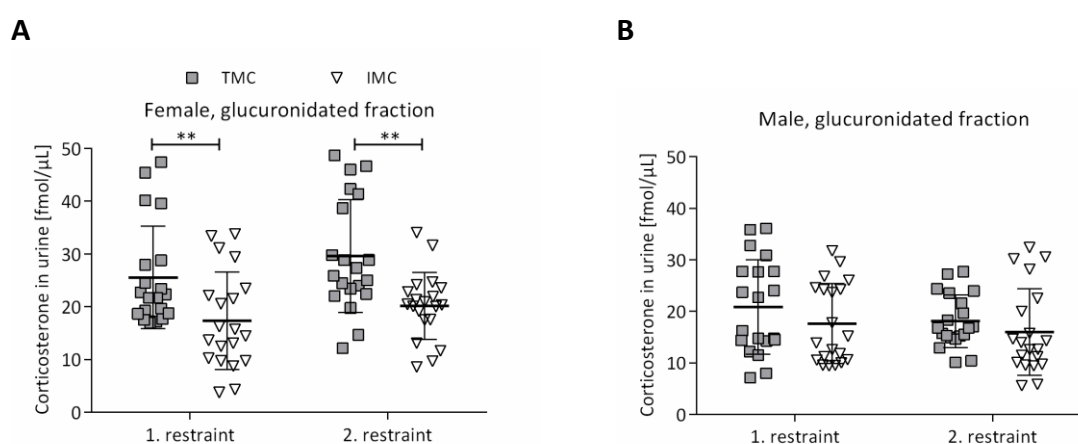


Figure 59. Corticosterone concentration in urine [fmol/ μ L] during first and second restraints in either Tecniplast metabolic cage or Innovative metabolic cage. A: Female mice. B: Male mice. Differences between TMC vs. IMC were calculated by independent-samples t test or Mann-Whitney U test. Corticosterone concentrations in urine for first and second restraint were analyzed separately. ** $P \leq 0.01$. Data are presented as mean (standard deviation). TMC: Tecniplast metabolic cage ($n = 20$), IMC: Innovative metabolic cage ($n = 20$).

Correlation between corticosterone in urine and cold stress parameters

Correlation analyses were conducted between urinary corticosterone concentrations and cold stress parameters including the Fur Score (FS, on a scale of 1 to 4), body surface temperature [$^{\circ}$ C], and cage temperature [$^{\circ}$ C]. Data of first and second restraint were analyzed separately including all mice, females or males. A significant correlation could only be detected for females between urinary corticosterone concentrations and cold stress parameters (see **Table 10**). Urinary corticosterone concentration showed a significant correlation with reference to the FS after first restraint ($r = 0.478$, $P \leq 0.05$, see **Figure 60**). This can be expressed as follows: as the FS increases (fur state deteriorates), stress hormone secretion into urine increases.

Table 10. Correlation analyses between corticosterone concentrations in urine (native and glucuronidated fraction) [fmol/ μ L] and Fur Score, body surface temperature [$^{\circ}$ C], cage temperature [$^{\circ}$ C] (cold stress). Pearson or Spearman correlation analyses were conducted. Data are expressed as correlation coefficients (* $P \leq 0.05$).

Corticosterone in urine [fmol/ μ L]	Cold stress	No. of restraint	All mice n=40	Female n=20	Male n=20
	Fur Score		first	0.200	0.478 *
second			-0.118	0.370	0.221
Body surface temperature [$^{\circ}$ C]		first	-0.125	-0.037	-0.212
		second	-0.273	-0.369	-0.025
Cage temperature [$^{\circ}$ C]		first	-0.138	-0.333	0.104
		second	-0.201	-0.418	-0.032

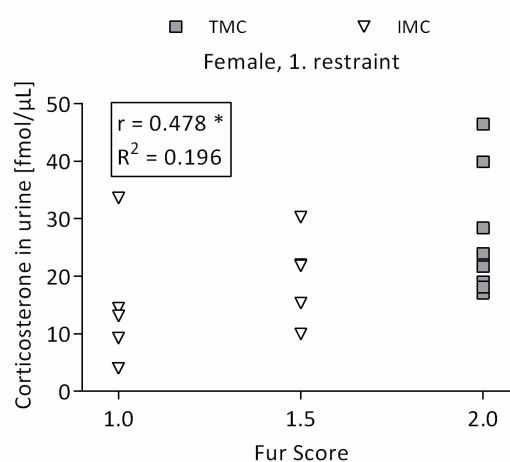


Figure 60. Correlation analysis between corticosterone concentrations in urine (native and glucuronidated fraction) [fmol/ μ L] and Fur Score of female mice after first restraint. Spearman correlation analyses were conducted. Data are expressed as correlation coefficients, significance level (* $P \leq 0.05$), and coefficient of determination (R^2).

4.4.2 Corticosterone levels in feces

In the frame of stress monitoring, fecal corticosterone metabolites (FCM) were quantified in fecal samples, which were collected during 24 h single housing. Females excreted a significantly higher amount of FCM in the TMC compared to controls after both 24 h restraints ($P \leq 0.05$, see **Figure 61 A**). FCM concentrations in IMC and control cages were comparable for female mice. Concerning male mice, FCM concentrations were significantly elevated after TMC restraint compared to controls (1st restraint: $P \leq 0.05$, 2nd restraint: $P \leq 0.01$; see **Figure 61 B**). Concerning the first restraint, significantly increased FCM levels of male mice were detected after IMC restraint as compared to controls ($P \leq 0.001$).

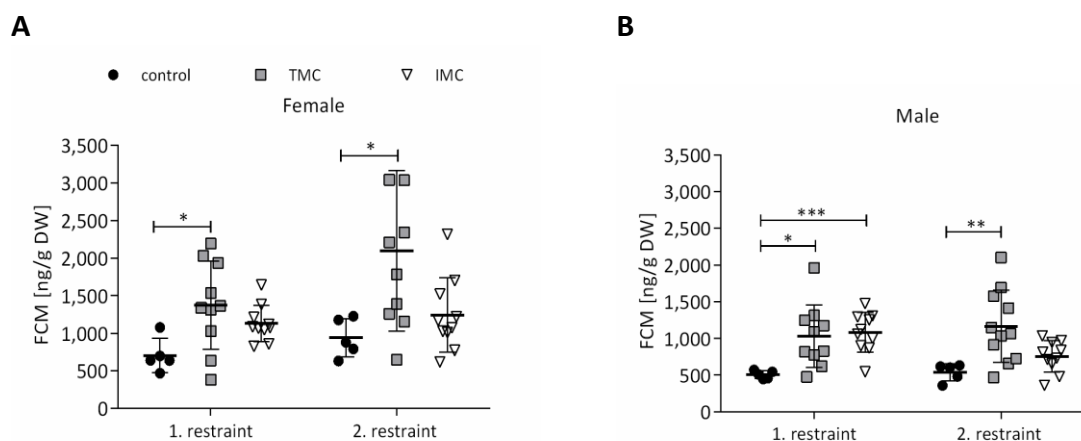


Figure 61. Fecal corticosterone metabolites (FCM) concentration [ng/g DW] during first and second restraints in the three tested cage types. A: Female mice. B: Male mice. Differences between control vs. TMC, control vs. IMC, and TMC vs. IMC were calculated by one-way ANOVA. FCM concentrations of first and second restraint were analyzed separately. * $P \leq 0.05$, ** $P \leq 0.01$, *** $P \leq 0.001$. Data are presented as mean (standard deviation). Control: control cage ($n = 5$), TMC: Tecniplast metabolic cage ($n = 10$), IMC: Innovative metabolic cage ($n = 10$).

4.4.2.1 Correlation between fecal corticosterone metabolites and cold stress parameters

To contextualize FCM concentrations to the cold stress experienced during metabolic cage restraint, correlation analyses were performed (see **Table 11**). FCM concentrations correlated significantly with FS data referring to all mice (1st restraint: $P \leq 0.01$, $r = 0.375$, see **Figure 62 A**; 2nd restraint: $P \leq 0.05$, $r = 0.344$, see **Figure 62 D**), females (1st restraint: $P \leq 0.05$, $r = 0.485$, see **Figure 62 B**; 2nd restraint: $P \leq 0.01$, $r = 0.579$, see **Figure 62 E**), and males (1st restraint: $P \leq 0.01$, $r = 0.570$, see **Figure 62 C**; 2nd restraint: $P \leq 0.001$, $r = 0.650$, see **Figure 62 F**) after both 24 h restraints. Only body surface temperature showed significant correlations compared to FCM concentrations for the second restraint alone (all mice: $P \leq 0.05$, $r = -0.304$, see **Figure 62 G**; female: $P \leq 0.05$, $r = -0.466$, see **Figure 62 H**). The correlation analyses revealed that as the FS increased, FCM concentrations also increased. In turn, as body surface temperature increased, FCM concentrations decreased.

Table 11. Correlation analyses between concentrations of fecal corticosterone metabolites (FCM) [ng/g DW] and Fur Score (FS), body surface temperature [°C], cage temperature [°C] (cold stress). Pearson or Spearman correlation analyses were conducted. Data are expressed as correlation coefficients (* $P \leq 0.05$, ** $P \leq 0.01$, *** $P \leq 0.001$).

	Cold stress	No. of restraint	All mice	Female	Male
			n=50	n=25	n=25
Fecal corticosterone metabolites [ng/g DW]	Fur Score	first	0.375 **	0.485 *	0.570 **
		second	0.344 *	0.579 **	0.650 ***
	Body surface temperature [°C]	first	-0.167	0.038	-0.377
		second	-0.304 *	-0.466 *	-0.344
Cage temperature [°C]	first	-0.210	-0.077	0.003	
	second	-0.141	-0.331	-0.236	

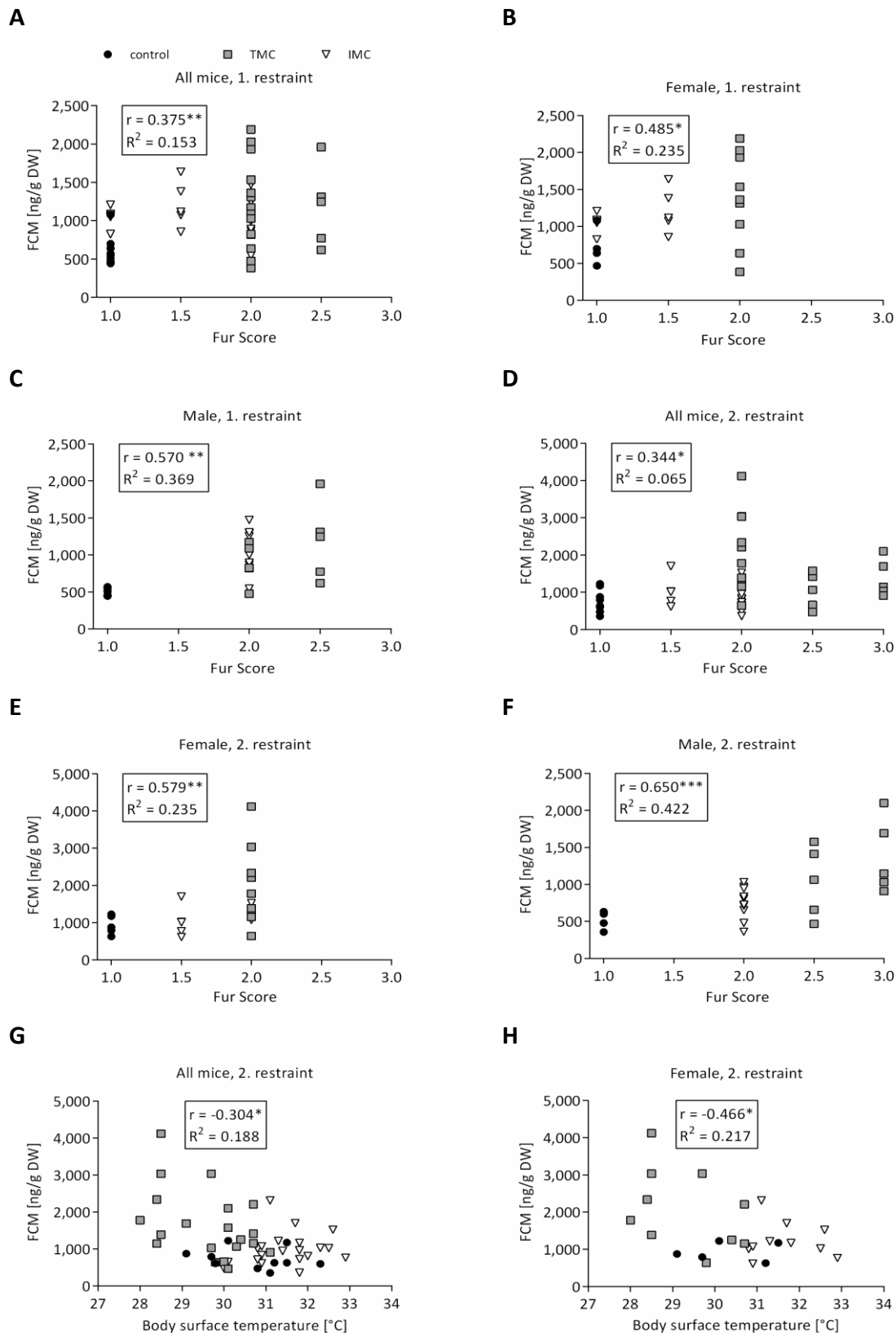


Figure 62. Correlation analyses between concentrations of fecal corticosterone metabolites (FCM) [ng/g DW] and Fur Score (FS), body surface temperature [°C] (cold stress). Pearson or Spearman correlation analyses were conducted. Data are expressed as correlation coefficients, significance level (* $P \leq 0.05$, ** $P \leq 0.01$, *** $P \leq 0.001$), and coefficient of determination (R^2).

In summary, it can be stated that corticosterone excretion into urine relating to female mice is significantly higher during TMC restraint compared to the IMC. FCM concentrations were additionally quantified for mice housed in control cages while TMC restraint induces a higher FCM excretion than husbandry in control cages. This was true for both sexes and restraints. It can be postulated that the TMC induces a greater stress response than the IMC, because FCM levels in IMC were comparable to FCM levels in control cages except for males during first restraint. Particularly, FS correlated positively with corticosterone excretion into feces (FCM), which indicates that the FS assigned by the independent scorers reflect the measured FCM levels.

4.4.2.2 Comparison of fecal corticosterone metabolites with Fur Scores of mice

Another subject of analysis was the matched FCM concentrations of each mouse and their respective FS data. The FS scale goes from 1 to 4 and is assigned as objectively as possible by the independent scorers. A FS of 1 describes a state without impairment to welfare, because it describes a well-groomed, smooth, and shiny fur state. A FS of 1 was therefore set as the threshold value (see **Figure 63** A-B). Separating the FCM concentrations into “well-groomed” (FS = 1) and “less-groomed” (FS > 1) subgroups resulted in a significant difference between the two subgroups concerning both sexes ($P \leq 0.001$). Therefore, a lower FS is associated with a lower FCM concentration and *vice versa*.

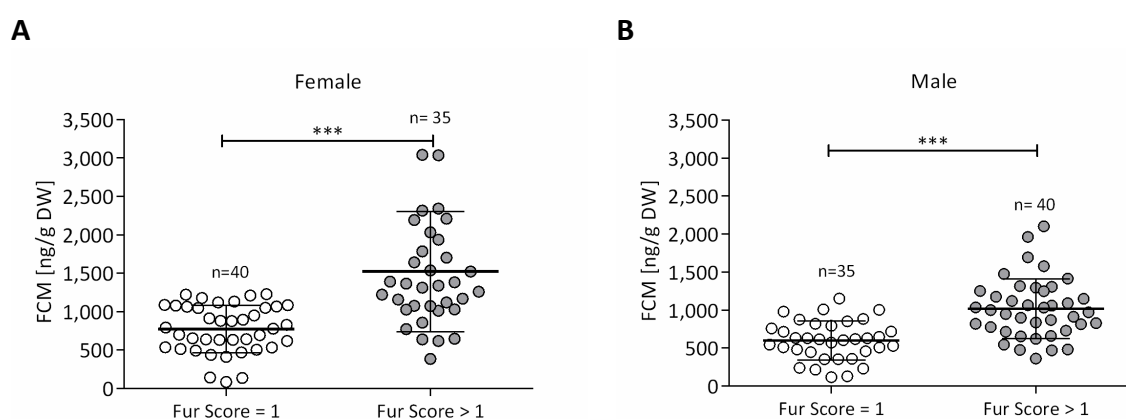


Figure 63. Fecal corticosterone metabolites (FCM) concentrations [ng/g DW] were matched to Fur Scores (FS) for each mouse. A: Female mice. B: Male mice. FS were subdivided in two groups: FS = 1 and FS > 1. Differences between both FS categories were calculated by independent-samples t-test or Mann-Whitney U test. * $P \leq 0.001$. Data are presented as mean (standard deviation).**

5. Discussion

The welfare of mice is negatively impacted by metabolic cage restraint due to various stressors. The grid cage floor can cause pain in their hind paws due to sensitization of the plantar nerves, and the absence of nest-building or burrowing opportunities deprives them of natural behaviors. Additionally, there are no hiding places and enrichment as well as nesting materials are lacking. Solitary housing also causes social and thermal stress as mice cannot interact with conspecifics or huddle for warmth [7,8].

This thesis describes the significant potential of the Innovative metabolic cage (IMC) in improving conventional methods of restraining mice in metabolic cages. A systematic comparison of the self-built IMC with a commercially available metabolic cage from Tecniplast GmbH, the Tecniplast MC (TMC), was undertaken with a focus on enhancing the welfare of mice. In the first place, the acquired knowledge shall contribute to refinement of the conditions for mice restrained in metabolic cages in the frame of necessary animal experiments. The knowledge attained can aid in accurately characterizing the stress physiology of laboratory mice, specifically through the examination of behavioral changes and metabolism. The C57BL/6J mouse strain, the most used and well-known inbred mouse strain in biomedical research, was chosen as an exemplary representative for other mouse strains [110–112]. This improved metabolic cage construction of the IMC represents the first attempt to decrease stress for laboratory mice during restraint in metabolic cages on various levels including the reduction of cold and metabolic stress as well as distress in general, which will be discussed in detail in the following sections.

5.1 Stress during restraint in metabolic cages affects mouse welfare and behavior

5.1.1 Outward appearance of mice after metabolic cage restraint

One objective of this thesis pursued the analysis of the extent to which the mouse welfare is affected by the IMC and the TMC in direct comparison. First, the grooming state of the fur and facial expression of mice was investigated by applying the Fur Score (FS) and the Mouse Grimace Scale (MGS).

A clear deterioration of the grooming state expressed as a higher FS was observed for both sexes after both TMC and IMC restraints compared with controls. Males additionally possessed a significantly higher FS in the TMC compared with the IMC after the first restraint and this tendency was also observed for the second restraint.

In the context of another study, the FS was also elevated for male BALB/c mice restrained in the TMC as opposed to controls. Kalliokoski *et al.* (2013) [7] assigned a FS of approximately 3 to the TMC experimental group and a FS of 1 to the control group, which is in the same range regarding both treatment groups as in the present study. This increase in FS induced by the TMC was attributed to a decreased grooming behavior, which can be interpreted as an indicator for impairment of welfare. Furthermore, the less groomed fur state, which leads to an increased FS, may serve as heat insulation mechanism for mice to better tolerate cold temperatures by fluffing up their fur [7]. The apparent cold stress of mice during metabolic cage restraint will be discussed in chapter 5.2 Indications of cold stress reduction during restraint in the Innovative metabolic cage.

To anticipate the results of the video analyses in the next section, female mice exerted self-grooming significantly more often during the first metabolic cage restraint while male mice groomed significantly more frequently during both metabolic cage restraints compared with controls. No significant differences in grooming frequency between the IMC and TMC were observed.

Grooming can be applied as a stress indicator and to study the underlying neuronal mechanisms of behavior while “barbering” is the exaggerated form of increased grooming and is considered an abnormal behavior [113,114]. Importantly, the assigned higher FS of mice restrained in metabolic cages do not match the higher frequency of grooming scored on the basis of video analyses. Self-grooming represents an innate, frequently occurring behavior in rodents and mammals in general. Rodents groom up to 30% of the time during which they are awake. Grooming was scored at specific points in time during the predefined time frames of video recordings, but the duration of grooming as well as number of bouts could be further considered. Furthermore, scoring of grooming behavior could be realized in a higher time resolution to might be able to explain this contradiction.

The position of ears as one facial unit referring to the MGS represented the most reliable parameter concerning the analysis of facial expressions of C57BL/6J mice after metabolic cage restraint. A higher score for ear position describes ears being pulled apart and deviating from their base position indicating experienced pain and (restraint) stress [50,115]. Also, the behavioral patterns grooming and sleeping share common characteristics with pain and stress [115]. In detail, the score for ear position was significantly higher after TMC restraint compared with the IMC after the second restraint. This was true for both sexes considered separately and together. For male mice after second restraint, the ear position score was also significantly higher after TMC restraint compared with controls.

However, it must be pointed out that the interrater reliability regarding ear position scores of the second restraint amounted to $\kappa = 0.167$, which refers to a “slight” interrater reliability. An interrater reliability of at least “fair” is preferred, which is defined in the range from $\kappa = 0.21$ to $\kappa = 0.40$. Considering both sexes in terms of ear position - also indicated a significantly higher ear position score for mice in the TMC as opposed to the IMC after the first restraint with a “moderate” interrater reliability of $\kappa = 0.519$. In another study, the MGS was applied for C57BL/6JRj mice after ketamine/xylazine anesthesia where nose as well as cheek bulge revealed the poorest agreement between scorers, which is also consistent with the study at hand [106].

Application of the MGS is quite challenging because scorers need to be effectively trained and unbiased. To address this difficulty, scorers from different fields of expertise could be chosen, who are not directly involved in the animal study. In this study, three colleagues; a scientist, a veterinarian, and a laboratory technician; rated mouse faces. One of the scorers was excluded since interrater reliability was not achieved including scores of the biased scorer since impartiality could not be ensured. Hohlbaum *et al.* (2020) [106] also emphasized that agreement between MGS scores is dependent on the observers’ experience levels. The scorers were all trained at the same time how to apply the MGS, but their experience was at beginner level, because they utilized this scientific tool for the first time in the frame of this study.

As scoring of mouse faces outside of the animal house by unbiased scorers is preferred, videos and photos need to be captured. As mice are moving during photo capture, the quality is often diminished. That is why photos were taken in shutter priority, but video recordings of mice from different angles may be preferred for the subsequent application of the MGS. Although it might be impractical, live scoring of mouse faces could also be considered as suggested by Miller and Leach (2015) [116]. Especially whisker position and cheek bulge are often not clearly visible, and thus cannot be accurately scored or scores represent an approximation. Interestingly, Miller and Leach (2015) [116] demonstrated that the MGS scores obtained from live scoring were significantly lower compared with retrospective scoring from images.

The black fur color of C57BL/6J mice has proven to be challenging in terms of assigning the FS as well as the scoring of particular MGS facial action units. Based on the differences between mouse strains such as fur color, it was suggested that MGS scores should be developed for respective mouse strains. C57BL/6J mice possess in general a low baseline regarding MGS Scores [116]. The grooming state as well as the ear position of C57BL/6J mice are unequivocally altered by metabolic cage restraint while the TMC has shown the tendency to induce a more pronounced deterioration in fur condition and ear position in comparison with the IMC. The FS and MGS, in particular the facial action unit ear position, therefore proved their utility as tools for the assessment of mouse welfare after metabolic cage restraint and can even partially explain differences between metabolic cage types.

5.1.2 Behavioral response to metabolic cage restraint and reference to neurotransmitters in sampled brain areas

Change of behavior can be considered as the reaction of an organism to the fulfillment of demand and the reduction of harm. The metabolic cage restricts i.a. freedom of movement and cognitive performance of mice. As the metabolic cage environment is ill-equipped lacking numerous environmental stimuli and the natural behavioral repertoire is limited, mouse welfare is definitely to some extent impaired. Therefore, metabolic cage restraint is thought to elicit a behavioral response in mice to cope with this stressful situation.

Two different behavioral tests were conducted directly after metabolic cage restraint - the Open Field Test (OFT) and Elevated Plus Maze (EPM). The OFT is often applied to assess the exploratory behavior and motor performance of mice while the EPM is more a test utilized for estimation of the anxiety and stress level of laboratory rodents [97–99]. Female and male C57BL/6J mice spent most of the testing time in the closed arms of the EPM while the middle zone of the OFT was visited for the longest time. This could serve as a first indicator that mice, including the controls, were stressed attributed to the solitary housing conditions and/or new environment of the testing arena. The same trend was also observed for number of entries into respective zones concerning both behavioral tests.

Females tended to be more active after the TMC restraint compared with the IMC, which has been demonstrated by a greater willingness to explore the OFT and EPM arena. For example, after the second 24 h restraint (t_2), females entered the center of the EPM more often after TMC restraint. Also at t_2 , female mice transferred out of the TMC into the EPM were active for a significantly longer period of time during 5 min testing. Concerning male mice, activity during the OFT after the first IMC restraint (t_1) tended to be higher compared with the TMC. This suggests that the female's exploratory drive was triggered after termination of the TMC restraint, what could indicate a relief. This increase in activity after TMC restraint regarding females could be associated with the elevated "escape behavior" counted during both TMC restraints as opposed to the IMC. "General activity" during the second restraint in the TMC was also significantly increased compared with the IMC for females. Other studies have shown that pre-exposure of mice to a novel environment directly before conducting the EPM increases motor activity, which could be assigned to the metabolic cage restraint before behavioral testing [117]. Also, differences in activity behavior between female and male mice during and after metabolic cage restraint could be due to the female's stage of estrous cycle. Since we did not assess the female's estrous cycle stage prior start of experiments, this limiting factor must be considered. However, it can be argued that the females were at least in the same cycle stage, which is attributed to the Lee-Boot effect since they were kept exclusively in female groups prior to the study. To circumvent this issue Walf and Frye (2007) [117] performed an ovariectomy of females before behavioral testing, but this invasive surgical procedure represents an additional burden to the mice besides the metabolic cage restraint, which is out of the scope of this study.

Based on behavioral tests it was indicated that control mice were less stressed compared with mice restrained in metabolic cages. For example, at t_2 a significant decrease in total distance traveled was observed for female mice after control cage housing in comparison with restraint in metabolic cages. In addition, also at t_2 , male mice were mobile for significantly longer in the EPM after metabolic cage restraint in relation to control cage housing. Therefore, this decrease in active behavior after housing in control cages could reflect a less stressed state of the mice, which could be explained by a less pronounced relief after termination of 24 h single housing in enriched control cages. Video analyses support this finding while female mice during the first restraint and male mice during both restraint periods in metabolic cages groomed significantly more often compared to controls. As previously mentioned, increased grooming can indicate stress in laboratory rodents. Van den Boom *et al.* (2017) [114] introduced an automated classification of self-grooming in mice using open-source software that is applicable for mice in an OFT and EPM, what can also be used in future studies for the analysis of grooming behavior during the performance of behavioral tests. Control cages were enriched with a house, nesting and bedding material as well as a wooden stick for gnawing. The enrichment material and house limited the view into the nesting area during video analysis, which is why scored behavior assigned to “immobility” and “grooming” in control cages in relation to metabolic cages should be interpreted with cautions. Houses made out of red plastic material instead of cardboard could be utilized. As mice cannot see the color red, but perceive them as being grey or dark, a hiding place for the mice is still provided and the scorer can also properly identify the animals’ behavior.

Since data collected during the OFT and EPM were partly inconsistent, the light-dark box test could also be conducted after metabolic cage restraint in order to study anxiety-like behavior based on approach-avoidance conflict [118]. It can be postulated that mice are more challenged in the light-dark box due to the extreme contrast between the light and dark compartment compared with the OFT, which is uniformly illuminated. Nevertheless, the OFT is a suitable tool for the assessment of locomotion, which could have been altered after 24 h sitting on the grid cage floor. The EPM, as the light-dark box, represents a more challenging test setup of four elevated arms with two closed and two open arms. Interestingly, Kuleskaya and Voikar demonstrated that a black floor of the OFT compared with a white floor promoted the exploratory behavior of C57BL/6 mice [118]. In the present study the floor of the OFT was dark gray in color suggesting a beneficial effect on the activity of tested mice. The application of the Social Interaction Test after metabolic cage restraint is another potential behavioral test to be conducted as already used by Whittaker *et al.* (2016) [12] in rats. Rearing was significantly increased after metabolic cage restraint compared to open-top cage housing during the Social Interaction Testing [12]. The behavioral category escape behavior in the present study included rearing. This test was also applied in the context of a study where male C57BL/6J mice were exposed to chronic unpredictable mild stress [119]. Whether the Social Interaction Test is suitable for the assessment of explorative and social behavior in mice after metabolic cage restraint, should to be investigated in the future.

To increase the reliability of scored behavior during video analysis, automated assessment of mouse behavior during metabolic cage restraint is less error-prone. Behavioral testing was conducted with the automated video tracking system ©ANY-maze, but recorded videos were manually analyzed based on pre-defined categories of an exclusive ethogram. Therefore, the value of machine learning in the context of artificial intelligence might achieve a more accurate, automated measurement of mouse behavior by circumventing biased scoring of an individual behavior analyst [28,120,121]. Throughput of behavioral analyses could also be massively increased by automation.

In order to further analyze alterations in behavioral patterns due to metabolic cage restraint on molecular level, the neurotransmitters dopamine (DA), 3,4-dihydroxyphenylacetic acid (DOPAC), 3-methoxytyramine (3-MT) and serotonin (SRT) were quantified. DA enhances mood and levels of energy when extracellular levels are increased, while at high levels, it can induce hyperactivity and compulsive as well as erratic behavior. Furthermore, DA is essential for feeding and movement [74]. No trends in DA concentrations within extracted brain areas; *caudate putamen* (CPU), *nucleus accumbens* (NAC), *hypothalamus* (HTM), ventral tegmental area (VTA), and *substantia nigra* (SN); were detected among the three tested cage types.

The instability of neurotransmitter extracts, especially of DA in perchloric mouse brain homogenates, was addressed by addition of the antioxidants L-cysteine and/or ascorbic acid to the extraction buffer to circumvent stability issues [122,123]. An innovative method for neurotransmitter analysis in the rat brain was recently introduced by applying stable isotope labeling derivatization following magnetic dispersive solid phase extraction and subsequent ultra-high performance liquid chromatography-tandem mass spectrometry in multiple reaction monitoring (MRM) mode [124]. As a consequence, possibilities for improvement regarding the applied LC-MS/MS method could be considered to ensure stability of primarily DA, but also of further neurotransmitters, to be quantified.

In toxin-induced mouse models for Parkinson's disease, researchers found out that C57BL/6 mice possess higher intrinsic DA levels in the striatum compared to other mouse strains [74]. It could be postulated that DA levels within the investigated brain areas, especially in CPU and NAC belonging to the striatum, were not affected by stressful conditions during metabolic cage restraint. Because of the general high abundance of DA in the striatum, C57BL/6J mice might be more tolerant to extrinsic interfering factors. The short restraint period of 24 h in metabolic cages might be an additional plausible reason.

Tyrosine hydroxylase immunohistochemistry of brain slices could be prepared additionally for visualization of dopaminergic anatomy, morphometry and cell counting. Importantly, tyrosine hydroxylase immunohistochemistry stains all catecholaminergic neurons that either produce DA, norepinephrine (NE) or epinephrine, while dopamine- β -hydroxylase can be solely utilized as an adrenergic marker [74]. Therefore, immunohistochemistry should be carried out with both markers to prevent mix-ups. To investigate how much of the local available Tyrosine is utilized for either NE or DA synthesis constitutes a comprehensive analysis.

Most mouse models were established to investigate specific dopaminergic pathologies including Parkinson's disease and Huntington's disease in terms of errors in motor function. In contrast to these mouse models having defined neuroanatomic lesions induced by selected neurotoxins, genetically altered mice possess gene modifications for proteins taking part in DA synthesis, metabolism, or neurotransmission [77]. As a consequence, genetically altered mice possess global DA dysfunction. Importantly, these mice show minimal pathophysiology besides a frequently modified behavior [74]. Since changes in behavior were already indicated after metabolic cage restraint, it might be worth investigating specific genetic alterations to draw conclusion on DA metabolism in terms of experienced stress and behavioral syndromes evolving from such experiences as e.g. post-traumatic stress disorder.

Pharmacological inhibition of the enzyme catechol-o-methyltransferase (COMT) by tolcapone significantly elevated DA levels in the ventral *hippocampus* of rats, but not in their striatum. Since the ventral *hippocampus* is preferentially involved in anxiety behavior, this brain region could be additionally extracted and DA concentrations subsequently assessed in future experiments [80]. Including the ventral *hippocampus* in analyses might give more insight into anxiety-related mechanisms possibly induced during metabolic cage restraint.

Investigation of DA levels in murine brain areas after the first restraint in metabolic cages might have produced clearer results, because DA discharge of neurons stops when events become predictable. Therefore, a habituation effect of mice to metabolic cage restraint cannot be excluded, even if other data do not indicate this, as mice were transferred into cages twice in total. Moreover, DA is involved in novelty detection and a phasic mode of discharge is not triggered in an habitual environment [77].

The DA metabolite DOPAC was significantly elevated or tended to be increased for female mice after restraint in the IMC compared to controls in the CPU and NAC. Concerning male mice, DOPAC was significantly increased in the HTM after restraint in the IMC compared with controls and the TMC.

The pronounced differences in female DOPAC levels within the CPU and NAC area can be explained based on the dorsal and ventral mesostriatal system, where dopaminergic neurons project from the *substantia nigra pars compacta* (SNc) and VTA to the striatum including CPU and NAC. DA levels were highest in the striatum of vehicle treated female and male rats in the context of another study with mean concentrations of 4.3 ng/mg tissue [80]. Mean DA concentrations in the present study ranged from 2.4 to 5.0 ng/mg wet weight within the CPU and NAC area after control cage housing and restraint in both metabolic cage types for both sexes, which are in the same range as the previously described study. Laatikainen *et al.* (2013) [80] also quantified DOPAC in the striatum of vehicle treated female and male rats possessing mean concentrations of approximately 0.75 ng/mg tissue. Concerning female mice in this study, mean DOPAC concentrations after IMC restraint in the CPU amounted to 1.72 ng/mg wet weight while controls possessed concentrations of 0.97 ng/mg wet weight. Within the NAC area of female mice, mean DOPAC concentrations were even higher and amounted to 2.98 ng/mg wet weight in the IMC in comparison with control concentrations of 2.08 ng/mg. DOPAC concentrations of mice increased considerably in the striatum, CPU and NAC, during IMC restraint compared with controls. Particularly noticeable are the enhanced female DOPAC concentrations after IMC restraint in the NAC area compared with the CPU area. This suggests that the ventral mesostriatal system is triggered to a greater extent during IMC restraint compared with the other cage types and this increase in DOPAC levels could be associated with an enhanced motivation, feeding behavior and welfare [74,76,77]. To further extend the hypothesis, DA levels increase during IMC restraint and therefore, the metabolic product DOPAC was increased at the time of brain extraction 4-6 h after termination of the experiment. Indeed this hypothesis can be supported with a study conducted by Bergamini *et al.* (2018) [125] in which male C57BL/6J mice were exposed to chronic social stress for 15 d and a decreased DA turnover was detected in the NAC brain area resulting in lower DOPAC/DA ratios. A reduction in DA turnover in the basal ganglia is associated with a depressive mood.

An imbalance in the direct and indirect pathways within the basal ganglia results in either increased or reduced motor activity [74]. As glutamate and gamma amino butyric acid (GABA) are the neurotransmitters controlling the direct and indirect pathways by binding to DA D1 or D2 receptors, the increase in DOPAC levels during IMC restraint yields no greater gain in knowledge. DA signals are mediated within the dorsal and ventral mesostriatal system, but not between the cerebral cortex and hypothalamic nuclei. It can be postulated that the indirect pathway is stimulated during IMC restraint leading to reduced motility. "Escape behavior" was significantly more frequently observed during TMC than IMC restraint at almost all points in time concerning both sexes. "General activity" was also significantly higher for female mice during the second measurement and for male mice during the first measurement of TMC restraint compared to IMC restraint. The abundance of the two DA receptors, D1 and D2, could be additionally investigated, but also enkephalin and substance P might be quantified. DA receptor expression can be quantified on mRNA and protein level *via* quantitative reverse transcription real-time PCR. Araki, Sims, and Bhide (2007) [126] found an increased DA D2 receptor expression in the striatum of embryonic and postnatal brains of CD1 mice, which is involved in the indirect pathway. If the DA D2 receptor is also predominantly expressed in the striatum of 12 week old C57BL/6J mice after metabolic cage restraint, it can be assumed that the indirect pathway prevails. Activity analyses over longer time periods, possibly throughout the 24 h metabolic cage restraint *via* utilization of the e.g. InfraMot system would give a more detailed insight than scoring activity behavior during selected time slots.

Since no significant differences were detected for DA among tested cage types, but for its metabolites, a comprehensive analysis of the brain metabolome could be suggested. DOPAC and 3-MT solely represent two pre-selected metabolites while DA can also be degraded to 3,4-dihydroxyphenylethanol by aldehyde dehydrogenase (AD) besides the formation of DOPAC. In addition, norepinephrine (NE) and epinephrine are predominantly metabolized to 3,4-dihydroxyphenylethanol. As homovanilic acid represents the main degradation product of DA, this metabolite could be also quantified in future approaches [81]. DA mainly undergoes phase II conjugation. DA glucuronide, but not DA sulfate, was detected in mouse brain microdialysis samples [127]. In conclusion, hallmarks of DA metabolism were investigated in the present study and many other metabolites of DA besides DOPAC and 3-MT exist, which could be incorporated into future analyses. One benefit of metabolic cage restraint is the ability to collect urinary samples. DA metabolites could be also quantified from urine to add another sample matrix to be analyzed, but it needs to be considered that DA is not solely synthesized in the brain, but also in the gastrointestinal tract [81]. Nevertheless, pilot studies could be performed to detect if DA metabolism deregulation is induced by metabolic cage restraint. Importantly, the analysis of DA metabolites from urine represents a non-invasive method compared to brain microdialysis, which is often applied for quantification of neurotransmitters in the murine brain [128].

Aspects of the dorsal mesostriatal system were also examined more closely while correlating activity parameters collected during the OFT and EPM with DA and 3-MT concentrations in the CPU and SN. The dorsal mesostriatal system takes an important part in motor control and activity. No trends were detected in DA levels between tested cages within specific brain areas and 3-MT was solely significantly increased in the CPU of male controls in comparison with TMC restraint, but significant correlations were detected. DA and 3-MT in CPU and SN correlated negatively with activity parameters including total distance traveled, average speed, and time spent (im)mobile in the OFT and EPM.

This means that the further the distance traveled, the higher the speed, and the more time spent mobile in the OFT and EPM, the fewer neurotransmitter concentrations were quantified. For this reason, comprehensive, interlinking analyses are probably more effective than merely determining a single parameter regardless of the overall study context and drawing conclusions about it. This interlinking approach is especially important in the field of behavioral analyses of mice, because these are preys and might often conceal their behavior.

SRT analyses regarding specific brain areas did not indicate trends for specific cage types with respect to an increase or decrease in concentrations. SRT modulates anxiety-related circuits, which is particularly relevant to this study in relation to the behavioral response of mice regarding metabolic cage restraint [129]. SRT takes part in the regulation numerous behaviors besides the anxiety context including stress-associated behaviors, happiness and appetite.

Regarding methodological considerations of conducted brain analyses, neurotransmitters were extracted from five to six murine brains while the group size amounted to ten mice for each sex. Since five areas of each mouse brain were investigated, workload and measuring time of almost 40 min per sample with the HPLC-MS/MS needed to stay within the limits. Therefore, it can be postulated that analysis of additional samples might confirm reported findings or reveal trends in SRT concentrations with 10 mice per experimental subgroup. As suggested before, brain slices of specific areas could be subjected to immunostaining prior to neurotransmitter extraction. The most commonly utilized SRT marker is tryptophan hydroxylase 2 (TPH2), which represents the abundant isoform of TPH besides TPH1 in the brain [86].

The extracted brain areas were primarily selected according to the pathway of basal ganglia and the associated nuclei including the dopaminergic ventral and dorsal mesostriatal systems. That is presumably why effects in SRT concentrations were not detected. The HTM, which was also included in the investigations, represents one target of the dorsal raphe nucleus (DRN). However, the *amygdala*, *hippocampus*, and *thalamus* among other brain areas, are assigned as the main projection areas of serotonergic neurons. Nevertheless, the serotonergic and dopaminergic system are thought to interact with each other, which therefore supports the measurement of SRT in the basal ganglia, but probably not exclusively [87]. Most importantly, the extraction and analysis of the ventral *hippocampus* would need to be focused on, because it projects to limbic structures; such as NAC, HTM, prefrontal cortex; and thus is considered to have an impact on mood related behavior. To give an example, optical stimulation of ventral *hippocampus* projections to NAC were shown to elevate anxiety-related behaviors [84].

The primary metabolite of SRT is 5-hydroxyindoleacetic acid (5-HIAA), which is able to pass the blood brain barrier in contrast to SRT. 5-HIAA is detectable in urine and blood and can be measured *via* HPLC-MS/MS [85]. SRT turnover is often assessed in studies analyzing mental illnesses and could be applied for investigating a potentially altered SRT metabolism induced by metabolic cage restraint whereby urine samples are collected anyway. As SRT is either synthesized within the brain or gastrointestinal tract, 5-HIAA derives and accumulates from both metabolic pathways. In addition, large nucleotide amino acid levels and tryptophane could have been quantified in plasma samples *via* HPLC since the calculated ratio of both parameters can be utilized to assess the availability of tryptophane in the brain for subsequent SRT synthesis [83].

Whether the tryptophane availability in the brain was unchanged in connexion with unchanged SRT levels in specific brain areas could thus have been clarified in order to ensure that the mice were supplied with sufficient amounts of dietary amino acid during metabolic cage restraint.

Novelty-suppressed feeding is commonly applied to assess anxiety-related behavior of laboratory rodents after treatment with anxiolytics and antidepressants such as selective serotonin reuptake inhibitors. Hyponeophagia represents a conflict-based testing method, because animals are deprived of food for 24 h and need to decide whether to approach the food located in the illuminated center or not [84,130]. The 24 h fasting period could relate to the reduced food intake during the 24 h metabolic cage restraint, especially concerning the TMC. Therefore, the main output of this test is the latency to eat, which will also be shortly discussed in chapter 5.3.2 Increase in food intake during Innovative metabolic cage restraint. The outcome of this behavioral test could further elucidate the impact of metabolic cage restraint on mouse welfare and additionally aid to discuss the collected behavioral data in combination with the measured neurotransmitters in the brain areas.

In previous studies, the analgesic effect of SRT modulating antidepressants was shown. A study conducted by Martin *et al.* (2017) [83] demonstrated that acute tryptophane depleted probands possessed significantly decreased SRT plasma concentrations and were more sensitive to pain perception 4-6 h after treatment. As metabolic cage restraint is often conducted for successive days or even weeks, the pain induced by the grid floor is possibly unbearable, which could be associated with reduced SRT levels in the brain. As this refinement project focussed on a short and endurable metabolic cage restraint for mice, this hypothesis cannot be addressed and potential fluctuations in brain SRT levels cannot be excluded during prolonged restraint.

In conclusion, the unaffected DA and SRT concentrations in the five investigated brain areas can be considered positively as no impact of metabolic cage restraint on murine neurotransmission could indicate a lower degree of suffering. Therefore, this finding highlights the need to keep the restraint period of mice in metabolic cages as short as possible and also to repeat metabolic cage restraint, only if really necessary, with an appropriate resting period in between. As has already been shown, it is essential to incorporate relevant metabolites into analyses to determine the DA and SRT turnover. Probably the most important result includes the increase of DOPAC after restraint in the IMC compared with controls (females: CPU, NAC; males: HTM), because this finding could indicate an improved condition of the mouse in terms of welfare and motivation, especially when elevated in the NAC region referring to the ventral mesostriatal pathway. This finding is further supported with an increased “escape behavior” (females: t_1 , t_2 ; males: t_1) and “general activity” (females: t_2 , males: t_1) during TMC compared with IMC restraint referring to a restless state of mice in the TMC. The higher activity of female mice during behavioral testing after termination of the TMC restraint sessions could be explained as kind of a relief.

5.1.3 Adrenal secretion of corticosterone is reduced during restraint in the Innovative metabolic cage

For an objective assessment of the stress level of mice during single housing in either TMC or IMC, the glucuronidated fraction of corticosterone and native corticosterone was quantified in the 24 h urine collection. Additionally, fecal corticosterone metabolites (FCM) were measured in feces collected in all investigated cage types, including controls. Corticosterone is a functional parameter of the *zona fasciculata* cells located in the adrenal cortex and represents the major stress hormone of mice. Female mice showed significantly elevated corticosterone concentrations in urine during TMC as opposed to the IMC restraint concerning both housing periods. For males no significant differences between cages could be detected for neither of the two points in time. FCM concentrations for female and male mice in the TMC were significantly higher compared with controls after both restraints. After the first IMC restraint period, male mice excreted significantly higher concentrations of FCM compared with controls.

When exposed to chronic stress, the hypothalamic-pituitary-adrenocortical (HPA) axis can show both response habituation and response facilitation. Habituation occurs when the same (homotypic) stressor is delivered repeatedly, and is characterized by progressive diminution of glucocorticoid responses to the stimulus [43]. In case of two 24 h restraints in the metabolic cages with a 6 d resting period in between, a habituation cannot be assumed, because excreted corticosterone concentrations remained elevated during second TMC restraint compared with either the IMC (urine, females) or controls (feces, both sexes). The timescale from which chronic stress is present, is not clearly defined. The present experimental setup, which extended over 2 weeks, can be considered as chronic stress since a 15 d period was defined as chronic social stress with reference to another study [125]. In contrast, study setups investigating chronic unpredictable stress exceed over 4 weeks [119,131]. Mice in the present study were transferred between cages for six times during the 2 week intervention, but more importantly, were handled for more than ten times due to behavioral testing, body weight (BW), and body composition determination. Male mice were kept isolated after the first 24 h metabolic cage restraint while females were returned to their group constellations. These interventions besides the metabolic cage restraint might further contribute to continuous stress experienced throughout the experiment. The postulated absence of an habituation to metabolic cage restraint based on corticosterone excretion negates the adduced hypothesis in chapter 5.1.2 Behavioral response to metabolic cage restraint and reference to neurotransmitters in sampled brain areas concerning neuronal DA discharge.

Interestingly, a gender-dependent dimorphism regarding the adrenal weight of rodents was proven before. In a study with F1 offspring of Naval Medical Research Institute mice crossed with C57BL/6J mice, females possessed a higher adrenal gland weight, greater cortex volumes and a larger *zona fasciculata* than males [47]. Concerning the present study, the adrenal gland weight was also significantly elevated for female mice compared with male mice, but no cage-dependent effect was detected for females and males analyzed separately and for both sexes considered together (data not shown). Whether the increased corticosterone levels in female urine samples are attributable to sex differences, or indicate a higher stress level of females, leads to the discussion of a sex-dependent excretion route of corticosterone in mice.

The route of steroid excretion is indeed different between male and female mice, as shown in a study of Touma *et al.* (2003) [52]. Urine and feces of male and female C57BL/6J mice was collected after administration of radiolabelled corticosterone intraperitoneally. Male mice excreted $71.7 \pm 4.0\%$ of corticosterone metabolites *via* feces whereas females excreted $56.2 \pm 4.4\%$. Regarding the urinary excretion, females excreted $43.8 \pm 4.4\%$ of metabolized corticosterone while males only excreted about $28.3 \pm 4.0\%$ [52]. In addition, female BALB/c mice were shown to excrete 60% of corticosterone in the urine and 40% in feces after intravenous injection of corticosterone [132]. To emphasize again, the urinary corticosterone concentration in the TMC was significantly elevated in comparison with the IMC, which was solely detected for females. Therefore, it can be postulated that male mice were equally stressed, but the lower excretion of corticosterone *via* urine does not show the anticipated effect in the selected matrix, but it does in feces. Taken together, quantification of corticosterone in urine and feces is preferred to map the entire excretion and to avoid drawing the wrong conclusions concerning the animal's stress level.

Besides the sex-specific route of excretion, the estrus cycle of females needs to be considered. Estrogen and progesterone levels fluctuate in plasma of female mice during specific cycle stages, e.g. estrogen concentrations are highest in the proestrus while progesterone concentrations are lacking in the metestrus [133,134]. An increase in 17β -estradiol follows an elevated HPA activity. That is why a bidirectional interaction between the hypothalamic-pituitary-gonadal axis and HPA axis is considered [42,131]. Also, a reduction in glucocorticoid receptor abundance of the *hippocampus* induced by estrogen is considered. This could result in a suppressing effect of estrogen levels on the negative feedback loop of the HPA axis leading to an elevation of the stress axis activity [135]. The cycle status of females in the present experiment was not determined even though it is considered scientific consensus.

The applied C57BL/6J inbred mouse strain possesses an inbreeding coefficient of $\geq 98\%$, which renders genetic predisposition comparable among mice. The binding affinity of corticosterone to the *hippocampus* is potentially reduced for C57BL/6 mice in contrast to BALB/c mice, suggesting that this mouse strain is particularly stress-resistant. After a 2 h restraint in a conical plastic tube, the serum corticosterone concentration of C57BL/6 mice was approximately 60% of that obtained for BALB/c mice [136]. As a matter of principle, an increased adrenal synthesis of corticosterone is nonetheless correlated with an increase in HPA axis activity, which can also be applied to the C57BL/6J mouse strain.

Post-traumatic stress disorder was the subject of another study, where human induced pluripotent stem cell-derived glutamatergic neurons from combat veterans were investigated among others. Glucocorticoid hypersensitivity in neurons of veterans suffering from post-traumatic stress disorder was found and also genes were identified contributing to the glucocorticoid response. The authors concluded that genetic and environmental risk factors definitely act a part in individual differences in response to trauma exposure [137]. Characterization of mouse strains, sex-specific differences not to be neglected, in terms of glucocorticoid hypersensitivity after stressful experimental interventions could therefore be essential for accurate interpretation of corticosterone concentrations as well as processes effected by glucocorticoids.

The animal personality of a single mouse represents an additional important point as individual variation modifies the reaction to a stressor, in this case the metabolic cage. The study of individual variation can aid in filling knowledge gaps in e.g. physiology and behavior. The behavioral domain aggression is thought to be the main determinant how an animal copes with a stressor involving the endocrine HPA axis activity. A proactive (aggressive and bold) and reactive (non-aggressive and shy) animal personality can further be adduced. Proactive mice would actively cope with the stressor and react more courageously to a challenging situation leading to a noradrenergic stimulation induced by a sympathetic activation. Reactive personalities on the other hand, would stay passive in the presence of a stressor based on their balanced character [20]. The ambivalence of a stress response regarding an association between corticosterone concentrations and behavior was reported. The authors postulated that the differences are founded on species or strain differences, the period of time of stressor exposure, the social state including dominant or subordinate male animals or the coping style entailing a proactive or passive type. Dominant male BALB/c mice acted more offensively and excreted higher post-stress levels of corticosterone compared with subordinates. Subordinate BALB/c males showed more submissive behaviors while the active subordinates, for which flight behavior was more pronounced, possessed the lowest corticosterone levels after experimentally induced social stress [138]. Based on these study results, an association between the behavioral trait of proactivity and an increase in corticosterone excretion can be suspected. Mice of both sexes showed significantly higher FCM concentrations in the TMC compared with control animals and for females significantly higher urine corticosterone levels were detected during TMC restraint as opposed to the IMC. This increase in corticosterone excretion in the TMC appears to be associated with a higher activity level of mice in the TMC expressed as escape and general behavior. As male mice were group housed prior to the first 24 h metabolic cage restraint, their social state could also have had an effect on their corticosterone excretion levels. Since the experimental group effects were quite clear based on obtained statistical significance of video-based behavioral analyses and corticosterone concentrations in urine and feces, analyses on individual mouse level appear to be less useful regarding the present study.

Within the frame of another metabolic cage study, corticosterone metabolites in fecal samples were also analyzed in male BALB/c mice during restraint in the TMC while the FCM output was ten times higher during TMC restraint in comparison with controls [7]. FCM excretion of male C57BL/6J mice in the present study has significantly increased twofold after both 24 h TMC restraints (1st restraint: 1029.88 ng/g DW, 2nd restraint: 1162.68 ng/g DW) compared to control cage housing (1st restraint: 504.38 ng/g DW, 2nd restraint: 537.06 ng/g DW). Even though male BALB/c mice were restrained in the TMC for a prolonged period of 3 weeks, the FCM output has remained at the same high level. The authors therefore concluded that the males did not habituate to the TMC, even after a 3 week period. This strain-specific difference in the magnitude of FCM excretion to the same stressor can be related to differences in the experimental methods for quantification of corticosterone in fecal samples (in-house enzyme immunoassay - fecal corticosterone metabolites with a 5 α -3 β ,11 β -triol structure, University of Osnabrück vs. commercial competitive enzyme-linked immunosorbent assay, Corticosterone enzyme-linked immunosorbent assay, EIA-4164; DRG Instruments GmbH), but also to the earlier discussed stress resistance of C57BL/6J mice. The quantified urinary corticosterone concentrations of mice in the study at hand are not directly comparable with other studies, because, to our knowledge, this innovative method for mice was not published before. Chu *et al.* (2020) [139] quantified corticosterone in mouse plasma *via* liquid chromatography-atmospheric pressure chemical ionization tandem-mass spectrometry. Stress was induced in male and female BALB/c mice by 1 h restraint stress in a 50 mL conical tube.

Mean plasma corticosterone concentrations amounted to 496.18 fmol/ μ L and 154.71 fmol/ μ L for stressed and control males respectively [139]. In contrast, the maximum corticosterone concentration in urine concerning the present study amounted to 29.91 fmol/ μ L. The comparability of the different sample matrices, measuring tools as well as the study design need to be taken into account. BALB/c mice were acutely stressed while C57BL/6J mice in this study were rather chronically stressed. The established method for the quantification of corticosterone in murine urine samples is highly specific in contrast to conventional enzyme and radio immunoassays since molecules possessing a specific mass-to-charge-ratio are detected with the LC/MS-MS technology.

Correlation analyses between FCM concentrations and FS data revealed that if the fur condition has worsened, FCM concentrations have accordingly increased. A FS of 1 does not describe an impairment of welfare, which is why a FS of 1 was set as the threshold value [95]. A low FS (= 1) matches low excreted FCM concentrations while a high FS (> 1) matches high FCM concentrations demonstrating that the assigned FS by two independent experimenters match this selected laboratory stress parameter.

As glucocorticoids promote hepatic glucose production, including gluconeogenesis as well as glycogenolysis, and excreted corticosterone concentrations were highest during TMC restraint, depletion of hepatic glycogen stores after restraint in the TMC as opposed to the IMC is replicable. Glucocorticoids further regulate pancreatic α and β cell function, which secrete insulin and glucagon. The main purpose of glucocorticoids entails the maintenance of sufficiently high plasma glucose levels during stressful episodes in order to ensure maximal brain function [48,140]. Interestingly, various studies have suggested that the HPA axis is activated in either case, when the organism is in a positive and a negative energy balance state [32,42].

Sampling methods including blood withdrawal, urine and feces collection are an additional source of stress and should therefore be implemented in the experimental design to avoid falsification of the measured glucocorticoid concentrations. That is why blood was only withdrawn at the very end of experiments to avoid an additional stress factor. Of course, the investigation of a more acute stress response to metabolic cage restraint could have been interesting since peak corticosterone concentrations are detectable within the first 10 min in plasma after presence of a stressor [141]. In urine and feces there is a time delay of approximately 2 h and 4-10 h respectively, depending on the daytime and therefore the level of activity [52].

Measured corticosterone concentrations in both matrices, urine and feces, clearly indicated a higher adrenal excretion during the 24 h TMC restraint. Therefore, an enhanced activation of the HPA axis and the entailed secretion of corticosterone plus its metabolites is more strongly evoked by restraint in the TMC as opposed to the IMC and controls. Here, the data from the females suggested that the TMC represented the greater stressor compared to the IMC since FCM concentrations for the IMC and control cages were in the same order of magnitude regarding both restraints. However, rating an increased HPA activity and corticosterone excretion as exclusively adverse should be evaluated with consideration for several reasons. First, mice are flight animals and it could therefore be vital to increase corticosterone excretion for the purpose of behavioral modification, such as an increase in alertness [32]. Second, elevated circulating corticosterone levels might be crucial for the adaptation of physiological processes in challenging situations including the glucose regulation discussed before. Nevertheless, strong fluctuations in corticosterone excretion certainly indicate an adaptation, possibly an imbalance, of physiological processes in the organism, which reacts to an external stressor.

5.2 Indications of cold stress reduction during restraint in the Innovative metabolic cage

5.2.1 Room temperature and the resulting cage temperature

Due to the fact that metabolic cages are empty, non-enriched cages lacking conspecifics; nesting, bedding, and enrichment material; the cold stress for mice is increased compared with conventional housing conditions [7,8]. In the present study, a clear increase in cage temperature during the 24 h restraint in the IMC as opposed to the TMC was demonstrated, reflecting the positive effect of the reduced IMC volume.

In the literature it was suggested that individually housed mice should be kept at 23-25°C [63]. This room temperature recommendation agrees with the present results on cage temperature. Here, the determined mean cage temperature based on all three tested cages; control cage, IMC, and TMC; amounted to approximately 23°C at a mean standard room temperature of 21.9°C. As a direct comparison of room and cage temperature is not valid, a repetition of the current study at different room temperature intervals is mandatory as suggested by Kingma, Frijns, and van Marken (2012) [142].

The resulting cage temperatures mainly depend on the set room temperature, the cage volume, and the BW of mice. Mice with a higher BW can carry more heat insulation and therefore might be more tolerant towards lower ambient temperatures [60]. For male C57BL/6J mice, a significant increase in IMC temperature compared with the TMC was detected after both restraints whereas this trend was only observed for females during the first restraint. Females possessed a significantly lower BW at all investigated points in time during the experiment suggesting a lower heat insulation and a lower capacity to warm up the IMC even if the cage volume was reduced.

5.2.2 Body surface temperature as a proxy for body core temperature

The body surface temperature was also assessed besides the cage temperature, because it can serve as a proxy for body core temperature [143]. Significant differences between body surface temperatures after restraint in respective cages were detected. Male mice body surface temperature was significantly increased for controls compared with the TMC and for the IMC compared with the TMC after second restraint. Female mice possessed a significantly increased body surface temperature after IMC restraint compared with the TMC and control cage housing regarding the second restraint. Since this thesis focuses on refinement measures regarding the enhancement of mouse welfare during metabolic cage restraint, which implies the reduction of cold stress among other things, a non-invasive measuring technique was selected. The body surface temperature of mice, but also the cage temperature, was therefore measured with a thermal camera instead of applying e.g. rectal thermometry [10]. During rectal thermometry, mice are often hand-restrained and the probe is inserted into the rectum, which could induce stress hyperthermia [143]. Importantly, mice do not need to be handled or fixated for taking thermal images. The thermal camera is simply held over the cage.

FCM concentrations significantly correlated with the body surface temperature of female mice and all mice concerning the second restraint period. A negative relation between the two parameters was found, which describes that the FCM decreases when the body surface temperature increases. This association indicates that the body surface temperature can indeed be used to assess animal welfare, at least for females. Due to their lower BW, it can be suggested that females are more prone to reach an hypothermic state during metabolic cage restraint than males. The sex (estrus cycle) and the body constitution of mice were suggested to represent two factors being decisive for maintenance of body core temperature, the proxy body surface temperature in the present study [142]. It was shown in other studies that male BALB/c and C57BL/6 mice can better tolerate solitary housing than their female conspecifics [7,8].

Concerning the body constitution of C57BL/6J mice in the present study, lean mass (LM) and fat mass (FM) was significantly different between males and females at all investigated points in time while females possessed a higher FM and males a higher LM (data not shown). The sex difference in body composition regarding LM and FM could be adapted to explain the differences in measured body surface temperatures, as sex and body constitution are the two factors being decisive for maintenance of body core temperature [142]. If small mammals are exposed to the cold and/or starved, they go into torpor in order to save energy, resulting in a decreased metabolic rate [60]. Males during second restraint in the TMC showed a significant increase in immobility compared with the IMC. Therefore, it can be suggested that male mice compensated the increased heat loss during TMC restraint due to reduction in activity. Immobility of males in control cages was further significantly elevated as opposed to the IMC, which might reflect that it is less likely for males to enter a critical metabolic state in the IMC since their activity did not need to be decreased.

The measuring site for assessment of the body surface temperature *via* infrared thermography should be predefined as temperatures vary across the mouse body [143]. The middle of the mouse back (interscapular to thoracolumbar region) was defined as the measuring point, but even if the temperature was measured at a fixed point, other confounders need to be taken into account. First, infrared thermography can underestimate the animal's temperatures due to e.g. reflections of the fur [143]. This could be avoided by shaving the section of fur determined for measurement, but potential disadvantages need to be considered such as increased heat loss at this skin area. Second, thermal images were taken between 08:00 am and 10:00 am representing the inactive phase of mice. During inactive time intervals, mice raise up their fur for heat insulation purposes, called piloerection. In contrast, during active time intervals, a greater surface area of mice is exposed to the surrounding environment [66]. As already discussed in chapter 5.1.1 Outward appearance of mice after metabolic cage restraint, also between 08:00 am and 10:00 am, increased FS were assigned after both metabolic cage restraints compared with controls. This decreased grooming state might have resulted from the attempt to effectively save energy for the maintenance of the body core temperature.

One study (2020) [144] introduced the concept of the thermoneutral point, which describes an ambient temperature below which energy expenditure increases and above which body temperature increases. For C57BL/6J mice, a diurnal fluctuation around 4°C between the light and dark phase, or inactive and active phase, regarding the thermoneutral point was demonstrated. Therefore, assessment of the animals' body surface temperature in a frequent manner, instead of the beginning and the termination of the 24 h metabolic cage restraint, might have provided a more detailed insight into body temperature fluctuation [144]. Male C57BL/6J mice possess a mean deep body temperature of 36.3°C, which was determined in a study where radiotelemeters were implanted in mice [145]. In this study, a cut-off value was set at 31°C based on the mean of measured body surface temperatures in all tested cage types, for both sexes and restraints. Temperatures below 31°C should probably not be reached, because otherwise a hypothermic state of the mice cannot be excluded during single housing. Whether this difference between deep body temperature and body surface temperature of approximately 5°C represents the actual thermal gradient has to be proven in future studies.

The non-invasive measurement of body surface temperatures of laboratory mice by means of thermal imaging represents a suitable proxy for their body temperature, if sources of confounders are considered and controlled as extensively as possible. Thermal imaging is an effective tool for first-line detection of hypothermic conditions in laboratory animals, which could be applied on a frequent basis to ensure housing conditions in metabolic cages appropriate to the welfare of laboratory animals.

5.2.3 Brown adipose tissue: adaptive non-shivering thermogenesis

The mRNA expression of Uncoupling protein 1 (*Ucp1*) in the interscapular brown adipose tissue (BAT) of mice after restraint in metabolic cages and control cages was quantified as the body temperature is i.a. maintained through the process of non-shivering thermogenesis in BAT [64,146]. No significant differences in *Ucp1* mRNA expression were quantified among tested metabolic cage types relative to controls.

Since the cage temperature in the IMC was significantly higher compared to the TMC after both restraints and the body surface temperature after second restraint in the IMC was also significantly elevated compared with the TMC, an upregulation of *Ucp1* in BAT after TMC restraint compared with the IMC would have been coherent. It is stated that if the BAT is activated, the metabolic efficiency decreases since less of the consumed energy is stored in fat depots of the body [60]. Accordingly, the absence of BAT activation might result from the need of mice to save energy during metabolic cage restraint. The improvement of energy turnover, increase in metabolic efficiency, is more vital than BAT activation following the upregulation of *Ucp1* mRNA expression for the maintenance of the body temperature.

SRT besides NE acts a part in the sympathetic stimulation of thermogenesis [147]. Fibers originating from the DRN connect to the ventromedial hypothalamic nucleus, release SRT, and thereby stimulate the BAT [60]. When SRT was directly injected into the ventromedial hypothalamic nucleus of female Sprague-Dawley rats, BAT was activated by an increased firing rate of sympathetic nerves to the BAT [148]. As measured SRT concentrations were comparable among cage types in the HTM, could explain the low responses at the *Ucp1* mRNA level in BAT.

A study that was conducted with *Ucp1* deficient mice on a C57BL/6J background demonstrated that mice kept at thermoneutrality (29°C) became obese independent of the type of diet (high-fat vs. control diet). The authors concluded that diet-induced thermogenesis is solely carried out by the BAT while BAT activity additionally acts on the ambient temperature [149]. Importantly, diet-induced thermogenesis has been demonstrated after feeding of mice with high-fat, “cafeteria” diets. The induction of thermogenesis was explained by either combusting excessive energy intake or extracting the maximum amount of protein out of the protein-diluted diet [60,70]. Therefore, it remains to be elucidated if a normal chow diet (see **Supplemental Table 9: Composition of diet**) can induce diet-induced thermogenesis and the extent to which the ambient temperature is involved.

As another explanatory approach, thermal images of the mouse inter-scapular skin and the lumbar back-skin could have been taken. Therefore, BAT thermogenesis can be assessed by calculating the difference between both measured temperatures, which might have achieved more conclusive results [143]. The infrared results on BAT thermogenesis could have been set in context with the *Ucp1* mRNA expression in BAT afterwards. Rodents possess BAT in the interscapular, subscapular, axillary, perirenal and periaortic regions [70]. In the present study, interscapular BAT was extracted from mice after euthanasia. The withdrawal of BAT from another part of the body might have been an useful addition to the current data situation concerning *Ucp1* mRNA expression.

In addition, white adipose tissue (WAT) could have been extracted followed by mRNA isolation, cDNA synthesis, and analysis of *Ucp1* mRNA expression *via* qRT-PCR. In this case potential “browning” of WAT is addressed. If beige adipose tissue formation is stimulated during metabolic cage restraint considering the discussed cold stress, *Ucp1* expression might accordingly be upregulated such as in BAT [71,150]. Studies have already demonstrated differences in *Ucp1* expression between different parts of the body depending on the adipose tissue type, but also within the same location such as the neck area, which contains all three types of adipose tissue: WAT, BAT, and beige adipose tissue [71,151]. Accordingly, it could be investigated whether *Ucp1* expression was underestimated in the present study, because *Ucp1* was apparently not upregulated in BAT, but trends might have been detected in beige adipose tissue (former WAT). However, it remains to be clarified whether a 24 h cold stress, especially in the TMC, can trigger such an adaptive response in adipose tissue, i.e. whether a definable threshold stimulus exists. A study conducted with male NMRI mice exposed to 4°C demonstrated that the highest values of *Ucp1* mRNA in BAT were expressed after 4 h [152].

Glucocorticoids were shown to directly block leptin receptors and thereby prevent the progression of the signal cascade for BAT activation, which can be reversed by removal of adrenal steroids as demonstrated in a study conducted with adrenalectomized rats [60,153]. An enhanced corticosterone secretion by the adrenal glands, especially during restraint in the TMC, might therefore prevent BAT recruitment. FCM concentrations during both 24 h restraints in the TMC were significantly higher compared with controls. This was true for both sexes. The *Ucp1* mRNA expression in BAT was in fact comparable between the TMC compared with controls. Therefore, it is not clear if the isolation stress in the control cage also may have been a factor and if the excreted FCM levels for controls were sufficiently high to inhibit BAT activation here as well.

To study the mechanism of non-shivering thermogenesis in BAT in more detail, the peroxisome proliferator-activated receptor gamma coactivator 1 alpha (PGC1 α) could be investigated in future experiments. PGC1 α is strongly expressed in the BAT and was found to be a transcriptional regulator of adaptive thermogenesis [71,154]. This coactivator is induced by i.a. cold exposure and acts primarily through the peroxisome proliferator-activated receptor gamma (PPAR γ). PGC1 α is essential for cold-induced activation of brown adipocytes as well for the formation of beige adipose tissue [71]. *Ucp1* expression in BAT is induced by PGC1 α , whereby this coactivator confers transcriptional specificity to PPAR γ and also induces activation of this nuclear receptor specifically on the *Ucp1* promoter [61,154]. Therefore, the mRNA expression as well as protein levels of *Ucp1*, PGC1 α , and PPAR γ in both adipose tissue types, BAT and WAT, could be assessed *via* qRT-PCR (mRNA) and Western Blotting or LC-MS/MS analyses (protein) to gain further insight into adaptive thermogenesis within the adipose tissue during restraint in metabolic cages. In case PGC1 α is ectopically expressed, this protein directly stimulates mitochondrial number and oxidative metabolism. Mitochondrial DNA is hereby elevated which results in an increase in nuclear- and mitochondrial-encoded mitochondrial genes. For the induction of mitochondrial genes, initiated by PGC1 α , the levels of the nuclear respiratory factor 1, nuclear respiratory factor 2, and the estrogen-related receptor α are largely induced [61,154]. Consequently, nuclear respiratory factor 1, nuclear respiratory factor 2 and estrogen-related receptor α represent further potential targets for elucidating the mechanism of adaptive thermogenesis in the mitochondria of the BAT. As PGC1 α is controlled by a large repertoire of ligands, the previously mentioned receptors and transcription factors merely represent a selection of possible targets.

Importantly, besides an ectopic expression, PGC1 α can be modified post-translationally as well as PGC1 α splicing variants have already been identified, which renders this mechanistic examination even more complex.

It was shown that *Ucp1* ablated mice were unable to induce non-shivering thermogenesis when exposed to 4°C, but still produced sufficient amounts of heat to survive for several weeks. This was explained by a training effect of muscles supporting shivering thermogenesis [155]. According to that, BAT-derived thermogenesis could solely be an optional approach for heat loss compensation in a cold environment and attention must also be focused on shivering thermogenesis. For a comprehensive insight into the complex of themes concerning heat loss and thermoregulation during metabolic cage restraint, shivering thermogenesis also needs to be addressed. Studying shivering thermogenesis is more challenging than analyzing non-shivering thermogenesis, which is possible on a molecular level. One option includes the recording of electromyograms by implanting surface electrodes on the mouse [156]. As this represents an invasive methods, the expected gain in knowledge must be set against the expected suffering of the mice.

The existing temperatures in both metabolic cages were probably not sufficiently low to induce a pronounced response on *Ucp1* mRNA level. This can be interpreted as positive, because an adaptation of non-shivering thermogenesis might be associated with a compensation of cold stress and a reduction in animal welfare. Cage temperatures in the TMC were significantly lower compared with the IMC. Therefore, an increase in metabolic efficiency due to the apparent cold stress in the TMC might have been triggered resulting in an unchanged *Ucp1* mRNA expression in BAT for TMC housed mice. More research is needed to clarify why the *Ucp1* mRNA expression was also unchanged for female and male mice kept in the IMC, but also why *Ucp1* mRNA expressions of female and male controls remained at the same level.

5.3 The Innovative metabolic cage effectively preserves energy resources of mice

5.3.1 Reduced body weight, lean and fat mass loss due to application of the Innovative metabolic cage

A BW loss of more than 20% is often defined as termination criterion for animal experiments, because it is associated with severe suffering [157]. Female and male mice lost significantly more BW during TMC restraint as compared with the IMC and controls concerning both 24 h periods.

In the study conducted by Kalliokoski *et al.* (2013) [7] male BALB/c mice lost approximately 8% of their initial BW after a 1 d restraint in the TMC. BW loss of male C57BL/6J mice in the present study was higher with mean BW losses of 13.1% and 14.9% after the first and second restraint in the TMC respectively. BW represents a critical parameter defining the lower critical temperature of mice [63]. As male mice possess a higher average BW than females, it can be postulated that they are more robust towards becoming hypothermic [63,158]. A higher sensitivity of females in contrast to males towards BW loss could be determined since females lost significantly more BW during IMC restraint compared with controls. This was true for both restraints. Talbot *et al.* (2020) [157] discussed if BW reduction is a sufficient and critical parameter, which can be utilized as an humane endpoint. BW reduction though depends on the animal model and study content, which is because BW loss alone could possibly not provide the adequate accuracy and further parameters need to be flexibly implemented tailored to the respective experiment [157]. Even if BW loss was eminently increased during TMC restraint, female and male mice regained BW after 6 d of resting with BW being comparable to the baseline assessment. It is therefore advisable to also define the length of the resting period after an intervention during which the BW of mice is monitored and can be regained. Of course, BW development of mice during experiments should consider the mouse strain, age, and sex since BW is clearly dependent on these parameters.

The LM and FM of mice was further assessed shortly before and after metabolic cage restraint while LM and FM loss was highest after TMC restraint as opposed to IMC restraint and controls. This was true for both sexes after both 24 h restraints except for females after the first restraint concerning FM loss. Loss of LM was more pronounced than FM loss for females, which might be due to the higher FM content of females compared with males. Importantly, LM loss in the IMC differed significantly from the TMC, but not from control cages while LM loss in the TMC was significantly different from control cages.

FM depots have a positive effect on tissue insulation. Studies have already demonstrated that subjects possessing an increased FM, including whole body fat as in the present study, can withstand cold temperatures for an extended period of time without noticeably increasing heat production [142]. The decrease in FM during TMC restraint therefore had counter-productive effects on tolerating the lower prevalent cage temperature, mainly in the TMC. The less pronounced FM loss of females could be referred to their higher FM. During exposure of mice to the cold, an increased induction of the adipose depot turnover rate in terms of adaptation mechanisms including heat production can be suggested. It is important to state that mice in the TMC might also have reached a fasted state, which will be discussed in chapter **5.3.2** Increase in food intake during Innovative metabolic cage restraint.

If cold stress is present and mice are in a fasted state, lipolysis in adipose tissue could have been promoted by forming ketone bodies from unesterified fatty acids. These unesterified fatty acids are released from the fat depots and thus represent the metabolic fuel. Ketone bodies are synthesized in the liver in the context of ketogenesis, but can also be utilized from extrahepatic tissue [90]. The less pronounced decrease in FM during metabolic cage restraint regarding female mice could also result from the increased urinary corticosterone secretion particularly in the TMC. An activation of glucocorticoid receptors specifically induces lipid mobilization and triglyceride accumulation as seen in Cushing's syndrome [48].

The less pronounced BW, FM, and LM loss during IMC restraint unequivocally indicates a less affected metabolic phenotype, which coincides with collected data on food intake as well as hepatic glycogen levels as discussed in chapter 5.3.2 Increase in food intake during Innovative metabolic cage restraint and in chapter 5.3.3 Glycogen stores in the liver are depleted to a lesser extent during restraint in the Innovative metabolic cage.

5.3.2 Increase in food intake during Innovative metabolic cage restraint

Food intake tended to increase or was significantly increased during IMC compared with TMC restraint regarding the second restraint period. This was true for both sexes. Males also tended to ingest more food in the IMC as opposed to the TMC during the first restraint, which suggests that the males adapt well to the angled food hopper of the IMC. The fecal output was also accordingly significantly increased during IMC restraint in comparison with the TMC.

The number of excreted fecal boli was assessed during 5 min behavioral testing as an indicator of stress since an increase in fecal boli excretion can be associated with an elevated anxiety level [159]. Male mice excreted significantly higher amounts of fecal boli in the EPM after IMC restraint compared with males restrained in the TMC. Therefore, it is plausible that this increase in fecal boli after IMC restraint was not exclusively associated with the stress level, but also with the quantity of food priorly taken up. Also, the number of fecal pellets excreted during behavioral testing tended to or was significantly increased for both sexes after second control cage housing in comparison with TMC restraint suggesting a higher food intake during housing in control cages rather than an increase in anxiety level.

Conducted video analyses also support the enhanced food uptake during IMC restraint, since the behavioral category other activities was significantly increased during IMC compared with TMC restraint concerning both restraints and sexes. This category includes feeding besides drinking, urination, and defecation. Besides food intake, the latency to feed could be integrated into future studies as an additional readout for anxiety-like behavior. It was shown that the latency to eat in a novel environment is increased for female and male C57BL/6J mice [160]. The increased food intake of mice during restraint in the IMC could be accompanied with a shorter latency to feed, which would additionally support the application of the IMC in contrast to the TMC.

Independent of the cold stress topic, it was shown that BAT is inactivated and *Ucp1* is downregulated if rats are fasted or the accessibility to the food is restricted [60,161,162]. On the contrary, an increase in *Ucp1* mRNA expression within interscapular BAT was observed after feeding a high-energy diet [163]. On the basis of the cited studies, there is a clear association between food intake and BAT activity, which could also apply to this study. However, to fully uncover this relationship, at least the food consumption of the control mice would have to be determined. It is important to state that in the present study the same standard chow diet (see **Supplemental Table 9**) was fed during restraint in all three tested cage types.

To additionally assess satiety of mice after restraint in different cages, quantification of leptin in blood samples, which were collected after euthanasia from the *vena cava*, can be suggested. Margareto, Marti, and Martinez (2001) [163] observed a significant positive association between BAT *Ucp1* mRNA levels with serum leptin after feeding a high-energy diet. Another study demonstrated that rats held in the cold (5°C) consume the approximately fourfold amount compared with controls kept at warmer temperatures besides BAT recruitment and activation of thermogenesis. Importantly, this activation of BAT was not directly caused by the higher food intake since BAT recruitment was also observed when rats in the cold were pair-fed with controls [60]. By reference to these studies, analyses of leptin in blood samples of mice could examine the potential links between food intake and BAT activation in terms of *Ucp1* mRNA expression more closely. Of course, food intake of controls should be assessed in future experiments to fill this knowledge gap.

The increase in food intake during IMC restraint is accompanied with an increase in the DA metabolite DOPAC in the CPU and NAC of females and the HTM of males after IMC restraint. DA is involved in feeding behavior since dopaminergic neurons respond to appetite stimuli. Especially in case of DA transmission impairment within NAC, a loss of appetite was observed [77]. Since the metabolite DOPAC was increased in NAC, a high DA turnover can be assumed. Therefore, an increase in food taken up during IMC restraint might be associated with elevated DOPAC levels in the NAC of mice restrained in the IMC. Serotonergic neurons in the HTM contribute to the regulation of feeding behavior, but no trends in SRT concentration in any of the investigated brain areas were detected regarding differences between cage types. To return to leptin, this anorexigenic hormone is able to inhibit SRT synthesis and/or release what causes a reduction in appetite. To elaborate, leptin binds to the leptin receptor expressed on raphe nuclei neurons, which are located in the brain stem, and thereby hinders SRT synthesis and/or release by these raphe nuclei neurons. Then reduced serotonergic signals reach hypothalamic neurons, the arcuate neurons to be specific, where less SRT binds to primarily Htr1a receptors inducing appetite [88].

The administration form of food needs to be considered for the TMC since stuck food pellets could block the supply of further pellets. The food hopper of the TMC is mounted horizontally while the food hopper of the IMC is at an angle. In case of stuck food pellets in the TMC, mice are not able to meet their energy demand. TMC restraint could therefore be repeated with a powdered diet as in the study conducted by Kalliokoski *et al.* (2013) [7] where male BALB/c mice were restrained in the TMC and a powdered diet was provided *ad libitum*. Food intake of male BALB/c mice ranged from approximately 0.15 g/g BW to 0.25 g/g BW during 24 h TMC restraint [7]. In contrast, male C57BL/6J mice consumed 0.07 g/g BW to 0.12 g/g BW in the TMC over the same time period. Whether this difference in food consumption is attributable to the different mouse strains or to the consistency of the presented diet needs to be investigated. Usage of a powdered diet in the IMC is not possible due to the angled fence.

In conclusion, the increase in food intake during IMC restraint could be mainly explained by the improved accessibility to the food hoppers compared with the TMC resulting in a higher food uptake. Concerning the TMC, the body's energy expenditure levels during the 24 h restraint were presumably exceeding the energy intake. This might have been further aggravated by the reduced accessibility to food pellets in the TMC. The higher energy demand of mice in the TMC could arise from the previously discussed elevated cold stress. The generation of a stress response including behavioral and physiological adaptations, such as neurotransmitter synthesis or corticosterone excretion, might require additional energy.

5.3.3 Glycogen stores in the liver are depleted to a lesser extent during restraint in the Innovative metabolic cage

Glycogen concentration in liver tissue of mice was quantified by histological and biochemical methods. Both methods clearly showed a significant reduction in glycogen concentration after restraint in the TMC compared with the IMC. This was true for both sexes. Concerning the biochemical method, glycogen stores of males were also significantly decreased in the TMC compared with controls while the glycogen content of females was comparable between the IMC and controls. Glycogenolysis was analyzed in the context of the present study since this pathway predominates during short-term fasting periods to provide the organism with sufficient glucose [90]. An increase in liver weight could be associated with refilling the tissue with i.a. glycogen. Liver weight was indeed significantly reduced for females and males after TMC restraint compared with the IMC, which is consistent with the measured glycogen concentrations.

The data here clearly indicate a negative energy balance of mice after TMC restraint. A negative energy balance describes the state of an organism when energy expenditure exceeds energy intake. BW, LM, and FM reduction is strongly pronounced in the TMC while food intake was decreased, especially during second restraint. Additionally, food intake was significantly correlated with liver glycogen content where a lower food intake reflects a lower glycogen content in the liver, which is assigned to the TMC. Therefore, it can be suggested that glycogen stores of the liver were utilized to counteract the body's increasing glucose demand during TMC restraint.

Hammad *et al.* (1982) [91] adapted male ICR mice to a controlled feeding schedule including access to food for 6 h and deprivation of food for 18 h. At the 6th hour, hepatic glycogen content reached its maximum while glycogen stores were continuously decreasing during the 18 h fasting period and were depleted in the end. The fasting period is to some extent comparable to restraint in the TMC in which significantly less food was consumed compared with the IMC. Therefore, the depletion in hepatic glycogen could be explained on the basis of reduced food intake. ICR mice were housed on a grid floor in order to prevent coprophagy, which renders the study setup comparable to the present study [91].

Hammad *et al.* (1982) [91] also measured blood glucose of mice, which amounted to 4.6 mmol/L as mean fasting level and raised up to 10.5 mmol/L after feeding. The mean blood glucose of male C57BL/6 mice amounted to 10.2 mmol/L in the context of another study, which were injected with 0.25 mg/kg epinephrine intraperitoneally 15 min before blood glucose measurement [92]. In the present study, the mean blood glucose level of all C57BL/6J mice amounted to 10.7 mmol/L at the end of experiments (data not shown). Even no significant differences in blood glucose levels were detected among cage types, it is obvious that blood glucose was elevated at the end of experiments and was not in the range of fasting glucose levels. In order to analyze glycogen metabolism, especially the breakdown during TMC restraint, more precisely, the measurement of insulin and glucagon in plasma samples besides blood glucose in whole blood samples would be conceivable.

It is known that an increase in catecholamines induces an increase in hepatic glucose production. Dibe *et al.* (2020) [92] investigated the effect of epinephrine (adrenaline) on glycogen levels in the liver of male C57BL/6 mice, which were either trained or sedentary for 12 d. Interestingly, epinephrine injected intra-peritoneally in sedentary mice induced higher blood glucose levels as well as reduced glycogen levels in the liver compared with trained males. The authors therefore suggested that prior exercise training decreases the effect of epinephrine on the liver's glycogen stores as training confers a "glycogen sparing effect" [92].

Whether mice were more "trained" after the second restraint in the TMC or the IMC is difficult to discuss since collected data suggest that mice rather approached a catabolic metabolic state in the TMC compared with the IMC. Data on LM loss further demonstrate the development of a catabolic metabolic state, and precisely not muscle growth, particularly during TMC restraint. However, it has become clear that mice were more active during TMC restraint expressed as escape behavior and general activity in relation to the IMC. It can be postulated that mice in the TMC therefore needed to mobilize extra energy sources, which is suggested by an elevated hepatic glycogen breakdown. Also, mice in the TMC might have moved increasingly to keep themselves warm and/or because their paws were hurting induced by the wide grid flooring, but this was at the expense of glycogen stores in the liver. An activation of the sympathetic nervous system during exercise induces the production of epinephrine and norepinephrine [92]. As a consequence, measuring (nor)epinephrine levels in the plasma and brain of mice could further create a link between hepatic glycogen depletion and the specific metabolic cage type in terms of activity patterns. Epinephrine is a direct metabolite of DA and since DA in the brain of mice has already been analyzed in this study, it would be a logical conclusion to include the metabolite epinephrine in future studies.

In conclusion, the liver glycogen stores were significantly depleted after TMC restraint, which points towards a higher glucose demand of mice in the TMC. The lower food intake resulting in less available glucose is not to be neglected and could therefore potentiate the reduction in glycogen stores. As a putatively higher stress potential is emanating from the TMC, an increase in glucocorticoids might have reinforced the breakdown of glycogen besides the increase in activity [140].

5.4 Further refinement measures for the improvement of metabolic cages

The IMC represents an effective refinement measure for the restraint of mice in metabolic cages. Based on the observations during the first test use of the IMC, the cage construction can be further improved including the following suggestions:

(1) Hiding places could be introduced in the form of a red plastic house fixed to the grid bottom or a red foil could be adhered on the outside of the cage to dim the light.

The red plastic refuge should be in the form of an igloo that urine and feces can fall off. The guideline of the Swiss Confederation indeed states that 30% of the surface of completely transparent metabolic cages should be dimmed towards the light source, but also a lookout should be provided for the animals [16].

(2) Small-scale enrichment could be supplied by installing grids vertical to the cage floor.

Mice would be given the opportunity for climbing by optimal use of space. Creating additional free movement is particularly important due to the reduction of the IMC cage volume, which was chosen in order to alleviate the cold stress of mice.

(3) The IMC can be heated from the exterior by arranging infrared lamps in front of the cage or by placing the IMC in an incubator. An exterior isolation of the IMC is also conceivable.

The cage temperature needs to be continuously monitored during first tests to prevent dehydration of mice. An upper limit for the cage temperature should be set priorly, ideally in combination with a shutdown of the infrared lamp or incubator. Even though cold stress of mice during metabolic cage restraint is often addressed due to single housing and the open grid cage floor, heat accumulation needs to be also considered, especially regarding the reduced cage volume of the IMC [16].

Recommendations for restraint of mice in metabolic cages could be written in more detail. The standard room temperature in animal houses is defined in the range of 20-22°C [62,63]. However, it is also important to designate resulting cage temperature ranges in dependence of cage volumes since applied metabolic cages from different manufacturers are often not directly comparable. The incorporation of climatic conditions during metabolic cage restraint is particularly important since metabolic cages are distinctly different from conventional cage housing. Metabolic cages possess an open cage floor and nesting as well as bedding material is absent. Additionally, mice are single housed.

Taken together, additional information that should be integrated in European guidelines include:

- Diameter, height, and volume of the metabolic cage types.
- Strain, sex, and body weight concerning mouse characteristics.

To give an example why this information is required. The IMC possesses a floor area of 110.3 cm² and a cage height of 12.5 cm. This is in compliance with the European Directive regarding the floor area per animal (100 cm²) that should be provided for mice possessing body weights over 30 g [5]. If mouse strains, such as New Zealand obese mice instead of lean C57BL/6J mice, are restrained in the IMC, the practicability of this metabolic cage type is to be questioned. This is because New Zealand obese mice possess body weights higher than 30 g [164,165]. The extracted advantages from the cage volume reduction for C57BL/6J mice could be negated by an unjustifiable impairment of welfare for New Zealand obese mice.

6. Conclusion

The metabolic cage represents an open cage system possessing a primarily functional construction, highly detached from species-appropriate husbandry conditions, but the visual and olfactory contact can be maintained between single housed mice. The stress-inducing restraint of mice in metabolic cages in the course of experiments ought not to be neglected and the refinement of housing conditions in metabolic cages is therefore particularly important to focus on.

The Innovative metabolic cage (IMC) demonstrates the first attempt to redesign the conventional way of metabolic cage restraint by retaining the essential features for urine and feces collection as well as monitoring of food and water intake. Animal welfare should be enhanced to the maximum extent possible while implementing the IMC, an innovative alternative to metabolic cage restraint. The IMC was directly compared with a commercially available metabolic cage from Tecniplast GmbH (TMC). A thorough severity assessment was undertaken by comparing the IMC with the TMC.

Here, the improvement of metabolic cage restraint in the form of the IMC should be elaborated by aiming to demonstrate that this cage type least affects the metabolic phenotype of mice. Based on this data collection, it can be stated that the IMC first of all reduces the general distress level of mice. Secondly, an alleviation of cold stress in the IMC was indicated and thirdly, the preservation of energy resources can be highlighted by applying the IMC. This dissertation thus contributes significantly to the improvement of housing conditions of conventional metabolic cage restraint and identifies suggestions on how metabolic cage restraint can be further revised.

By using the IMC, the variation in data collected during metabolic cage restraint of mice is reduced, therefore implying a significant improvement in data validity. Accordingly, data gathered during animal experiments applying conventional metabolic cage models should be evaluated with uncertainty. The consequent implementation of the 3R principle, especially the refinement of experimental procedures of indispensable animal experiments, is therefore in the interest of science. Thus, when high animal welfare standards are applied with the use of the IMC, in turn, the pursuit of robust scientific quality can be assumed.

References

- [1] J. Zurlo and E. Hutchinson, "Food for Thought ... Refinement," *ALTEX*, vol. 31, no. 1, pp. 4–10, 2014.
- [2] R. C. Hubrecht and E. Carter, "The 3Rs and Humane Experimental Technique: Implementing Change," *Animals : an open access journal from MDPI*, vol. 9, no. 10, 2019.
- [3] J. D. Bailoo, T. S. Reichlin, and H. Würbel, "Refinement of experimental design and conduct in laboratory animal research," *ILAR journal*, vol. 55, no. 3, pp. 383–391, 2014.
- [4] B. Vollmar, P. Dabrock, B. Fleischmann et al., "Tierversuche in der Forschung: Das 3R-Prinzip und die Aussagekraft wissenschaftlicher Forschung," *Handreichung der Ständigen Senatskommission für tierexperimentelle Forschung der DFG zur Planung und Beschreibung tierexperimenteller Forschungsprojekte*, pp. 1–20, 2019.
- [5] European Parliament of the Council, "Directive 2010/63/EU of 2010 on the protection of animals used for scientific purposes," 22 September 2010.
- [6] National Research Council of the National Academies, "Guide for the care and use of laboratory animals," *Washington, DC: National Academies Press*, 2011.
- [7] O. Kalliokoski, K. R. Jacobsen, H. S. Darusman et al., "Mice do not habituate to metabolism cage housing—a three week study of male BALB/c mice," *PloS one*, vol. 8, no. 3, 1–11, 2013.
- [8] A. Kovalčíková, M. Gyurászová, R. Gardlík et al., "The effects of sucrose on urine collection in metabolic cages," *Laboratory animals*, vol. 53, no. 2, pp. 180–189, 2019.
- [9] C. C. Hoppe, K. M. Moritz, S. M. Fitzgerald et al., "Transient Hypertension and Sustained Tachycardia in Mice Housed Individually in Metabolism Cages," *Physiological Research*, no. 58, pp. 69–75, 2009.
- [10] H. Prior, H. Blunt, L. Crossman et al., "Refining Procedures within Regulatory Toxicology Studies: Improving Animal Welfare and Data," *Animals : an open access journal from MDPI*, vol. 11, no. 11, pp. 1–16, 2021.
- [11] Z. Sahin, H. Solak, A. Koc et al., "Long-term metabolic cage housing increases anxiety/depression-related behaviours in adult male rats," *Archives of Physiology and Biochemistry*, vol. 125, no. 2, pp. 122–127, 2019.
- [12] A. L. Whittaker, K. A. Lymn, and G. S. Howarth, "Effects of Metabolic Cage Housing on Rat Behavior and Performance in the Social Interaction Test," *Journal of applied animal welfare science : JAAWS*, vol. 19, no. 4, pp. 363–374, 2016.
- [13] Z. Sahin, "Metabolic cages can be used for social isolation stress rather than metabolism studies with their current form," *Türk Bilimsel Derlemeler Dergisi*, no. 1, pp. 115–120, 2022.
- [14] B. T. Kurien, N. E. Everds, and R. H. Scofield, "Experimental animal urine collection: a review," *Laboratory animals*, vol. 38, no. 4, pp. 333–361, 2004.
- [15] M. J. Stechman, B. N. Ahmad, N. Y. Loh et al., "Establishing normal plasma and 24-hour urinary biochemistry ranges in C3H, BALB/c and C57BL/6J mice following acclimatization in metabolic cages," *Laboratory animals*, vol. 44, no. 3, pp. 218–225, 2010.
- [16] Schweizerische Eidgenossenschaft and Bundesamt für Lebensmittelsicherheit und Veterinärwesen BLV, "Fachinformation Tierversuche: Das Halten von Versuchstieren in Stoffwechselkäfigen und Stoffwechselboxen 2.06," 2017.
- [17] Schweizerische Eidgenossenschaft, "Verordnung des BLV über die Haltung von Versuchstieren und die Erzeugung gentechnisch veränderter Tiere sowie über die Verfahren bei Tierversuchen (Tierversuchsverordnung)," 2010.
- [18] L. Benner, S. Krämer, and K. Siegeler, "Belastungseinschätzung bei Versuchstieren Teil 2: Orientierungshilfen für die Arbeit," *Versuchstierkunde kompakt*, no. 3, pp. 12–17, 2019.
- [19] Animal Research Review Panel, "Guideline 20: Guidelines for the Housing of Rats in Scientific Institutions," *Orange NSW, Australia*, pp. 1–74, 2007.
- [20] V. Careau and T. Garland, "Performance, personality, and energetics: correlation, causation, and mechanism," *Physiological and biochemical zoology : PBZ*, vol. 85, no. 6, pp. 543–571, 2012.
- [21] C. Schirmer, M. A. Abboud, S. C. Lee et al., "Home-cage behavior in the Stargazer mutant mouse," *Scientific reports*, vol. 12, no. 1, pp. 1–8, 2022.
- [22] L. Lewejohann, C. Reinhard, A. Schrewe et al., "Environmental bias? Effects of housing conditions, laboratory environment and experimenter on behavioral tests," *Genes, Brain and Behavior*, no. 5, pp. 64–72, 2006.

- [23] J. P. Garner, B. N. Gaskill, C. Rodda et al., "Mouse Ethogram - An ethogram for the Laboratory Mouse," <https://mousebehavior.org/ethogram/>.
- [24] C. B. Gurumurthy and K. C. K. Lloyd, "Generating mouse models for biomedical research: technological advances," *Disease models & mechanisms*, vol. 12, no. 1, pp. 1–10, 2019.
- [25] Marc Spehr, "Soziale Signale erschnüffeln: chemische Kommunikation und das Vomeronasalorgan," *Neuroforum*, pp. 157–164, 2010.
- [26] J. P. McGann, "Poor human olfaction is a 19th-century myth," *Science (New York, N.Y.)*, vol. 356, no. 6338, pp. 1–6, 2017.
- [27] H. Schröder, N. Moser, and S. Huggenberger, eds., *Neuroanatomy of the Mouse*, Springer International Publishing, Cham, 2020.
- [28] V. Voikar and S. Gaburro, "Three Pillars of Automated Home-Cage Phenotyping of Mice: Novel Findings, Refinement, and Reproducibility Based on Literature and Experience," *Frontiers in behavioral neuroscience*, vol. 14, pp. 1–15, 2020.
- [29] D. Réale, S. M. Reader, D. Sol et al., "Integrating animal temperament within ecology and evolution," *Biological Reviews*, no. 82, pp. 291–318, 2007.
- [30] T. Burton, S. S. Killen, J. D. Armstrong et al., "What causes intraspecific variation in resting metabolic rate and what are its ecological consequences?," *Proceedings. Biological sciences*, vol. 278, no. 1724, pp. 3465–3473, 2011.
- [31] A. K. Gebczyński and M. Konarzewski, "Locomotor activity of mice divergently selected for basal metabolic rate: a test of hypotheses on the evolution of endothermy," *Journal of evolutionary biology*, vol. 22, no. 6, pp. 1212–1220, 2009.
- [32] S. M. Smith and W. W. Vale, "The role of the hypothalamic-pituitary-adrenal axis in neuroendocrine responses to stress," *Basic research*, pp. 383–395, 2006.
- [33] E. Carstens and G. P. Moberg, "Recognizing Pain and Distress in Laboratory Animals," *Institute for Laboratory Animal Research*, no. 41, pp. 62–71, 2000.
- [34] K. Lorenz, *Vergleichende Verhaltensforschung: Grundlagen der Ethologie*, 1978.
- [35] D. Fraser, D. M. Weary, E. A. Pajor et al., "A Scientific Conception of Animal Welfare that Reflects Ethical Concerns," *Animal Welfare*, no. 6, pp. 187–205, 1997.
- [36] C. M. Wade and M. J. Daly, "Genetic variation in laboratory mice," *Nature genetics*, vol. 37, no. 11, pp. 1175–1180, 2005.
- [37] M. Jennings, G. R. Batchelor, P. F. Brain et al., "Refining rodent husbandry: the mouse: Report of the Rodent Refinement Working Party," *Laboratory animals*, vol. 32, pp. 233–259, 1998.
- [38] M. Busch, S. Chourbaji, P. Dammann et al., "Tiergerechte Haltung von Labormäusen: Ausschuss für Tiergerechte Labortierhaltung," *GV-SOLAS Gesellschaft für Versuchstierkunde*, pp. 1–25, 2014.
- [39] J. O. Wolff and P. W. Sherman, *Rodent Societies. An Ecological & Evolutionary Perspective*, University of Chicago Press, Chicago and London, 2007.
- [40] M. Leger, E. Paizanis, K. Dzahini et al., "Environmental Enrichment Duration Differentially Affects Behavior and Neuroplasticity in Adult Mice," *Cerebral cortex (New York, N.Y. : 1991)*, vol. 25, no. 11, pp. 4048–4061, 2015.
- [41] B. N. Gaskill, C. J. Gordon, E. A. Pajor et al., "Heat or insulation: behavioral titration of mouse preference for warmth or access to a nest," *PloS one*, vol. 7, no. 3, 1–11, 2012.
- [42] J. P. Herman, H. Figueiredo, N. K. Mueller et al., "Central mechanisms of stress integration: hierarchical circuitry controlling hypothalamo-pituitary-adrenocortical responsiveness," *Frontiers in neuroendocrinology*, vol. 24, no. 3, pp. 151–180, 2003.
- [43] J. P. Herman, M. M. Ostrander, N. K. Mueller et al., "Limbic system mechanisms of stress regulation: hypothalamo-pituitary-adrenocortical axis," *Progress in neuro-psychopharmacology & biological psychiatry*, vol. 29, no. 8, pp. 1201–1213, 2005.
- [44] L. Schiffer, L. Barnard, E. S. Baranowski et al., "Human steroid biosynthesis, metabolism and excretion are differentially reflected by serum and urine steroid metabolomes: A comprehensive review," *The Journal of steroid biochemistry and molecular biology*, vol. 194, pp. 1–25, 2019.
- [45] M. J. Sheriff, B. Dantzer, B. Delehanty et al., "Measuring stress in wildlife: techniques for quantifying glucocorticoids," *Oecologia*, vol. 166, no. 4, pp. 869–887, 2011.

- [46] R. Palme, "Non-invasive measurement of glucocorticoids: Advances and problems," *Physiology & Behavior*, vol. 199, pp. 229–243, 2019.
- [47] M. Bielohuby, N. Herbach, R. Wanke et al., "Growth analysis of the mouse adrenal gland from weaning to adulthood: time- and gender-dependent alterations of cell size and number in the cortical compartment," *American journal of physiology. Endocrinology and metabolism*, no. 293, pp. 139–146, 2007.
- [48] A. Joharapurkar, N. Dhanesha, G. Shah et al., "11 β -Hydroxysteroid dehydrogenase type 1: potential therapeutic target for metabolic syndrome," *Pharmacological reports*, no. 64, pp. 1055–1065, 2012.
- [49] M. Häggström and D. Richfield, "Diagram of the pathways of human steroidogenesis," *WikiJournal of Medicine*, vol. 1, no. 1, 2014.
- [50] K. Hohlbaum, B. Bert, S. Dietze et al., "Severity classification of repeated isoflurane anesthesia in C57BL/6JRj mice-Assessing the degree of distress," *PloS one*, vol. 12, no. 6, 1-21, 2017.
- [51] R. Palme, C. Touma, N. Arias et al., "Steroid extraction: Get the best out of faecal samples," *WTM*, no. 100, pp. 238–246, 2013.
- [52] C. Touma, N. Sachser, E. Möstl et al., "Effects of sex and time of day on metabolism and excretion of corticosterone in urine and feces of mice," *General and Comparative Endocrinology*, vol. 130, no. 3, pp. 267–278, 2003.
- [53] R. Palme, S. Rettenbacher, C. Touma et al., "Stress hormones in mammals and birds: comparative aspects regarding metabolism, excretion, and noninvasive measurement in fecal samples," *Annals of the New York Academy of Sciences*, vol. 1040, pp. 162–171, 2005.
- [54] A. Han, A. Marandici, and C. Monder, "Metabolism of Corticosterone in the Mouse," *The Journal of biological chemistry*, no. 258, pp. 13703–13707, 1983.
- [55] J. J. Millspaugh and B. E. Washburn, "Use of fecal glucocorticoid metabolite measures in conservation biology research: considerations for application and interpretation," *General and Comparative Endocrinology*, vol. 138, no. 3, pp. 189–199, 2004.
- [56] J. F. Hoffman, A. X. Fan, E. H. Neuendorff et al., "Hydrophobic Sand Versus Metabolic Cages: A Comparison of Urine Collection Methods for Rats (*Rattus norvegicus*)," *Journal of the American Association for Laboratory Animal Science*, vol. 57, no. 1, pp. 51–57, 2018.
- [57] Y. Zhen, K. W. Krausz, C. Chen et al., "Metabolomic and Genetic Analysis of Biomarkers for PPAR α Expression and Activation," *Molecular and cellular endocrinology*, vol. 21, no. 9, pp. 2136–2151, 2007.
- [58] D. Beyoğlu, Y. Zhou, C. Chen et al., "Mass isotopomer-guided decluttering of metabolomic data to visualize endogenous biomarkers of drug toxicity," *Biochemical pharmacology*, vol. 156, pp. 491–500, 2018.
- [59] T. Wang, Y. M. Shah, T. Matsubara et al., "Control of steroid 21-oic acid synthesis by peroxisome proliferator-activated receptor alpha and role of the hypothalamic-pituitary-adrenal axis," *The Journal of biological chemistry*, vol. 285, no. 10, pp. 7670–7685, 2010.
- [60] B. Cannon and J. Nedergaard, "Brown adipose tissue: function and physiological significance," *Physiological reviews*, vol. 84, no. 1, pp. 277–359, 2004.
- [61] B. B. Lowell and B. M. Spiegelman, "Towards a molecular understanding of adaptive thermogenesis," *Nature*, vol. 404, no. 6778, pp. 652–660, 2000.
- [62] R. J. Seeley and O. A. MacDougald, "Mice as experimental models for human physiology: when several degrees in housing temperature matter," *Nature metabolism*, vol. 3, no. 4, pp. 443–445, 2021.
- [63] J. R. Speakman and J. Keijer, "Not so hot: Optimal housing temperatures for mice to mimic the thermal environment of humans," *Molecular metabolism*, vol. 2, no. 1, pp. 5–9, 2012.
- [64] C. L. Karp, "Unstressing intemperate models: how cold stress undermines mouse modeling," *The Journal of experimental medicine*, vol. 209, no. 6, pp. 1069–1074, 2012.
- [65] F. Vialard and M. Olivier, "Thermoneutrality and Immunity: How Does Cold Stress Affect Disease?," *Frontiers in immunology*, vol. 11, pp. 1–11, 2020.
- [66] A. W. Fischer, B. Cannon, and J. Nedergaard, "Optimal housing temperatures for mice to mimic the thermal environment of humans: An experimental study," *Molecular metabolism*, vol. 7, pp. 161–170, 2018.
- [67] V. Golozoubova, H. Gullberg, A. Matthias et al., "Depressed thermogenesis but competent brown adipose tissue recruitment in mice devoid of all hormone-binding thyroid hormone receptors," *Molecular endocrinology (Baltimore, Md.)*, vol. 18, no. 2, pp. 384–401, 2004.

- [68] M. A. Griggio, "The participation of shivering and nonshivering thermogenesis in warm and cold-acclimated rats," *Comparative Biochemistry and Physiology – Part A: Molecular & Integrative Physiology*, vol. 73, no. 3, pp. 481–484, 1982.
- [69] J. Nedergaard, V. Golozoubova, A. Matthias et al., "UCP1: the only protein able to mediate adaptive non-shivering thermogenesis and metabolic inefficiency," *Biochimica et biophysica acta*, vol. 1504, no. 1, pp. 82–106, 2001.
- [70] T. C. L. Bargut, M. B. Aguila, and C. A. Mandarim-de-Lacerda, "Brown adipose tissue: Updates in cellular and molecular biology," *Tissue & cell*, vol. 48, no. 5, pp. 452–460, 2016.
- [71] A. Fenzl and F. W. Kiefer, "Brown adipose tissue and thermogenesis," *Horm Mol Biol Clin Invest*, no. 19, pp. 25–37, 2014.
- [72] B. Cannon and J. Nedergaard, "Brown adipose tissue: function and physiological significance," *Physiological reviews*, vol. 84, no. 1, pp. 277–359, 2004.
- [73] A. Eskilsson, K. Shionoya, S. Enerbäck et al., "The generation of immune-induced fever and emotional stress-induced hyperthermia in mice does not involve brown adipose tissue thermogenesis," *FASEB journal : official publication of the Federation of American Societies for Experimental Biology*, vol. 34, no. 4, pp. 5863–5876, 2020.
- [74] C. J. Zeiss, "Neuroanatomical phenotyping in the mouse: the dopaminergic system," *Veterinary pathology*, vol. 42, no. 6, pp. 753–773, 2005.
- [75] G. Ayano, "Dopamine: Receptors, Functions, Synthesis, Pathways, Locations and Mental Disorders: Review of Literatures," *Journal of Mental Disorders and Treatment*, vol. 2, no. 2, pp. 1–4, 2016.
- [76] T. Macpherson, M. Morita, and T. Hikida, "Striatal direct and indirect pathways control decision-making behavior," *Frontiers in psychology*, vol. 5, pp. 1–7, 2014.
- [77] A. Nieoullon and A. Coquerel, "Dopamine: a key regulator to adapt action, emotion, motivation and cognition," *Current Opinion in Neurology*, no. 16, S3-S9, 2003.
- [78] Y. Smith, M. D. Bevan, E. Shink et al., "Microcircuitry of the direct and indirect pathways of the basal ganglia," *Neuroscience*, no. 2, pp. 353–387, 1998.
- [79] A. Nambu, H. Tokuno, and M. Takada, "Functional significance of the cortico-subthalamo-pallidal 'hyperdirect' pathway," *Neuroscience research*, vol. 43, no. 2, pp. 111–117, 2002.
- [80] L. M. Laatikainen, T. Sharp, P. J. Harrison et al., "Sexually dimorphic effects of catechol-O-methyltransferase (COMT) inhibition on dopamine metabolism in multiple brain regions," *PloS one*, vol. 8, no. 4, 1-8, 2013.
- [81] J. Meiser, D. Weindl, and K. Hiller, "Complexity of dopamine metabolism," *Cell communication and signaling : CCS*, vol. 11, no. 34, pp. 1–18, 2013.
- [82] F. Schumacher, S. Chakraborty, B. Kleuser et al., "Highly sensitive isotope-dilution liquid-chromatography-electrospray ionization-tandem-mass spectrometry approach to study the drug-mediated modulation of dopamine and serotonin levels in *Caenorhabditis elegans*," *Talanta*, vol. 144, pp. 71–79, 2015.
- [83] S. L. Martin, A. Power, Y. Boyle et al., "5-HT modulation of pain perception in humans," *Psychopharmacology*, vol. 234, no. 19, pp. 2929–2939, 2017.
- [84] C. N. Yohn, M. M. Gergues, and B. A. Samuels, "The role of 5-HT receptors in depression," *Molecular brain*, vol. 10, no. 28, pp. 1–12, 2017.
- [85] C. Kriegebaum, L. Gutknecht, A. Schmitt et al., "Serotonin now: part 1 Neurobiology and Developmental Genetics," *Fortschritte der Neurologie Psychiatrie*, no. 78, pp. 319–331, 2010.
- [86] L. Zhou, M.-Z. Liu, Q. Li et al., "Organization of Functional Long-Range Circuits Controlling the Activity of Serotonergic Neurons in the Dorsal Raphe Nucleus," *Cell reports*, vol. 18, no. 12, pp. 3018–3032, 2017.
- [87] S. K. Ogawa, J. Y. Cohen, D. Hwang et al., "Organization of monosynaptic inputs to the serotonin and dopamine neuromodulatory systems," *Cell reports*, vol. 8, no. 4, pp. 1105–1118, 2014.
- [88] F. Oury and G. Karsenty, "Towards a serotonin-dependent leptin roadmap in the brain," *Trends in endocrinology and metabolism: TEM*, vol. 22, no. 9, pp. 382–387, 2011.
- [89] P. J. Roach, A. A. Depaoli-Roach, T. D. Hurley et al., "Glycogen and its metabolism: some new developments and old themes," *The Biochemical journal*, vol. 441, no. 3, pp. 763–787, 2012.
- [90] L. Rui, "Energy Metabolism in the Liver," *Comprehensive Physiology*, no. 4, pp. 177–197, 2014.
- [91] E. S. Hammad, J. S. Striffler, and R. R. Cardell, "Morphological and biochemical observations on hepatic glycogen metabolism in mice on a controlled feeding schedule. I. Normal mice," *Digestive diseases and sciences*, vol. 27, no. 8, pp. 680–691, 1982.

- [92] H. A. Dibe, L. K. Townsend, G. L. McKie et al., "Epinephrine responsiveness is reduced in livers from trained mice," *Physiological reports*, vol. 8, no. 3, 1-14, 2020.
- [93] J. Guillen, "FELASA Guidelines and Recommendations," *Journal of the American Association for Laboratory Animal Science*, vol. 51, no. 3, pp. 311–321, 2012.
- [94] M. Mähler Convenor, M. Berard, R. Feinstein et al., "FELASA recommendations for the health monitoring of mouse, rat, hamster, guinea pig and rabbit colonies in breeding and experimental units," *Laboratory animals*, vol. 48, no. 3, pp. 178–192, 2014.
- [95] Y. S. Mineur, D. J. Prasol, C. Belzung et al., "Agonistic Behavior and Unpredictable Chronic Mild Stress in Mice," *Behavior Genetics*, no. 33, pp. 513–519, 2003.
- [96] D. J. Langford, A. L. Bailey, M. L. Chanda et al., "Coding of facial expressions of pain in the laboratory mouse," *Nature methods*, vol. 7, no. 6, pp. 447–449, 2010.
- [97] C. Bodden, S. Siestrup, R. Palme et al., "Evidence-based severity assessment: Impact of repeated versus single open-field testing on welfare in C57BL/6J mice," *Behavioural brain research*, vol. 336, pp. 261–268, 2018.
- [98] R. D. Brose, E. Lehrmann, Y. Zhang et al., "Hydroxyurea attenuates oxidative, metabolic, and excitotoxic stress in rat hippocampal neurons and improves spatial memory in a mouse model of Alzheimer's disease," *Neurobiology of aging*, vol. 72, pp. 121–133, 2018.
- [99] F. Karl, A. Griebshammer, N. Üçeyler et al., "Differential Impact of miR-21 on Pain and Associated Affective and Cognitive Behavior after Spared Nerve Injury in B7-H1 ko Mouse," *Frontiers in molecular neuroscience*, vol. 10, no. 219, pp. 1–15, 2017.
- [100] K. B. J. Franklin and G. Paxinos, eds., *The mouse brain in stereotaxic coordinates*, Elsevier Academic Press, Amsterdam, 2008.
- [101] K. J. Livak and T. D. Schmittgen, "Analysis of relative gene expression data using real-time quantitative PCR and the 2⁻(Delta Delta C(T)) Method," *Methods (San Diego, Calif.)*, vol. 25, no. 4, pp. 402–408, 2001.
- [102] J. Henkel, K. Buchheim-Dieckow, J. P. Castro et al., "Reduced Oxidative Stress and Enhanced FGF21 Formation in Livers of Endurance-Exercised Rats with Diet-Induced NASH," *Nutrients*, vol. 11, no. 2709, pp. 1–15, 2019.
- [103] I. Walter and S. Klaus, "Maternal high-fat diet consumption impairs exercise performance in offspring," *Journal of nutritional science*, vol. 3, 1-9, 2014.
- [104] C. Touma, R. Palme, and N. Sachser, "Analyzing corticosterone metabolites in fecal samples of mice: a noninvasive technique to monitor stress hormones," *Hormones and behavior*, vol. 45, no. 1, pp. 10–22, 2004.
- [105] B. Hauser, T. Deschner, and C. Boesch, "Development of a liquid chromatography-tandem mass spectrometry method for the determination of 23 endogenous steroids in small quantities of primate urine," *Journal of chromatography. B, Analytical technologies in the biomedical and life sciences*, vol. 862, pp. 100–112, 2008.
- [106] K. Hohlbaum, G. M. Corte, M. Humpenöder et al., "Reliability of the Mouse Grimace Scale in C57BL/6J Mice," *Animals : an open access journal from MDPI*, vol. 10, no. 9, pp. 1–12, 2020.
- [107] T. K. Koo and M. Y. Li, "A Guideline of Selecting and Reporting Intraclass Correlation Coefficients for Reliability Research," *Journal of chiropractic medicine*, vol. 15, no. 2, pp. 155–163, 2016.
- [108] R. J. Landis and G. G. Koch, "The Measurement of Observer Agreement for Categorical Data," *Biometrics*, no. 33, pp. 159–174, 1977.
- [109] L. M. Keubler, N. Hoppe, H. Potschka et al., "Where are we heading? Challenges in evidence-based severity assessment," *Laboratory animals*, vol. 54, no. 1, pp. 50–62, 2020.
- [110] R. M. J. Deacon, C. L. Thomas, J. N. P. Rawlins et al., "A comparison of the behavior of C57BL/6 and C57BL/10 mice," *Behavioural brain research*, vol. 179, no. 2, pp. 239–247, 2007.
- [111] J. O. Hendrickx, S. de Moudt, E. Calus et al., "Age-related cognitive decline in spatial learning and memory of C57BL/6J mice," *Behavioural brain research*, vol. 418, pp. 1–5, 2022.
- [112] K. Mekada, K. Abe, A. Murakami et al., "Genetic differences among C57BL/6 substrains," *Experimental animals*, vol. 58, no. 2, pp. 141–149, 2009.
- [113] P. Kahnau, A. Jaap, U. Hobbiesiefken et al., "A preliminary survey on the occurrence of barbering in laboratory mice in Germany," *Animal Welfare*, vol. 31, no. 4, pp. 433–436, 2022.

- [114] B. J. G. van den Boom, P. Pavlidi, C. J. H. Wolf et al., "Automated classification of self-grooming in mice using open-source software," *Journal of neuroscience methods*, vol. 289, pp. 48–56, 2017.
- [115] D. L. Langford, A. L. Bailey, M. L. Chanda et al., "Coding of facial expressions of pain in the laboratory mouse," *Nature methods*, vol. 7, no. 6, pp. 447–449, 2010.
- [116] A. L. Miller and M. C. Leach, "The Mouse Grimace Scale: A Clinically Useful Tool?," *PloS one*, vol. 10, no. 9, pp. 1–10, 2015.
- [117] A. A. Wolf and C. A. Frye, "The use of the elevated plus maze as an assay of anxiety-related behavior in rodents," *Nature protocols*, vol. 2, no. 2, pp. 322–328, 2007.
- [118] N. Kuleshkaya and V. Voikar, "Assessment of mouse anxiety-like behavior in the light-dark box and open-field arena: role of equipment and procedure," *Physiology & Behavior*, vol. 133, pp. 30–38, 2014.
- [119] Q. Lu, A. Mouri, Y. Yang et al., "Chronic unpredictable mild stress-induced behavioral changes are coupled with dopaminergic hyperfunction and serotonergic hypofunction in mouse models of depression," *Behavioural brain research*, vol. 372, pp. 1–10, 2019.
- [120] W. Hong, A. Kennedy, X. P. Burgos-Artizzu et al., "Automated measurement of mouse social behaviors using depth sensing, video tracking, and machine learning," *Proceedings of the National Academy of Sciences of the United States of America*, vol. 112, no. 38, pp. E5351–60, 2015.
- [121] F. de Chaumont, E. Ey, N. Torquet et al., "Live Mouse Tracker: real-time behavioral analysis of groups of mice," *bioRxiv preprint*, pp. 1–31, 2018.
- [122] K. Thorré, M. Pravda, S. Sarre et al., "New antioxidant mixture for long term stability of serotonin, dopamine and their metabolites in automated microbore liquid chromatography with dual electrochemical detection," *Journal of chromatography. B, Biomedical sciences and applications*, vol. 694, no. 2, pp. 297–303, 1997.
- [123] G. E. de Benedetto, D. Fico, A. Pennetta et al., "A rapid and simple method for the determination of 3,4-dihydroxyphenylacetic acid, norepinephrine, dopamine, and serotonin in mouse brain homogenate by HPLC with fluorimetric detection," *Journal of pharmaceutical and biomedical analysis*, vol. 98, pp. 266–270, 2014.
- [124] X.-E. Zhao, Y. He, S. Zhu et al., "Stable isotope labeling derivatization and magnetic dispersive solid phase extraction coupled with UHPLC-MS/MS for the measurement of brain neurotransmitters in post-stroke depression rats administered with gastrodin," *Analytica chimica acta*, vol. 1051, pp. 73–81, 2019.
- [125] G. Bergamini, J. Mechtersheimer, D. Azzinari et al., "Chronic social stress induces peripheral and central immune activation, blunted mesolimbic dopamine function, and reduced reward-directed behaviour in mice," *Neurobiology of stress*, vol. 8, pp. 42–56, 2018.
- [126] K. Y. Araki, J. R. Sims, and P. G. Bhide, "Dopamine receptor mRNA and protein expression in the mouse corpus striatum and cerebral cortex during pre- and postnatal development," *Brain Research*, vol. 1156, pp. 31–45, 2007.
- [127] P. Uutela, L. Karhu, P. Piepponen et al., "Discovery of dopamine glucuronide in rat and mouse brain microdialysis samples using liquid chromatography tandem mass spectrometry," *Analytical chemistry*, vol. 81, no. 1, pp. 427–434, 2009.
- [128] V. I. Chefer, A. C. Thompson, A. Zapata et al., "Overview of brain microdialysis," *Current protocols in neuroscience*, Chapter 7, Unit 7.1, 2009.
- [129] C. A. Lowry, P. L. Johnson, A. Hay-Schmidt et al., "Modulation of anxiety circuits by serotonergic systems," *Stress (Amsterdam, Netherlands)*, vol. 8, no. 4, pp. 233–246, 2005.
- [130] B. A. Samuels and R. Hen, "Novelty-Suppressed Feeding in the Mouse: Chapter 7," *Neuromethods*, vol. 63, pp. 107–121, 2011.
- [131] R. S. Eid, S. E. Lieblich, P. Duarte-Guterman et al., "Selective activation of estrogen receptors α and β : Implications for depressive-like phenotypes in female mice exposed to chronic unpredictable stress," *Hormones and behavior*, vol. 119, pp. 1–18, 2020.
- [132] O. Kallioikoski, J. Hau, K. R. Jacobsen et al., "Distribution and time course of corticosterone excretion in faeces and urine of female mice with varying systemic concentrations," *General and Comparative Endocrinology*, vol. 168, no. 3, pp. 450–454, 2010.
- [133] A. F. Ajayi and R. E. Akhigbe, "Staging of the estrous cycle and induction of estrus in experimental rodents: an update," *Fertility research and practice*, vol. 6, no. 5, pp. 1–15, 2020.

- [134] S. L. Byers, M. V. Wiles, S. L. Dunn et al., "Mouse Estrous Cycle Identification Tool and Images," *PloS one*, vol. 7, no. 4, pp. 1–5, 2012.
- [135] B. B. Turner, "Sex differences in the binding of type I and type II corticosteroid receptors in rat hippocampus," *Brain Research*, vol. 581, no. 2, pp. 229–236, 1992.
- [136] M. S. Flint and S. S. Tinkle, "C57BL/6 mice are resistant to acute restraint modulation of cutaneous hypersensitivity," *Toxicological sciences : an official journal of the Society of Toxicology*, vol. 62, no. 2, pp. 250–256, 2001.
- [137] C. Seah, M. S. Breen, T. Rusielewicz et al., "Modeling gene × environment interactions in PTSD using human neurons reveals diagnosis-specific glucocorticoid-induced gene expression," *Nature neuroscience*, vol. 25, no. 11, pp. 1434–1445, 2022.
- [138] B. Pletzer, W. Klimesch, K. Oberascher-Holzinger et al., "Corticosterone response in a resident-intruder-paradigm depends on social state and coping style in adolescent male Balb-C mice," *Neuroendocrinology Letters*, no. 5, pp. 585–590, 2007.
- [139] L. Chu, N. Li, J. Deng et al., "LC-APCI+-MS/MS method for the analysis of ten hormones and two endocannabinoids in plasma and hair from the mice with different gut microbiota," *Journal of pharmaceutical and biomedical analysis*, vol. 185, pp. 1–13, 2020.
- [140] T. Kuo, A. McQueen, C. Tzu-Chieh et al., "Regulation of Glucose Homeostasis by Glucocorticoids," *Advances in Experimental Medicine and Biology*, vol. 872, pp. 99–126, 2018.
- [141] M. Benedetti, R. Merino, R. Kusuda et al., "Plasma corticosterone levels in mouse models of pain," *European Journal of Pain*, vol. 16, pp. 803–815, 2012.
- [142] B. Kingma, A. Frijns, and W. van Marken Lichtenbelt, "The thermoneutral zone: implications for metabolic studies," *Frontiers in bioscience (Elite edition)*, vol. 4, no. 5, pp. 1975–1985, 2012.
- [143] C. W. Meyer, Y. Ootsuka, and A. A. Romanovsky, "Body Temperature Measurements for Metabolic Phenotyping in Mice," *Frontiers in physiology*, vol. 8, no. 520, pp. 1–13, 2017.
- [144] V. Škop, J. Guo, N. Liu et al., "Mouse Thermoregulation: Introducing the Concept of the Thermoneutral Point," *Cell reports*, vol. 31, no. 2, pp. 1–10, 2020.
- [145] C. G. Tankersley, R. Irizzary, S. Flanders et al., "Functional Genomics of Sleep and Circadian Rhythm: Selected Contribution: Circadian rhythm variation in activity, body temperature, and heart rate between C3H/HeJ and C57BL/6J inbred strains," *Journal of Applied Physiology*, no. 92, pp. 870–877, 2002.
- [146] Y.-H. Tseng, A. M. Cypess, and C. R. Kahn, "Cellular bioenergetics as a target for obesity therapy," *Nature reviews. Drug discovery*, vol. 9, no. 6, pp. 465–482, 2010.
- [147] B. A. de Fanti, D. A. Gavel, J. S. Hamilton et al., "Extracellular hypothalamic serotonin levels after dorsal raphe nuclei stimulation of lean (Fa/Fa) and obese (fa/fa) Zucker rats," *Brain Research*, vol. 869, pp. 6–14, 2000.
- [148] T. Sakaguchi and G. A. Bray, "Effect of norepinephrine, serotonin and tryptophan on the firing rate of sympathetic nerves," *Brain Research*, vol. 492, pp. 271–280, 1989.
- [149] H. M. Feldmann, V. Golozoubova, B. Cannon et al., "UCP1 ablation induces obesity and abolishes diet-induced thermogenesis in mice exempt from thermal stress by living at thermoneutrality," *Cell metabolism*, vol. 9, no. 2, pp. 203–209, 2009.
- [150] A. J. Kowaltowski, "Cold Exposure and the Metabolism of Mice, Men, and Other Wonderful Creatures," *Physiology (Bethesda, Md.)*, vol. 37, no. 5, pp. 253–259, 2022.
- [151] J. Nedergaard and B. Cannon, "How brown is brown fat? It depends where you look," *Nature medicine*, vol. 19, no. 5, pp. 540–541, 2013.
- [152] A. Jacobsson, M. Muhleisen, B. Cannon et al., "The uncoupling protein thermogenin during acclimation: indications for pretranslational control," *American journal of physiology. Regulatory, integrative and comparative physiology*, vol. 267, no. 4, pp. 1–9, 1994.
- [153] A. M. Madiehe, L. Lin, C. White et al., "Constitutive activation of STAT-3 and downregulation of SOCS-3 expression induced by adrenalectomy," *American journal of physiology. Regulatory, integrative and comparative physiology*, vol. 281, no. 6, R2048–58, 2001.
- [154] C. Handschin and B. M. Spiegelman, "Peroxisome proliferator-activated receptor gamma coactivator 1 coactivators, energy homeostasis, and metabolism," *Endocrine reviews*, vol. 27, no. 7, pp. 728–735, 2006.

- [155] V. Golozoubova, E. Hohtola, A. Matthias et al., "Only UCP1 can mediate adaptive nonshivering thermogenesis in the cold," *FASEB journal : official publication of the Federation of American Societies for Experimental Biology*, vol. 15, no. 11, pp. 2048–2050, 2001.
- [156] H. C. Scholle, F. Biedermann, D. Arnold et al., "A surface EMG multi-electrode technique for characterizing muscle activation patterns in mice during treadmill locomotion," *Journal of neuroscience methods*, vol. 146, no. 2, pp. 174–182, 2005.
- [157] S. R. Talbot, S. Biernot, A. Bleich et al., "Defining body-weight reduction as a humane endpoint: a critical appraisal," *Laboratory animals*, vol. 54, no. 1, pp. 99–110, 2020.
- [158] Y. Yang, D. L. Smith, K. D. Keating et al., "Variations in body weight, food intake and body composition after long-term high-fat diet feeding in C57BL/6J mice," *Obesity (Silver Spring, Md.)*, vol. 22, no. 10, pp. 2147–2155, 2014.
- [159] S. L. McFadden and B. L. Hooker, "Comparing Perika St. John's Wort and Sertraline for Treatment of Posttraumatic Stress Disorder in Mice," *Journal of dietary supplements*, vol. 17, no. 3, pp. 300–308, 2020.
- [160] M. Francois, I. Canal Delgado, N. Shargorodsky et al., "Assessing the effects of stress on feeding behaviors in laboratory mice," *eLife*, vol. 10, pp. 1–20, 2022.
- [161] J. B. Young, E. Saville, N. J. Rothwell et al., "Effect of diet and cold exposure on norepinephrine turnover in brown adipose tissue of the rat," *The Journal of clinical investigation*, vol. 69, no. 5, pp. 1061–1071, 1982.
- [162] N. J. Rothwell and M. J. Stock, "Effect of chronic food restriction on energy balance, thermogenic capacity, and brown-adipose-tissue activity in the rat," *Bioscience reports*, vol. 2, no. 8, pp. 543–549, 1982.
- [163] J. Margareto, A. Marti, and J. A. Martínez, "Changes in UCP mRNA expression levels in brown adipose tissue and skeletal muscle after feeding a high-energy diet and relationships with leptin, glucose and PPARgamma," *The Journal of nutritional biochemistry*, vol. 12, no. 3, pp. 130–137, 2001.
- [164] C. John, J. Grune, C. Ott et al., "Sex Differences in Cardiac Mitochondria in the New Zealand Obese Mouse," *Frontiers in endocrinology*, vol. 9, no. 732, pp. 1–9, 2018.
- [165] S. Moradi Tuchayi, J. Tam, G. R. Wojtkiewicz et al., "Injectable slurry for selective destruction of neck adipose tissue in New Zealand obese mouse model," *Sleep & breathing = Schlaf & Atmung*, vol. 24, no. 4, pp. 1715–1718, 2020.

List of Abbreviations

ACTH	Adrenocorticotropin
AD	Aldehyde dehydrogenase
ANOVA	Analysis of variance
ATP	Adenosine triphosphate
BAT	Brown adipose tissue
BC	Body composition
BH ₄	Tetrahydrobiopterin
BMR	Basal metabolic rate
BW	Body weight
cAMP	Cyclic adenosine monophosphate
cDNA	Complementary DNA
CE	Collision energy
COMT	Catechol-O-methyltransferase
CPU	<i>Caudate putamen</i>
CRH	Corticotropin releasing hormone
CYP	Cytochrome P450
DA	Dopamine
ddH ₂ O	Double-distilled water
DHOPA	11 β ,20 α -Dihydroxy-3-oxopregn-4-en-21-oic acid
Dife	German Institute of Human Nutrition
DNA	Deoxyribonucleic acid
DOPAC	3,4-Dihydroxyphenylacetic acid
DRN	Dorsal raphe nucleus
DW	Dry weight
E. coli	<i>Escherichia coli</i>
EE	Energy expenditure
e.g.	<i>Exempli gratia</i> , for example
EIA	Enzyme Immunoassay
EPM	Elevated Plus Maze
ESI	Electrospray ionization
FAD/FADH ₂	Flavin adenine dinucleotide
FCM	Fecal corticosterone metabolites
FM	Fat mass
Frag	Fragmentor voltage
FS	Fur Score
G-1-P/G-6-P	Glucose-1-phosphate/Glucose-6-phosphate
GABA	Gamma amino butyric acid
GLUT2	Glucose transporter 2
GPH	Glycogen phosphorylase
GPH-P	Phosphorylated glycogen phosphorylase
GR	Glucocorticoid receptor
GS	Glycogen synthase
GS-OH	Dephosphorylated glycogen synthase
H ₂ O	Water
HDOPA	11 β -Hydroxy-3,20-dioxopregn-4-en-21-oic acid
HPA	Hypothalamic-pituitary-adrenocortical
HPLC	High performance liquid chromatography
Hprt1	Hypoxanthine-guanine phosphoribosyltransferase 1
HTM	<i>Hypothalamus</i>
i.a.	<i>Inter alia</i>

ICC	Interrater/Intraclass correlation coefficient
i.e.	<i>Id est</i>
IMC	Innovative metabolic cage
LC	<i>Locus coeruleus</i>
LC-MS/MS	Liquid chromatography tandem-mass spectrometry
lgp	Lateral globus pallidus
LM	Lean mass
MAO	Monoamine oxidase
mgp	Medial globus pallidus
MGS	Mouse Grimace Scale
MR	Mineralocorticoid receptor
MRL	Max Rubner Laboratory
MRM	Multiple Reaction Monitoring
mRNA	Messenger RNA
m/z	Mass-to-charge ratio
NAC	<i>Nucleus accumbens</i>
NAD ⁺ /NADH	Nicotinamide adenine dinucleotide
NADP/NADPH	Nicotinamide adenine dinucleotide phosphate
NE	Norepinephrine
NMR	Nuclear magnetic resonance
O ₂	Molecular oxygen
OFT	Open Field Test
PAS	Periodic Acid Schiff
PCR	Polymerase chain reaction
PGC1 α	Peroxisome proliferator-activated receptor gamma coactivator 1-alpha
pH	<i>Potentia hydrogenii</i>
PKA	Protein kinase A
PPAR	Peroxisome proliferator-activated receptor
PVN	<i>Nucleus paraventricularis</i>
qRT-PCR	Quantitative reverse transcription PCR
R ²	Coefficient of determination
RNA	Ribonucleic acid
RT	Room temperature
SPF	Specified pathogen free
SN	<i>Substantia nigra</i>
SNC	<i>Substantia nigra pars compacta</i>
SNr	<i>Substantia nigra pars reticulata</i>
SRT	Serotonin
STN	Subthalamic nucleus
TMC	Tecniplast metabolic cage
TPH	Tryptophan hydroxylase
<i>Ucp1</i>	Uncoupling protein 1
UDP	Uridine diphosphate
UDP-G	Uridine diphosphate glucose
UTP	Uridine triphosphate
VMAT	Vesicular monoamine transporter
VTA	Ventral tegmental area
WAT	White adipose tissue
3-MT	3-Methoxytyramine
5-HIAA	5-Hydroxyindoleacetic acid
5-HTP	L-5-Hydroxytryptophan

List of Figures

Figure 1. The hypothalamic-pituitary-adrenocortical axis schematically displayed.	11
Figure 2. Biosynthesis of corticosterone.	13
Figure 3. Thermoregulatory response depending on ambient temperature.	16
Figure 4. Energy metabolism in mitochondria of the brown adipose tissue.	18
Figure 5. Schematic illustration of the dorsal mesostriatal and the ventral mesostriatal system in the murine brain.	19
Figure 6. Hypothetical connection between basal nuclei concerning the direct and the indirect pathway proceeding within the dopaminergic system.	21
Figure 7. Biosynthesis and degradation of dopamine.....	22
Figure 8. The serotonergic system of the central nervous system.	24
Figure 9. Biosynthesis and degradation of serotonin.	25
Figure 10. Glycogen metabolism in the liver.....	27
Figure 11. Study design of the conducted animal experiment shown as a time progression.	31
Figure 12. Comparison of applied metabolic cage types in animal experiment.....	32
Figure 13. Mouse Grimace Scale: three-point scale of the five facial units.....	34
Figure 14. Sample photos of mice taken with the thermal imaging camera during restraint in A: control cage, B: Tecniplast metabolic cage, and C: Innovative metabolic cage.	35
Figure 15. Experimental setup of A: Elevated Plus Maze and B: Open Field Test.	37
Figure 16. Shelf system and cage position for the video observation of mice during restraint in the control cage and metabolic cages.	37
Figure 17. Representation of observation intervals per mouse in the respective cage system.....	38
Figure 18. Photographs of food hoppers pertaining to the used metabolic cage types.	40
Figure 19. A: Used brain block for the preparation of coronal slices from murine brain. B: Dissection of respective brain areas.	41
Figure 20. Dissection of brain areas of interest.	43
Figure 21. Chemical structures of A: Corticosterone, B: Corticosterone-d8, C and D: respective fragments.	49
Figure 22. Chemical structures of A: Dopamine, B: Dopamine-d4, C: Serotonin, D: Serotonin-d4, E: 3,4-Dihydroxyphenylacetic acid, F: 3,4-Dihydroxyphenylacetic acid-d5, G: 3-Methoxytyramine, and H: [¹³ C, ^D ₅]-3-Methoxytyramine.	51
Figure 23. Scores of respective facial action units of the applied Mouse Grimace Scale are shown. ...	57
Figure 24. Cage temperature after 24 h single housing in the three different cage types.....	58
Figure 25. Body surface temperature after 24 h single housing in the three different cage types.....	59
Figure 26. Relative mRNA expression of Uncoupling protein 1 in brown adipose tissue of mice after second restraint in the three different cage types.	60
Figure 27. Weight of interscapular brown adipose tissue of mice after second restraint in the three different cage types.....	60
Figure 28. Number of excreted fecal boli within the Elevated Plus Maze Arena after first and second restraints in the three different cage types.	62
Figure 29. Number of excreted fecal boli within the Open Field Test after first and second restraints in the three different cage types.....	63
Figure 30. Spent time in either center, open arms or closed arms of the Elevated Plus Maze Arena after first and second restraints in the three different cage types.....	64
Figure 31. Spent time in either center, middle zone or outer zone of the Open Field Test Arena after first and second restraints in the three different cage types.....	65

Figure 32. Entries into either center, open arms or closed arms of the Elevated Plus Maze Arena after first and second restraints in the three different cage types.....	66
Figure 33. Entries into either center, middle zone or outer zone of the Open Field Test Arena after first and second restraints in the three different cage types.....	67
Figure 34. Total distance in the Elevated Plus Maze after first and second restraints in the three different cage types.....	68
Figure 35. Total distance in the Open Field Test after first and second restraints in the three different cage types.....	69
Figure 36. Activity in the Elevated Plus Maze Arena subdivided into total time (im)mobile after first and second restraints in the three different cage types.	70
Figure 37. Activity in the Open Field Test subdivided into total time (im)mobile after first and second restraints in the three different cage types.	71
Figure 38. Counts of behavioral categories during first restraint of females in the three different cage types.	73
Figure 39. Counts of behavioral categories during second restraint of females in the three different cage types.....	75
Figure 40. Counts of behavioral categories during first restraint of males in the three different cage types.	77
Figure 41. Counts of behavioral categories during second restraint of males in the three different cage types.....	79
Figure 42. Dopamine concentrations in five different brain areas.	81
Figure 43. 3,4-Dihydroxyphenylacetic acid concentrations in four different brain areas.	82
Figure 44. 3-Methoxythiramine concentrations in five different brain areas.	84
Figure 45. Serotonin concentrations in five different brain areas.....	86
Figure 46. Correlation between the concentration of neurotransmitters dopamine and 3-methoxythiramine in caudate putamen or substantia nigra of male mice and the total distance, average speed, and activity in either the Elevated Plus Maze or the Open Field Test after second restraint.	90
Figure 47. Body weight referenced to baseline measurement and body weight change during restraint in the three tested cage types.....	92
Figure 48. Lean mass change after first and second restraints in the three tested cage types.	93
Figure 49. Fat mass change after first and second restraints in the three tested cage types.	94
Figure 50. Food intake during first and second restraints in the metabolic cage types.	94
Figure 51. Water intake during first and second restraints in the metabolic cage types.	95
Figure 52. Fecal output during first and second restraints in the metabolic cage types.....	95
Figure 53. Excreted urine volume during first and second restraints in the metabolic cage types.	96
Figure 54. Sample photos of liver slices stained with Periodic acid Schiff/Hematoxylin.....	97
Figure 55. Differences in percentage areas stained positive with Periodic Acid Schiff relative to controls are depicted for liver slices of female and male mice after second restraint in either Tecniplast metabolic cage or Innovative metabolic cage.....	98
Figure 56. Glycogen concentration in liver after second restraint in the three different cage types. .	98
Figure 57. Correlation of glycogen concentration in liver with food intake during metabolic cage restraint.	99
Figure 58. Liver weight of female and male mice after the second restraint in three different cage types.	99
Figure 59. Corticosterone concentration in urine during first and second restraints in either Tecniplast metabolic cage or Innovative metabolic cage.	100

Figure 60. Correlation analysis between corticosterone concentrations in urine and Fur Score of female mice after first restraint. 101

Figure 61. Fecal corticosterone metabolites concentration during first and second restraints in the three tested cage types. 102

Figure 62. Correlation analyses between concentrations of fecal corticosterone metabolites and Fur Score, body surface temperature..... 103

Figure 63. Fecal corticosterone metabolites concentrations were matched to Fur Scores for each mouse. 104

List of Tables

Table 1. Recommendations of minimum enclosure size, floor area per animal, and minimum enclosure height for mice in stock and during procedures depending in body weight [5].	4
Table 2. Recommendation of minimum floor area and height of metabolic cages for restraint of mice [16].	4
Table 3. Fur Score: detailed evaluation scheme.	33
Table 4. Exclusive ethogram applied for video analysis of mice during restraint in different cage systems.	38
Table 5. LC-ESI-MS/MS parameters for measurement of corticosterone in urine samples.	50
Table 6. LC-ESI-MS/MS parameters for measurement of neurotransmitters in brain areas.	52
Table 7. Fur Scores of C57BL/6J mice at baseline, after first, and second restraints in control and metabolic cages.	54
Table 8. Inter-rater reliability of each facial action unit of the applied Mouse Grimace Scale.	56
Table 9. Correlation between the concentration of the neurotransmitters dopamine and 3-methoxytyramine in the caudate putamen or substantia nigra and the total distance, average speed, and activity in either the Elevated Plus Maze or the Open Field Test after second restraint.	88
Table 10. Correlation analyses between corticosterone concentrations in urine (native and glucuronidated fraction) and Fur Score, body surface temperature, cage temperature (cold stress).	101
Table 11. Correlation analyses between concentrations of fecal corticosterone metabolites and Fur Score, body surface temperature, cage temperature (cold stress).	102
Supplemental Table 1. Chemicals.	147
Supplemental Table 2. Buffers and solutions.	148
Supplemental Table 3. Kits.	148
Supplemental Table 4. Sequences of murine primers for quantitative Reverse Transcription PCR. .	148
Supplemental Table 5. Standards.	149
Supplemental Table 6. Equipment for animal experiment.	149
Supplemental Table 7. Laboratory equipment.	150
Supplemental Table 8. Consumable material for animal experiment.	152
Supplemental Table 9. Composition of diet.	153
Supplemental Table 10. Consumable material for laboratory analyses.	155
Supplemental Table 11. Software.	156

Units

am	<i>ante meridiem</i> , before noon
bp	base pair
cm	centimeter
cm ²	square centimeter
d	day
dm ³	cubic decimeter
eV	electron-volt
fmol	femtomole
x g	g-force, 9.81 m/s ²
g	gram
h	hour
IU	International unit
kg	kilogram
L	liter
m	meter
M	molar
μg	microgram
μL	microliter
μm	micrometer
μM	micromolar
mg	milligram
min	minute
MJ	megajoule
mL	milliliter
mm	millimeter
mM	millimolar
mmol	millimole
ms	milliseconds
mol	mole
ng	nanogram
nm	nanometer
nM	nanomolar
oz.	fluid ounce
pm	<i>post meridiem</i> , afternoon
pmol	picomole
psi	pound-force per square inch
rpm	revolutions per minute
s	second
U	unit
V	volt
°C	degree Celsius
%	percent
°	degree

Supplemental information

S1 Materials

S1.1 Reagents

Supplemental Table 1. Chemicals

Substance	Supplier
Acetic acid (concentrated)	Carl Roth GmbH & Co. KG, Karlsruhe, Germany
Acetonitrile (LiChrosolv, hypergrade for LC-MS)	Sigma-Aldrich Chemie GmbH, Taufkirchen, Germany
Acetonitrile (HiPerSolv CHROMANORM)	VWR International GmbH, Darmstadt, Germany
β -glucuronidase from <i>E. Coli</i> (25,000 U)	Sigma-Aldrich Chemie GmbH, Taufkirchen, Germany
β -Mercaptoethanol	VWR International GmbH, Darmstadt, Germany
Brilliant Blue G250	Carl Roth GmbH & Co. KG, Karlsruhe, Germany
Bromphenol blue	Sigma-Aldrich Chemie GmbH, Taufkirchen, Germany
Caustic soda (1 N)	Carl Roth GmbH & Co. KG, Karlsruhe, Germany
Chloroform	Carl Roth GmbH & Co. KG, Karlsruhe, Germany
Disodium phosphate (anhydrous)	Altmann Analytik GmbH & Co. KG, Munich, Germany
DNase I (RNase-free, 1 U/ μ L)	ThermoFisher Scientific, Waltham, United States
Deoxyribonucleotide triphosphate Mix (10 mM)	ThermoFisher Scientific, Waltham, United States
Distillation-pure water (30 ppb)	Merck Chemicals GmbH, Darmstadt, Germany
Double-distilled water (reverse osmosis, Mini Ro 10-15-EP)	Veolia Water Technologies GmbH, Celle, Germany
ESI-L Low Concentration Tuning Mix	Agilent Technologies, Waldbronn, Germany
Ethanol (rotisol)	Carl Roth GmbH & Co. KG, Karlsruhe, Germany
Ethylenediaminetetraacetate (50 mM)	ThermoFisher Scientific, Waltham, United States
Formic acid ($\geq 99\%$, for LC-MS)	VWR International GmbH, Darmstadt, Germany
Formic acid (98%)	Sigma-Aldrich Chemie GmbH, Taufkirchen, Germany
Glycerol	Carl Roth GmbH & Co. KG, Karlsruhe, Germany
Hydrochloric acid (1 M)	Carl Roth GmbH & Co. KG, Karlsruhe, Germany
Isoflurane CP [®]	CP-Pharma Handelsgesellschaft mbH, Burgdorf, Germany
Isopropanol (2-propanol - rotisol)	Carl Roth GmbH & Co. KG, Karlsruhe, Germany
Methanol (LiChrosolv, hypergrade for LC-MS)	Merck Chemicals GmbH, Darmstadt, Germany
Methanol (HiPerSolv CHROMANORM)	VWR International GmbH, Darmstadt, Germany
Methyl tert-butyl ether (HiPerSolv CHROMANORM)	VWR International GmbH, Darmstadt, Germany
Nuclease-free H ₂ O (DEPC-treated)	Carl Roth GmbH & Co. KG, Karlsruhe, Germany
Roth poly d(T) ₁₂₋₁₈ primer	Carl Roth GmbH & Co. KG, Karlsruhe, Germany
Perchloric acid (70%)	Sigma-Aldrich Chemie GmbH, Taufkirchen, Germany
Phosphoric acid (85%)	Carl Roth GmbH & Co. KG, Karlsruhe, Germany
RevertAid Reverse Transcriptase	ThermoFisher Scientific, Waltham, United States
Sodium carbonate (anhydrous)	Carl Roth GmbH & Co. KG, Karlsruhe, Germany
Sodium hydroxide (1 N)	Carl Roth GmbH & Co. KG, Karlsruhe, Germany
Sodium thiosulfate pentahydrate	Merck Chemicals GmbH, Darmstadt, Germany
SYBR Green/Fluorescein qPCR Master Mix	ThermoFisher Scientific, Waltham, United States
Tris base	Carl Roth GmbH & Co. KG, Karlsruhe, Germany
TRIzol [™] Reagent	Thermo Fisher Scientific, Waltham, United States
Water for HPLC (HiPerSolv CHROMANORM) filtered at 0.2 μ m	VWR International GmbH, Darmstadt, Germany

S1.2 Buffers and solutions

Supplemental Table 2. Buffers and solutions

Buffers and solutions	Composition/Supplier
Bradford Assay Dye	100 mg Brilliant Blue G250 in 50 mL ethanol and 100 mL phosphoric acid (85%) (total volume: 1 L H ₂ O suitable for HPLC)
Extraction buffer for neurotransmitters in brain areas	0.002 M sodium thiosulfate pentahydrate in 0.2 M perchloric acid (70%)
Protein Assay Dye Reagent Concentrate (Phosphoric Acid Solution, Methanol)	Bio-Rad Laboratories, Inc., Feldkirchen, Germany
Reaction buffer with MgCl ₂ , 10x (DNase I, RNase-free Kit)	Thermofisher Scientific, Waltham, United States
Reaction buffer, 5x (Revertaid™ First Strand cDNA Synthesis Kit)	Thermofisher Scientific, Waltham, United States
Sodium phosphate buffer (0.25 M, pH 6.9)	35 mL of 0.5 M sodium dihydrogen phosphate, 65 mL 0.5 M disodium phosphate, 100 mL ddH ₂ O
Solution 1 (Starch Kit)	Dissolve in 6 mL H ₂ O suitable for HPLC
Solution 2 (Starch Kit)	Dissolve in 27 mL H ₂ O suitable for HPLC
Solution 3 (Starch Kit)	Dissolve in 1100 µL H ₂ O suitable for HPLC and 220 µL hexokinase-suspension

S1.3 Kits

Supplemental Table 3. Kits

Kit	Supplier
DNase I, RNase-free (1 U/µL) Kit	Thermofisher Scientific, Waltham, United States
Revertaid™ First Strand cDNA Synthesis Kit	Thermofisher Scientific, Waltham, United States
Starch Kit	R-Biopharm AG, Darmstadt, Germany

S1.4 Oligonucleotides

Supplemental Table 4. Sequences of murine (*m*) primers for quantitative Reverse Transcription PCR (qRT-PCR)

Primer	Primer sequence (5' → 3')	Fragment size [bp]
β-actin (<i>mβ-actin</i>)	fw: CCAGCCTTCCTTCTTGGGTAT rv: GGGTGTAACGAGCTCAG	374
Hypoxanthine-guanine phosphoribosyltransferase 1 (<i>mHprt1</i>)	fw: TGGATACAGGCCAGACTTTGTT rv: CAGATTCAACTTGCCTCATC	162
Uncoupling protein 1 (<i>mUcp1</i>)	fw: TGGTGAACCCGACAATTCC rv: GGCCTCACCTTGGATCTGAA	141

S1.5 Standards

Supplemental Table 5. Standards

Internal standards	Supplier
Corticosterone-d8 in acetonitrile	Cayman Chemical Company, Ann Arbor, United States
Dopamine-d ₄ hydrochloride in 0.2 M perchloric acid	CDN Isotopes Inc., Quebec, Canada
Serotonin-d ₄ creatinine sulfate complex in H ₂ O suitable for HPLC	CDN Isotopes Inc., Quebec, Canada
3,4-Dihydroxyphenylacetic acid-d ₅ in H ₂ O suitable for HPLC	Alsachim, Illkirch Graffenstaden, France
[13C1D5]3-Methoxythyramine in H ₂ O suitable for HPLC	Alsachim, Illkirch Graffenstaden, France
Protein standard	Supplier
Protein standard, bovine serum albumin (200 mg/mL)	Sigma-Aldrich Chemie GmbH, Taufkirchen, Germany
Other standard	Supplier
Glycogen from bovine liver	Sigma-Aldrich Chemie GmbH, Taufkirchen, Germany

S1.6 Equipment for animal experiment and laboratory analyses

Supplemental Table 6. Equipment for animal experiment

Animal experiment equipment	Type	Supplier	Scope of application
Cages	Open polycarbonate cage of type III, 800 cm ²	EHRET GmbH Life Science Solutions, Freiburg im Breisgau, Germany	Home cage
	Open polycarbonate cage of type II, 350 cm ²	Tecniplast GmbH, Hohenpeißenberg, Germany	Control cage and single housing cage for males
Camera with interchangeable lens	α 6000	Sony, Tokio, Japan	Mouse Grimace Scale
Tecniplast metabolic cage (TMC)	Metabolic cages for individual mice, 3600M021	Tecniplast GmbH, Hohenpeißenberg, Germany	Single housing of mice
Infrared camera	DCS-932L	D-Link GmbH, Eschborn, Germany	Video recording in MC/control cage
Innovative metabolic cage (IMC)	-	Self-constructed from Mr. Röder at DIfE	Single housing of mice
Lens	70 mm, F2.8 DG, MACRO, Filter size: 49 mm	Sigma GmbH, Rödermark, Germany	Mouse Grimace Scale
Lighting	Seveno, LED lamp	Obi Group Holding SE & Co. KGaA, Wermelskirchen, Germany	Illumination of behavioral testing arenas
Nuclear Magnetic Resonance	500, Basic Model	Echo-MRI™, Zinsser Analytic GmbH, Eschborn, Germany	Body composition
Plastic tubing	20, Ø 4.5 cm	Self-constructed from Mr. Röder at DIfE	Body composition
Restrainer	10.5 cm x 7.5 cm x 6 cm, hole for tail: 1 cm	Self-constructed from Mr. Röder at DIfE	Blood collection from tail tip

Room-divider	Paravent AIR, QM1.0	Schneider GmbH & Co. KG, Hamburg, Germany	Delimitation of behavioral testing arenas
	2x Paravent 4 panel	Quick-Star GmbH, Recklingshausen, Germany	
Scale	PLJ Max 800 g, Min 0.02 g, d = 0.001 g	KERN & SOHN GmbH, Balingen, Germany	Body weight
	BP121S Max 120 g, d = 0.1 mg	Sartorius AG, Göttingen, Germany	Organ weight
	440-47N Max 2000 g, d = 0.1 g	KERN & SOHN GmbH, Balingen, Germany	Weight of food and water supply of MC
Steel Brain Matrix	51386	Stoelting Co., Dublin, Ireland	Dissection of brain into coronal slices
Thermal imaging camera	E50	FLIR, Frankfurt am Main, Germany	Thermal images of mice in MC/ control cages
Water bottle	Tecniplast 63, 100 mL, 1-3 oz.	Tecniplast GmbH, Hohenpeißenberg, Germany	Water supply in home cage
	Short caps: ACCP2511 opening \varnothing : 1.0 mm, outer \varnothing : 6.5 mm length nipple: 25 mm/in		Water supply in IMC
	Long caps: ACCP6521 opening \varnothing : 2.2 mm, outer \varnothing : 8 mm length nipple: 65 mm/in		Water supply in TMC
Webcam	C920 Pro HD, 1080 p, 30 fps	Logitech, Lausanne, Switzerland	Recording of mice during behavioral testing

Supplemental Table 7. Laboratory equipment

Laboratory equipment	Type	Supplier
Beadruptor	12, SKU 19-050A	Omni International, Inc, Kennesaw, United States
Centrifuge	Benchtop centrifuge, 064141	Carl Roth GmbH & Co. KG, Karlsruhe, Germany
	Heraeus Fresco 21	Thermo Fisher Scientific, Waltham, United States
	Mikro 200R	Andreas Hettich GmbH & Co. KG, Tuttlingen, Germany
	Universal 320 R	Andreas Hettich GmbH & Co. KG, Tuttlingen, Germany
Column	Kinetex C8 150 x 4.60 mm, 2.6 μ m, 100 A	Phenomenex Inc., Torrance, USA
	YMC-Triart PFP 150 x 3.0 mm, 3 μ m, 12 nm	Thermo Fisher Scientific, Waltham, United States
Fine scale	ABJ-NM, ABS-N Max 220 g, Min 0.01 g, d=0.1 mg	KERN & SOHN GmbH, Balingen, Germany
High performance liquid chromatography system	1260 Infinity II	Agilent Technologies, Inc., Waldbronn, Germany
	1260 Infinity	
Light Cycler	Light Cycler® 480 II, 5267	Roche Diagnostics GmbH, Mannheim, Germany

Mass spectrometer	6495 Triple Quad LC/MS interface: electrospray ion source	Agilent Technologies, Inc., Waldbronn, Germany
	6470 Triple Quad LC/MS interface: electrospray ion source	
Microplate reader	iMark	Bio-Rad Laboratories, Inc., Feldkirchen, Germany
	PowerWave XS2	BioTek Instruments GmbH, Bad Friedrichshall, Germany
Microscope	Olympus BX50 camera: Olympus XC50	Evident Europe GmbH, Hamburg, Germany
NanoDrop	NanoDrop One	Thermo Fisher Scientific, Waltham, United States
Oven	UN30, SingleDISPLAY	Memmert GmbH + Co. KG, Schwabach, Germany
pH meter	Knick 766 Calimatic	Knick, Elektronische Meßgeräte GmbH & Co., Berlin, Germany
Pipette	Multichannel - Research Plus 8 channel, 30 - 300 µL	Eppendorf SE, Hamburg, Germany
	Multipipette - E3x 1 µL - 50 mL	
	Single channel - Research Plus 0.1 - 2.5 µL, 0.5 - 10 µL, 2 - 20 µL, 10 - 100 µL, 20 - 200 µL, 100 - 1000 µL, 500 - 5000 µL	
Pre-column	YMC-Triart PFP 3 µm, 3 x 10 mm	Thermo Fisher Scientific, Waltham, United States
Stirrer	Yellowline, MSH basic	IKA®-Werke GmbH & Co. KG, Staufen, Germany
Thermocycler	Mastercycler gradient	Eppendorf SE, Hamburg, Germany
Thermomixer	5436	Eppendorf SE, Hamburg, Germany
Ultrasonic bath	Bandelin Sonorex	BANDELIN electronic GmbH & Co.KG, Berlin, Germany
Vacuum concentrator	Jouan RC 10.22, RCT 90, Serial No. 30109174	Gemini B.V., Apeldoorn, Netherlands
Vacuum controller	PVK 610, Vacu-Box	MLT AG Labortechnik, Wangen, Switzerland
Vortex generator	D-6012	neoLab Migge GmbH, Heidelberg, Germany
	Vortex-Genie 2	Scientific Industries, Inc., New York, United States

S1.7 Consumable material for animal experiment and laboratory analyses

Supplemental Table 8. Consumable material for animal experiment

Consumable material	Type	Supplier	Scope of application
Bedding material	Aspen wood, grain size: 2-5 mm, height: 1.5 mm, 211.56 g	ssniff Spezialdiäten GmbH, Soest, Germany	Home and control cage enrichment
Cardboard house	16 cm x 12 cm x 8 cm	LBS Biotechnology, United Kingdom	Home and control cage enrichment
Cellulose tissue	Green, H3-towel system classic, 23 cm x 24.8 cm	Essity Professional Hygiene Germany GmbH, Mannheim, Germany	
Food	Pelleted, rat/mouse maintenance, V 1534-300	ssniff Spezialdiäten GmbH, Soest, Germany	Food supply
Gnawing bar	Aspen wood, 100 x 20 x 20 mm	ssniff Spezialdiäten GmbH, Soest, Germany	Home and control cage enrichment
Histoset	Uni-Safe, white	Engelbrecht - Medizin- und Labortechnik GmbH, Edermünde, Germany	Embedding of tissue in paraffin
Nestlet	Cotton, 5 x 5 cm	ZOONLAB GmbH, Castrop-Rauxel, Germany	Home and control cage enrichment
Scalpel	AESCU LAP®, disposable scalpel, Cutfix	B. Braun SE, Melsungen, Germany	Organ removal and cut off from tail tip

Supplemental Table 9: Composition of diet

Product #	V 1534-300
Ingredient	
<u>Amino Acids [%]:</u>	
Arginine	1.19
Lysine	1.10
Histidine	0.49
Leucine	1.39
Isoleucine	0.79
Valine	0.92
Threonine	0.72
Tryptophan	0.25
Methionine	0.38
Glutamic acid	4.22
Phenylalanine	0.89
Phenylalanine+ Tyrosine	1.50
Glycine	0.89
Cystine	0.35
Methionine + Cysteine	0.73
Aspartic acid	1.84
Proline	1.31
Alanine	0.87
Serine	1.01
<u>Raw nutrients [%]:</u>	
Starch	35.2
Sucrose	5.3
Crude fiber	4.9
Crude ash	6.4
Crude protein	19.0
Crude fat	3.3
Nitrogen-free extractives	54.2
<u>Mineral substances [%]:</u>	
Calcium	1.00
Phosphorus	0.70
Calcium/Phosphorus	1.43 : 1
Sodium	0.24
Magnesium	0.22
Potassium	0.92
<u>Fatty acids [%]:</u>	
C 12:0	-
C 14:0	0.01
C 16:0	0.45
C 18:0	0.09
C 20:0	0.01
C 16:1	0.01
C 18:1	0.62
C 18:2	1.76
C 18:3	0.23

Vitamins [per kg]:

Vitamin A	25,000 IU (\cong 7,500 μ g/kg retinol \cong 15,000 μ g/kg beta-carotene)
Vitamin D ₃	1,500 IU (\cong 37.5 μ g/kg vitamin D ₃)
Vitamin E	135 mg
Vitamin K	20 mg
Thiamin (B ₁)	86 mg
Riboflavin (B ₂)	32 mg
Pyridoxin (B ₆)	31 mg
Cobalamin (B ₁₂)	150 μ g
Nicotinic acid	153 mg
Pantothenic acid	59 mg
Folic acid	10 mg
Biotin	710 μ g
Choline	1,370 mg

Trace elements [per kg]:

Iron	186 mg
Manganese	68 mg
Zinc	91 mg
Copper	15 mg
Iodine	2.1 mg
Selenium	0.3 mg
Gross energy	16.2 MJ/kg
Convertible Energy	13.5 MJ/kg

Supplemental Table 10. Consumable material for laboratory analyses

Consumable material	Type	Supplier
96-well PCR plate	LC 480	Biozym Scientific GmbH, Hessisch Oldendorf, Germany
Ceramic beads	1.4 mm, SKU 19-645	Omni International, Inc, Kennesaw, United States
Combitips®	0.2 mL, 2.5 mL, 5 mL	Eppendorf SE, Hamburg, Germany
Glass vials	1.5 mL short thread bottle, 32 x 11.6 mm, clear glass; 9 mm polypropylene cap, 6 mm punch hole	IVA Analysentechnik GmbH & Co. KG, Meerbusch, Germany
Microinserts	0.25 mL, 31 x 6 mm, clear glass, 15 mm tip	IVA Analysentechnik GmbH & Co. KG, Meerbusch, Germany
Microtiter plate	96 well	Greiner AG, Kremsmünster, Austria
Needles for single use	-	Henke Sass Wolf, Tuttlingen, Germany
Pipette tips	0.1 - 20 µL	Carl Roth GmbH & Co. KG, Karlsruhe, Germany
	2 - 200 µL	Eppendorf SE, Hamburg, Germany
	100 - 1200 µL	Carl Roth GmbH & Co. KG, Karlsruhe, Germany
Reaction vessels	1.5 mL Graduated Tube Natural, EasyGrip Cap Mixed	Starlab International GmbH, Hamburg, Germany
	0.5 mL, 1.5 mL, 2.0 mL, SafeSeal	Sarstedt AG & Co. KG, Nümbrecht, Germany
	1.5 mL, SafeSeal, low protein-binding	
	5 mL	Carl Roth GmbH & Co. KG, Karlsruhe, Germany
	15 mL	
50 mL	VWR International GmbH, Darmstadt, Germany	
Spin-X centrifuge tube filter	8161, 0.22 µm cellulose acetate in 2.0 mL polypropylene tube	Corning GmbH, Kaiserslautern, Germany
Stuffed pipette tips	10 µL, 200 µL, 1250 µL	Biozym Scientific GmbH, Hessisch Oldendorf, Germany

S1.8 Software

Supplemental Table 11. Software

Software	Scope of application	Supplier
©ANY-maze version 4.99	Behavioral tests	Stoelting Europe, Dublin, Ireland
cellSens™	Histology: photographs	Evident Europe GmbH, Hamburg, Germany
D-ViewCam	Video recording in cages	D-Link GmbH, Eschborn, Germany
Graphpad Prism version 6	Graphs	Graphstats Technologies Private Limited, Bangalore, India
IBM® SPSS® Statistics	Statistics	IBM Deutschland GmbH, Ehningen, Germany
ImageJ (NIH)	Histology: analysis of photographs	Public domain
LightCycler®	qRT-PCR	Roche Deutschland Holding GmbH, Mannheim, Germany
MassHunter (quantitative analysis)	Serotonin and dopamine concentrations in brain areas	Agilent Technologies Germany GmbH & Co. KG, Waldbronn, Germany
Microplate Manager®6 (MPM6)	Protein assay, glycogen analyses	BioRad Laboratories GmbH, Feldkirchen, Germany
Skyline Targeted Mass Spec Environment	Corticosterone concentrations in urine	MacCoss Lab Software, Open source

Conferences

Oral presentation

1. Wittek L, Nitezki T, Raila J, Krämer S. Vergleich von Metabolischen Käfigtypen - Analyse von Refinement-Maßnahmen und metabolischen Parametern bei Labormäusen. Deutsche Veterinärmedizinische Gesellschaft (DVG), 2021.
2. Wittek L, Nitezki T, Raila J, Krämer S. Wie stark sind Labormäuse wirklich durch den Einsatz des Metabolischen Käfigs belastet? Gesellschaft für Versuchstierkunde Society of Laboratory Animal Science (GV-SOLAS), 2021.
3. Wittek L, Nitezki T, Raila J, Krämer S. Der Metabolische Käfig - eine kritische Analyse potentieller Belastungen. Gesellschaft für Versuchstierkunde Society of Laboratory Animal Science (GV-SOLAS), 2020.
4. Siegeler K, Wittek L, Krämer S. Von der Notwendigkeit der objektivierbaren Belastungseinschätzung. Ursula M. Händel-Tierschutzpreis der Deutschen Forschungsgemeinschaft (DFG), Gießen, 2020.

Curriculum vitae

Diese Seite enthält persönliche Daten und wurde aus der Arbeit entfernt.

Acknowledgements

Diese Seite enthält persönliche Daten und wurde aus der Arbeit entfernt.

Eidesstaatliche Erklärung

Hiermit versichere ich, dass die vorliegende Dissertation mit dem Titel:

„Comparison of metabolic cages - analysis of refinement measures on the welfare and metabolic parameters of laboratory mice”

in der Abteilung Physiologie und Pathophysiologie der Ernährung der Universität Potsdam selbstständig und ausschließlich unter Verwendung der angegebenen Quellen und Hilfsmittel angefertigt wurde. Ebenfalls bestätige ich, dass diese Arbeit weder in gleicher noch in ähnlicher Form bisher an einer anderen Hochschule eingereicht wurde.

Nuthetal, June 2023

Laura Wittek